Understanding therapy resistance in glioblastoma using proteomics approach

By

JACINTH RAJENDRA

LIFE09201204011

TATA MEMORIAL CENTRE

MUMBAI

A thesis submitted to the

Board of Studies in Life Sciences in partial fulfillment of requirements for the Degree of

DOCTOR OF PHILOSOPHY

of

HOMI BHABHA NATIONAL INSTITUTE

January 2019

Homi Bhabha National Institute

Recommendations of the Viva Voce Committee

As members of the Viva Voce Committee, we certify that we have read the dissertation prepared by **Ms. Jacinth Rajendra** entitled "**Understanding therapy resistance in Glioblastoma using proteomics approach**" and recommend that it may be accepted as fulfilling the thesis requirement for the award of Degree of Doctor of Philosophy.

S N Dalal — 21/01/2019

Chairman – Dr. Sorab Dalal — Date:

Shilpee Dutt — 21/1/19

Guide/Convener – Dr. Shilpee Dutt — Date:

Ellora Sen — 21/01/2019

External Examiner – Dr. Ellora Sen — Date:

V Prasanna — 21/01/2019

Member – Dr. Prasanna Venkatraman — Date:

Dibyendu Bhattacharya — 21/01/2019

Member - Dr. Dibyendu Bhattacharya — Date:

Final approval and acceptance of this thesis is contingent upon the candidate's submission of the final copies of the thesis to HBNI.

I hereby certify that I have read this thesis prepared under my direction and recommend that it may be accepted as fulfilling the thesis requirement.

Date: 21/01/2019

Place: Navi Mumbai

Shilpee Dutt 21/01/2019

Dr. Shilpee Dutt

Guide

STATEMENT BY AUTHOR

This dissertation has been submitted in partial fulfilment of requirements for an advanced degree at Homi Bhabha National Institute (HBNI) and is deposited in the Library to be made available to borrowers under rules of the HBNI.

Brief quotations from this dissertation are allowable without special permission, provided that accurate acknowledgement of source is made. Requests for permission for extended quotation from or reproduction of this manuscript in whole or in part may be granted by the Competent Authority of HBNI when in his or her judgment the proposed use of the material is in the interests of scholarship. In all other instances, however, permission must be obtained from the author.

Navi Mumbai, Jacinth Rajendra

Date: 21.1.2019

DECLARATION

I, hereby declare that the investigation presented in the thesis has been carried out by me. This work is original and has not been submitted earlier as a whole or in part for a degree / diploma at this or any other Institution / University.

Navi Mumbai,

Date: 21.1.2019 Jacinth Rajendra

List of Publications arising from the thesis
Journal

1. **Enhanced proteasomal activity is essential for long term survival and recurrence of innately radiation resistant residual glioblastoma cells. Jacinth Rajendra**, Keshava K. Datta, Sheikh Burhan Ud Din Farooqee, Rahul Thorat, Kiran Kumar, Nilesh Gardi, Ekjot Kaur, Jyothi Nair, Sameer Salunkhe, Ketaki Patkar, Sanket Desai, Jayant Sastri Goda, Aliasgar Moiyadi, Amit Dutt, Prasanna Venkatraman, Harsha Gowda and Shilpee Dutt**. Oncotarget. 2018 Jun 12; 9(45): 27667–27681.**

Chapters in books and lectures notes : N/A

Conferences

Platform presentation

1. **Indian Association of Cancer Research (IACR) – April 2016** held in New Delhi, India on April 2016 for the abstract entitled: Differential proteomic analysis reveals role of a novel serine threonine kinase DCLK3 and 14-3-3 zeta in innately radiation resistant and relapse cells of Glioblastoma. **Jacinth Rajendra**, Keshava Datta, Raja Reddy, Nilesh Gardi, Ekjot Kaur, Ketaki Patkar, Aliasgar, Kakoli Bose, Amit Dutt, Harsha Gowda, Shilpee Dutt

2. **Indian society for neurooncology conference (ISNOCON) - April 2018** held at AIIMS, New Delhi from 5th April to 8th April 2018 for the abstract entitled : Enhanced proteasome activity is essential for long term survival and recurrence of innately radiation resistant residual glioblastoma cells

3. **INDO – US Proteogenomics conference 2018** held at ACTREC, TMC, Mumbai from 7th Dec – 11th Dec 2018 for the abstract entitled : Integrin independent recruitment of paxillin identifies it as a novel drug target in recurrent GBM. **Jacinth Rajendra**, Jyothi Nair, Anagha Acharekar, Ekjot Kaur, Shilpee Dutt. **Awarded 1st Prize**

Poster Presentation

1. International Proteomics Symposium Conference held at IIT Bombay on December 2014 for the abstract entitled: Differential Proteome reveals major role of metabolic pathways in conferring radio resistance to recurrent Glioblastoma. **Rajendra J**, Datta Keshava, Gardi N, Patkar K, Dutt A, Gowda H, Dutt S

2. Tata Memorial Centre 75th Platinum Jubilee Celebrations held in Mumbai on February 2016 for the abstract entitled as: Differential proteomic analysis reveals role of a novel serine threonine kinase DCLK3 and 14-3-3 zeta in innately radiation resistant and relapse cells of Glioblastoma.
   Jacinth Rajendra, Keshava Datta, Raja Reddy, Nilesh Gardi, Ekjot Kaur, Ketaki Patkar, Aliasgar, Kakoli Bose, Amit Dutt, Harsha Gowda, Shilpee Dutt

3. International Conference on Enzymology held at ACTREC, TMC , Mumbai on January 2017 for the abstract entitled : Identification of a novel serine threonine kinase DCLK3 and immunoproteasome subunit PA28α: Potential therapeutic targets for innately radiation resistant glioblastoma cells
   Jacinth Rajendra, Keshava Datta, Sheikh Burhan Ud Din Farooqee, Raja Reddy, Nilesh Gardi, Ekjot Kaur, Ketaki Patkar, Aliasgar Moiyad, Prasanna Venkataraman, Kakoli Bose, Amit Dutt, Harsha Gowda, Shilpee Dutt.*

4. Annual Meeting of American Association for Cancer Research" held at Washington, DC from April 1st – April 5th 2017 for the abstract entitled: Identification of proteasome pathway and a novel serine threonine kinase DCLK3: Potential therapeutic targets for innately radiation resistant glioblastoma cells.

Others

1. **Radiation-induced homotypic cell fusions of innately resistant glioblastoma cells mediate their sustained survival and recurrence.** Kaur E, **Rajendra J**, Jadhav S, Shridhar E, Goda JS, Moiyadi A, Dutt S.**Carcinogenesis. 2015 Jun; 36(6):685-95**

2. **Unique spectral markers discern recurrent Glioblastoma cells from heterogeneous parent population.** Ekjot Kaur, Aditi Sahu, Arti R. Hole, **Jacinth Rajendra**, Rohan Chaubal, Nilesh Gardi, Amit Dutt, Aliasgar Moiyadi, C. Murali Krishna & Shilpee Dutt Scientific Reports **volume6**, Article number: 26538 (2016)

Navi Mumbai,

Date: 21.1.2019 Jacinth Rajendra

Dedicated to my loving mother

Late Mrs. Jasmine Rajendra

Acknowledgments

I take this opportunity to express my heartfelt gratitude and thankfulness to all those who have walked along with me through this challenging journey and motivated me to overcome the odds.

Firstly, I would like to thank my mentor Dr. Shilpee Dutt for giving me the opportunity to pursue my Ph.D. under her guidance. Her mentorship has molded me to think beyond barriers in research. I am grateful to her for motivating me as a scientist and a mentor. Her constant support, persuasion, and encouragement through all my experiences during these six years has helped me grow as a research scientist.

I extend my earnest gratefulness to Dr. Rajiv Sarin (Ex-Director, ACTREC) and Dr. S.V. Chiplunkar (Director, ACTREC) for providing the infrastructure of ACTREC and other eminent facilities which helped me pursue my research interest successfully. I would also like to thank ACTREC funds for the fellowship, Homi Bhabha National Institute (HBNI) and Tata Memorial Centre (TMC) for providing me with the financial assistance to present my work at an international platform.

I also express thanks to my doctoral committee members: Dr. Sorab Dalal (Chairperson, ACTREC), Dr. Dibyendu Bhattacharya (ACTREC), Dr. Prasanna Venkatraman (ACTREC), Dr. Harsha Gowda (Institute of Bioinformatics, Bangalore) and my ex-chairperson Dr. Rita Mulherkar for their critical and valuable insights.

I want to further acknowledge Dr.Prasanna Venkatraman and Dr. Harsha Gowda who were also my collaborators in this study. I want to thank Dr. Prasanna for helping me with her expertise and resources for a part of my thesis work related to proteasome biology. I also want to thank Dr. Harsha Gowda for providing me the platform to perform all my proteomic experiments.

A special word of appreciation to Dr. Amit Dutt for his immense support and encouragement both professionally and personally. I want to especially thank him for his valuable suggestions and honest opinions in my study. It has been a privilege to seek guidance and knowledge from a well-known scientist who has also been recognized globally for his significant contribution to medical sciences in India.

I thank my clinical collaborators: Dr. Aliasgar Moiyadi (for providing the GBM samples for this study, Dr. Jayant Sastri Goda for his support and guidance during the radiation experiments performed on the orthotopic GBM mouse model. I also want to sincerely thank Dr. Rahul Thorat (ACTREC) for his immense patience, support, encouragement while helping me with orthotopic injections during the *in vivo* experiments.

The growth of a budding researcher also largely depends on the lab environment which is maintained by the members who work as a team. So, I take this opportunity to thank my seniors: Ekjot Kaur, Priya Puri & Gauri Patade who were part of the initial years of my Ph.D. I thank

them for their warmth and patient cooperation with which they helped me start my Ph.D. I especially thank Ekjot Kaur and Priya Puri who were not only accommodating seniors but they were also my companions who supported me both professionally and personally. I also thank Priti Parikh for sharing a great bond of friendship with me during her tenure in our lab. A special thanks to Smita Ma'am and Ganesh Sir for their diligent assistance during the course of my Ph.D.

I also want to acknowledge my peers – Sameer Salunkhe, Jyothi Nair, Anagha Acharekar, and Saket Vatsa Mishra for maintaining a very warm and dynamic environment in the lab. Their genuine love, respect, support and fun-loving attitude played a vital role in boosting my confidence and motivation to accomplish my goal. I also want to thank all the trainees who worked with me to assist me during my study – Louella, Tejal, Samreen, Puloma, Samadri, Gargi & Elton. A special thanks to Burhan, Keshava Datta and Kiran Kumar who worked with me in collaboration for a part of my study.

I extend my thanks to the members of our extended lab family: The former and present Dutt Lab Members –Pawan Upadhayay, Prajish Iyer, Rohan Chaubal, Nilesh Gardi, Pratik Chandrani, Mukul Godbole, Manoj Sir, Hemant Dhamne, Vidya, Sanket Desai, Asim Joshi, Bhaskar and Neelima for their professional and friendly support.

I'd like to also thank my batch mates - Bhushan Thakur, Sameer Salunkhe, Prajish Iyer, Pratik Chaudhari, Bhavik Jain, Gopal, Arunabha, Saujanya & Mukul for being a source of encouragement and relaxation through delightful gatherings and outings.

This journey wouldn't have been possible without the love and care from my close friends, family members, and spiritual mentors. I want to especially thank my lovely friends outside my lab and ACTREC - Bhushan Thakur, Joel Christie, Shalini Dimri, Apoorva Bhope & Kunal Onkar, Aakanksha Sharma, Swathi Maddali, Rachita Murali, Dr.Preeti Gupta, Vandana Bhalla, Edward James, Angelin James & Ebi Suganya who never hesitated to be my listening ear in times of difficulties. Their love and companionship helped me cope up during hard times.

Our roots define our being in this world which stems from our family. My family has been my pillar of strength during the entire tenure of my Ph.D. I want to especially thank and acknowledge my father Mr. D. Rajendra who not only supported me with his unconditional love for me but he also backed me up with his ceaseless prayers which have brought me this far. I want to thank him for patiently enduring my absence even through his ailing moments so that I could focus on my Ph.D. and complete it. Words won't be enough to express my gratitude towards my elder sister Janet Rajendra who stood beside me through all the odds and tarried along with me through these years. I thank her for being my motivator and the source of emotional strength. She has been more than just a sister to me. I thank her for inspiring me to dream beyond my limits and encouraging me at every step of my Ph.D. journey. I would also like to thank my brother in law – Mr. Sunil Chetti for his love, support and timely advice when I needed it the most. I also thank the elders of my family who supported me with their love and prayers – Josephine Ebenezer, Dr. Helen Roberts & Hepzibah Angela.

I would also like to thank my spiritual mentors – James Ebenezer, Eunice Anita, Renuka Samuel & T.D Samuel. I want to especially thank them for being a source of encouragement and for helping me keep my perspectives in place during tough times of my Ph.D.

Last but not the least I thank the Lord Almighty for giving me the wisdom, strength, and grace to bring this to completion. All glory, honor, and praise be to the God who enables and to the God who sustains with his unending love and grace.

Jacinth Rajendra

Table of contents

SYNOPSIS **1**

SYNOPSIS OF PH. D. THESIS **2**

1 INTRODUCTION AND REVIEW OF LITERATURE **16**
1.1 Glioblastoma 17
1.2 Standard of care 20
1.3 Prognosis 21
1.4 Recurrence and therapy resistance 22
1.5 Proteomics and Cancer 24
1.6 Mass spectrometry-based quantitative proteomics in cancer 25
1.7 Isobaric tagged relative and absolute quantification (iTRAQ) 27
1.8 Differential proteomic studies in glioblastoma 28
1.9 Rationale 31

2 MATERIAL AND METHODS **33**
2.1 Cell Culture and Patient samples 34
2.2 Drug Treatment 35
2.3 Radiation treatment 35
2.4 Trypan blue assay 35
2.5 Clonogenic survival assay 35
2.6 RNA extraction, cDNA synthesis, and qPCR 36
2.7 Protein Extraction 36
2.8 iTRAQ labeling 36
2.9 SCX FRACTIONATION 37
2.10 LC-MS/MS analysis 37
2.11 Protein identification and quantitation 38
2.12 Bioinformatics Analysis 38
2.13 Western Blot analysis 39
2.14 MTT cytotoxicity assay 39
2.15 Luciferase based NFkB promoter activity 39
2.16 Proteasome activity assay 40
2.17 Orthotopic xenograft mouse experiments 40
2.18 Radiation and drug treatment of orthotopic GBM mouse model. 41
2.19 Bioluminescence imaging of orthotopic tumor xenografts 41
2.20 Bacterial purification of GST-tagged 14-3-3 ζ 41
2.21 GST pull-down assay using GST tagged 14-3-3 ζ as bait 42
2.22 Statistical methods 42

3 CHARACTERIZATION OF THE RADIATION RESISTANT AND THE RELAPSE POPULATION. **43**

3.1 Introduction **44**

3.2 Results **48**
3.2.1 Survival response of Relapse cells to a lethal dose of radiation 48
3.2.2 Relapse glioblastoma cells demonstrate enhanced malignant properties..... 50
3.2.3 Presence of MNGCs post radiation and chemotherapy in glioblastoma..... 52
3.2.4 Presence of MNGCs in other cancers. 54

3.3 Discussion..... **57**

4 DIFFERENTIAL PROTEOMIC ANALYSIS OF PARENT, RADIATION RESISTANT AND RELAPSE POPULATION USING QUANTITATIVE PROTEOMIC **60**

4.1 Identification and functional validation of pathways deregulated in RR and R cells 61
4.1.1 Introduction 61
4.1.2 Results 65
4.1.3 Discussion 87

4.2 Identification and functional validation of candidate protein 14-3-3 zeta in RR cells 90
4.2.1 Introduction 90
4.2.2 Results 95
4.2.3 Discussion 101

5 SUMMARY AND CONCLUSION **104**
5.1 Summary..... **105**
5.2 Conclusion **108**

6 REFERENCES **110**

7 APPENDIX..... **121**

8 PUBLICATIONS..... **124**

List of figures

Figure 1 Age-adjusted and age-specific incidence rates for glioblastoma at diagnosis and gender, CBTRUS statistical report: NPCR and SEER, 2006–2010. 17

Figure 2 Distribution of glioblastoma in different regions of the brain. 18

Figure 3 MRI of the brain Image courtesy of George Jallo, MD 19

Figure 4 Common alterations involved in glioblastoma. Image adopted from (1) 24

Figure 5 Schematic representation of proteomic analysis using mass spectrometry (4) 25

Figure 6 Different types of quantitative proteomic techniques. 27

Figure 7 Chemical structures for iTRAQ 28

Figure 8 Formation of MNGCs. Image adopted from (1) 44

Figure 9 Schema showing the multi-step in-vitro radiation model recapitulating the progression of GBM and demonstrating the non-proliferative phase (76) 47

Figure 10 Cellular model to capture the inaccessible residual cells. 48

Figure 11 Radiation response of relapse (R1) cells to second round of lethal dose of radiation 49

Figure 12 Radioresistance of R1 and R2 compared to P 50

Figure 13 Wound healing assay for parent and relapse cells 50

Figure 14 Boyden chamber assay for comparing the invasion of Relapse cells as compared to Parent 51

Figure 15 Schematic representation of the experiment to examine the presence of MNGCs in response to standard therapy 52

Figure 16 monitoring the presence of MNGCs in response to therapy. 53

Figure 17 Clonogenic survival curves of different cancer cell lines. 54

Figure 18 Growth kinetics of cell lines post radiation 55

Figure 19 Morphological changes in response to radiation. 56

Figure 20 Presence of MNGCs in other cancer. 56

Figure 21 Different types of proteasomes 63

Figure 22 Nf-kB an indirect target of proteasomes (2) 64

Figure 23 In vitro radiation resistant model 66

Figure 24 A schematic representation of the proteomics workflow. 67

Figure 25 Proteomic analysis of the parent (P), radiation resistant (RR), relapse(R) 68

Figure 26 Unsupervised clustering of differential proteins. 69

Figure 27 Pathway analysis of the cluster 2 and cluster 3 70

Figure 28 Deregulated pathways in the radiation resistant and relapse population.....72

Figure 29. Validation of proteomics data 73

Figure 30 Proteasome activity and expression of beta catalytic subunits in RR cells. **B** 75

Figure 30 Proteasome activity and expression of beta catalytic subunits in RR cells. .....**Error! Bookmark not defined.**

Figure 31. Dose determination of bortezomib in SF268.....**Error! Bookmark not defined.**

Figure 32. Effect of proteasome inhibition on proteasome activity in vitro in RR cells ..**Error! Bookmark not defined.**

Figure 33 Effect of proteasome inhibition on cell viability of RR cells in vitro. .....**Error! Bookmark not defined.**

Figure 34 Western blot for protein expression of activated NfκB (phosphorylated p65) in the P (Parent) and RR (Radiation resistant) cells 81

Figure 35 Heat map representation of gene expression values of NFkB target genes.Figure 34 Western blot for protein expression of activated NfκB (phosphorylated p65) in the P (Parent) and RR (Radiation resistant) cells.....81

Figure 35 Heat map representation of gene expression values of NFkB target genes. 82

Figure 36 Luciferase based reporter assay for the transcriptional activity of NFkB 83

Figure 37 Tumorigenic potential of RR cells compared to P 84

Figure 38 Tumorigenic potential of BTZ pretreated P and RR cells.....85

Figure 39 Schematic representation for studying the effect of intraperitoneal injections of bortezomib along with radiation treatment of mice intracranially injected with parent GBM cells. 86

Figure 40 Effect of proteasome inhibition on the tumorigenic potential of the cells in vivo ..87

Figure 41 Proposed model for the study 90

Figure 42 Structure of 14-3-3 91

Figure 43 14-3-3 pathways to maintain normal cellular homeostasis. 92

Figure 44 Overexpression of 14-3-3 zeta in different cancers.....93

Figure 45 Expression of 14-3-3 ζ in TCGA patient samples dataset.....95

Figure 46 Expression of 14-3-3 zeta.....96

Figure 47 Identification of ζ interacting partners using GST pull down assay.....97

Figure 48 Mitochondrial function of RR compared to R.....100

Figure 49 Mitochondrial morphology of P and RR cells.....101

List of tables

Table 1 List of proteasome subunits differentially expressed in all biological replicates. 74

Table 2 Downregulated proteasome target proteins 78

Table 3 List of interacting proteins identified in RR cells. 97

Table 4 List of interacting proteins functionally classified 99

Synopsis

Homi Bhabha National Institute

SYNOPSIS OF Ph. D. THESIS

1. **Name of the Student: JACINTH RAJENDRA**

2. **Name of the Constituent Institution: TMC-ACTREC**

3. **Enrolment No. : LIFE09201204011**

4. **Title of the Thesis: Understanding therapy resistance in Glioblastoma using proteomics approach**

SYNOPSIS

Introduction

Glioblastoma are the most aggressive and malignant form of brain tumor associated with poor prognosis and refractory to the first line of treatment adopted: surgery and chemo-radiation. It accounts for about 3.5% of all the malignant tumors, 15 % of all malignant primary brain tumors and 50% of all gliomas. Despite undertaking the multimodal therapy the median survival for these patients is not more than 12 – 15 months and recurrence is inevitable.(2, 3) Recurrence in GBM is one of the major contributing factors of high morbidity and mortality of GBM. This is attributed to a subpopulation of cells that survive initial therapies and cause tumour re-growth (4, 5). However, targeting residual resistant cells of glioma is challenging since they are invisible in MRIs post initial treatment and they are inaccessible from the patient biopsies for biological studies (6, 7). Extensive research is being done to identify effective therapeutic targets for this lethal tumor but effective development of therapeutics that can interfere specifically with the function of these residual resistant cells largely remains unmet due to lack

of identification of differential molecular events that make this subpopulation of residual resistant cells different from the bulk tumor cells. (8-13)

We have previously reported development of a cellular model of radiation resistance using GBM cell lines and primary cultures from patient samples, which recapitulate the clinical scenario of resistance and enable us to capture residual radiation resistant (14) cells (15) and understand their molecular mechanism of survival.

Rationale

There are numerous studies in glioblastoma looking at the differential gene expression in therapy resistant glioma cells.(5, 16-18) But gene expression not always correlate with the protein expression and the identification of any therapeutically relevant pathway from these studies still remains as elusive as before. Proteomics directly addresses the functional effectors of cellular and disease processes.(19, 20) Till date majority of proteomics studies in glioblastoma have focused on identification of differential proteins amongst different on GBM cell lines, patient samples or within the same tumour to investigate the heterogeneity of glioblastoma, mechanism of chemoresistance and identification of diagnostic biomarkers. (21-32) Since proteins are the effector molecules for almost all the cellular pathways therefore here we want to analyze the proteome of the radio-resistant and relapse cells. Thus, this study is based on the hypothesis that the glioblastoma radio-resistant residual cells undergo a change in their protein repertoire which promotes their survival and leads to relapse. Identification of differential proteins in the radiation resistant residual cells and relapse cells will provide invaluable insights into the cellular pathways of resistant cells and will help in the identification of therapeutically relevant drug targets to eliminate resistant cells.

Basis of the project- This study will be done using an in vitro radiation resistant model that has previously been established in our lab (15) from Glioblastoma cell lines U87MG and SF268 and primary cultures from patient samples. The radiation resistant cells were obtained by subjecting the glioma grade IV cells (U87MG, SF268 and two primary patient samples) to lethal dose of radiation (at which ~10%

population survive) determined using clonogenic survival assay. It was observed that in all the cell cultures, a small population of cells (~10% or less) that we call "Radiation resistant" escape apoptosis and survive. These surviving cells exhibit a transient non-proliferative, multinucleated and giant cell phenotype for a period of 1 week or less and then resume their growth similar to their parent population to form "Relapse population".

Accordingly, by identifying the differential proteins in radiation resistant we should be able to understand the molecular mechanism used by these cells to overcome therapy induced stress and apoptosis. Hence in this study a quantitative proteomics approach has been adopted identify the functional role of differentially expressed proteins in influencing radiation surviving mechanism in Glioblastoma.

Aim of my thesis project is to understand the molecular pathways influencing therapy surviving glioblastoma cells using a proteomic approach.

The Specific Objectives are:

1. Characterization of the radiation resistant and the relapse population.
2. Identification of the differential proteome in radioresistant Glioblastoma cell line: SF268 using quantitative proteomic approaches and protein identification by Mass Spectrometry.
3. Pathway analysis and functional validation of differentially identified proteins

Objective 1 - Characterization of the radiation resistant and the relapse population.

Following aspects of the radiation resistant and relapse will be studied: -

1. Does the relapse population have more aggressive nature compared to the parent population?
2. Are radiation resistant with a multinucleated and giant phenotype radiation specific phenotype or they are formed in combination with chemotherapy?
3. Are multinucleated and giant cells formed in other cancers post radiation

Work Plan

1. To analyze whether this multinucleated and giant phenotype of the radiation resistant is radiation specific, U87MG cells will be monitored by cell counting and microscopic observation under 4 conditions: a) Daily dose of 2Gy radiation b) Daily dose of 2Gy + Temozolomide (TMZ) (25µM) c) Daily dose of 25µM TMZ d) Lethal dose of radiation – 8Gy. The fractionated dose of radiation and temozolomide will be administered until ≤ 10% cells are left behind post treatment.
2. Further, to assess the aggressive behavior of relapse cells, the parent and relapse cells of GBM cell lines and patient samples will be compared for their invasive and migrating phenotype using the matrigel based boyden chamber assay and wound healing assay.

Work Done

1.1 Multinucleated and Giant cells (MNGCs) are not radiation specific but are also formed upon Temozolomide treatment (alone and with radiation).

A fractionated dose of total 26Gy and 25µM was administered until less than 10% cells survived. It was observed that the cells that received only 26Gy radiation or daily dose of only 25µM remained in a non-proliferative phase for 31days and 41days, respectively. However, the cells that were given both IR and TMZ did not survive. The presence of Multinucleated and Giant cells (MNGCs) were quantified at regular intervals in all conditions. It was found that the percentage of MNGCs in the cells that were administered only 2Gy IR and 2Gy IR + TMZ were more compared to untreated and only TMZ treatment. This showed that MNGCs are indeed formed in response to radiation and chemotherapy treatment and are involved in Tumor relapse.

1.2 Multinucleated and Giant cells (MNGCs) are not GBM specific and formed in other cancers.

4 different cancerous cell lines were studied, one colorectal cell line HT29, one lung cancer cell line H1975, and two breast cancer cell line- MCF7 and T47D and their lethal dose were determined by Clonogenic survival assay. All 4 cell lines were subjected to a lethal dose of radiation and monitored

for the presence of non-proliferative multinucleated and giant cells. HT29 T47D and MCF7 remained in a non-proliferative phase and then followed by relapse. The lung cancer cell line H1975 did not form relapse cells. Instead, the cells after the radiation with lethal does completely attained senescence at 6th day and no further traces of proliferation was seen. The RR cells formed from each of the cell line displayed presence of multinucleated and giant cells along with increased expression of pro-survival genes and SASPs.

1.2 Relapse cells are more migrating and invasive than the parent cells

The matrigel based invasion assay and wound healing assay for migration was performed in Parent and Relapse population of SF268, U87MG and 3 Patient Samples. The Relapse population of the 2 GBM cell lines and one patient sample showed a significant increase in the invasion and migrating potential as compared to the Relapse population.

1.3 Relapse cells display similar response to radiation as the Parent

Relapse population of SF268 and U87MG was subjected to its respective lethal dose of radiation i.e. 6.5Gy and 8Gy, respectively and monitored the growth of the cells by trypan blue counting every alternate day. Cells remained in a non-proliferative phase for just 4 – 5 days as in the case when the untreated cells were subjected to the same dose of radiation. However, after a period of 4-5 days the cells resumed growth to form the second relapse population. This suggests that just as the parent exhibited the presence of a subpopulation of cells that had the ability to escape radiation, similarly, the relapse population also displayed the presence of radiation resistant cells. Additionally, a clonogenic survival assay revealed similar radiosensitivity of the two relapse populations as compared to the parent.

Objective 2 - Identification of the differential proteome in radioresistant Glioblastoma cell line: SF268 using quantitative proteomic approaches and protein identification by Mass Spectrometry.

We will use the three populations: Parent, Radiation resistant and Relapse Population from the two Glioblastoma cell line SF268. The differentially expressed proteins will be determined across the three populations using Isobaric tag for relative and absolute quantitation (iTRAQ) which is a MS-based approach for the relative quantification of proteins, relying on the derivatization of primary amino groups in intact proteins using isobaric tag for relative and absolute quantitation. Due to the isobaric mass design of the iTRAQ reagents, differentially labeled proteins do not differ in mass; accordingly, their corresponding proteolytic peptides appear as single peaks in MS scans. The isotope-encoded reporter ions that can only be observed in MS/MS spectra allow for calculating the relative abundance (ratio) of the peptide(s) identified by this spectrum. The candidate differentially expressed proteins will be further confirmed by western blot in another GBM cell line (U87MG) and other patient samples.

Work Done

Quantitative proteomic analysis of radio resistant (RR) and relapse (R) cells

Three populations: Parent(P), Radiation Resistant (RR) and Relapse(R) Population from the Glioblastoma cell line SF268 was used for performing differential proteomic analysis using Isobaric tag for relative and absolute quantitation (iTRAQ).

824 proteins were found to be differentially expressed in radiation escapers as compared to parent cells out of which 431 proteins were downregulated (Fold change <0.7) and 393 proteins were up-regulated (Fold Change >1.5). 874 proteins were differentially expressed in relapse population as compared to parent cells of SF268 out of which 523 proteins were downregulated (<0.7) and 351 proteins were up-regulated (>1.5). (Fig 2.A).1392 proteins were differentially regulated in Relapse vs Radiation Resistant out of which 747 proteins were upregulated (>1.5) and 645 were downregulated (<0.7).

The iTRAQ data was validated by western blot of few candidate proteins such as EGFR, HRAS, and YBX3. The expression of these proteins was correlated with the expression pattern in the iTRAQ data set.

Similarly, the iTRAQ analysis of the three SF268 populations: Parent, Radiation Resistant and Relapse population was performed in five biological independent experiments.

Objective 3 - Pathway analysis of differentially expressed proteins and functional validation of the identified proteins in the primary patient samples.

Work Plan

The list of differentially expressed proteins identified will be analyzed for their collaborative role in any cellular signaling pathway by performing pathway analysis using KEGG database and Molecular Signature Database. The expression of proteins found in the relevant pathways will be validated using western blot in the three populations of cell lines: U87, SF268 and Patient Samples. Proteins from the statistically significant pathway will be studied for its functional role in the formation of radiation resistant cells and relapse. To understand the functional role of a pathway, the protein expression will be inhibited either by shRNA /siRNA mediated knockdown or a pharmacological inhibitor. Following the inhibition of the proteins we will check the involvement of candidate proteins in therapy resistance by subjecting the cells to different doses of radiation and analyzing the clonogenic potential of these cells compared to sensitive and untreated resistant cells to check the reversal of resistant phenotype of these cells.

Work Done

3.1 Unsupervised clustering of proteomics data identifies protein clusters uniquely differential in each population

In order to determine the pattern of expression of proteins and the commonality in the function of proteins as the cell progresses from Parent, Radiation Resistant to Relapse phase Unsupervised hierarchal clustering was performed using gene expression data sets from the three comparisons (R vs

RR , R vs P and RR vs P). This segregated the data set into five clusters depending on the pattern of differential expression across the three populations. 134 proteins were found to be dowregulated in the radiation escapers and relapse as compared to the parent cells (C1). 783 proteins were majorly upregulated in Relapse population but were showed downregulation / similar expression in radiation escapers as compared to the parent (C2). 641 proteins were upregulated in the RE population as compared to the other two population (C3). The expression of 165 proteins remains at a basal level in the P and RR population however their expression goes down in the relapse cells (C4) and 70 proteins show an increase in expression in the Radiation Escapers and Relapse population as compared to the P cells (C5). The major two clusters that were further analysed were cluster 2 and 3 which comprised of maximum genes.

3.2 Pathway analysis reveals deregulation of proteasome and protein turnover machinery proteins in RR population and deregulation of focal adhesion pathway in relapse cells

Gene ontology and enrichment analysis of the entire differential proteins found in the RR compared to the parent cells, revealed 24 pathways enriched with upregulated and downregulated proteins. Of these, 8 pathways were enriched with upregulated proteins and 16 pathways were enriched with downregulated proteins. However, proteasome pathway was the most deregulated pathway based on the associated genes filter (k/K ratio). Proteomic analysis from three biological replicates also revealed significant deregulation of proteasome pathway in the RR population.

Correlating the phenotype of increased migration and invasive capacity of Relapse cells, the proteomic analysis revealed upregulation of genes involved in focal adhesion – ITGB5, ICAM1, VASP, FN1, PPR12A, and FLNB. These genes were screened in the relapse cells of U87MG and three patient samples at mRNA level by real time PCR. ITGB5 was the only gene found to be upregulated at the transcript and protein level in the relapse cells of cell lines and patient samples.

FUNCTION VALIDATION

Functional validation of proteasome pathway was further carried out to understand the survival mechanism of RR cells.

3.3 RR cells display enhanced proteasome activity and survival dependency on proteasome activity *in vitro* and *in vivo*

In order to confirm the increase in proteasome pathway in the RR population, Proteasome activity assay was performed in the RR population of SF268, U87 and 2 Patient Samples. The RR population of both the cell lines and Patient samples showed increased proteasome activity. To study the effect of proteasome inhibition on radioresistance in vitro the Parent and RR population were treated with different doses of Bortezomib – 0.1nM, 1nM and 10nM and checked for proteasome activity inhibition and cell viability. It was found that RR population was more sensitive to proteasome inhibition at 10nM conc. The RR population also exhibited increased radiosensitivity in the presence of the proteasome inhibitor when subjected to different doses of radiation.

The subtle effect of bortezomib seen *in vitro* after 72 hrs. post treatment is significantly enhanced in reducing tumorigenicity of the treated cells *in vivo*, suggesting a slow and prolonged effect of proteasome inhibition on the survival of the cells. A significant effect of proteasome inhibition was observed on the overall survival of mice which were injected with pre-treated RR-BTZ cells along with an increased % of tumour free mice when BTZ was administered intraperitoneally along with radiation.

3.4 Proteasomes indirectly regulate RR cell survival via the NFkB activation

Furthermore, the levels of activated NFkB was checked by western blot in the P and RR cells of cell lines and patient samples. The RR cells displayed increased levels of activated NFkB in both the cell lines and PS1. Furthermore, the transcript levels of 9 NFkB target genes (TNF-α, IL6, IkB-a, IFN-γ, ICAM1, COX2, NOD4, p16, SOD2) were screened in RR cells of the cell lines and patient sample by real-time PCR. At least 6 genes out of the 9 in SF268, U87 and PS1 harbour increased expression of phospho-NFkB suggesting the presence of a transcriptionally active NFkB in RR cells. To directly assess the NFkB transcriptional activity in the RR cells of U87, we monitored the relative promoter activity of the luciferase based NFkB reporter constructs in the P and RR cells. The RR cells showed a significant increase (20 fold) in NFkB transcriptional activity as compared to the parent population (P). Importantly, administration of the proteasome inhibitor (Bortezomib) in the P and RR cells

diminished this activity by 1.5 and 3.0-fold demonstrating the dependency of NFkB activity on the proteasome activity. A synergistic inhibitory effect was observed in the presence of IkB-alpha construct and bortezomib in the P and RR cells. However, the RR cells displayed a much higher reduction as compared to the P cells

CONCLUSION AND DISCUSSION

The aim of this study was to identify the processes deregulated in the innately radiation resistant residual (RR) population as we have previously shown that these are the cells responsible for relapse in glioblastoma. iTRAQ based quantitative proteomic analysis on the parent (P), innately radiation resistant residual (RR) and relapse (R) population revealed significantly deregulation of the proteasome pathway in the RR cells. Contrary to other reports, the RR cells displayed enhanced expression and activity of proteasome subunits, which triggered NFkB signalling. Pharmacological inhibition of proteasome activity led to impeded NFkB transcriptional activity, radio-sensitization of RR cells *in vitro*, and significantly reduced capacity of RR cells to form orthotopic tumours *in vivo*. We demonstrate that combination of proteasome inhibitor with radio-therapy abolish the inaccessible residual resistant cells thereby preventing GBM recurrence. However, the exact mechanism downstream to higher proteasome expression and NFkB activity in the RR cells needs to be further explored. Nonetheless, this study establishes that proteasomes aid the survival of the innate radiation resistant population via NFkB pathway and hence can be valuable targets for precluding relapse in glioblastoma. Apart from the identification of biological processes governing the survival of RR cells, proteomic revealed deregulation of focal adhesion proteins in the Relapse cells as a candidate gene that can be explored further. This correlated with the enhanced invasion and migrating properties demonstrated by the relapse cells inspite of having a similar response to the lethal dose of radiation as compared to the parent cells. Further, the multinucleated and giant cells (MNGCs) formed in RR cells are not specific to radiation in Glioblastoma but are formed in response to chemotherapy and in other cancers too. To summarize, this study has revealed new insights on the radiation resistant residual cells and relapse cells that can be further explored for a deeper knowledge of radioresistance and recurrence in glioblastoma.

References

1. Stupp R1 MW, van den Bent MJ, Weller M, Fisher B, Taphoorn MJ, Belanger K, Brandes AA, Marosi C, Bogdahn U, Curschmann J, Janzer RC, Ludwin SK, Gorlia T, Allgeier A, Lacombe D, Cairncross JG, Eisenhauer E, Mirimanoff RO. Radiotherapy plus concomitant and adjuvant temozolomide for glioblastoma. N Engl J Med. 2005 March 10;352:9.
2. Stupp R1 HM, Mason WP, van den Bent MJ, Taphoorn MJ, Janzer RC, Ludwin SK, Allgeier A, Fisher B, Belanger K, Hau P, Brandes AA, Gijtenbeek J, Marosi C, Vecht CJ, Mokhtari K, Wesseling P, Villa S, Eisenhauer E, Gorlia T, Weller M, Lacombe D, Cairncross JG, Mirimanoff RO. Effects of radiotherapy with concomitant and adjuvant temozolomide versus radiotherapy alone on survival in glioblastoma in a randomised phase III study: 5-year analysis of the EORTC-NCIC trial. 2009;10.
3. Glas M, Rath BH, Simon M, Reinartz R, Schramme A, Trageser D, et al. Residual tumor cells are unique cellular targets in glioblastoma. Annals of neurology. 2010 Aug;68(2):264-9. PubMed PMID: 20695020. Pubmed Central PMCID: 4445859.
4. Kelley K, Knisely J, Symons M, Ruggieri R. Radioresistance of Brain Tumors. Cancers. 2016 Mar 30;8(4). PubMed PMID: 27043632. Pubmed Central PMCID: 4846851.
5. Weller M, Cloughesy T, Perry JR, Wick W. Standards of care for treatment of recurrent glioblastoma--are we there yet? Neuro-oncology. 2013 Jan;15(1):4-27. PubMed PMID: 23136223. Pubmed Central PMCID: 3534423.
6. Roy S, Lahiri D, Maji T, Biswas J. Recurrent Glioblastoma: Where we stand. South Asian journal of cancer. 2015 Oct-Dec;4(4):163-73. PubMed PMID: 26981507. Pubmed Central PMCID: 4772393.
7. Reardon DA. Therapeutic Advances in the Treatment of Glioblastoma: Rationale and Potential Role of Targeted Agents. The Oncologist. 2006;11(2):152-64.
8. Zhang X. Glioblastoma multiforme: Molecular characterization and current treatment strategy (Review). Experimental and Therapeutic Medicine. 2011.
9. Weller M, Cloughesy T, Perry JR, Wick W. Standards of care for treatment of recurrent glioblastoma--are we there yet? Neuro-Oncology. 2012;15(1):4-27.
10. Mangum R. Glioma Stem Cells and their Therapy Resistance. Journal of Carcinogenesis & Mutagenesis. 2012;01(S1).
11. Kanu OO, Mehta A, Di C, Lin N, Bortoff K, Bigner DD, et al. Glioblastoma multiforme: a review of therapeutic targets. Expert Opin Ther Targets. 2009 Jun;13(6):701-18. PubMed PMID: 19409033. Epub 2009/05/05. eng.
12. Wurth R, Barbieri F, Florio T. New Molecules and Old Drugs as Emerging Approaches to Selectively Target Human Glioblastoma Cancer Stem Cells. Biomed Res Int. 2014;2014:126586. PubMed PMID: 24527434. Pubmed Central PMCID: 3909978.
13. Roger Stupp MD, Warren P. Mason, M.D., Martin J. van den Bent, M.D.,, Michael Weller MD, Barbara Fisher, M.D., Martin J.B. Taphoorn, M.D.,, Karl Belanger MD, Alba A. Brandes, M.D., Christine Marosi, M.D.,, Ulrich Bogdahn MD, Jürgen Curschmann, M.D., Robert C. Janzer, M.D.,, Samuel K. Ludwin MD, Thierry Gorlia, M.Sc., Anouk Allgeier, Ph.D.,, Denis Lacombe MD, J. Gregory Cairncross, M.D., Elizabeth Eisenhauer, M.D.,, et al. Radiotherapy plus Concomitant and Adjuvant Temozolomide for Glioblastoma. The new england journal of medicine. 2005.
14. Kaur E, Rajendra J, Jadhav S, Shridhar E, Goda JS, Moiyadi A, et al. Radiation-induced homotypic cell fusions of innately resistant glioblastoma cells mediate their sustained survival and recurrence. Carcinogenesis. 2015 Jun;36(6):685-95. PubMed PMID: 25863126.
15. Zhang X, Zhang W, Cao WD, Cheng G, Zhang YQ. Glioblastoma multiforme: Molecular characterization and current treatment strategy (Review). Exp Ther Med. 2012

Jan;3(1):9-14. PubMed PMID: 22969836. Pubmed Central PMCID: 3438851. Epub 2012/09/13. Eng.
16. Kumar DM, Patil V, Ramachandran B, Nila MV, Dharmalingam K, Somasundaram K. Temozolomide-modulated glioma proteome: role of interleukin-1 receptor-associated kinase-4 (IRAK4) in chemosensitivity. Proteomics. 2013 Jul;13(14):2113-24. PubMed PMID: 23595970.
17. ZHANG AWaG. Differential gene expression analysis in glioblastoma cells and normal human brain cells based on GEO database. ONCOLOGY LETTERS. 2017 07 September;14.
18. Mann APM. Proteomics to study genes and genomes. NATURE. 2000;405 |.
19. Picotti P, Bodenmiller B, Aebersold R. Proteomics meets the scientific method. Nature methods. 2013 Jan;10(1):24-7. PubMed PMID: 23269373.
20. . !!! INVALID CITATION !!!
21. Khwaja FW, Reed MS, Olson JJ, Schmotzer BJ, Gillespie GY, Guha A, et al. Proteomic identification of biomarkers in the cerebrospinal fluid (CSF) of astrocytoma patients. Journal of proteome research. 2007 Feb;6(2):559-70. PubMed PMID: 17269713. Pubmed Central PMCID: 2566942.
22. Vogel TW, Zhuang Z, Li J, Okamoto H, Furuta M, Lee YS, et al. Proteins and protein pattern differences between glioma cell lines and glioblastoma multiforme. Clinical cancer research : an official journal of the American Association for Cancer Research. 2005 May 15;11(10):3624-32. PubMed PMID: 15897557.
23. de Aquino PF, Carvalho PC, Nogueira FC, da Fonseca CO, de Souza Silva JC, Carvalho Mda G, et al. A Time-Based and Intratumoral Proteomic Assessment of a Recurrent Glioblastoma Multiforme. Frontiers in oncology. 2016;6:183. PubMed PMID: 27597932. Pubmed Central PMCID: 4992702.
24. Zhang P, Guo Z, Zhang Y, Gao Z, Ji N, Wang D, et al. A preliminary quantitative proteomic analysis of glioblastoma pseudoprogression. Proteome science. 2015;13:12. PubMed PMID: 25866482. Pubmed Central PMCID: 4393599.
25. Hudler P, Kocevar N, Komel R. Proteomic approaches in biomarker discovery: new perspectives in cancer diagnostics. TheScientificWorldJournal. 2014;2014:260348. PubMed PMID: 24550697. Pubmed Central PMCID: 3914447.
26. Kalinina J, Peng J, Ritchie JC, Van Meir EG. Proteomics of gliomas: initial biomarker discovery and evolution of technology. Neuro-oncology. 2011 Sep;13(9):926-42. PubMed PMID: 21852429. Pubmed Central PMCID: 3158015.
27. Collet B, Guitton N, Saikali S, Avril T, Pineau C, Hamlat A, et al. Differential analysis of glioblastoma multiforme proteome by a 2D-DIGE approach. Proteome science. 2011;9(1):16. PubMed PMID: 21470419. Pubmed Central PMCID: 3083325.
28. Niclou SP, Fack F, Rajcevic U. Glioma proteomics: status and perspectives. Journal of proteomics. 2010 Sep 10;73(10):1823-38. PubMed PMID: 20332038.
29. Thaker NG, Zhang F, McDonald PR, Shun TY, Lewen MD, Pollack IF, et al. Identification of survival genes in human glioblastoma cells by small interfering RNA screening. Molecular pharmacology. 2009 Dec;76(6):1246-55. PubMed PMID: 19783622. Pubmed Central PMCID: 2784725.
30. Hill JJ, Moreno MJ, Lam JC, Haqqani AS, Kelly JF. Identification of secreted proteins regulated by cAMP in glioblastoma cells using glycopeptide capture and label-free quantification. Proteomics. 2009 Feb;9(3):535-49. PubMed PMID: 19137551.
31. Furuta M, Weil RJ, Vortmeyer AO, Huang S, Lei J, Huang TN, et al. Protein patterns and proteins that identify subtypes of glioblastoma multiforme. Oncogene. 2004 Sep 2;23(40):6806-14. PubMed PMID: 15286718.

Publications in Refereed Journal:

a. Published: **Jacinth Rajendra**, Keshava K. Datta, Sheikh Burhan Ud Din Farooqee, Rahul Thorat, Kiran Kumar, Nilesh Gardi, Ekjot Kaur, Jyothi Nair, Sameer Salunkhe, Ketaki Patkar, Sanket Desai, Jayant Sastri Goda, Aliasgar Moiyadi, Amit Dutt, Prasanna Venkataraman, Harsha Gowda, Shilpee Dutt. **Enhanced proteasomal activity is essential for long term survival and recurrence of innately radiation resistant residual glioblastoma cells. Oncotarget Accepted : 26 April 2018**

b. Accepted: N/A

c. Communicated: N/A

Other Publications:

- Kaur E[1], **Rajendra J[1]**, Jadhav S[1], Shridhar E[1], Goda JS[1], Moiyadi A[1], Dutt S[2].**Radiation-induced homotypic cell fusions of innately resistant glioblastoma cells mediate their sustained survival and recurrence.** *Carcinogenesis. 2015 Jun;36(6):685-95*
- Ekjot Kaur[1], Aditi Sahu[2], Arti R. Hole[2], **Jacinth Rajendra[1]**, Rohan Chaubal[3], Nilesh Gardi[3],Amit Dutt[3], Aliasgar Moiyadi[4], C. Murali Krishna[2] & Shilpee Dutt[1] **Unique spectral markers discern recurrent Glioblastoma cells from heterogeneous parent population** ***Scientific Reports | 6:26538 | DOI: 10.1038/srep26538***

a. Book/Book Chapter : N/A

b. Conference/Symposium

- **Oral Presentation** at **Indian Association Of Cancer Research (IACR) – April 2016 held in New Delhi , India on April 2016** for the abstract entitled: Differential proteomic analysis reveals role of a novel serine threonine kinase DCLK3 and 14-3-3 zeta in innately radiation resistant and relapse cells of Glioblastoma.
- **Oral Presentation at ISNOCON 2018 held at AIIMS, New Delhi from 5th April to 8th April 2018** for the abstract entitled **:** Enhanced proteasomal activity is essential for long term survival and recurrence of innately radiation resistant residual glioblastoma cells
- **Poster Presentation** at **International Proteomics Symposium Conference held at IIT Bombay on December 2015** for the abstract entitled : Differential Proteome reveals major role of metabolic pathways in conferring radioresistance to recurrent Glioblastoma.
- **Poster Presentation** at **Tata Memorial Centre 75th Platinum Jubilee Celebrations held in Mumbai on February 2016** for the abstract entitled as : Differential proteomic analysis reveals role of a novel serine threonine kinase DCLK3 and 14-3-3 zeta in innately radiation resistant and relapse cells of Glioblastoma.
- **Poster Presentation** at **International Conference on Enzymology held at ACTREC, TMC , Mumbai on January 2017** for the abstract entitled : Identification of a novel serine threonine kinase DCLK3 and immunoproteasome subunit PA28α: Potential therapeutic targets for innately radiation resistant glioblastoma cells

Identification of a novel serine threonine kinase DCLK3 and immunoproteasome subunit PA28α: Potential therapeutic targets for innately radiation resistant glioblastoma cells. **Jacinth Rajendra**, Keshava Datta, Sheikh Burhan Ud Din Farooqee, Raja Reddy, Nilesh Gardi, Ekjot Kaur, Ketaki Patkar, Aliasgar Moiyadi, Prasanna Venkataraman, Kakoli Bose, Amit Dutt, Harsha Gowda, Shilpee Dutt.

- **Poster Presentation at Annual Meeting of American Association For Cancer Research" held at Washington, DC from April 1st – April 5th 2017** for the abstract entitled : Identification of proteosome pathway and a novel serine threonine kinase DCLK3: Potential therapeutic targets for innately radiation resistant glioblastoma cells. **Jacinth Rajendra**, Keshava Datta, Sheikh Burhan Ud Din Farooqee, Raja Reddy, Nilesh Gardi, Ekjot Kaur, Ketaki Patkar, Aliasgar Moiyadi, Prasanna Venkataraman, Kakoli Bose, Amit Dutt, Harsha Gowda, Shilpee Dutt.*

Signature of Student: Jacinth

Date: 30·5·18

Doctoral Committee:

S. No.	Name	Designation	Signature	Date
1.	Dr. Sorab Dalal	Chairman	S. N. Dalal	30·5·18
2.	Dr. Shilpee Dutt	Guide/ Convener	Shilpee Dutt	30·5·18
3.	Dr. Dibyendu Bhattacharya	Member	[illegible]	30·5·18
4.	Dr. V. Prasanna	Member	V. Prasanna	30·5·18
5.	Dr. Harsha Gowda	Technical Advisor	[illegible]	30·5·18

Forwarded Through:

S.V. Chiplunkar 12/6/18

Dr. S.V. Chiplunkar
Director, ACTREC &
Chairperson, Academic &
Training Program, ACTREC

Prof. K. Sharma
Director, Academics
T.M.C.

Prof. K. S. Sharma
DIRECTOR - ACADEMICS, TMC
Mumbai - 400 012.

Version approved during the meeting of Standing Committee of Deans held during 29-30 Nov 2013

1 Introduction and Review of literature

This chapter introduces the clinical aspects of the most lethal form of brain tumor – Glioblastoma along with the challenges involved in treating this disease. This chapter also discusses the molecular characteristics of glioblastoma reported till date to understand therapy resistance of this tumor.

1.1 Glioblastoma

Glioblastoma is a highly aggressive diffuse glioma of astrocytic lineage. It is termed as Grade IV Glioma according to WHO classification. It accounts for about 3.5% of all the malignant tumors, 16 % of all malignant primary brain tumors and 50-60% of all gliomas (33-36). The average age-adjusted incidence rate of this tumor is 3.2 per 100,000 population (37, 38).

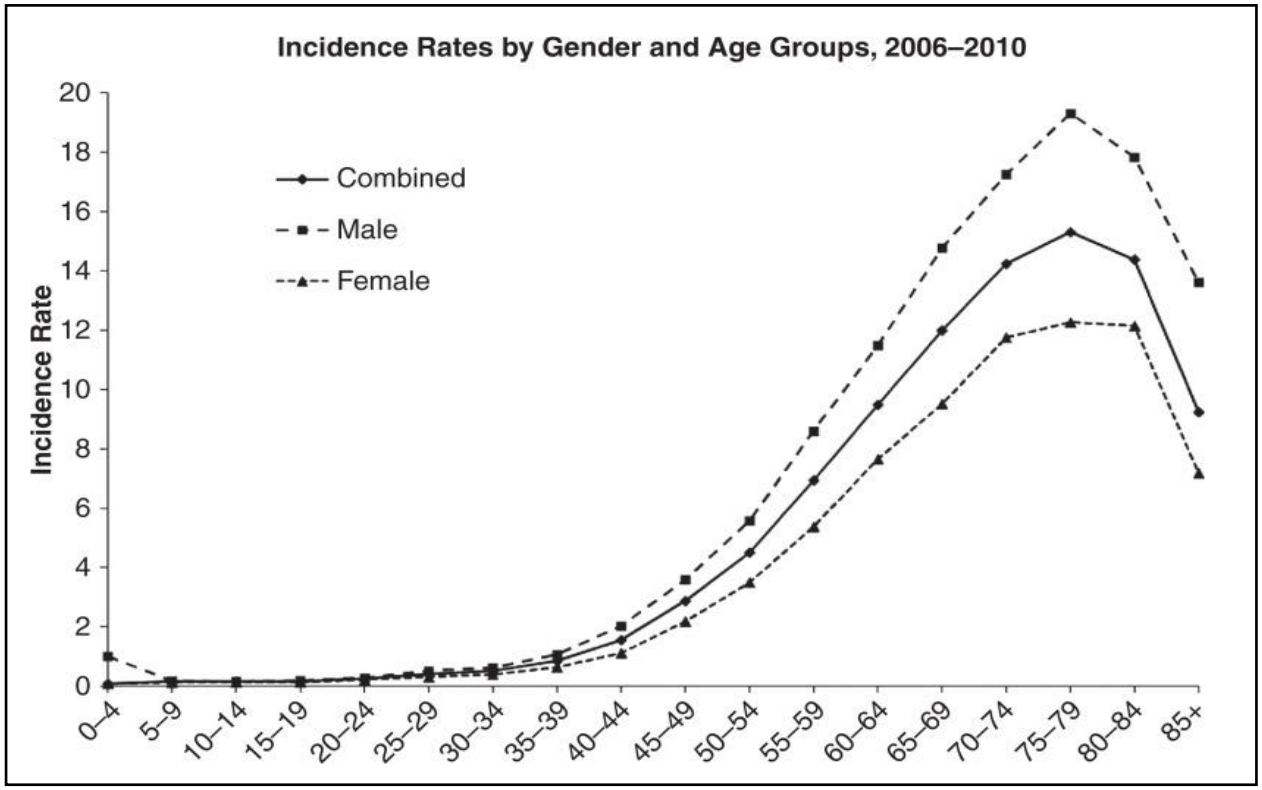

Figure 1 Age-adjusted and age-specific incidence rates for glioblastoma at diagnosis and gender, CBTRUS statistical report: NPCR and SEER, 2006–2010.

X-axis, age groups; Y-axis, incidence rates. Rates are per 100,000 and age-adjusted to the 2000 US standard population. NPCR, CDC's National Program of Cancer Registries; SEER, NCI's Surveillance, Epidemiology, and End Results program. (36)

Figure 1 illustrates the incidence rates for glioblastoma as per age and gender. Primary glioblastoma is most prevalent in older patients with a median age of 64 at diagnosis and its incidence increases in patients of age group 75 – 84 years. The incidence is 1.6 times higher in

males compared to females and 2.0 times higher in Caucasians compared to Africans and Afro-Americans, with lower incidence in Asians and American Indians (39). In India, the incidence rates of glioma varies from 5.8% in Mumbai, 6.7% in Bangalore, 3.5% in Chennai, 5.6% in Dibrugarh, and 28.2% in Trivandrum among males and 6.3% in Mumbai, 5.6% in Bangalore, 7.5% in Chennai, 0% in Dibrugarh, and 21.8% in Trivandrum among females as per the by Indian Council for Medical Research 2009 report. The demographic data from Tata Memorial Hospital based on 1-year prospective study conducted on 656 patients also revealed increased proportion of high-grade gliomas 151 cases (59.5%) amongst the total CNS tumors registered (39, 40).

It is a case of high-grade astrocytic neoplasm characterized by the presence of either microvascular proliferation and/or tumor necrosis. A highly invasive tumor which infiltrates to the normal surrounding brain parenchyma but remains confined to the central nervous system (41). It can arise in any lobe of the brain and even the brain stem and cerebellum, but more commonly occur in the frontal and temporal lobes (42). A recent study by Tyler et al, demonstrated that the localization of glioblastoma in the brain varies according to the molecular subtype of glioblastoma. The neural and mesenchymal glioblastoma formed tumors farthest in the cerebrum whereas the classical and proneural type localized in the temporal and frontal lobe as represented in figure 2 (43).

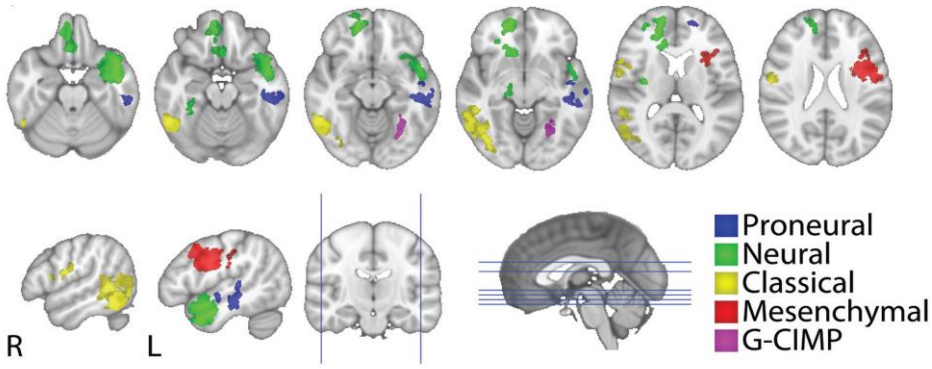

Figure 2 Distribution of glioblastoma in different regions of the brain.

Axial (row) and sagittal (second row) of statistically significant clusters ($p < 0.05$) by subtype.

However, the etiology of this tumor remains elusive. Radiation exposure is the few known risk factors associated with glioblastoma (39). Gliomas also develop in patients who have undergone radiation therapy for any other cancer type (44). Electromagnetic fields, formaldehyde, and nonionizing radiation from cell phones are still speculated causes of glioblastoma (45). Patients with hereditary syndromes such as Cowden, Turcot, Li-Fraumeni, Neurofibromatosis type 1 and type 2, Tuberous Sclerosis, and familial Schwannomatosis have also been associated with increased risk of glioma. The clinical presentation of patients with newly diagnosed glioblastoma varies greatly with the tumor size, localization and the anatomical features of the brain (46, 47). These patients display symptoms of increased intracranial pressure, including a headache and focal or progressive neurologic deficits, vomiting, nausea, and seizures.

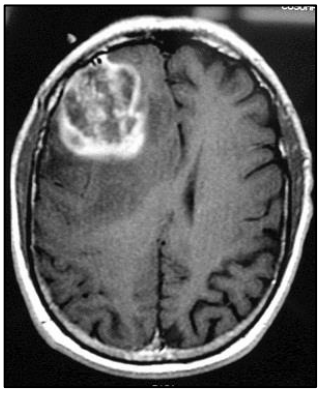

Figure 3 MRI of the brain Image courtesy of George Jallo, MD

The regular diagnostic techniques include computed tomography (CT) or magnetic resonance imaging (MRI) scan. On MRI, the tumor appears as an irregularly shaped mass with a dense ring of enhancement and hypointense center of necrosis due to the enhancement with gadolinium contrast (42). Figure 3 is a T1-weighted axial gadolinium-enhanced magnetic resonance image demonstrates an enhancing tumor of the right frontal lobe.

Advanced techniques like diffusion-weighted imaging (DWI), perfusion-weighted imaging (perfusion MR) and MR spectroscopy have enabled a better understanding of the pathophysiology of GB tumors and its differentiation from other brain tumor-mimics like infarction (39).

1.2 Standard of care

The standard mode of therapy includes maximal safe surgical resection, followed by concurrent radiation therapy along with an oral DNA alkylating chemotherapy agent, temozolomide (TMZ) (Temodar®), and then adjuvant chemotherapy with TMZ (48). Following surgery, radiation therapy using three-dimensional conformal beam or intensity-modulated RT is now the standard of care. A total dose of 60Gy is administered as 1.8-2 Gy fractions five days per week for six weeks. Simultaneously, TMZ is given at a dose of 75 mg/m2 daily for six weeks until radiation therapy is completed. This is based on the randomized phase 3 study conducted by Stupp et al that reported the increase in median survival to 15 months vs 12 months with radiotherapy and temozolomide vs radiotherapy alone, respectively (hazard ratio, 0.63; $P < .001$) (2, 3). Post one-month TMZ is restarted at 150 mg/m2 daily for five days for a month and then the dose is escalated to 200 mg/m2 for five consecutive days per month for the remainder of therapy. This TMZ cycle is continued till 6-18 months (44, 49). In spite of undergoing the standard mode of treatment, the tumor recurs in 90% of cases within 6 – 12 months. Apart from conventional therapies, various modifications have been done in the area of surgical resection and chemotherapy. Complete surgical resection of these tumors is a challenge due to its infiltration to eloquent areas of the brain such as speech, motor function, and the senses. To improve the extent of surgical resection, technologies such as image-guided surgery using 5-ALA, intra-operative MRI, or (diffusion tensor imaging) DTI neuronavigation are being adopted (50, 51). However, the cost and the need for specialized equipment, operators, and surgery suites limit the usage of such novel technologies. Bevacizumab or Avastin, a humanized vascular endothelial growth factor (*VEGF*) monoclonal antibody targeting blood vessel formation (VEGF-A target) was a new drug approved in 2009 for recurrent GBM (52). Although, preliminary results of large randomized trials have demonstrated improvement in the progression-free survival (PFS) it did not result in increased

overall survival (OS) (53). In October 2015 FDA approved the administration of Optune®, the device delivering tumor-treating fields (TTFields), along with TMZ for adults with newly diagnosed supratentorial GBM, following surgery and standard-of-care treatment. Optune plus TMZ demonstrated superior PFS of 7.1 months versus 4 months with TMZ alone, as well as superior OS of 20.5 months versus 15.6 months with TMZ alone (54). Interstitial brachytherapy using iodine-125 (I-125) has been employed as an adjuvant treatment for smaller brain tumors and has indicated an improvement in median survival for few highly selected patients (49).

Despite undergoing multimodal therapy, the median survival of the GB patients is not more than 12 – 15 months and recurrence is inevitable in >90% cases. Only about 10% of the patients survive till 5 years post therapy contributed by the high resistant nature of these tumor cells (7).

1.3 Prognosis

The clinical outcome of GB patients is mostly associated with poor prognosis. Long-term survivors of glioblastoma with a survival of > 2 yrs. are very rare since medium survival is not more than 12 – 15 months. The five-year survival rate is not more than 10% for such patients. Clinical predictors for survival in GB are tumor size, its anatomical location, Karnofsky Performance Score (KPS), recursive partition analysis (RPA), histopathological and radiological features namely MIB-1 labeling index, contrast enhancing tumors, amount of tumor necrosis on preoperative MRI, peritumoral edema and perfusion parameters (55). Current molecular prognosis markers include *IDH1/2* (isocitrate dehydrogenase 1/2) mutations and *MGMT* (O6-methylguanine-DNA methyltransferase) promoter methylation which are associated with good prognosis and better response to temozolomide in GB patients (47).

The molecular classification of GBM into four subgroups: classical, mesenchymal, proneural and neural by Verhaak et al based on 840 gene signatures have provided deeper insights into

the pathogenesis of this tumor (56). These classes differ in their genomic and transcript alterations along with the clinical outcomes. While the classical subgroup shows amplification of mutant *EGFR* variant III and loss of *PTEN*; the mesenchymal subtype exhibits *NF1* mutations, loss of *TP53* and *CDKN2A* and is associated with poor prognosis. Constituting of a younger group of patients, the proneural subgroup distinctly shows enrichment of *IDH1/2*, *TP53* mutations in along with amplification of *PDGFRA*, *CDK6*, *CDK4*, and *MET* and show a higher survival rate. Lastly, the neural subtype displays molecular signatures similar to that of neurons but does not show unique distinguishing alterations compared to other subtypes. Furthermore, Noushmehr et al using 'The Cancer Genome Atlas' (TCGA) dataset identified a distinct subtype of GBM tumors referred to as a glioma CpG island methylator phenotype (*G-CIMP*), displaying hyper-methylation at multiple loci (57). These *G-CIMP* samples had distinct molecular and clinical features, harboring IDH1 mutation at high frequency. The molecular profiling of GBM tumors has thus, further strengthened the understanding of its underlying biology. However, the existing knowledge of the tumour has not successfully been able to improve the clinical outcome of the patients.

1.4 Recurrence and therapy resistance

Recurrence is one of the key factors for poor prognosis in glioblastoma patients and remains a challenge in clinics. The relapsed tumors formed are confined to the margins of the primary site of the tumor in most cases with no invasion to other parts other than the brain (7). This pattern of recurrence has been attributed to the presence of highly infiltrative neoplastic cells in the inaccessible regions of the brain and an aberrant vasculature comprised hyperproliferative, leaky and unorganized blood vessels. Leading to an incomplete surgical resection of the primary tumor followed by radiation therapy along with chemotherapy, thus this multimodal therapy has proved to be the only palliative and not curative with recurrence being unavoidable. The other major reason for recurrence has been accredited to the presence

of both intrinsic and acquired resistant tumor cells which give rise to more aggressive recurrent tumors. Various studies have been carried out and are still being done to unravel the mechanisms of radio and chemoresistance. Chemo-resistance to the oral alkylating drug, temozolomide has been associated with the epigenetic silencing of the *MGMT* gene (O-6-methylguanine-DNA methyltransferase). It is a DNA repair enzyme that removes alkyl groups from the O-6 position of guanine. Its inactivation (due to promoter methylation) renders glioma cells more sensitive to chemotherapy but the tumors possessing unmethylated *MGMT* gene are more resistant to chemotherapy. Interestingly, patients harboring unmethylated *MGMT* demonstrate long-term survival, thus suggesting the involvement of other contributing factors in the therapy response. Several other factors are reported to contribute to therapy resistance such as genetic alterations, signaling pathways, microRNAs, hypoxia, the brain microenvironment, and glioma stem cells (GSCs). Over-expression of proteins like Epidermal growth factor receptor/variant VIII (EGFR/EGFRVIII), Platelet Derived Growth Factor Receptor (PDGFR), Phosphatidylinositide 3-kinase (PI3K), and Signal Transducer and Activator of Transcription (STAT3), Survivin, BIRC3 and altered metabolic proteins have also been reported in these resistant GBM cells (58, 59) .

Moreover, tumor suppressor genes such as p53, p21, p16, and *PTEN* are commonly mutated in GBMs while cell cycle regulators *CDK4* and MDM2 are amplified in approximately 13% of the tumors, pointing towards an important role these proteins might play in inducing genetic instability in these cells (60, 61). These genetic alterations are majorly responsible for the deregulation of signalling pathways involved in GBM like, growth factor tyrosine kinase receptor (TKR) triggered pathways, the Ras sarcoma (Ras) pathway, phosphatidylinositol 3-kinase (PI3K)/phosphatase and tensin homolog (PTEN)/AKT, retinoblastoma (RB)/cyclin-dependent kinase (CDK) N2A-p16INK4a, and the TP53/mouse double minute 2 (MDM2)/MDM 4/CDKN2A-p14ARF pathways as represented in figure 4 (62). Furthermore,

there are various signaling pathways such as the Notch, Wnt/β catenin and Hedgehog pathway that are known to promote resistance by aiding the highly tumorigenic cancer-initiating or glioma stem cells (GSC) to survive and repopulate the entire tumor post-therapy (63-66). Additionally, the ATM/Chk2/p53 pathway endorses glioma radioresistance by activating the DNA damage repair pathway and inducing cell cycle arrest (67, 68).

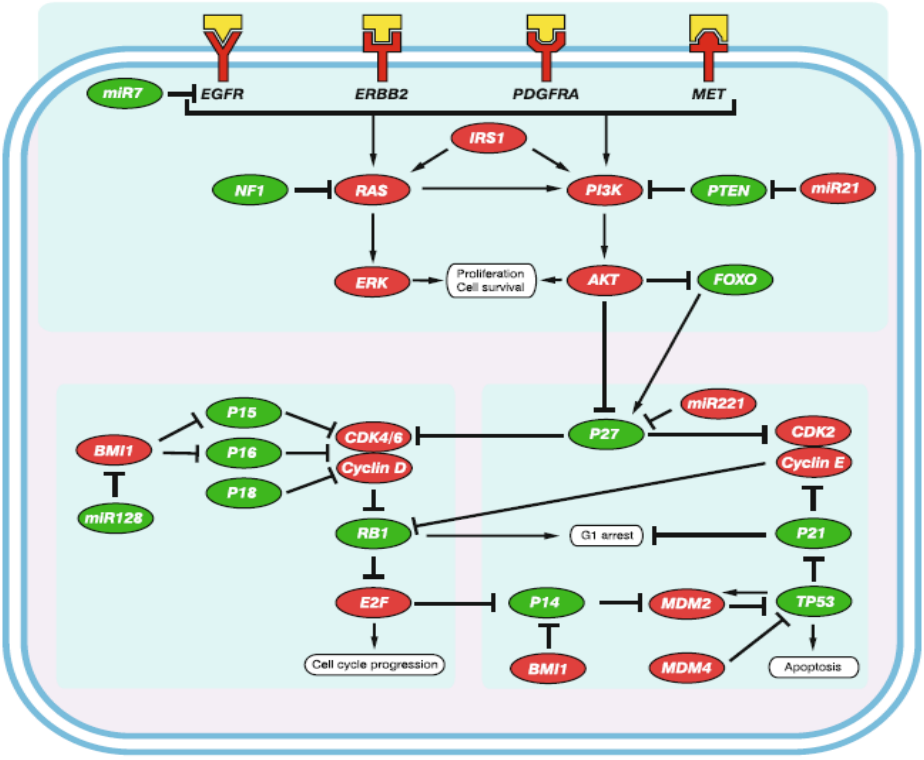

Figure 4 Common alterations involved in glioblastoma. Image adopted from (1)

1.5 Proteomics and Cancer

Cancer is an evolving disease driven by many complex biological processes. Although there has been an enormous development in the treatment strategies against this deadly disease, yet this disease remains to be completely surmounted. Its unconquered ability to ace over every therapeutic intervention is one of the major reasons for cancer recurrence and therapy resistance today. This disease is not just a consequence of genomic instability but also an amalgamation of deregulated cellular responses as a result of altered protein function. Thus, a comprehensive

understanding of the biological processes governing cancer progression requires an extensive knowledge of proteins, which are the ultimate effector molecules of cellular functions (69, 70). Proteomics, according to Kiernan is defined as "the use of quantitative protein-level measurements of gene expression to characterize biological processes (e.g., Disease processes and drug effects) and decipher the mechanisms of gene expression control "(71). The field of proteomics is broadly categorized into three main areas: (1) protein micro-characterization for large-scale identification of proteins and their post-translational modifications; (2) 'differential display' proteomics for comparison of protein levels with potential application in a wide range of diseases; and (3) studies of protein-protein interactions using techniques such as mass spectrometry or the yeast two-hybrid system. Since proteomics focuses on the gene products, which are the active agents in cells, it directly contributes to drug development as almost all drugs are directed against proteins. In cancer, proteomics has empowered scientists to monitor alterations in the protein expression both qualitatively and quantitatively. The ability to decode protein signatures in cancer using proteomics is valuable for more effective diagnosis, prognosis, and response to therapy (26, 72) .

1.6 Mass spectrometry-based quantitative proteomics in cancer

In order to decode protein signatures involved in an oncogenic transformation of a normal cell, it is essential to decipher the change in the protein repertoire as the cell transforms.

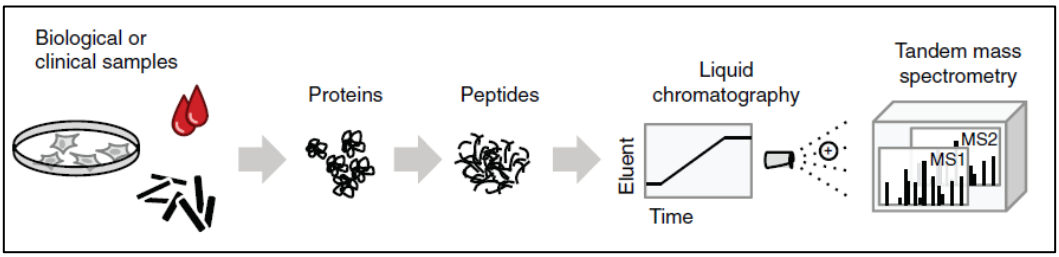

Figure 5 Schematic representation of proteomic analysis using mass spectrometry (4)

Hence, a comprehensive tool such as quantitative proteomics enables us to gain insights into the differential proteome of a cancerous cell compared to a non- transformed cell (73, 74). Over

the last two decades, mass spectrometry (MS)-based methods have become essential tools to understand the molecular mechanism of a diseased condition. MS-based proteomics is categorized as top-down proteomics and bottom-up proteomics. Top-down proteomics includes measurement of an intact protein. Bottom-down proteomics involves measuring the peptides as the substitutes for the protein of interest (figure 5). In bottom-up proteomics, the protein extract is digested into short peptides using trypsin and separated by liquid chromatography, either directly or after biochemical fractionation. The eluted peptides from the chromatography column are subjected to electrospray ionization and are directly sprayed into the mass spectrometer. There are two levels of MS measurement which occurs in tandem. First, a mass analyzer measures the mass-to-charge ratio (*m*/*z*) of peptide molecular ions (MS1) followed by detection of *m*/*z* values of fragment ions resulting from the fragmentation of specific peptide (75, 76).

The peptides present in the sample are identified by the specific fragment ion pattern of each peptide ion, together with its *m*/*z* value. The peptide sequences identified are then mapped to proteins, and the signal intensities of either peptides or fragment ions are used to estimate relative changes in abundance across samples.

Quantitative proteomic techniques can be gel based or non- gel based. Gel-based approach includes Two-Dimensional electrophoresis (2DE) or Difference gel electrophoresis (DIGE) which uses fluorescence-based labeling of the proteins prior to separation. However, both these approaches are less reproducible and less sensitive (77). Thus, to combat technical variability at various stages of sample handling and during measurements, non-gel-based techniques have been developed for an extensive and accurate quantification of proteins. The notion –gel-based tools vary according to the time point of the proteomics workflow at which the quantification strategy is incorporated. Below in figure 6 is an illustrative representation of the different types of labeled and label-free quantitative proteomic techniques.

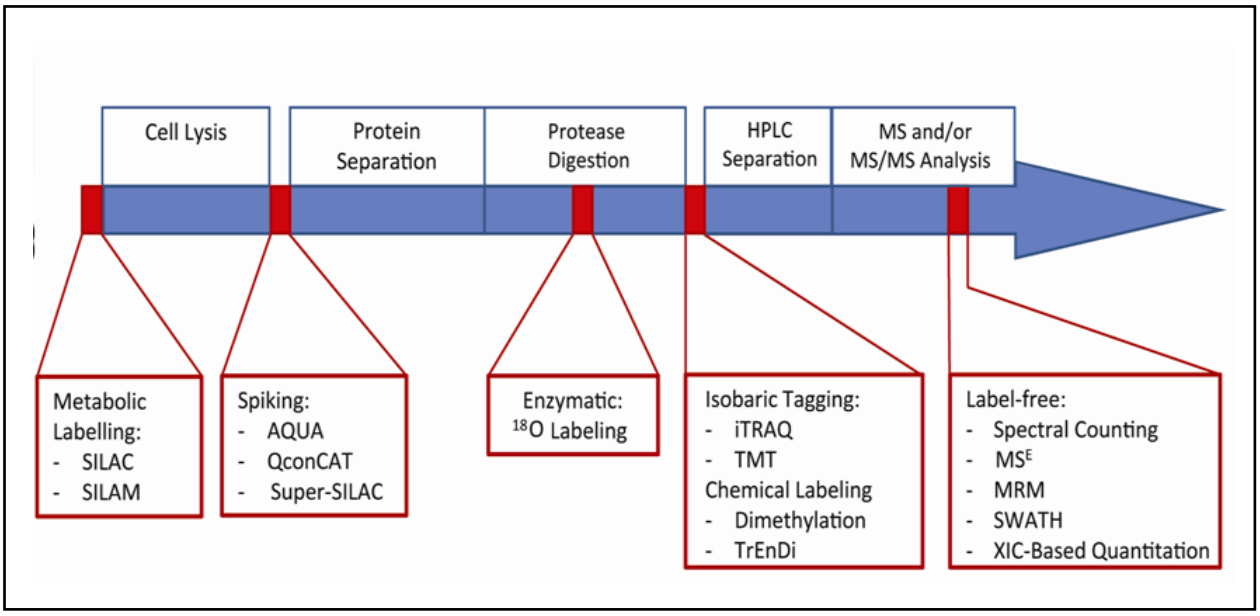

Figure 6 Different types of quantitative proteomic techniques.

These approaches can be classified as isotope- labeled and label-free MS. Isotope-labeling methods are categorized by introduction of stable isotope tags to proteins via chemical reactions using isotope-coded affinity tags (ICAT) and isobaric tag for relative and absolute quantification (iTRAQ), enzymatic labeling, for example using ^{18}O water for trypsin digestion, or via metabolic labeling (stable isotope labeling of amino acids in cell culture – SILAC).

1.7 Isobaric tagged relative and absolute quantification (iTRAQ)

This quantitative proteomic technique first developed by Ross et al is based on the derivatization of primary amino groups in intact proteins using the isobaric tag for relative and absolute quantitation (iTRAQ). The iTRAQ reagents are isobaric labels (figure 7) due to which differentially labeled proteins do not differ in mass; accordingly, their corresponding proteolytic peptides appear as single peaks in MS scans (78). The quantitative information is provided by isotope-encoded reporter ions that can only be observed in MS/MS spectra, which can be analyzed by the fragmentation behavior of ESI and MALDI ions of peptides generated from iTRAQ-labelled proteins using a TOF/TOF and/or a QTOF instrument

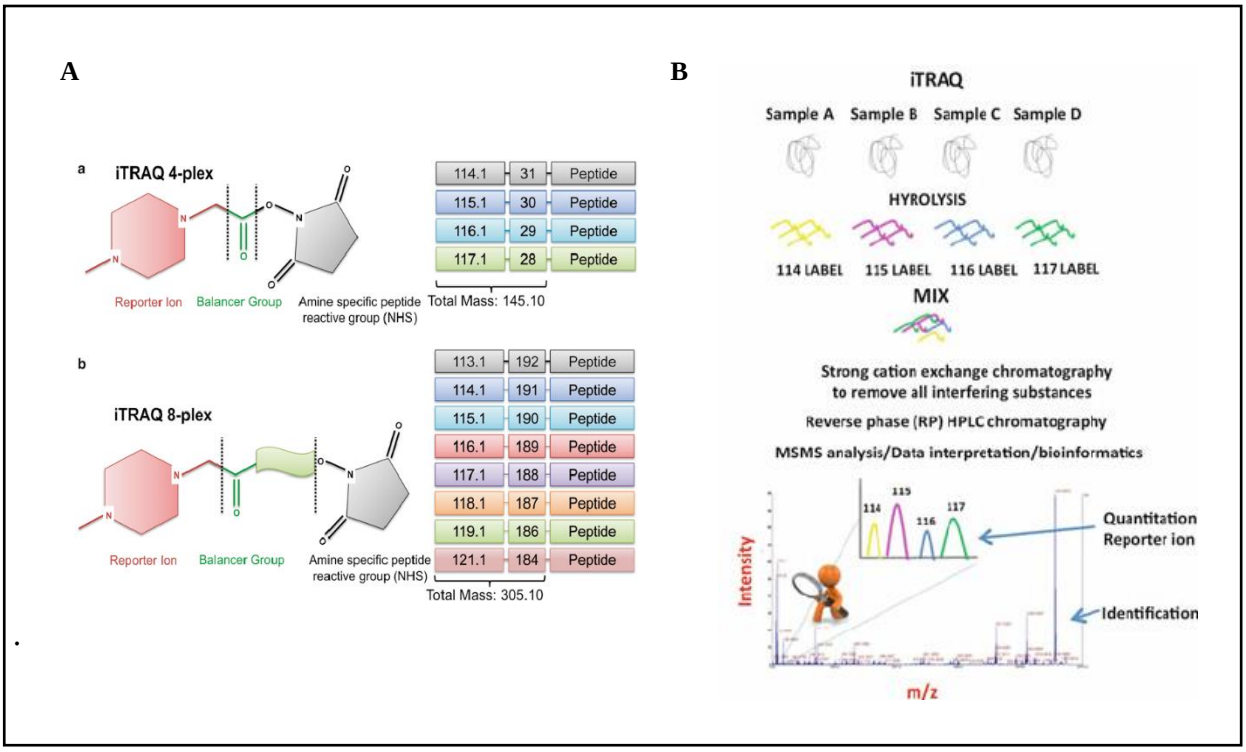

Figure 7 Chemical structures for iTRAQ

(A) 4-plex and (B) 8-plex isobaric Balancer + reporter ions add up to 145 Da in 4-plex and 304 Da in 8-plex experiments. In 8-plex, reporter mass of 120 is not present as it will give erroneous quantitation since phenylalanine ammonium ion is also observed at a mass of 120 Da (c) iTRAQ workflow

This technique allows simultaneous labeling and quantitation of four or eight samples in contrast to ICAT and SILAC. Since multiple samples are combined in one run, the instrument time for analyses can be reduced, and variations between different LC/MS runs does not hamper the results. Comparative studies for different isotope labels including differential gel electrophoresis (DIGE), ICAT, and iTRAQ showed that iTRAQ is more sensitive than ICAT (79).

1.8 Differential proteomic studies in glioblastoma

More than 100 papers appear in PubMed where researchers have used proteomic tools to identify proteins involved in different aspect of glioblastoma. However, most of these proteomic studies are to identify differential protein patterns among different cell lines or between cell lines and patient samples. Initial studies performed in glioblastoma employed two-dimensional gel electrophoresis (2D GE) approach to identify the proteins specifically or

differentially expressed in the high-grade gliomas. Furuta et al in 2004 adopted this technique to identify the protein differences amongst de novo primary glioblastoma tissues and secondary glioblastoma tissues. This study was performed in a total of 13 with 6 primary and 7 secondary glioblastoma tissues. Only 11 uniquely expressed proteins in any one the GBM tissues were sequenced and identified. These included Tenascin-X precursor, Unnamed protein, Enolase 1, Centrosome-associated protein 350, Epidermal growth factor receptor, EGFR, ERCC6, DUOX2, HNRPA3, WNT-11 protein precursor, Cadherin-related tumor suppressor homolog precursor, ADAMTS-19 (80). In 2005, Vogel et al implemented this technique to report the differences in protein expression amongst GBM cell lines as compared to primary glioblastoma tissues (23). Two-dimensional gel electrophoresis (2-DE) and cleavable Isotope-Coded Affinity Tag (cICAT) was also used by a group (81) to compare the cerebrospinal fluid (CSF) proteome in order to identify the tumor and grade specific biomarkers in patients suffering from histologically different grade brain tumors. Although 2D GE aided in the identification of differential proteins, however, the number of proteins identified and the identification of low abundant proteins such as receptors and signaling remained a challenge. The incorporation of isotope coated labels and label-free quantification techniques enabled identification of proteins which differed in abundance between two or three samples. In 2009, Rajcevic et al applied iTRAQ based quantitative proteomics technique to reveal increased metabolic activity and cellular cross-talk in angiogenic compared with invasive glioblastoma phenotype (82). Multidimensional Protein Identification Technology (MudPIT) was exploited to investigate resistance of glioblastoma to a naturally occurring terpene with chemotherapeutic properties known as perillyl alcohol (POH) in A172 cell line (83). Quantitative proteomic Isotope-Coded Protein Label (ICPL) analysis by Emmanuelle Com et al revealed alteration of several functional processes in the glioblastoma when they investigated protein expression between the four regions of GB on clinically relevant biopsies from 5 patients (84). Ravindra Varma

Polisetty et al performed iTRAQ analysis on membrane-enriched fractions of GBM tissues and identified deregulation of calcium signaling and other protein groups of regulatory functions. Kumar DM et al have identified temozolomide mediated alterations in glioma proteome (17, 85) . In order to identify a plasma-based biomarker in glioma patient, Gautam P et al have reported the serum proteome from glioblastoma patients (86). Quantitative proteomics has also been used to identify molecular signatures and develop predictive markers of pseudo-progression (PsPD) by Zhang et al, 2015. In this study, only three PsPD and three GBM patients were used for comparison. 530 proteins with significant fold changes were identified which belonged to the protein synthesis network and the cellular growth and proliferation network (25). In 2016, Rebecca S. Lescarbeau et al conducted a quantitative phosphoproteomic analysis on a genetically engineered murine proneural glioblastoma model to quantitate phosphotyrosine-mediated signaling using mass spectrometry. They interestingly identified phosphorylation of CDK1 pY15, associated with the G2 arrest as the most differentially phosphorylated site, with a 14-fold increase in phosphorylation in the tumors. The use of Wee1 kinase inhibitor - the kinase responsible for CDK1 Y15 phosphorylation against these tumors revealed Wee1 kinase to be a potential therapeutic target in glioblastoma. Quantitative proteomics is also being employed to study intra-tumor heterogeneity in glioblastoma (87, 88). The progress in the identification of differential proteins associated with glioblastoma progression, prognosis, heterogeneity and diagnostic values has been considerably significant using the advanced proteomic technologies. However, there is also a substantial need to exploit these technologies to understand the biology of radio-resistance and recurrence in glioblastoma. In this study, we applied iTRAQ based technology to decipher the differential proteins governing the survival of residual resistant cells and promoting relapse.

1.9 Rationale

There are numerous studies in glioblastoma looking at the differential gene expression in therapy-resistant glioma cells (5, 16-18). But gene expression not always correlate with the protein expression and the identification of any therapeutically relevant pathway from these studies still remains as elusive as before. Proteomics directly addresses the functional effectors of cellular and disease processes (19, 20). Till date majority of proteomics studies in glioblastoma have focused on identification of differential proteins amongst different GBM cell lines, patient samples or within a same tumor to investigate the heterogeneity of glioblastoma, mechanism of chemoresistance and identification of diagnostic biomarkers (23, 25-32, 81, 88). Our aim was to understand the mechanisms of radiation resistance and recurrence in GBM. Since proteins are the effector molecules for almost all the cellular pathways therefore here we want to analyze the proteome of the radio-resistant and relapse cells***. Thus, this study is based on the hypothesis that the glioblastoma radio-resistant residual cells undergo a change in their protein repertoire which promotes their survival and leads to relapse.*** Identification of differential proteins in the radiation resistant residual cells and relapse cells will provide invaluable insights into the cellular pathways of resistant cells and will help in the identification of therapeutically relevant drug targets to eliminate resistant cells.

This study was done using an *in vitro* radiation resistant model that has previously been established in our lab (15) from glioblastoma cell lines U87MG and SF268 and primary cultures of naive patient samples. The residual cells inaccessible from patient biopsies were obtained from the cellular model of resistance we developed. Radiation resistant cells were obtained by subjecting the glioma grade IV cells (U87MG, SF268, and two primary patient samples) to a lethal dose of radiation (at which ~10% population survive) determined using clonogenic survival assay. It was observed that in all the cell cultures, a small population of

cells (~10% or less) that we call "Radiation Resistant (RR)" escape apoptosis and survive. These surviving cells exhibit a transient non-proliferative, multinucleated and giant cell phenotype for a period of 1 week or more and then resume their growth similar to their parent population to form "Relapse population (R)". This system allowed us to collect parent, RR and R cells for functional studies. ***The aim of my thesis project is to understand the molecular pathways influencing therapy surviving glioblastoma cells using a proteomic approach.***

The Specific Objectives are:

4. Characterization of the radiation resistant and the relapse population.
5. Differential proteomic analysis of parent, radiation resistant and relapse population using quantitative proteomics

2 Material and methods

2.1 Cell Culture and Patient samples

GBM grade IV cell lines U87MG and SF268 were obtained from ATCC. Breast cancer cell lines MCF7 and T47D, colorectal cancer cell line HT29 and lung cancer cell line H1975 were kind gifts from Dr. Amit Dutt (ACTREC). These cell lines were authenticated in the laboratory by short tandem repeat profiling based on eight markers in. The cell lines were maintained in DMEM containing 10% (v/v) FBS, penicillin (200 U/ml), streptomycin (100 µg/ml) and incubated at 37°C in a humidified incubator with an atmosphere of 50 mL/L CO2.

The project was approved by the institutional review board and informed consent in the language understood by the patients was also taken prior to tumour collection. Tissue was collected after surgery from 20 patients with confirmed glioblastoma. Fresh tissue samples were collected in DMEM containing 400U/ml of pencillin, 200 µg/ml of streptomycin. Single cell suspension was made using Brain Tumor Dissociation Kit (P) (catalogue number 130-095-942) as per the kit instructions. The tissues were first washed with PBS to remove blood vessels and necrotic tissue from the tumour samples and then transferred the tissue into C-tube containing pre-heated 3890µl of buffer X, 50µl of enzyme N and 20µl of enzyme A. The tissues were then subjected for mechanical disruption using gentle MACS dissociator program h_tumor_02, followed by 15 minutes incubation at 37 °C under slow, continuous rotation. Further, the C tubes containing the samples were run on the gentleMACS Program h_tumor_03 and incubated for 10 minutes at 37 °C under slow, continuous rotation. In the final step, samples were run on gentleMACS Program m_brain_01 and the pellet was collected after centrifuging briefly and was seeded in DMEM: F12 media containing 15% (v/v) FBS, 1% of antibiotic cocktail containing fungizone and incubated at 37°C in a humidified incubator with an atmosphere of 5% CO_2.

2.2 Drug Treatment

20 mg capsule of temozolomide (Temonat from NATCO Company) was dissolved in DMSO according to manufacturer's guidelines. Cells were treated with the drug at 25µM concentration daily for three weeks.

2.3 Radiation treatment

The cells growing in 10% FBS containing media were washed with 1X PBS. The cells were incubated with 0.05% FBS containing DMEM for 72hrs. After 72hrs, cells were replaced by 10% FBS containing median and were irradiated using 60Co γ-rays at the respective lethal dose. The fractionated dose of 2Gy was administered for 13 days over a span of two weeks.

2.4 Trypan blue assay

10µl of cell suspension was diluted in 1:1 ratio with 0.4% Trypan Blue solution. Non-viable cells were blue and viable cells remained unstained. Cells were counted under the microscope in four 1 x 1 mm squares of one chamber and the average number of cells per square was determined.

2.5 Clonogenic survival assay

To determine the survival fraction at 2 Gy (SF2) as well as a lethal dose of radiation for all the cell lines, a clonogenic assay was carried out in a 60mm dish using 1000-3000 cells as per the plating efficiency of the glioma cultures. The colonies (>35 cells) were fixed with pre-chilled methanol: acetic acid (3:1), stained with 0.5% crystal violet and counted after 10-15 days of radiation. SF2 values and the lethal dose was calculated from the radiation-survival curve using SPSS software version 21®.

2.6 RNA extraction, cDNA synthesis, and qPCR

Total RNA was extracted by TRIZOL Reagent (Invitrogen) according to the manufacturer's protocol. cDNA was synthesized using the SuperScript III First-Strand kit (Invitrogen) as per the manual instructions. qPCR was carried out using Roche Light Cycler Master Mix using Light Cycler 480 real-time PCR system. GAPDH was used as an internal control. Relative changes of mRNA amounts were calculated using the ΔΔCt method. A list of all primers used for real-time PCR is provided in Annexure I.

2.7 Protein Extraction

10 million cells of the Parent (P), Radiation Resistant (RR) and Relapse (R) cells were grown under normal growth conditions. The media was aspirated and the cells were washed thrice with cold 1 X PBS after which the cells were scraped and pelleted down. The cell pellet was suspended in 150µl of 0.5% SDS Solution and sonicated with 10 pulses each for 10secs. The sonicated cells were centrifuged at 4000RPM for 15mins at 4ºC and the supernatant was used for the proteomic analysis. The protein concentration was determined using bicinchoninic acid assay and equal amounts of protein from the 3 conditions were taken for further analysis.

2.8 iTRAQ labeling

Protein extracts from the untreated, radiation resistant and relapse cells were digested with trypsin and the peptides were labeled with iTRAQ reagents according to the manufacturer’s instructions (iTRAQ Reagents Multiplex kit; Applied Biosystems/MDS Sciex, Foster City, CA). Briefly, 80 µg of protein from each sample was reduced, alkylated and digested with sequencing grade trypsin; (Promega, Madison, WI, USA). Peptides from P, RR and R were labeled with iTRAQ reagents containing 114, 115 and 116 reporter ions, respectively. The three labeled samples were pooled, vacuum-dried and subjected to fractionation by strong cation exchange (SCX) chromatography.

2.9 SCX FRACTIONATION

The pooled sample after iTRAQ labelling was resuspended in 1 ml of buffer A [10 mM KH2PO4, 25% (v/v) acetonitrile (ACN), pH 2.9] and separated on a SCX column (Zorbax 300-SCX, 5 µm, 2.1 mm ID × 50 mm, Agilent Technologies, Santa Clara, CA, USA) at a flow rate of 700 µl/min with a 40 min gradient [5 min, 0-5% buffer B (buffer A + 350 mM KCl); 5 min, 5-10%; 5 min, 10-23%; 5 min, 23-50%; 10 min, 50-100%; 10 min, 100% B]. One minute fractions were collected, vacuum-dried and desalted using a C18 cartridge (Pierce, Rockford, USA) as per the manufacturer's instructions. After desalting, consecutive fractions were pooled to obtain a total of thirteen fractions for LC-MS/MS analysis.

2.10 LC-MS/MS analysis

Nanoflow electrospray ionization tandem mass spectrometric analysis of peptide samples was carried out using LTQ-Orbitrap Velos (Thermo Scientific, Bremen, Germany) interfaced with Agilent's 1200 Series nanoflow LC system. The chromatographic capillary columns used were packed with Magic C18 AQ (particle size 5 µm, pore size 100Å; Michrom Bioresources, Auburn, CA, USA) reversed phase material in 100% ACN at a pressure of 1000 psi. The peptide sample from each SCX fraction was enriched using a trap column (75 µm × 2 cm) at a flow rate of 3 µl/min and separated on an analytical column (75 µm × 10 cm) at a flow rate of 350 ml/min. The peptides were eluted using a linear gradient of 7-30% ACN over 65 min. The mass spectrometric analysis was carried out in a data dependent manner with full scans acquired using the Orbitrap mass analyzer at a mass resolution of 60,000 at 400 m/z. For each MS cycle, twenty most intense precursor ions from a survey scan were selected for MS/MS and fragmentation detected at a mass resolution of 15,000 at m/z 400. The fragmentation was carried out using higher-energy collision dissociation (HCD) as the activation method with 40% normalized collision energy. The ions selected for fragmentation were excluded for 30 sec. The automatic gain control for full FT-MS was set to 1 million ions and for FT MS/MS

was set to 0.1 million ions with a maximum time of accumulation of 500 ms, respectively. For accurate mass measurements, the lock mass option was enabled.

2.11 Protein identification and quantitation

The MS data were analyzed using Proteome Discoverer (Thermo Fisher Scientific, Version 1.4). The workflow consisted of a spectrum selector and a reporter ion quantifier. MS/MS search was carried out using SEQUEST and MASCOT search algorithms against the NCBI RefSeq database (release 52 40) containing 31,811 proteins. Search parameters included trypsin as the enzyme with 1 missed cleavage allowed; oxidation of methionine was set as a dynamic modification while alkylation at cysteine and iTRAQ modification at N-terminus of the peptide and lysine were set as static modifications. Precursor and fragment mass tolerance were set to 20 ppm and 0.1. Da, respectively. False Discovery Rate (FDR) was calculated by searching the proteomic data against a decoy protein database. Only those Peptide Spectrum Matches (PSMs) that qualified a 1% FDR threshold were considered for further analysis. Unique peptide(s) for each protein identified was used to determine relative protein quantitation based on the relative intensities of reporter ions released during MS/MS fragmentation of peptides.

2.12 Bioinformatics Analysis

Heat Map representation for the differential genes on the basis of their relative peptide intensities was constructed using MeV software (v 4.9.0). Unsupervised Hierarchical clustering of the genes was done using Pearson Correlation method. Functional annotation and Gene enrichment pathway analysis were done using Cytoscape (v 3.5.1) ClueGo (v 1.8) and CluPedia (v 1.0) plugin with default parameters. KEGG and REACTOME pathway databases were used for reference.

2.13 Western Blot analysis

Cells were lysed using EBC lysis buffer (120 mM NaCl, 50 mM Tris-Cl (pH 8.0), 0.5% (v/v) Nonidet P-40, 50 μg/ml PMSF and protease, phosphatase inhibitor cocktail for 45 minutes on ice. The supernatant was collected and 40ug of protein was used for immunoblotting using anti-YBX3 (rabbit; 1:1000; Pierce), anti-PSMB4 (rabbit; 1:1000; Pierce), and anti-PSMD10 (rabbit; 1:1000; Pierce), anti-YWHAZ (rabbit; 1:1000; Pierce), anti-YWHAG (Mouse; 1:6000; Pierce), anti-YHWAS (rabbit; 1:1000; Pierce), Actin (Sigma; 1:4000 dilutions), was used as a loading control. Immune-reactive proteins were visualized using an enhanced chemiluminescence (ECL) reagent (Pierce).

2.14 MTT cytotoxicity assay

5000 cells/well were seeded in 96 well plates for overnight. Bortezomib (Bortenat 2mg; Natco Company) was added at different concentration i.e. 0.1nM, 1nM, 10nM and 100nM. After 72hrs 10 μL of MTT reagent (5mg/ml in PBS, Himedia TC191-1G) was added to each well and incubated for 4h. Crystals were dissolved using freshly prepared acidified isopropanol containing 10% triton X-100. Optical density was measured at 570nM by (SPECTROstar^{NANO}star spectrophotometer)

2.15 Luciferase based NFkB promoter activity

To measure NFkB promoter activity, cells were transiently transfected with NFkB-pGL4-luc2 and pGL4-hrl (5:1 ratio) or NFkB-pGL4-luc2 with pTRIPZ IkB-α and fold change (treated/untreated) was calculated as a ratio of firefly luciferase/ renilla luciferase (FL/RL) activity. The constructs were kind gifts from Dr. Prasanna Venkatraman, ACTREC. FL and RL activities were measured using Dual luciferase assay system (Promega) and the readings were recorded in a Berthold luminometer for period of 1 sec. All experiments were done in triplicate. Values represent mean ± SEM. ***$p<0.0005$ (t-test, n=3)

2.16 Proteasome activity assay

0.1 million cells were pelleted, washed twice with 1X PBS and resuspended in ATP buffer containing 50 mM Tris (pH 7.5), 5 mM MgCl2, 1mMATP, 10% glycerol and protease inhibitor cocktail (Sigma). Cell suspensions were ultra-sonicated for four cycles of 5 s each (with 1 s break after each 2 s) at 30 kHz on ice. Proteasome activity was measured using 50µM Suc-LLVY-7-amino-4-methyl coumarin substrate and fluorescence readings were taken at excitation 355 nm/emission 460 nm.

2.17 Orthotopic xenograft mouse experiments

All animal experiments were licensed through the Laboratory Animal Facility of ACTREC, TMC. Protocols were reviewed by the Institutional Animal Ethics Committee (IAEC). NUDE/SCID mice (6–8 weeks old) bred and maintained in an isolated facility within a specific pathogen-free environment were used for this study. $1*10^5$ pLenti6-luc2 U87MG cells stably expressing luciferase were intracranially injected for generating the orthotopic GBM model and for studying the tumorigenicity of pre-treated Parent and RR cells. $2.5 *10^5$ pLenti6-luc2 U87MG stably expressing luciferase were intracranially injected for studying the effect of proteasome inhibitor along with radiation. In order to perform an intracranial injection, the cells were suspended in 5µl 1X PBS prior to injection and kept on ice until injected. Prior to injecting the cells intracranially, the mice were anesthetized using an injection mix of Ketamine (120mg/kg)/Xylazine (mg/kg)/Saline and the mice were placed on the stereotaxic for stereotactic surgery. A 10 mm to 15 mm long incision was made on top of the skull. A small hole was drilled using a sterile 26-gauge sharp needle at 1 mm posterior to bregma and 2 mm lateral to coronal suture and 2.5 mm depth. The 5µl cell suspension was then loaded onto the Hamilton syringe and injected at a rate of 1 µl per minute for a total of 6-8 minutes. The tumors were allowed to grow and animals were sacrificed using CO_2 at the onset of disease symptoms, such as weight and activity loss, and the brains were removed.

2.18 Radiation and drug treatment of orthotopic GBM mouse model.

The mice were divided into four groups post 7 – 10 days of intracranial injection: Vehicle control, bortezomib (Bortenat 2mg, NATCO Company), Radiated group, Radiation and BTZ group. Radiation was delivered to the whole brain of anesthetized mice, immobilized in a plastic chamber using 60Co γ-rays. A total dose of 14Gy was administered over a period of 7 days. 0.5mg/Kg of bortezomib was administered intraperitoneally twice in a week for 2 weeks.

2.19 Bioluminescence imaging of orthotopic tumor xenografts

Mice were anesthetized with Ketamine/Xylazine and were administered luciferin (D-Luciferin potassium salt, 150 mg/kg, Calliper Life Sciences) via intraperitoneal injection. The images were acquired 10-12 minutes post-injection. The time chosen was based on the pharmacokinetics of luciferin which defines that maximum luminescence emission and greatest sensitivity of detection will be obtained when cell luminescence is detected after 10-15 mins of injection of luciferin. The selected imaging time was maintained as constant among all the animals to be imaged. Regions of interest encompassing the intracranial area of the signal were defined using Living Image software, and the total photons/s/sr/cm2 (photons per second per steradian per square cm) was recorded.

2.20 Bacterial purification of GST-tagged 14-3-3 ζ

The plasmid pGEX-4T encoding glutathione S-transferase (GST)-tagged-14-3-3 ζ protein, was a kind gift from Dr. Sorab Dalal. This plasmid was transformed using BL21 competent cells. The transformed culture was inoculated in 10 ml Luria broth - ampicillin containing medium and incubated overnight at 37° C shaking condition. Next day the start culture was inoculated in 100ml Luria broth - ampicillin containing medium and incubated until an $OD_{600\ nm}$ of 0.4–0.6 was reached. Bacteria were then grown in the presence of 0.1 mM of IPTG for 3 hrs. For protein purification, bacteria were collected by centrifugation and lysed with 1% Triton X – 100. The lysate was incubated with Glutathione sepharose beads (50% slurry) for 1 hr. in cold.

The beads were spun down and washed thrice with NET-N buffer (20mM Tris-HCl pH 8, 100mM NaCl, EDTA pH 8, 0.5% NP-40). The beads were resuspended in NTE-N buffer at stored at 4°C.

2.21 GST pull-down assay using GST tagged 14-3-3 ζ as bait

10 – 20 million cells were harvested and lysed using RBC lysis buffer (120 mM NaCl, 50 mM Tris-Cl (pH 8.0), 0.5% (v/v) Nonidet P-40, 50 µg/ml PMSF and protease, phosphatase inhibitor cocktail for 45 minutes on ice. The supernatant was collected and 500µg of lysate was incubated with 30 µl of GST tagged 14-3-3 ζ in the NET buffer for 1 – 2hrs in cold conditions on a rotator. The supernatant has collected the beads were washed with NET –N buffer 6-7 times. The beads were then boiled for 5 mins in the 2X lamilli buffer and loaded on an SDS PAGE gel. The gel was silver stained and the proteins bands were in-gel digested for protein identification by mass spectrometry.

2.22 Statistical methods

All data are represented as means ± standard error means (SEMs). The two-tailed Student's t-test was applied for statistical analysis. The Kaplan-Meier curve was plotted to generate the survival curves and to estimate the median survival values. Differences between survival curves were compared using a log-rank test.

3 Characterization of the radiation resistant and the relapse population.

3.1 Introduction

The tumor is a heterogeneous population with different cells designated to perform diverse functions for tumor growth and maintenance. During therapy, tumor cells undergo several kinds of cellular stress and adopt alternative measures to combat the toxic conditions detrimental for their survival. Cancer stem cells (CSCs), or tumor-initiating cells have largely been reported to govern therapy resistance and recurrence in various cancers (89-93). Various studies in glioblastoma and breast cancer report that CSCs possess innate resistance mechanisms against radiation- and chemotherapy-induced cancer cell death, enabling them to survive and initiate tumor recurrence (94-98). Several molecular mechanisms have been proposed to be adopted by CSCs, including amplified checkpoint activation and DNA damage repair as well as increased Wnt/β-catenin and Notch signaling (64, 99-101).

Another class of cells which are mostly overlooked in cancer studies are multinucleated and giant cells (MNGCs). MNGCs are one of the commonly present in granulomas that develop during various inflammatory reactions.

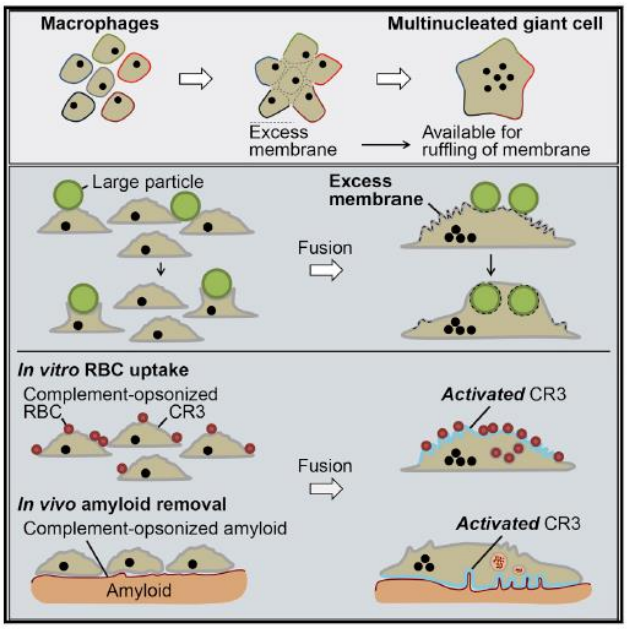

Figure 8 Formation of MNGCs. Image adopted from (1)

They are known to originate from the fusion of monocytes or macrophages (figure 8), but the exact mechanism of their genesis remains unclear (102). In cancer, MNGCs have been frequently observed in human cancer tissues and cell lines, mostly associated with late stages of the tumor (103). Failure of cytokinesis and endoreduplication has been shown to contribute to the formation of MNGCs that eventually generate polyploidy cells. Cell fusion is another mechanism reported to generate multinucleated cells during development. But in the context of cancer, such events are rare and have been implicated only in the virally induced transformation of the normal cells, enhancing the propensity to cause chromosomal instability and eventually resulting in aneuploidy (104). Some of the studies also report the multinucleated cells formation as a result of radiation, though these cells so reported eventually underwent cell death by mitotic catastrophe (105). The pre-existing MNGCs in tumors are thought to be responsible for increased resistance to therapies, however, the precise functional role of these cells in cancer is still not known (106). In several studies where the MNGC formation was observed after radiotherapy were overlooked. In fact, many authors equate multinucleation with cell death. Although a component of MNGCs that develop after therapeutic exposures is eliminated through apoptosis or other modes of cell death, compelling evidence reported in the past decade has demonstrated that the surviving MNGCs can contribute to cancer relapse by first entering a state of dormancy and ultimately giving rise to progeny with stem cell-like properties. MNGCs can give rise to tumor-repopulating cells through different mechanisms, including nuclear budding or burst similar to simple organisms like fungi . The contribution of MNGCs to cancer recurrence following therapeutic exposures has been well documented for ovarian, breast and colon cancers. According to Weihua et al, a single MNGC is sufficient to produce a metastatic tumor comprised mainly of mononuclear cells (107). An extensive study from our lab also reports the presence of a heterogenous subpopulation of radio-resistant cells which are innately resistant to the lethal dose of radiation (15). These cells after the exposure

to a lethal dose of gamma radiation are arrested at the G2/M phase of the cell cycle to become non-proliferative and undergo DNA damage repair. They remain in a non-proliferative phase for a limited time and then resume growth to form the relapse cells. The non-proliferative RR cells were found to be enriched with MNGCs which remain reversibly senescent without undergoing apoptosis until they start to divide and form the relapse population. The observation of reversible senescent phenotype is further confirmed by enhanced expression in SASPs (Senescent associated secretory proteins) such as GM-CSF, SCF IL-6 and IL-8. Concomitantly, these MNGC enriched RR cells showed enhanced expression of enhanced expression of anti-apoptotic genes *BIRC3* and *Bcl-xL* along with higher expression of pAKT – a well-known protein known to promote survival and resistance in glioblastoma. There is also a significant increase in the mRNA levels of p21 in the S, G2/M phase arrested resistant population along with higher levels of Cdk1 phosphorylated at the inhibitory site Tyr15 in the radiation resistant cells contributing to the arrest at the G2 phase of the cell cycle. pCdk1 (Y15) gets activated by Wee 1 kinase, a negative regulator of mitosis, therefore we hypothesized that an inhibitor to this protein would induce RR to undergo premature mitosis (108). Indeed, the RRs treated with the Wee 1 kinase inhibitor underwent apoptosis by day 5 of the treatment. Figure 9 is an illustrative representation of our previous findings based on which this present study has been performed.

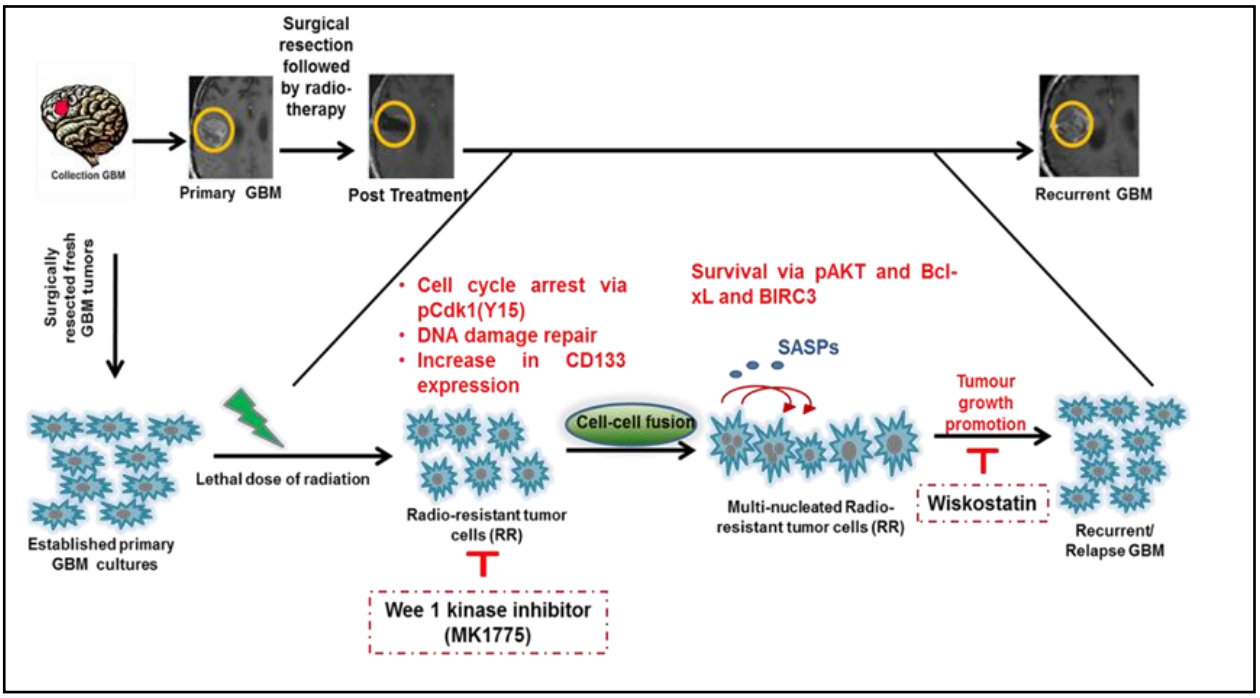

Figure 9 Schema showing the multi-step in-vitro radiation model recapitulating the progression of GBM and demonstrating the non-proliferative phase (76)

In this thesis, I wanted to see if the MNGCs were still formed when the glioblastoma cells are given combination treatment which is given in clinical settings (2Gy fractions over a span of 2 weeks) and chemotherapeutic drug TMZ at a clinically applied dosage. Further, this phenotype was also explored in other cancers to determine whether the therapy induced MNGCs formation is GBM specific or pertains to other cancer types too. Also, since recurrence is an inevitable phenomenon in GBM and is attributed to the highly infiltrative nature of this tumor type, this study also includes the investigation of the aggressive nature of the relapse cells in terms of their radiation response and invasion and migration properties.

3.2 Results

3.2.1 Survival response of Relapse cells to a lethal dose of radiation

Initial experiments performed on GBM cell lines SF268 and U87MG in the laboratory showed that when cells were subjected to a lethal dose of radiation few cells survived & remained in a non-proliferative phase for a week. After a week this residual resistant (RR) cells start dividing to form "Relapse cells" which grow in a similar manner to parent cells (figure 10 A&B).

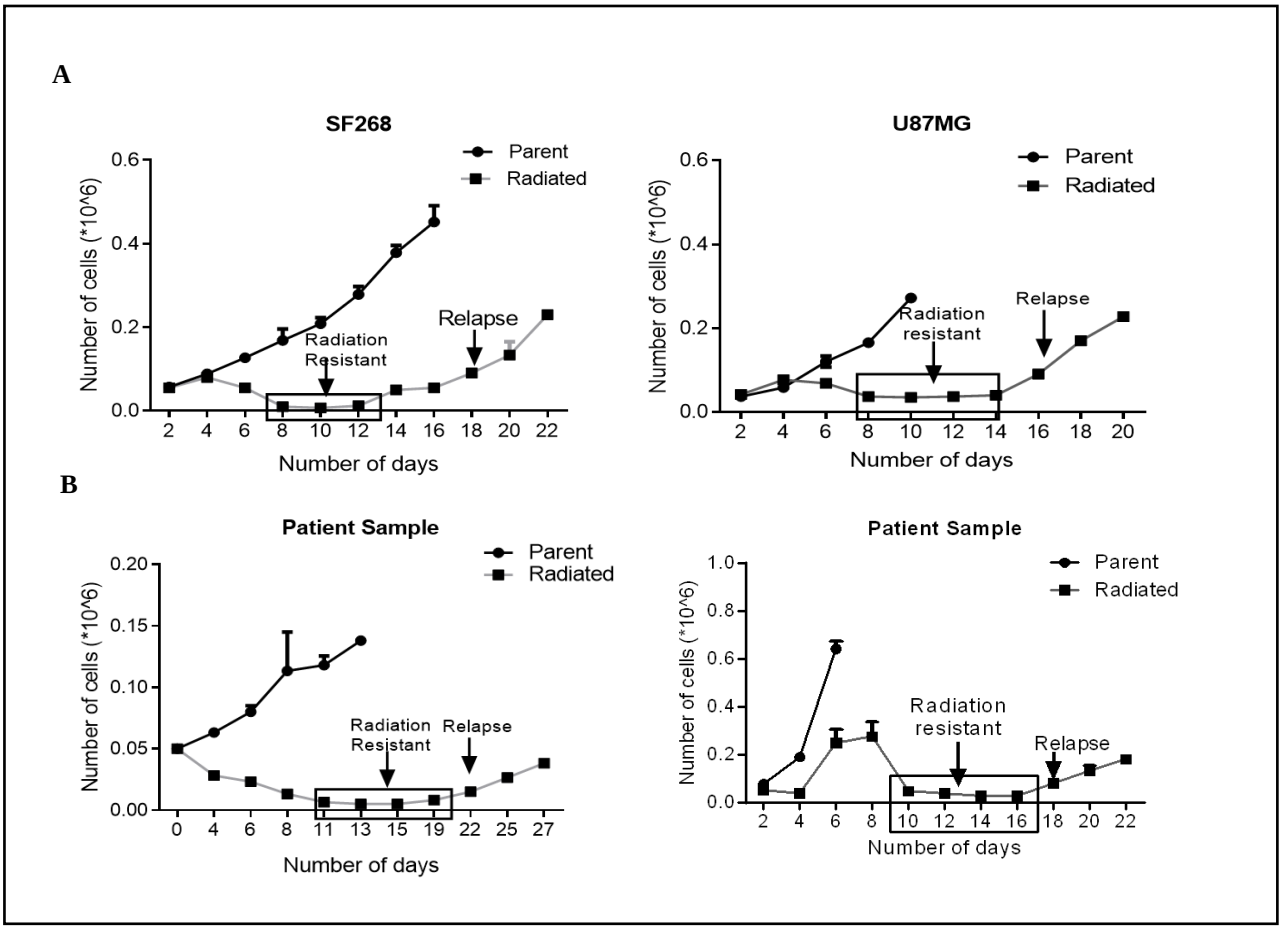

Figure 10 Cellular model to capture the inaccessible residual cells.

The graph represents the growth kinetics of (A) SF268, U87MG and (B) Two Patient Samples post lethal dose of radiation

In this study, the relapse cells were subjected to another round of lethal dose of radiation and the radiation response of the cells were observed to assess their radio-resistant property. It was observed that the same dose of radiation (8Gy) that could kill more than 90% of the parent population had less significant effect in terms of cell death on the relapse population. The cell

viability decreased to only 80% from initial 100% (as observed at day 10) in U87MG and 50% in SF268 (as observed on day 8). Suggesting that relapse population had acquired properties of resistance. The viability of these cells remained unaltered for 7-10 days in U87MG and 4-5 days in SF268. After the transient non-proliferative phase, they resumed growth to form the second relapse (R_2) population, similar to the first relapse (R_1) (Figure 11 A&B).

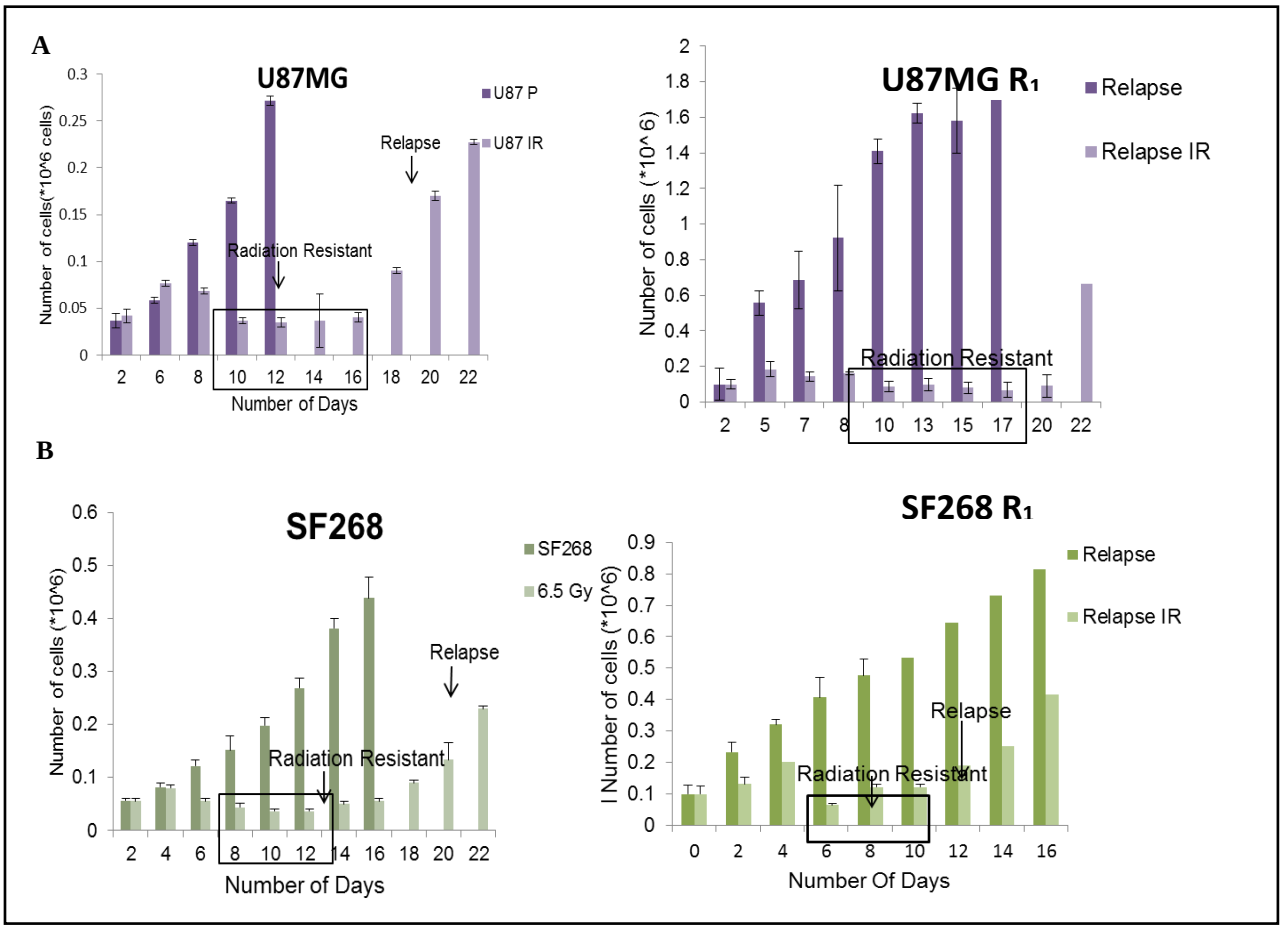

Figure 11 Radiation response of relapse (R1) cells to second round of lethal dose of radiation

(A) *Growth kinetics of U87MG P and R_1 cells post radiation. (B) Growth kinetics of SF268 P and R_1 post radiation, respectively.*

To examine their long-term clonogenic potential of relapse (R1 and R2), a clonogenic assay was performed on the P, R_1 & R_2 of U87MG and SF268. The D_0 (dose at which 37% of cells survive upon radiation treatment) of the R_2 was found to be 6.27 and 6.07 Gy whereas in R_1 it was found to be 6.09 and 5.9 Gy as compared to the parent population of U87MG, SF268,

respectively which was 5.78 and 5.77 Gy (figure 12 A & B). These data demonstrate an increase in the D_0 dose from Parent to R1 to an R_2 population which reflects that every time glioma cells are exposed to radiation the cells that survive acquire higher resistance than parent cells.

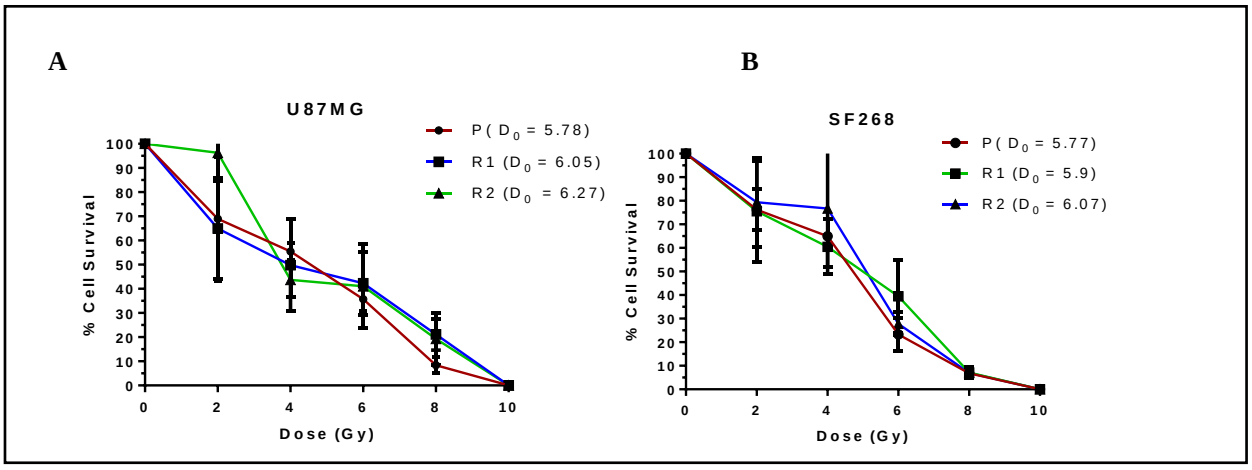

Figure 12 Radioresistance of R1 and R2 compared to P

(A& B) Clonogenic survival curve of Parent (P), 1st Relapse (R_1) and 2nd Relapse (R_2) in U87MG and SF268, respectively

3.2.2 Relapse glioblastoma cells demonstrate enhanced malignant properties

Recurrent glioblastoma tumors in clinics are more aggressive and infiltrate to the deeper region of the brain which makes therapeutic intervention a challenge. Hence, we wanted to assess

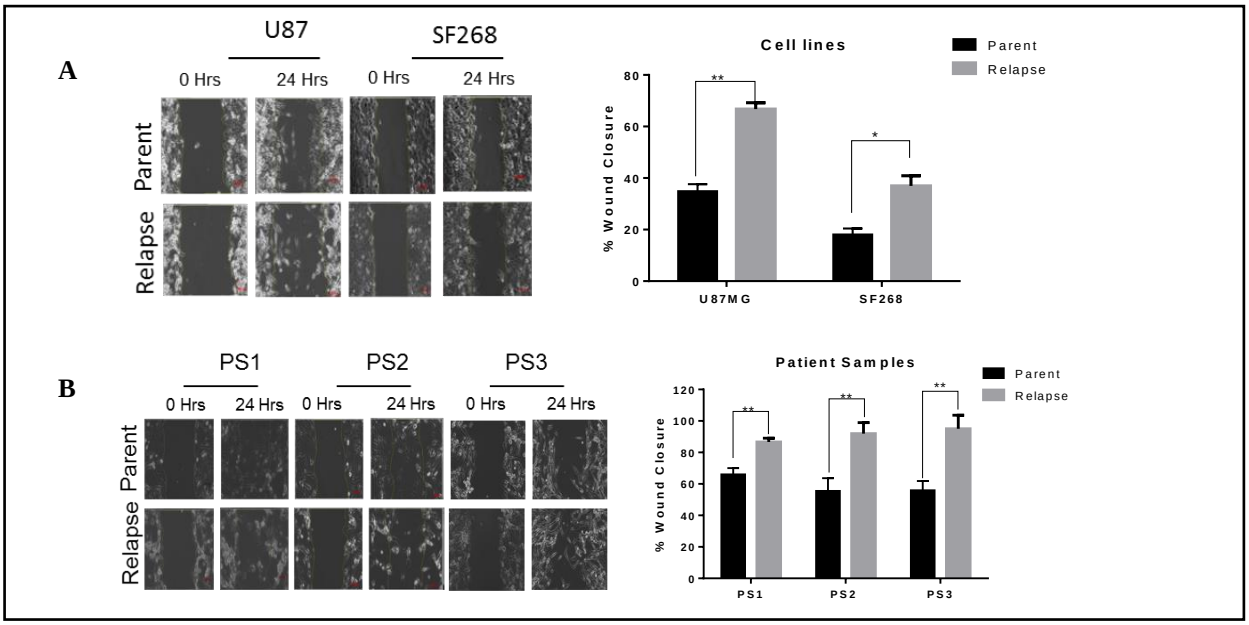

Figure 13 Wound healing assay for parent and relapse cells

(A & B) Representative images and graphical representation of wound healing assay in the parent and relapse cells of cell lines (U87MG, SF268) and patient samples (PS1, PS2 & PS3), respectively.

The migrating and invasive properties of the relapse cells formed in our *in vitro* radio-resistant model. For this, the relapse cells derived from cell lines (U87MG and SF268) as well as short-term cultures of 3 patient samples (PS1, PS2, and PS3) were taken. The migration potential was monitored by wound healing assay and it was found that relapse cells demonstrated a significant increase in migration in both cell lines and the three patient samples (figure 13 A & B). Furthermore, the invasive property of relapse cells was assessed by matrigel matrix invasion assay. The relapse cells of the cell lines demonstrated an increase in their invasion potential. However, the relapse cells of the patient samples showed similar invasion potential as compared to the parent (figure 14 A & B). Together, these data show that indeed the recurrent tumor cells acquire higher resistance and migration potential compared to the primary tumor.

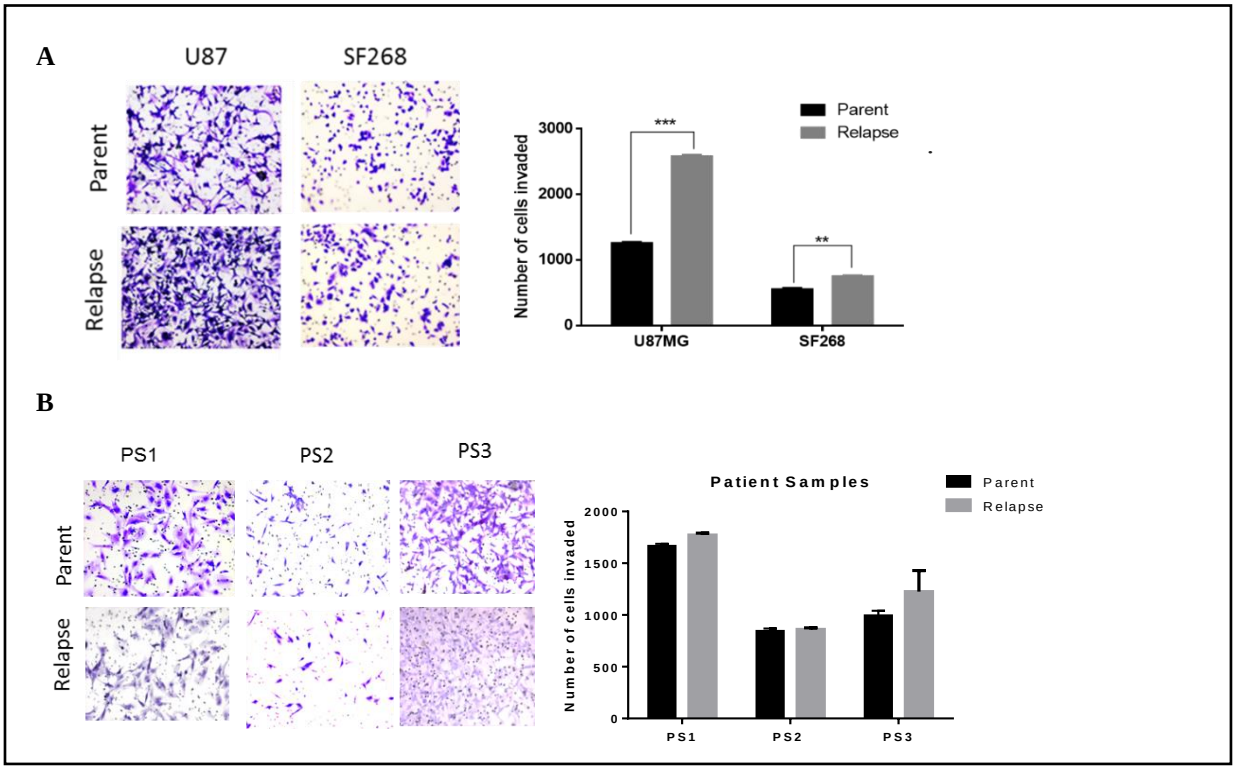

Figure 14 Boyden chamber assay for comparing the invasion of Relapse cells as compared to Parent

(A & B) Representative images and graphical representation of Matrigel matrix invasion assay in the parent and relapse cells of cell lines (U87MG, SF268) and patient samples (PS1, PS2 & PS3), respectively.

3.2.3 Presence of MNGCs post radiation and chemotherapy in glioblastoma

Our previously published study demonstrated the presence of MNGCs after the glioblastoma cells were exposed to a lethal dose of radiation. However, in clinics, the patients are administered a total radiation dose of 60 Gy over a span of 4-5 weeks in fractionated doses of 2Gy along with the chemotherapeutic drug temozolomide at 75mg/Kg body weight daily until the radiation therapy is given. We wanted to examine whether the MNGCs are formed even at a clinical dosage of radiation and chemotherapy.

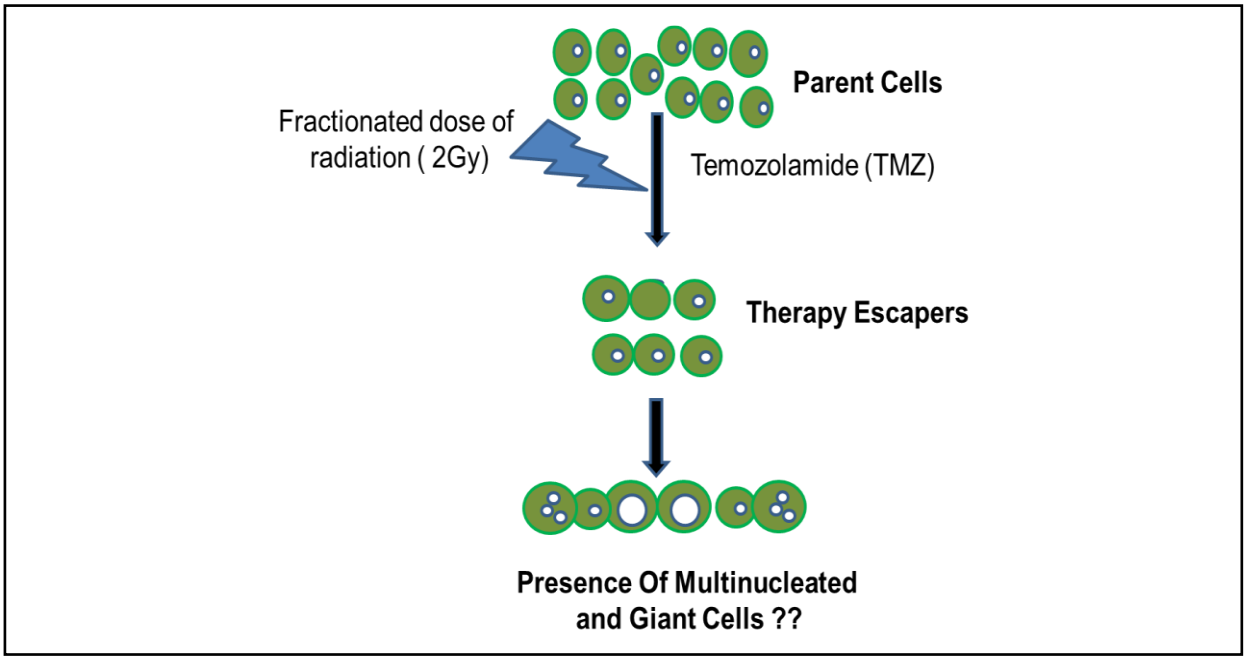

Figure 15 Schematic representation of the experiment to examine the presence of MNGCs in response to standard therapy

For this the U87MG cells were given the following treatment conditions: i) Untreated ii) Daily dose of fractionated dose of radiation (2Gy) until the less than 10 % cells were remaining. iii) A daily dose of temozolomide (25 µM – plasma concentration of temozolomide in the body) as illustrated in figure 15.

This experiment was performed to observe and quantitate the presence of therapy escapers similar to radiation escapers in presence of temozolomide (TMZ) and fractionated dose of radiation.

It was observed that the radiated cells underwent a drastic reduction in their cell viability after administration of 26Gy of radiation at day 15 (figure 16 A).

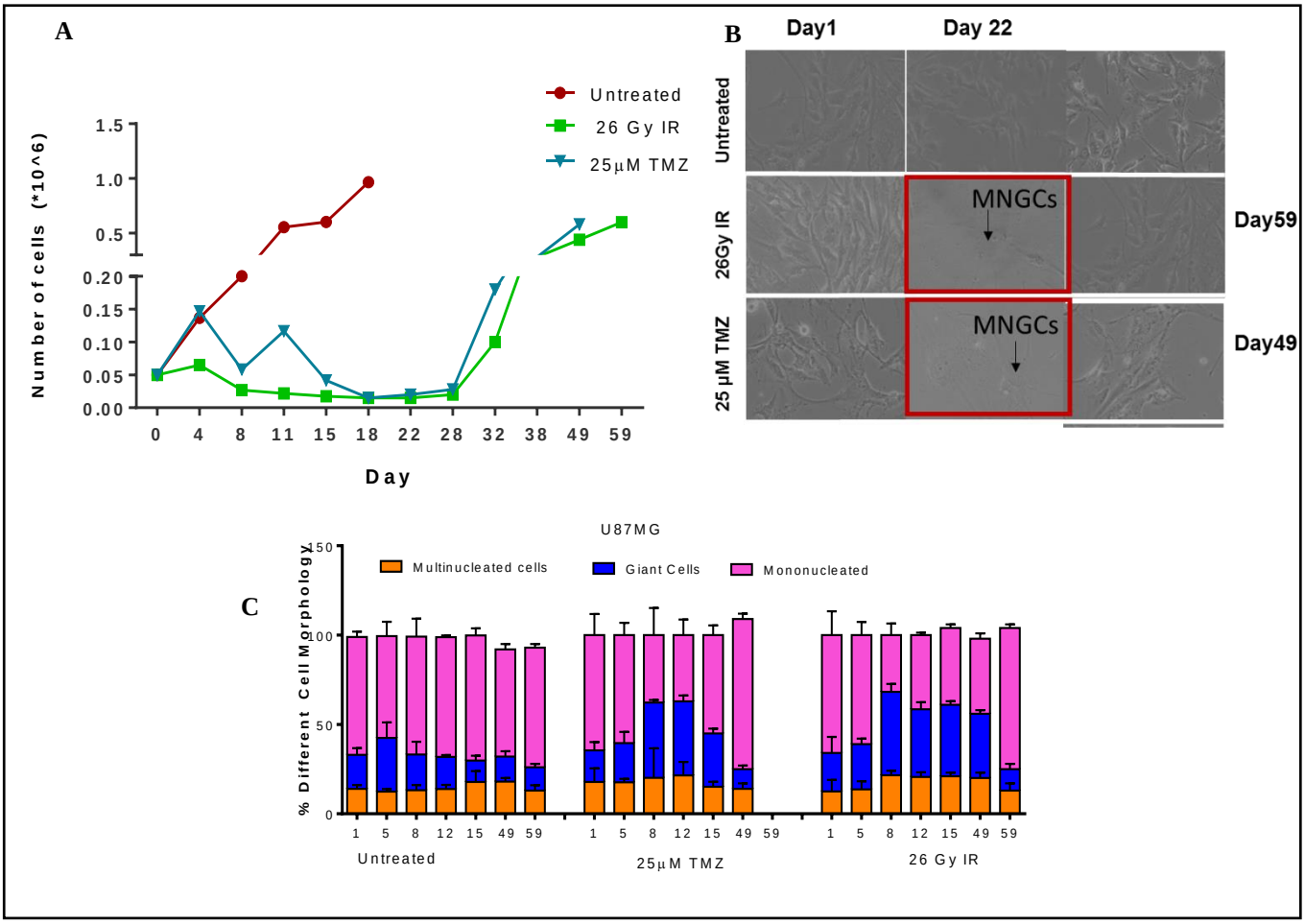

Figure 16 monitoring the presence of MNGCs in response to therapy.

(A) Growth kinetics of U87MG cells treated with a total of 26Gy radiation in 2Gy fractions for 13 days and daily administration of 25µM TMZ for 2 weeks. (B) Graphical representation of the % of Multinucleated, Giant cells and mononucleated cells present while the cells were treated. (C) Representative morphological images of U87MG cells in three different conditions on different days.

These cells remained in a non-proliferative phase for 17 days and resumed their growth to form relapse population. Similar to our previous results, the % of giant cells and multinucleated cells was > 50% in the non-proliferative cells until day 35 after which it gradually reduced as the cells resumed to grow back severely and further reduced to < 20% at day 59 (figure 16 B). Additionally, the cells that were treated with TMZ also showed a similar response. These cells

also started showing a significant reduction in cell number at day 15 and remained in a non-proliferative phase for about 20 days until the cells resumed their growth. More than 60% of non-proliferative cells were enriched with multinucleated and giant cells which diminished as the cells relapsed (figure 16 A, B & C). Thus, we conclude that MNGCs are formed in response to radiation and chemotherapy as well when administered in the clinical dosage.

3.2.4 Presence of MNGCs in other cancers.

Since MNGCs proved to be a vital component of the RR cells formed in glioblastoma, we expanded our study to other cancers. The lethal dose of radiation for 2 breast cancer cell lines (MCF7, T47D), colorectal cancer (HT29) and lung cancer (H1975) was determined using the clonogenic survival assay. The lethal dose of radiation was found to be 5.73 Gy, 6.99 Gy, 4.46 Gy and 4.24 Gy for MCF7, T47D, HT29, and H1975, respectively (figure 17 A, B, C, D).

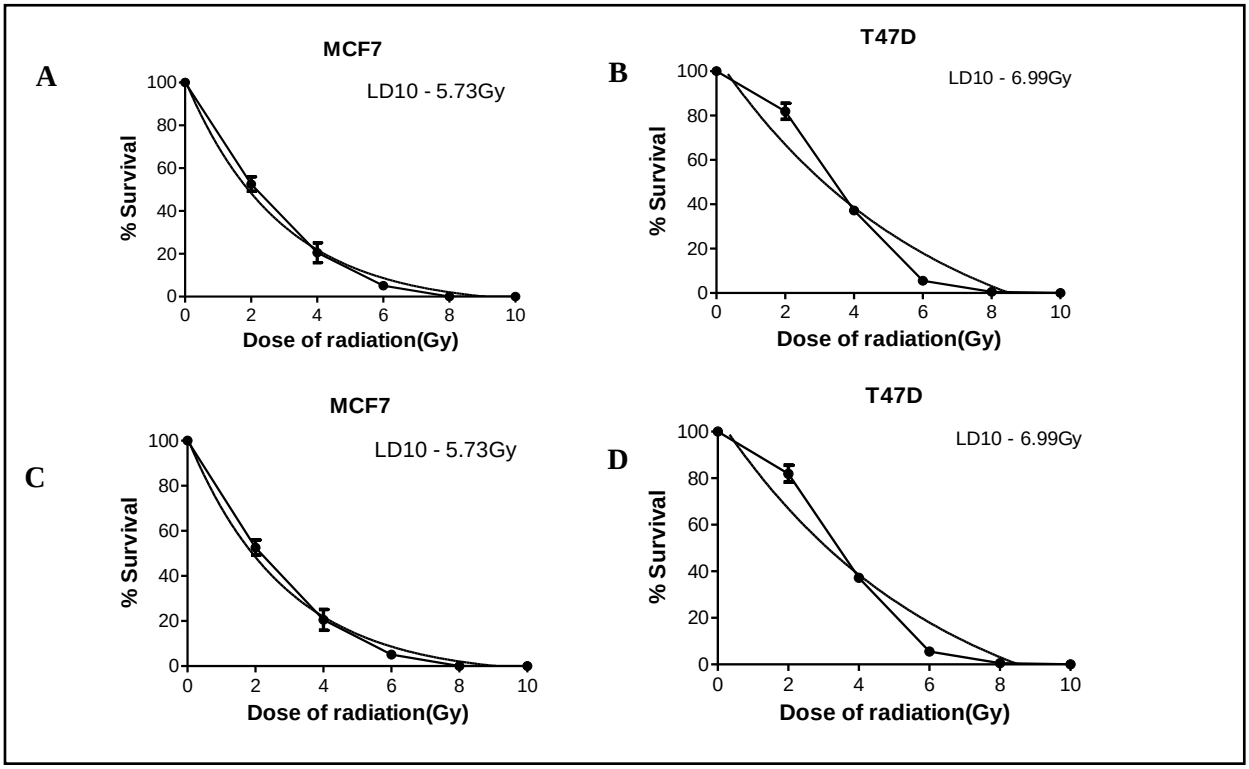

Figure 17 Clonogenic survival curves of different cancer cell lines.

These cell lines were then subjected to their respective lethal dose of radiation and monitored for cell viability and presence of MNGCs. Interestingly, it was observed that except for H1975, the other three cell lines exhibited the presence of non-proliferative cells (RR cells) following

radiation exposure. However, the time interval of the RR cells in the non-proliferative phase varied. MCF7 RR cells remained in an undivided state for almost 8-10 days, whereas T47D RR and HT29 RR cells where transiently non-proliferative only for 3-4 days (Figure 18 A, B, C & D).

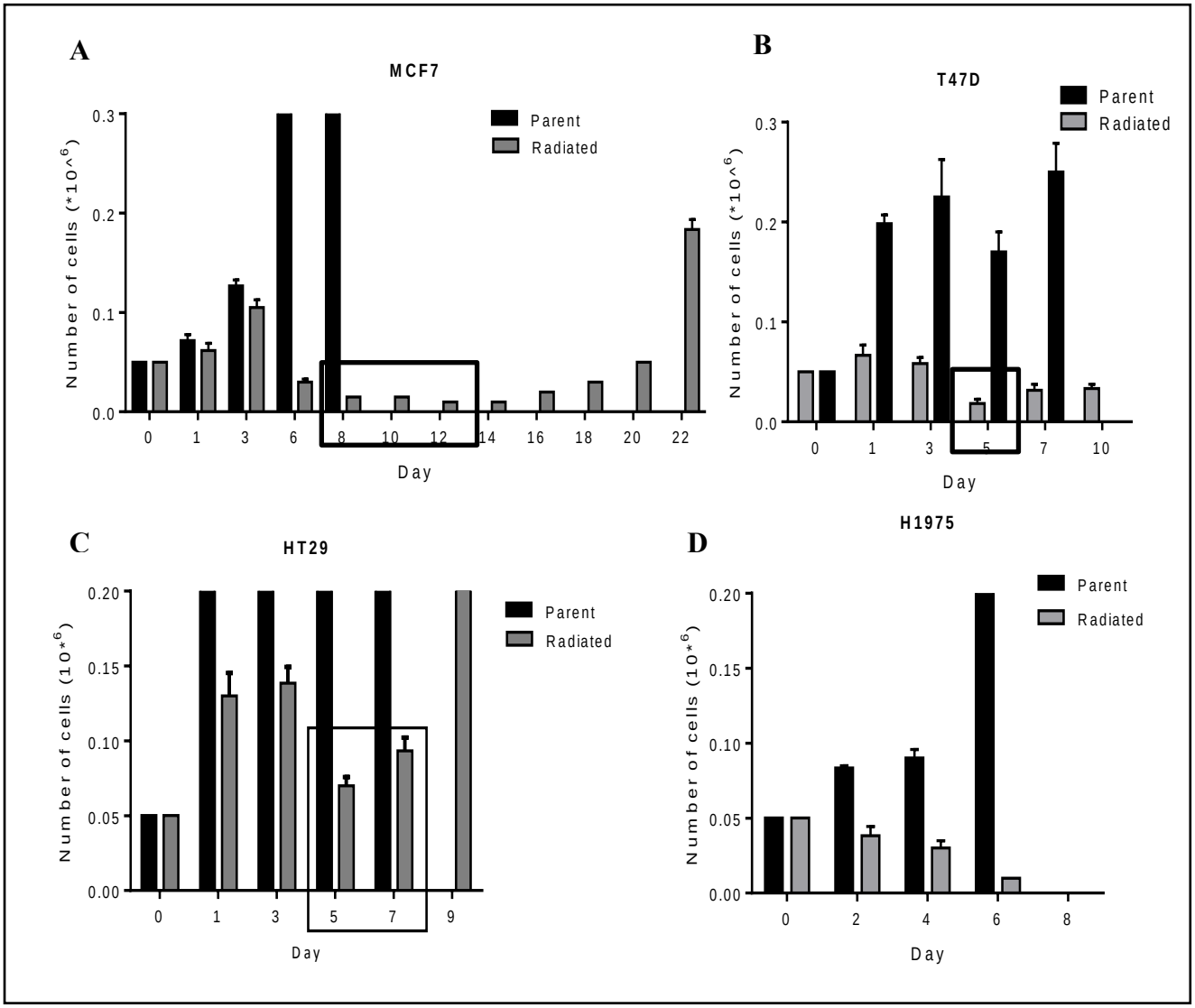

Figure 18 Growth kinetics of cell lines post radiation

Although the time period of the non-proliferative phase varied in these cell lines, in all 3 cases, the RR cells recommenced their growth to form the relapse cells. The RR cells of all the three cell lines were found to be enriched with MNGCs. (Figure 19 A, B, & C).

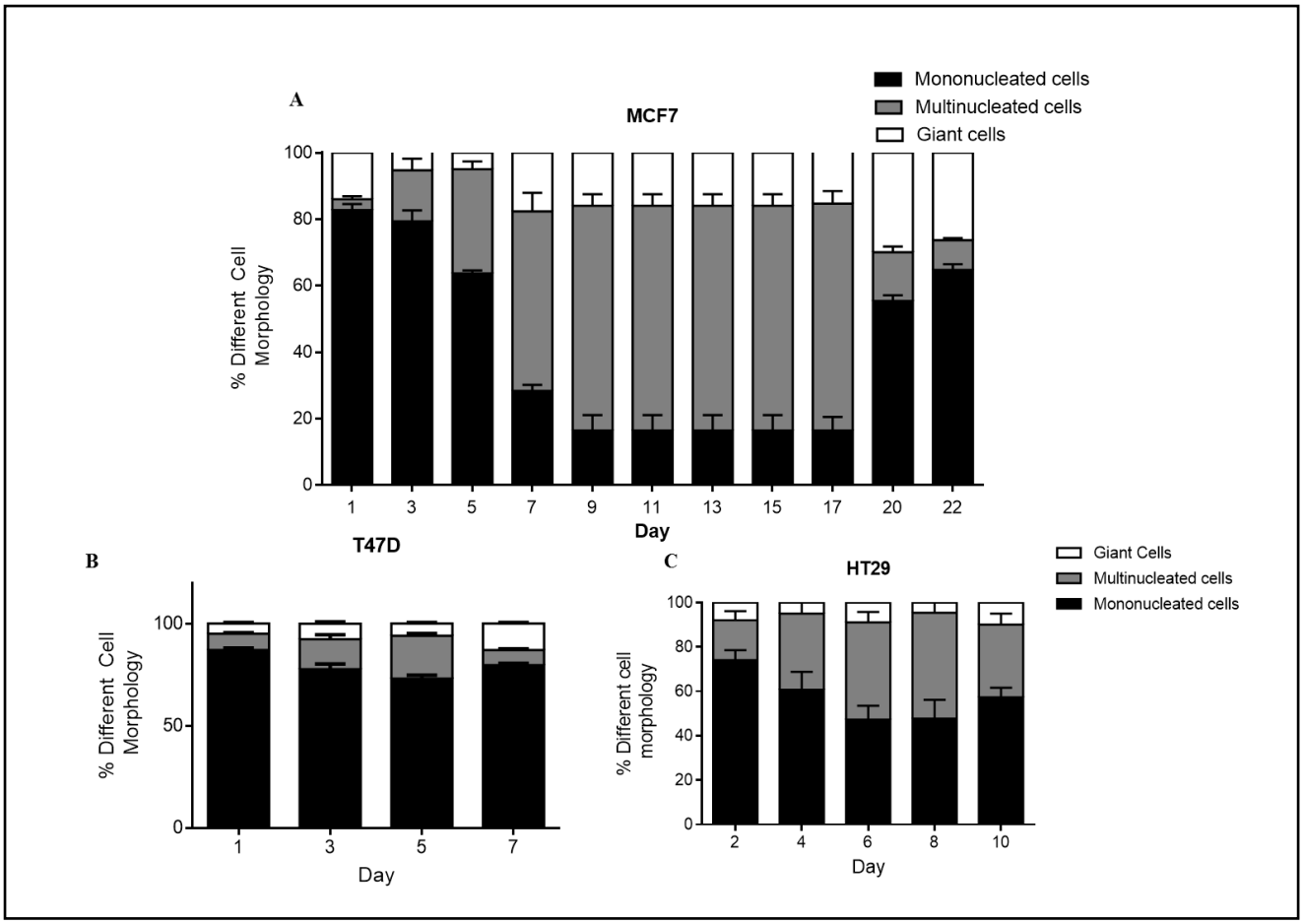

Figure 19 Morphological changes in response to radiation.

These RR cells also displayed increased expression of survival genes (SURVIVIN, BCLXL, BIRC3) and SASPs (IL-6, GM-CSF) along with p21 (figure 20).

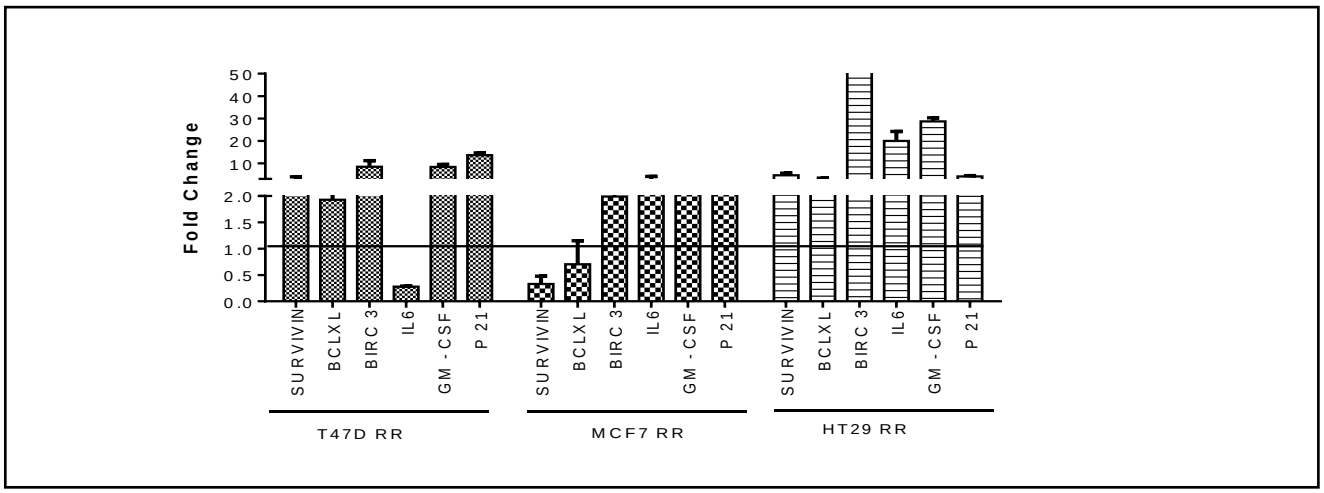

Figure 20 Presence of MNGCs in other cancer.

mRNA expression of survival, SASPs in the RR cells of T47D, MCF7 & HT29 as compared to the parent's cells

Taken together the data presented in this chapter demonstrate that the relapse cells are more aggressive in terms of their invasive and migrating properties compared to their parent cells. However, their survival response to radiation does not change significantly even after repeated exposure to lethal of radiation. Furthermore, the data shows that the presence of non-proliferative cells enriched with MNGCs is not a glioma-specific phenomenon or a radiation specific phenomenon. This phenotype was observed in the presence of clinically relevant dose of radiation and chemotherapy in GBM cell lines and in other cancers also.

3.3 Discussion

Glioblastoma comprises of > 60% of malignant gliomas due to its highly infiltrative nature and the ability of the cells to disperse. For this reason, recurrence in glioblastoma is an inevitable phenomenon owing to its aggressive nature and therapy resistance. The underlying cause for failure in the treatment of recurrent tumors is the lack of complete understanding of its biology. Therefore, it is necessary to conduct studies focussed on understanding the molecular differences between the primary and recurrent tumors. The lack of recurrent tissues available for biological studies is the foremost limiting factor for the small cohort. However, the scarcity in recurrent tissues due to inaccessibility of recurrent tumors for surgical resection, low tumor content and high necrotic tissue and insufficient paired samples of the primary and recurrent tumor makes it very difficult to understand the progression of glioblastoma from primary to recurrence. Thus, it is imperative essential to have resistance and recurrent model systems to be able to get insights into the biology of glioblastoma progression for a better understanding of glioblastoma progression.

Our *in vitro* radiation-resistant model empowers us to carry out studies on the relapse cells of GB cell lines (U87MG, SF268) as well as short-term cultures of patient samples, which are expanded from a subpopulation of innately radio-resistant cells after their respective parent

cells were exposed to a lethal dose of radiation. The relapse cells were found to be morphologically similar to their respective parent cells although they were formed after a transient non-proliferative phase of the MNGC enriched RR cells. Upon exposing the relapse cells to the second round of lethal dose of radiation, it was observed that the relapse cells showed a similar pattern of response to radiation as in the case of parent cells. Correspondingly, the R_1 cells also exhibited the presence of a subpopulation of cells which survived radiation and remained in a non-proliferative phase for 5-7 days and resumed growth to form R_2. The clonogenic survival assay revealed a no significant increase in radio-resistance as the cells progressed from P to R_1 to R_2. In this study, the aggressive nature of relapse cells was assessed. We first evaluated the radiation response of relapse cells as compared to parent cells. For which the relapse cells of U87MG and SF268 were subjected with the second round of lethal dose of radiation. However, R_1 cells showed a significant increase in their migrating and invasive potential as compared to the P. This data clearly indicates that the radiation therapy on recurrent tumors is ineffective. This incompetence of radiation therapy on recurrent tumors is due to the increased invasiveness of these tumors which makes them inaccessible for therapy along with the obstinate presence of pre-existing innate radio-resistant cells. These findings are consistent with the reports which have demonstrated radiation-induced invasiveness in glioblastoma. The results of this study in the relapse population provide a new in vitro platform which can be exploited in vivo to explore and dive deeper into the biology of innately radio-resistant and relapse cells.

Besides, we also determined whether the presence of MNGCs was the consequence of the sudden shock of a high dose of radiation or it is therapy induced. We observed that daily administration of radiation and temozolomide in vitro conditions also showed the presence of therapy resistant cells. The resistant cells formed after daily administration of TMZ and IR took a longer time to relapse compared to the radiation resistant cells formed after subjecting to a single round of lethal dose. The increased time span in the non-proliferative phase could be due to the prolonged exposure of cells to therapy which augmented cellular stress. Thus, the cells required an extended interval to combat stress and maintain

their oncogenic properties to relapse. Additionally, we also show that this phenomenon is not restricted to glioblastoma. In the study of different cancerous cell lines such as breast cancer (MCF7, T47D), colorectal cancer (HT29 and lung cancer (H1975) we show that in a heterogeneous mixture of cancerous cells, there exists a subpopulation of cells (RR cells) which is innately resistant to a lethal dose of radiation. Except in H1975, which is radio-sensitive and was taken as a negative control for the study, these RR cells, irrespective of the cancer type, display the presence of MNGCs which remain non-proliferative for a stipulated period of time and then resume growth. The time interval between the non-proliferative phase and the percentage of MNGCs in the RR cells varied amongst the different cell lines. MCF7 (p53 wild-type) exhibited a lengthier non-proliferative phase than T47D and HT29 which are p53 mutated cell lines. p53 functions as a transcription factor involved in cell-cycle control, DNA repair, apoptosis and cellular stress responses. However, besides inducing cell growth arrest and apoptosis, p53 activation also modulates cellular senescence and organismal aging. The increased expression of SASPs (IL-6, GM-CSF) indicates that the non-proliferating RR cells enter senescence post radiation exposure. The different time period of reversible senescent phase in the RR cells of the three cell types could be attributed to the difference in their p53 status. Thus, the formation of MNGCs is an adaptive nature of cancer cells to overcome therapy induced stress and we also showed in another studies from our lab that indeed the percentage of giant cells in the residual resistant population independently correlate with a poor patient survival (109). A detailed study of the molecular mechanism involved in their genesis would provide deeper insights into battle therapy resistance in cancer.

4 Differential proteomic analysis of parent, radiation resistant and relapse population using quantitative proteomic

This chapter includes the description of the differential proteomic analysis using iTRAQ technology in Parent, RR and R cells of SF268 in at least 3 biologically independent experiments. The dataset obtained was analyzed for relevant biological functions using two approaches: a) Pathway-based approach b) Candidate based approach. Thus this chapter is divided into two sections. The first section describes the identification and validation of the proteasome pathway as an essential part in the survival of RR cells. The second section is the identification and functional role of 14-3-3 zeta in glioblastoma and the RR cells of GBM.

4.1 Identification and functional validation of pathways deregulated in RR and R cells

4.1.1 Introduction

Glioblastoma is a heterogeneous tumor comprising of highly neovascular and infiltrating tumor cells. The complexity of this fatal disease is attributed to the multifaceted biological processes governing its progression. Despite the multimodal therapy adopted, recurrence is inevitable in Glioblastoma patients. The irrepressible recurrent tumors are reported to arise from a subpopulation of residual cells which are otherwise not visible in the MRIs post initial treatments. These residual cells are reported to be unique entities which are potential targets to combat therapy resistance. However, targeting residual resistant cells of glioma is challenging since they are inaccessible from the patient biopsies for biological studies (26)

A paradigm shift in the treatment modality for this tumor type requires a widespread understanding of the key molecular players and biological processes involved in enabling the residual cells to resist therapy and initiate relapse. Quantitative proteomics using iTRAQ based technology empowers us to explore the entire proteome which are the final effectors of a molecular process that gets altered as the cells transform from normal to cancerous type and later into an aggressive tumor (78). Isobaric tag for relative and absolute quantitation (iTRAQ) is an MS-based approach for the relative quantification of proteins, relying on the derivatization

of primary amino groups in intact proteins using the isobaric tag for relative and absolute quantitation. Due to the isobaric mass design of the iTRAQ reagents, differentially labeled proteins do not differ in mass; accordingly, their corresponding proteolytic peptides appear as single peaks in MS scans. The isotope-encoded reporter ions that can only be observed in MS/MS spectra allow for calculating the relative abundance (ratio) of the peptide(s) identified by this spectrum (78).

Many proteomics studies have been performed to explore different aspects of glioblastoma. However, the majority of proteomics studies in glioblastoma have focused on identification of differential proteins amongst different GBM cell lines, patient samples or within a same tumor to investigate the heterogeneity of glioblastoma, mechanism of chemoresistance and identification of diagnostic biomarkers (23, 86, 110). But, none of these studies could identify the survival mechanism of innately resistant cells due to their unavailability. This study identifies the proteomic signature of residual resistant and the relapse cells of glioblastoma from captured form the cellular model as described in chapter 1 of this thesis.

.

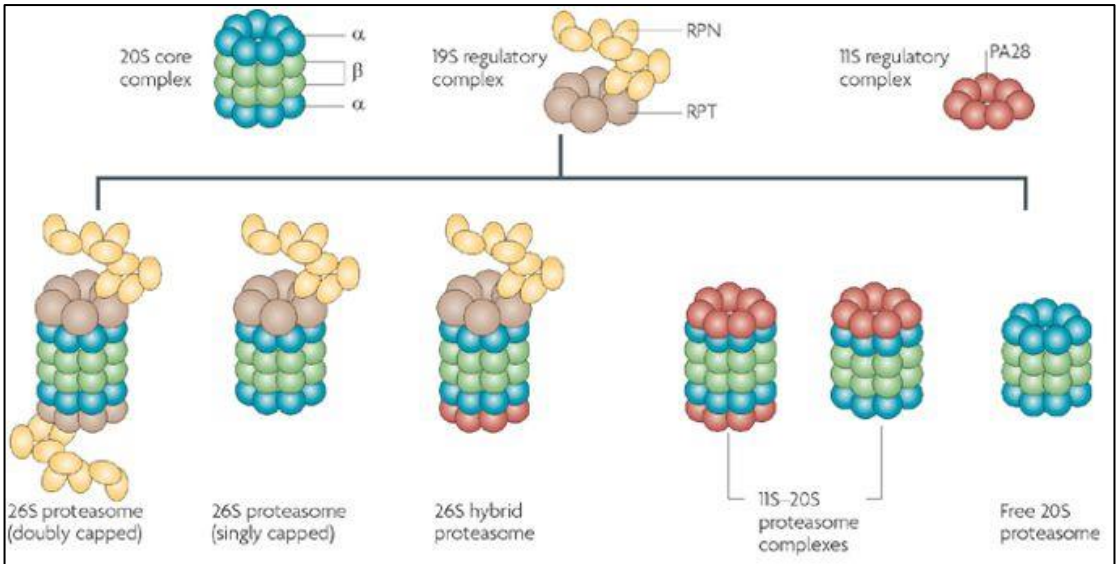

Figure 21 Different types of proteasomes

Nature Reviews | Neuroscience

The proteasome is a multimeric proteinase, abundant in all eukaryotic cells and controls degradation of intracellular proteins in a specific manner. This large 2MDa multisubunit complex functions by the association of 20S proteasomes to a variety of regulator complexes like a 19S regulator, PA28ab, PA28g, PA200, EMC29, PI31 as shown in figure 21. As a result, there are various types of proteasomes such as 26S proteasome (19Sreg - 20Sprot), 30S proteasome (19Sreg - 20Sprot - 19Sreg), hybrid proteasome (19Sreg - 20Sprot -PA28), PA28-proteasome (PA28 - 20Sprot - PA28) complexes and others (111).

26S Proteasome is known as the classical proteasome plays a vital role in maintaining cellular protein homeostasis by degrading many proteins, and regulating many cellular processes. It controls expression of short-lived cell cycle and cell death regulators and transcription factors, such as cyclin A, B and E, p21 and p27, p53, cJun, cFos, and nuclear factor κB (NF-κB) (112). Amongst these, NF-κB is a family of transcription factors that can form different heterodimers or homodimers with any of these 5 subunits: p50 (NF-κB1, p105), p52 (NF-κB2, p100), p65 (RelA), RelB, and c-Rel. Under normal conditions, NF-κB dimers are present in the cytoplasm bound to inhibitor-κB (IκB) proteins (113).

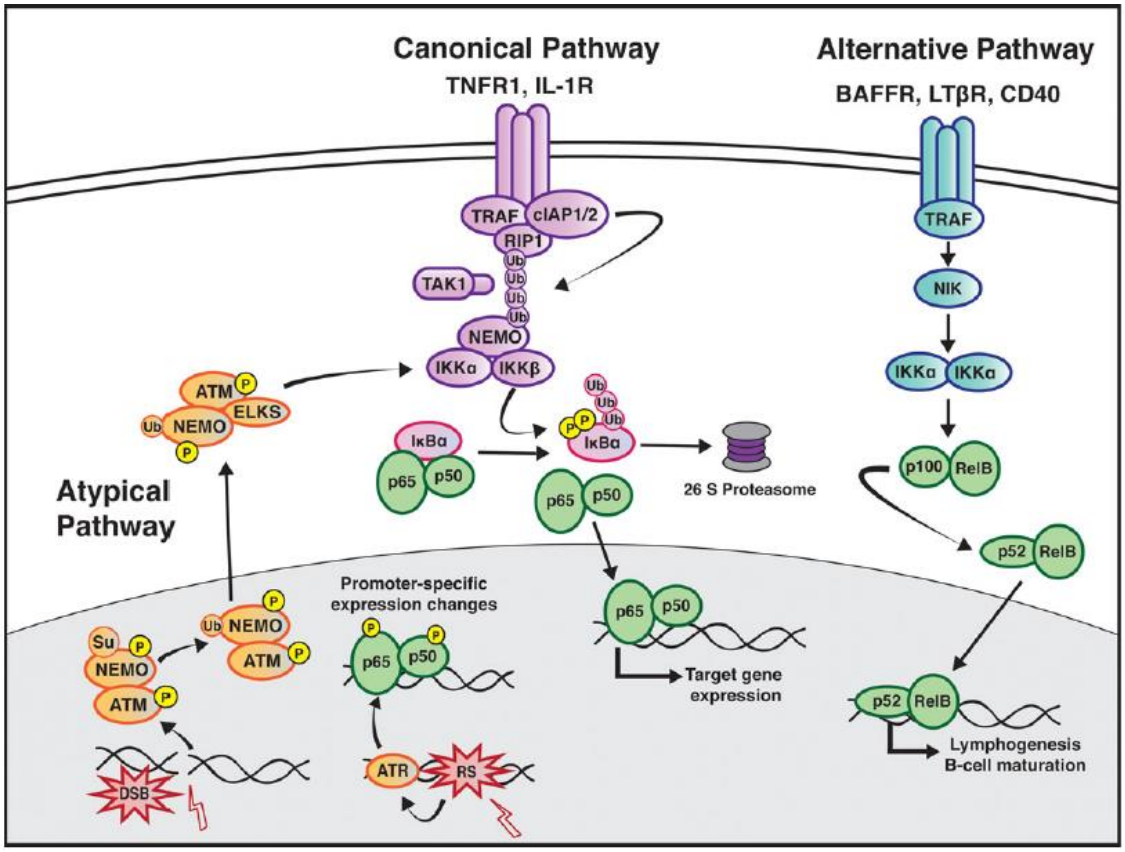

Figure 22 Nf-kB an indirect target of proteasomes (2)

The proteasome mediated degradation of phosphorylated form of IκB results in the activation and translocation of NF-kB to the nucleus where it binds to its target genes and regulates transcription. The tumor cells are more dependent on proteasomes to get rid of misfolded and damaged proteins due to their genomic instability and rapid proliferation. Thereby, preventing cellular stress and apoptosis. Also, there are some reports which show that the overexpression of proteasomal subunit proteins is involved in elevated levels of proteasome activity. Hence, proteasomes are well-known targets in cancer therapy. In the context of radio-resistance, proteasome activity has been found to be reduced in radio resistant cells (114-119). In this chapter, we show that innately radio-resistant GBM cells harbor increased expression of proteasomal subunits, enhanced proteasome activity and increased levels of proteasome substrate p-NFkB and a concordant increase of NFkB target genes. We demonstrate pharmacological inhibition of proteasomal activity reduces NFkB transcriptional activity and

radiosensitizes RR cells. Furthermore, the absence of proteasome activity in RR cells also significantly decreases their ability to form tumors *in vivo.*

Together, our proteomics data has delineated proteasomal pathway as one of the plausible targetable mechanisms that significantly contribute to the survival of innate radiation residual cells via the NFkB signaling cascade.

4.1.2 Results

4.1.2.1 Recapitulating the clinical scenario using innate radiation resistant (RR) and Relapse (R) cells from an in vitro radiation resistant model

To capture and understand the survival mechanisms of residual resistant cells of GBM, that are diagnostically undetectable post-treatment, we generated *in vitro* radiation resistant model derived from cell lines and patient samples (21) (Figure 23 A). Using the same protocol, in this study first the glioblastoma cell lines (SF268 and U87MG) and two short-term primary cultures of patient samples (PS1 and PS2) were subjected to their respective lethal dose of radiation (6.5Gy, 8Gy, 6Gy, 6.5Gy) as determined previously using clonogenic assay (21). Post-treatment initially the cells proliferate, but after 4-5 days post-treatment more than 90% cells died leaving behind a small population (< 10%) surviving cells. These cells are the innately radiation resistant residual cells (RR) which remain viable but non-proliferative for approximately 7-10 days and acquire Multinucleated Giant (MNGCs) phenotype. However, instead of undergoing mitotic catastrophe, RR cells resume growth to form the relapse (R) population. Figure 23 B shows graphs for SF268 and PS1 growth pattern of RR cells. The parent (P), innately radiation resistant (RR) and relapse (R) cells obtained from SF268 were then subjected to quantitative proteomic analysis. The three populations obtained from U87MG, PS1, and PS2 were used for validation and functional studies.

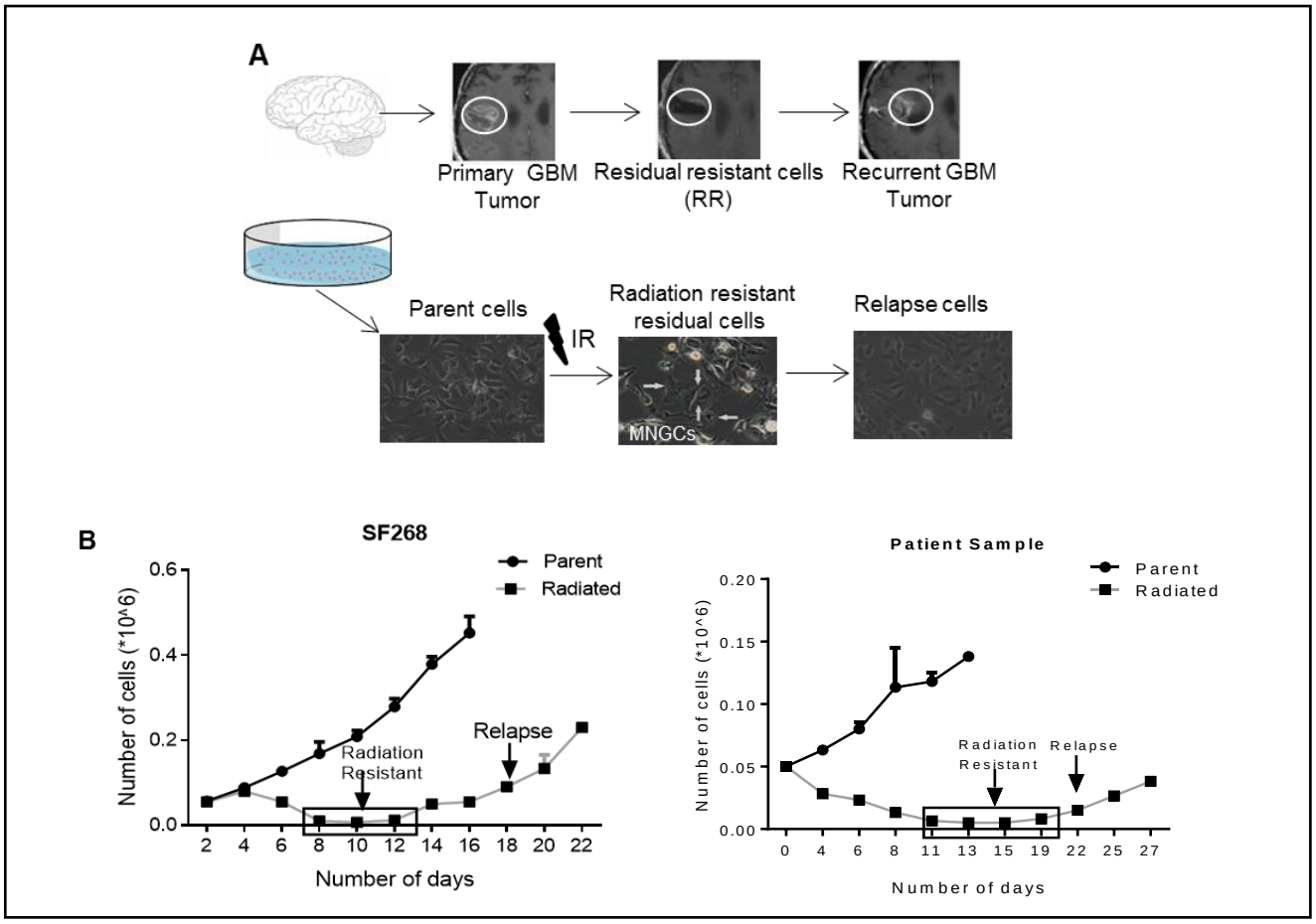

Figure 23 In vitro radiation resistant model

(A) The illustration depicts the clinical scenario in patient's pre and post-treatment in which post-surgery there is a significant regression or complete abolishment of the tumor observed. However, in > 90% cases tumor recurs. This clinical scenario was recapitulated in an in vitro model. The images represent the SF268 Parent, innate Radiation Resistant (RR) enriched with multinucleated giant cells (MNGCs) and Relapse (R) population. (B) The graph represents the growth kinetics of SF268 and Patient Sample post lethal dose of radiation.

4.1.2.2 Quantitative proteomic analysis of radioresistant (RR) and relapse (R) cell

iTRAQ based quantitative proteomic analysis was performed on the parent, RR and R cell population of SF268. Figure 24 illustrates the proteomics workflow. Equal amounts of protein from the Parent, RR and R populations was digested with trypsin and their tryptic peptides were labeled with 114, 115 and 116 isobaric reagents respectively for differential protein expression analysis. The iTRAQ-labelled peptide samples were pooled, fractionated and analyzed by LC-MS/MS. The data obtained were searched against National Centre for

Biotechnology Information RefSeq database (version 52 40) using Protein Discoverer (version 1.4) using MASCOT and SEQUEST.

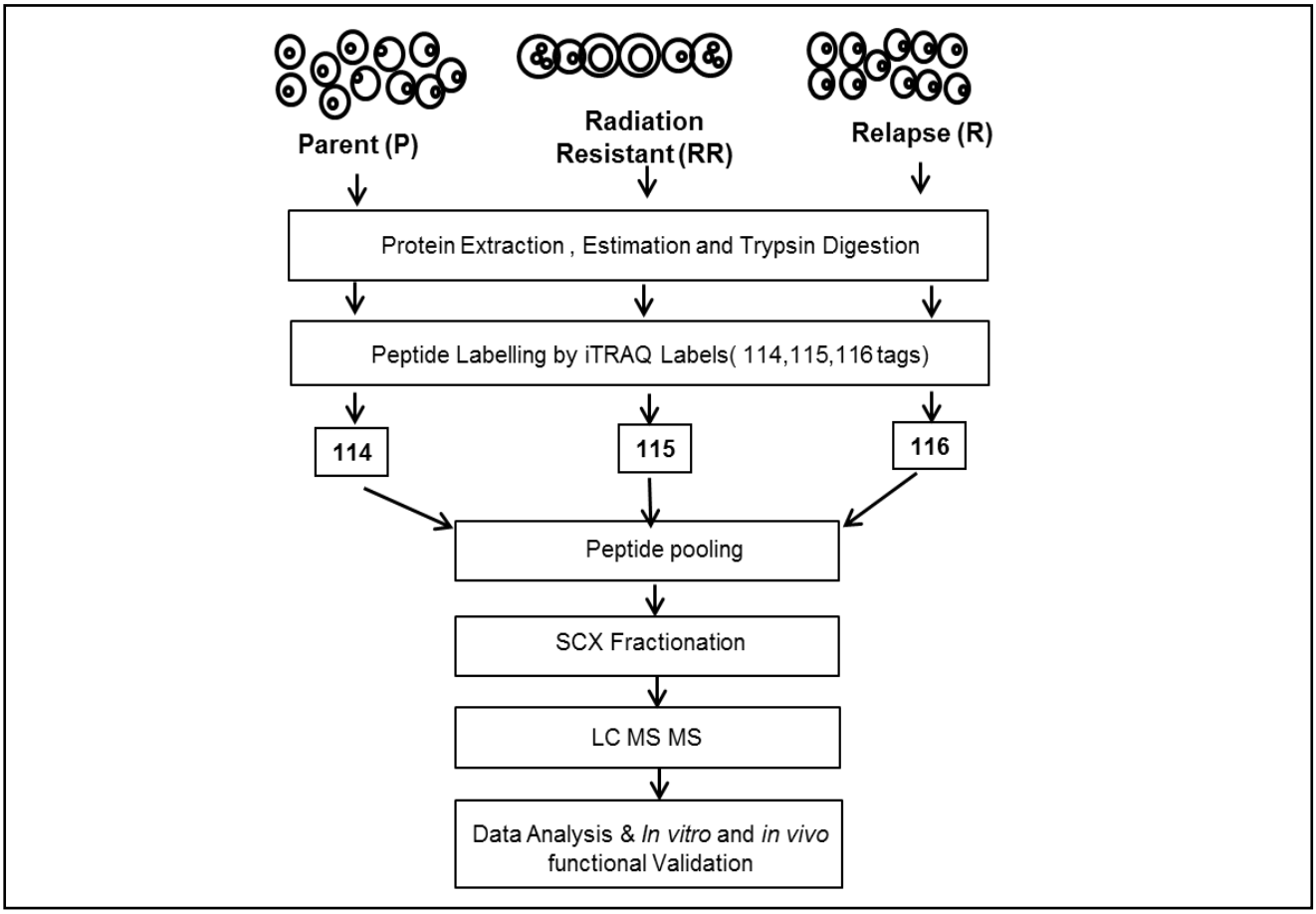

Figure 24 A schematic representation of the proteomics workflow.

Compared to parent cells 824 proteins were found to be differentially expressed in RR cells compared to parent cells out of which 393 proteins were up-regulated (fold change >1.5) and 431 proteins were downregulated (fold change <0.7) while 874 proteins were differentially expressed in relapse population of which 352 proteins were up-regulated (>1.5) and 522 proteins were downregulated (<0.7). 1,392 proteins were differentially regulated in R vs. RR out of which 747 proteins were upregulated (>1.5) and 645 were downregulated (<0.7) in the R population (Figure 25 A). iTRAQ data was validated by analyzing the expression levels of HRAS, EGFR, YBX3 (Figure 25 B). Relative peptide intensity values of the three proteins from mass spectrometry showed concurrent expression with the western blot data (Figure 25 C).

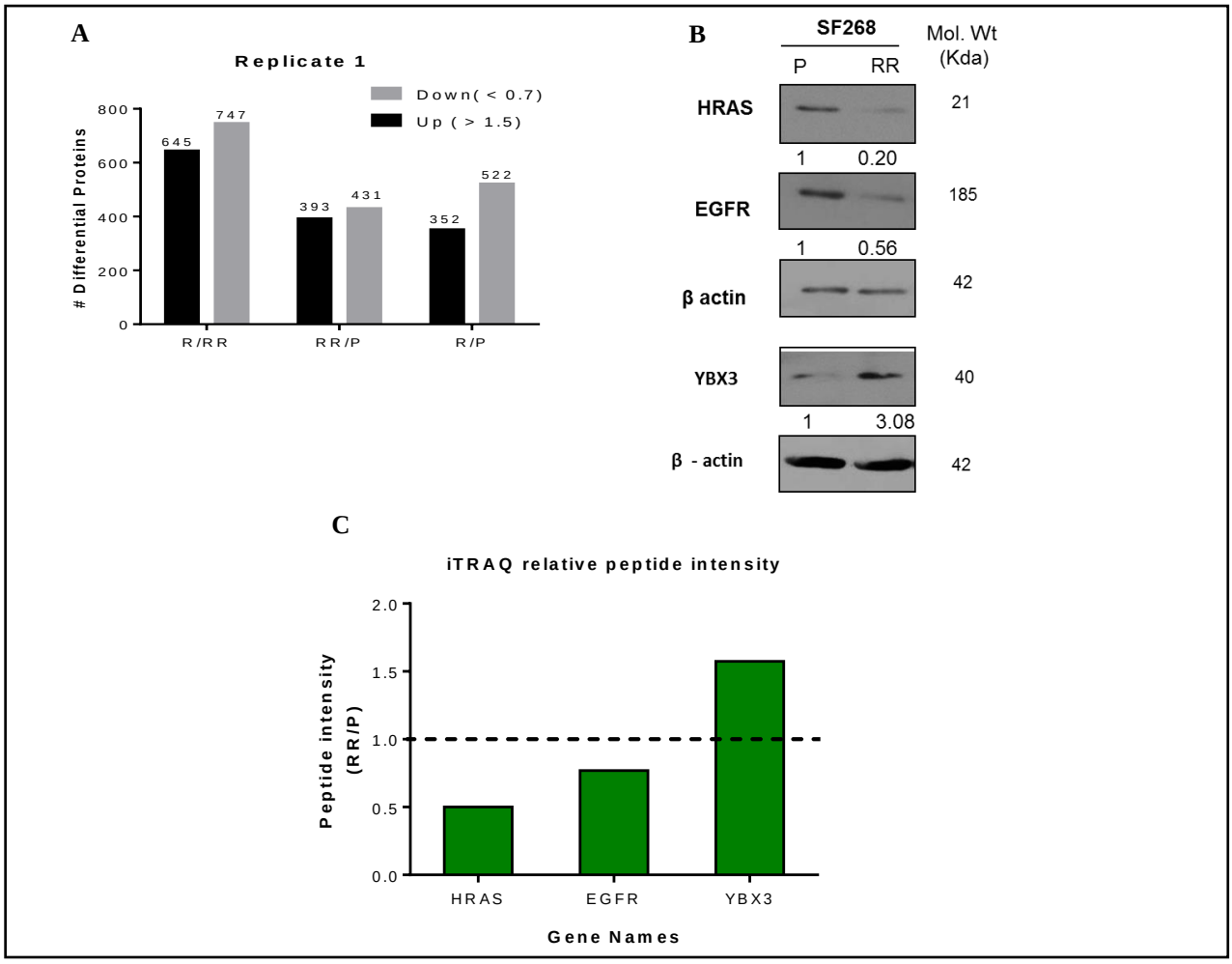

Figure 25 Proteomic analysis of the parent (P), radiation resistant (RR), relapse(R)

(A)Graphical representation of the number of differential proteins identified in the RR and R w.r.t P and R w.r.t RR by the proteomic analysis. Results in each bar graph are the composite data from three independent experiments performed in triplicate (mean ± SEM). (B) Western blots showing the expression of HRas, EGFR, YBX3 in Parent (P), Radiation Resistant (RR) and Relapse (R) population of SF268 cell line. β–actin was used as loading control. (C) Bar plot of the relative peptide intensity values of the mentioned proteins in RR/P and R/P as determined by iTRAQ.

4.1.2.3 Unsupervised clustering of proteomics data identifies protein clusters uniquely differential in each population.

Since a cell's phenotype is an outcome of a collective network of biological processes, it was hypothesized that proteins showing similar expression pattern will participate in similar biological processes. Therefore, we first identified the proteins showing co-expression, for which unique master differential gene list was compiled the at least one of the three binary comparisons (RR Vs. P, R Vs. P, R Vs. RR) which comprise of 1773 genes. Unsupervised

clustering was performed for these genes based on their respective relative protein abundance values as represented in a heat map. The expression pattern of each cluster is illustrated as a line plot (Figure 26).

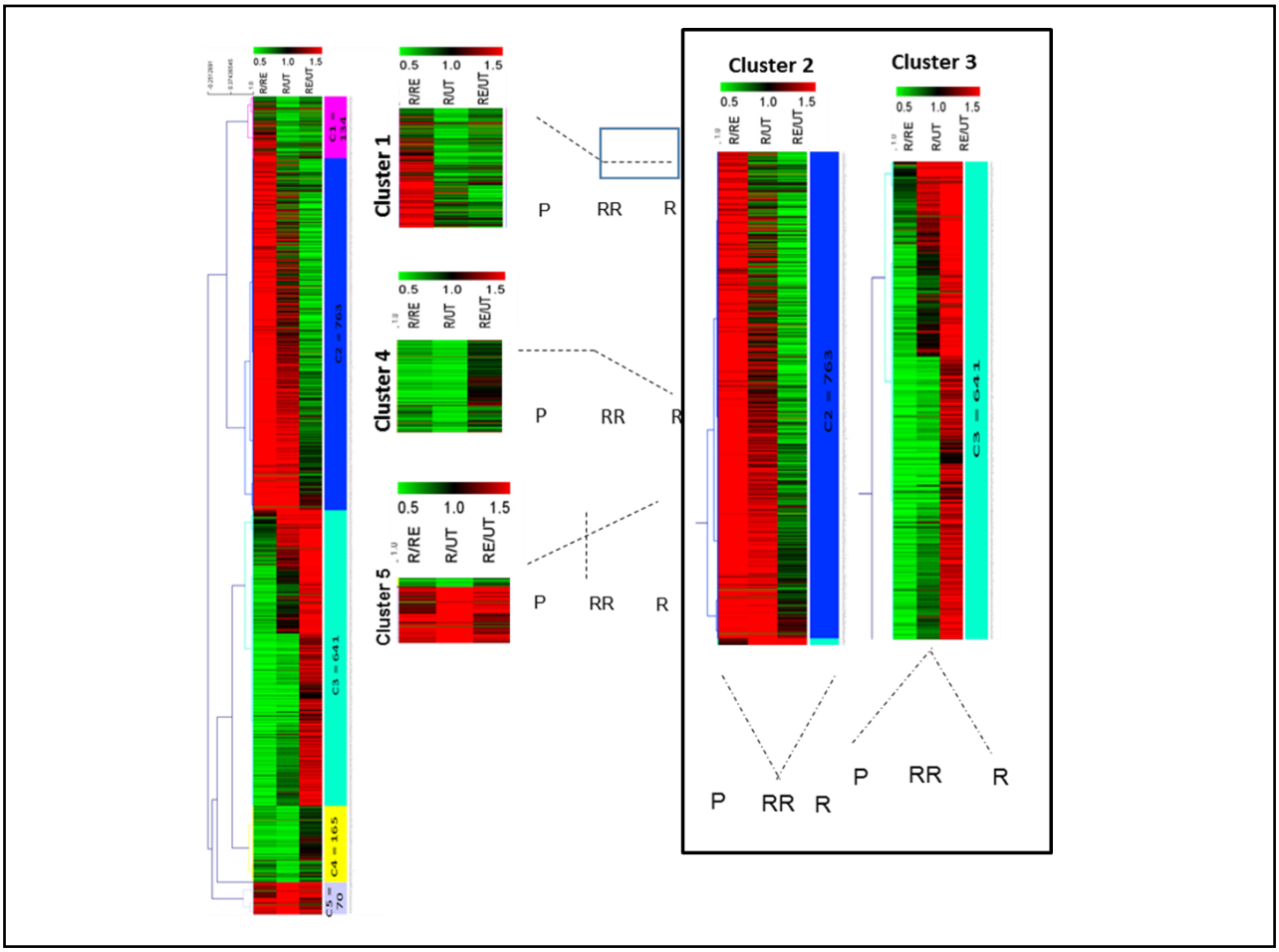

Figure 26 Unsupervised clustering of differential proteins.

Heat map representation of unsupervised hierarchical clustering of the proteins based on their relative peptide intensities in R w.r.t RR, RR w.r.t P and R w.r.t P. Red- Upregulation > 1.5, Green- Down

Analysis segregated the data set into five clusters (C1-C5) out of which two major clusters, cluster 2 and cluster 3 represented proteins that were exclusively enriched with uniquely downregulated and upregulated proteins in the RR population, respectively. Cluster 2 represents 783 proteins and Cluster 3 represents 641 proteins. Clusters 1, 4 and 5 comprised of proteins that showed a similar expression pattern in RR and R cells. 134 proteins were found to be downregulated in the RR and R as compared to the parent cells (cluster 1). The expression of 165 proteins remains at a basal level in the P and RR population however their expression

declines in the R cells (cluster 4) and 70 proteins show an escalation in expression in the RR and R as compared to the P cells (cluster 5). Since we were interested to know how the RR cells survive, we focused on the proteins classified in cluster 2 and cluster 3 which comprised of proteins uniquely downregulated and upregulated in the RR cells, respectively.

4.1.2.4 Pathway analysis reveals deregulation of proteasome and protein turnover machinery proteins in RR population and focal adhesion pathway in relapse population

To analyze the molecular pathway that might be involved in the survival and radiation resistance mechanisms of RR cell, pathway enrichment analysis of the deregulated proteins in

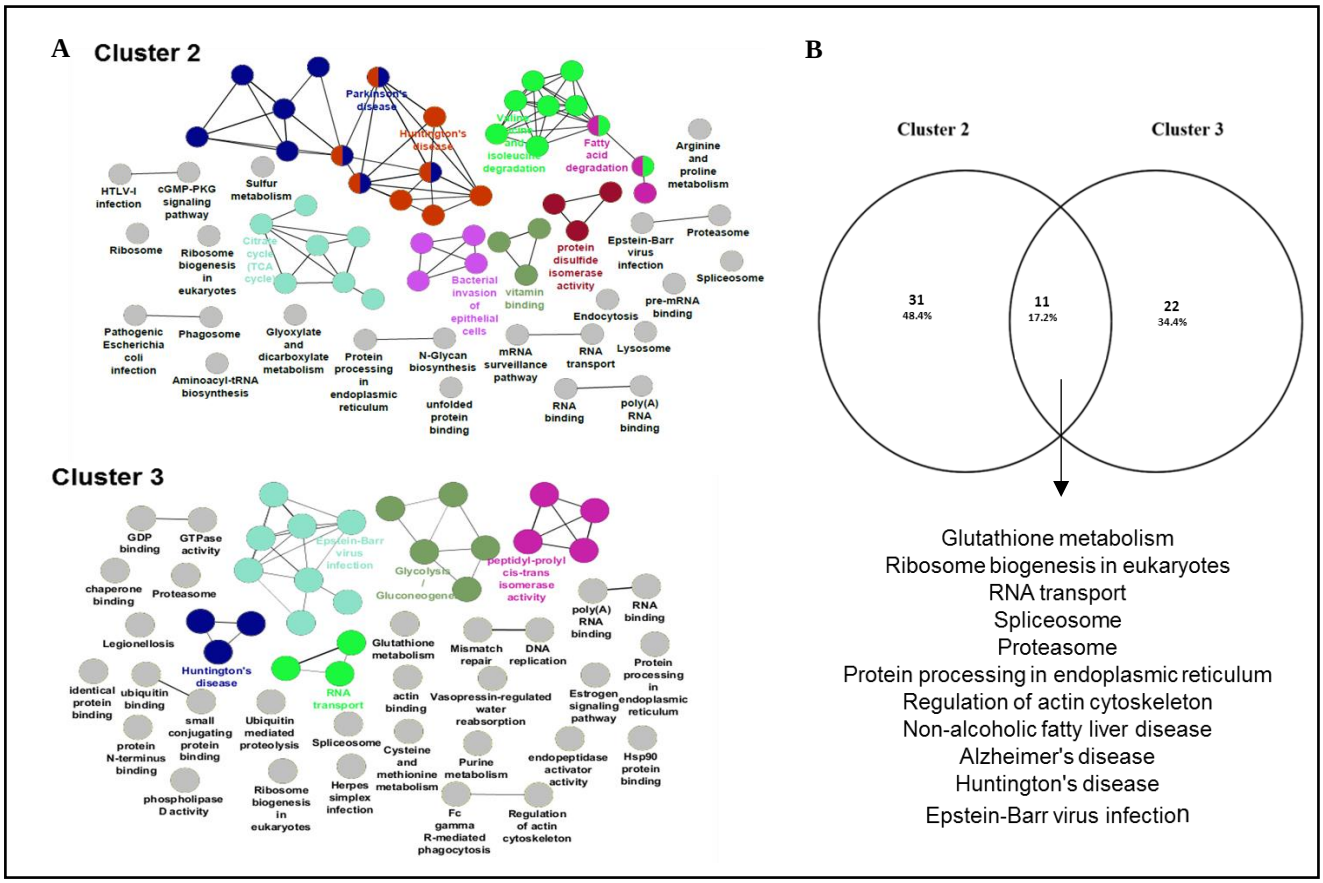

Figure 27 Pathway analysis of the cluster 2 and cluster 3

(A) Pathway analysis of the Genes in cluster 2 and cluster was collapsed into pathways using ClueGo and CluePedia plugin of Cytoscape with KEGG and REACTOME pathway databases. Each colored circle represents a pathway enriched with upregulated and downregulated protein in the RR cells but non-differential in the R cells. E. (B) Venn diagram for the overlap of pathways between cluster 2 and cluster 3

RR population compared to parent population in cluster 2 and cluster 3 was done using KEGG and REACTOME database (Figure 27 A). In total 42 pathways were deregulated in cluster 2, 33 pathways were deregulated in cluster 3. Interestingly, 11 pathways were commonly deregulated in both cluster 2 and 3 (Figure 27 B). These pathways included glutathione metabolism, ribosome biogenesis in eukaryotes, RNA transport, spliceosome, and proteasome, protein processing in endoplasmic reticulum, regulation of actin cytoskeleton, non-alcoholic fatty liver disease (NAFLD), Alzheimer's disease, Huntington's disease and Epstein - Barr virus infection. Additionally, gene ontology and enrichment analysis of the entire differential proteins found in the RR compared to the parent cells revealed 24 pathways enriched with upregulated (red circle) and downregulated proteins (green circle). Of these, 8 pathways were enriched with upregulated proteins and 16 pathways were enriched with downregulated proteins (Figure 28 A). Out of the 8 pathways that were enriched with upregulated proteins, 5 statistically significant (Term p-value < 0.05) pathways included Proteasome (8 proteins), Ubiquitin mediated proteolysis (10 proteins), Protein processing in Endoplasmic Reticulum (18 proteins), RNA Transport (17 proteins), oocyte meiosis (9 proteins). However, proteasome pathway was the most deregulated pathway based on the associated genes filter (k/K ratio) as shown in figure 28 B.

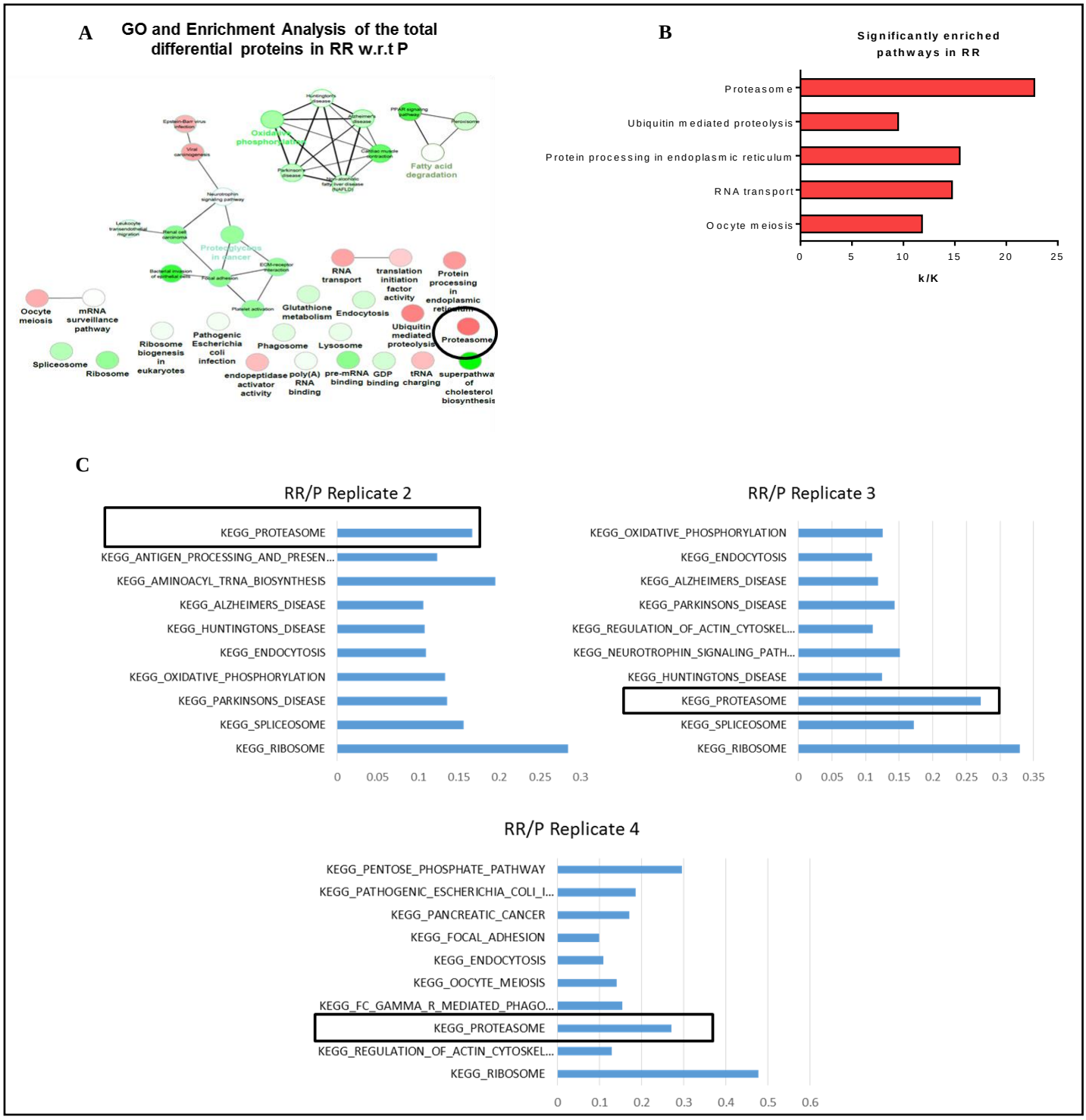

Figure 28 Deregulated pathways in the radiation resistant and relapse population

A) Pathway analysis of deregulated genes in Radiation Resistant (RR) vs. Parent (P) Genes deregulated in RR w.r.t P were collapsed into pathways using ClueGo and CluePedia plugin of Cytoscape with KEGG and REACTOME pathway databases. The color gradient shows the number of genes of each group associated with the pathway. Equal proportions of the two clusters are represented in white. (B) KEGG pathways enriched with upregulated proteins according to their k/K ratio. k – Number of genes identified from the pathway, K – Total number of genes curated in the KEGG database for a pathway. (C)Pathway analysis of deregulated proteins in all the biological replicates.

Proteomic analysis from three biological replicates also revealed significant deregulation of the proteasome pathway in the RR population (Figure 28 C). Proteasome subunits differential in all the four biological replicates has been represented in Table 1. Three subunits PSME1, PSMA7, and PSMB4 were used for validation by western blot (Figure 29 A, B & C). The data sets of all the replicates have been deposited to the ProteomeXchangeConsortium (http: //proteomecentral. proteomexchange.org) via the PRIDE partner repository.

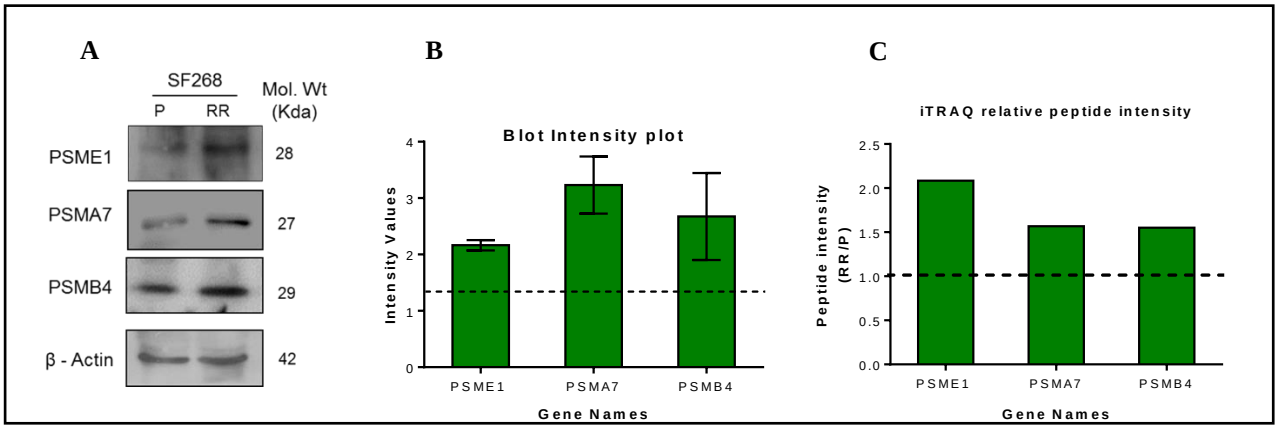

Figure 29. Validation of proteomics data

(A) Western blot showing the expression of PSME1, PSMA7 and PSMB4 parent (P), Radiation Resistant (RR) and Relapse (R) cells of SF268. β-actin was used as loading control. (B) Band intensity plot for the proteins validated by western blot using IMAGE J software. (C) Shows the relative peptide intensity values of the three proteins from iTRAQ analysis

4.1.2.5 RR cells display enhanced proteasome activity and survival dependency on proteasome activity in vitro

Since the RR population exhibited increased protein expression of proteasome subunits, we sought to observe if the expression correlated with proteasome activity. Therefore, proteasome activity was analyzed in the parent and RR cells of SF268, U87MG, PS1 and PS2 using florigenic substrate Suc-LLVY-Amc. Indeed the RR population of SF268, U87MG, PS1, and PS2 showed 22.18%, 35.60%, 20.63% and 71.63 % increase respectively in the proteasome activity compared to the parent cells (Figure 30 A). Among the 9 subunits overexpressed in the RR, 3 subunits are part of the 19S regulatory subunit – PSMC1, PSMD2, PSMD7;3 subunits

of the 20S core particle – PSMA1, PSMA7, PSMB4 and 1 subunits of the 11S regulatory subunits – PSME1.

Table 1 List of proteasome subunits differentially expressed in all biological replicates.

Gene Symbol	Protein Description	Σ# Unique Peptides	Σ# PSMs	Fold Change in RR/P
REPLICATE 1				
PSME1	proteasome activator complex subunit 1 isoform 1 [Homo sapiens]	4	4	2.085
PSMD7	26S proteasome non-ATPase regulatory subunit 7 [Homo sapiens]	3	6	1.977
PSMA1	proteasome subunit alpha type-1 isoform 3 [Homo sapiens]	1	2	1.634
PSMD2	26S proteasome non-ATPase regulatory subunit 2 [Homo sapiens]	9	12	1.632
PSMA7	proteasome subunit alpha type-7 [Homo sapiens]	4	13	1.568
PSMB4	proteasome subunit beta type-4 [Homo sapiens]	2	4	1.550
PSMC1	26S protease regulatory subunit 4 [Homo sapiens]	6	10	1.518
PSMA3	proteasome subunit alpha type-3 isoform 2 [Homo sapiens]	2	4	0.656
PSMD14	26S proteasome non-ATPase regulatory subunit 14 [Homo sapiens]	3	4	0.593
REPLICATE 2				
PSMD9	26S proteasome non-ATPase regulatory subunit 9 isoform 1	4	6	1.88
PSMD10	26S proteasome non-ATPase regulatory subunit 10 isoform 1	6	9	1.523
PSMC1	26S protease regulatory subunit 4	19	57	1.381
PSMC6	26S protease regulatory subunit 10B	16	48	1.356
PSMD8	26S proteasome non-ATPase regulatory subunit 8	10	21	1.356
PSMA4	proteasome subunit alpha type-4 isoform 1	10	35	1.294
PSME2	proteasome activator complex subunit 2	12	30	1.281
PSMD13	26S proteasome non-ATPase regulatory subunit 13 isoform 1	19	47	1.243
PSMD7	26S proteasome non-ATPase regulatory subunit 7	10	19	1.227
PSMD12	26S proteasome non-ATPase regulatory subunit 12 isoform 1	22	44	1.207
REPLICATE 3				
PSMD9	26S proteasome non-ATPase regulatory subunit 9 isoform 1	5	7	3.587
PSMC5	26S protease regulatory subunit 8 isoform 1	21	54	1.525
PSMB10	proteasome subunit beta type-10 precursor	1	1	1.445
PSME2	proteasome activator complex subunit 2	9	29	1.41
PSMD6	26S proteasome non-ATPase regulatory subunit 6 isoform 2	19	30	1.382
PSMD4	26S proteasome non-ATPase regulatory subunit 4	12	27	1.362
PSMA3	proteasome subunit alpha type-3 isoform 1	9	25	1.326
PSMD8	26S proteasome non-ATPase regulatory subunit 8	9	19	1.321
PSMC6	26S protease regulatory subunit 10B	18	52	1.318
PSMD13	26S proteasome non-ATPase regulatory subunit 13 isoform 1	17	43	1.302
PSMB7	proteasome subunit beta type-7 precursor	5	17	1.278
PSMD2	26S proteasome non-ATPase regulatory subunit 2 isoform 1	31	74	1.257
PSMD14	26S proteasome non-ATPase regulatory subunit 14	13	23	1.222
PSMC4	26S protease regulatory subunit 6B isoform 1	17	49	1.217
REPLICATE 4				
PSMD9	26S proteasome non-ATPase regulatory subunit 9 isoform 1	6	10	1.95
PSME2	proteasome activator complex subunit 2	9	35	1.77
PSMD8	26S proteasome non-ATPase regulatory subunit 8	11	22	1.579
PSMD4	26S proteasome non-ATPase regulatory subunit 4	12	26	1.489
PSMD7	26S proteasome non-ATPase regulatory subunit 7	11	23	1.411
PSMC4	26S protease regulatory subunit 6B isoform 1	23	70	1.382

Columns from the right represent the gene symbol, protein description, #- number of unique peptides identified, number of peptide score matches (PSMs) and the fold change of the proteins in RR w.r.t P.

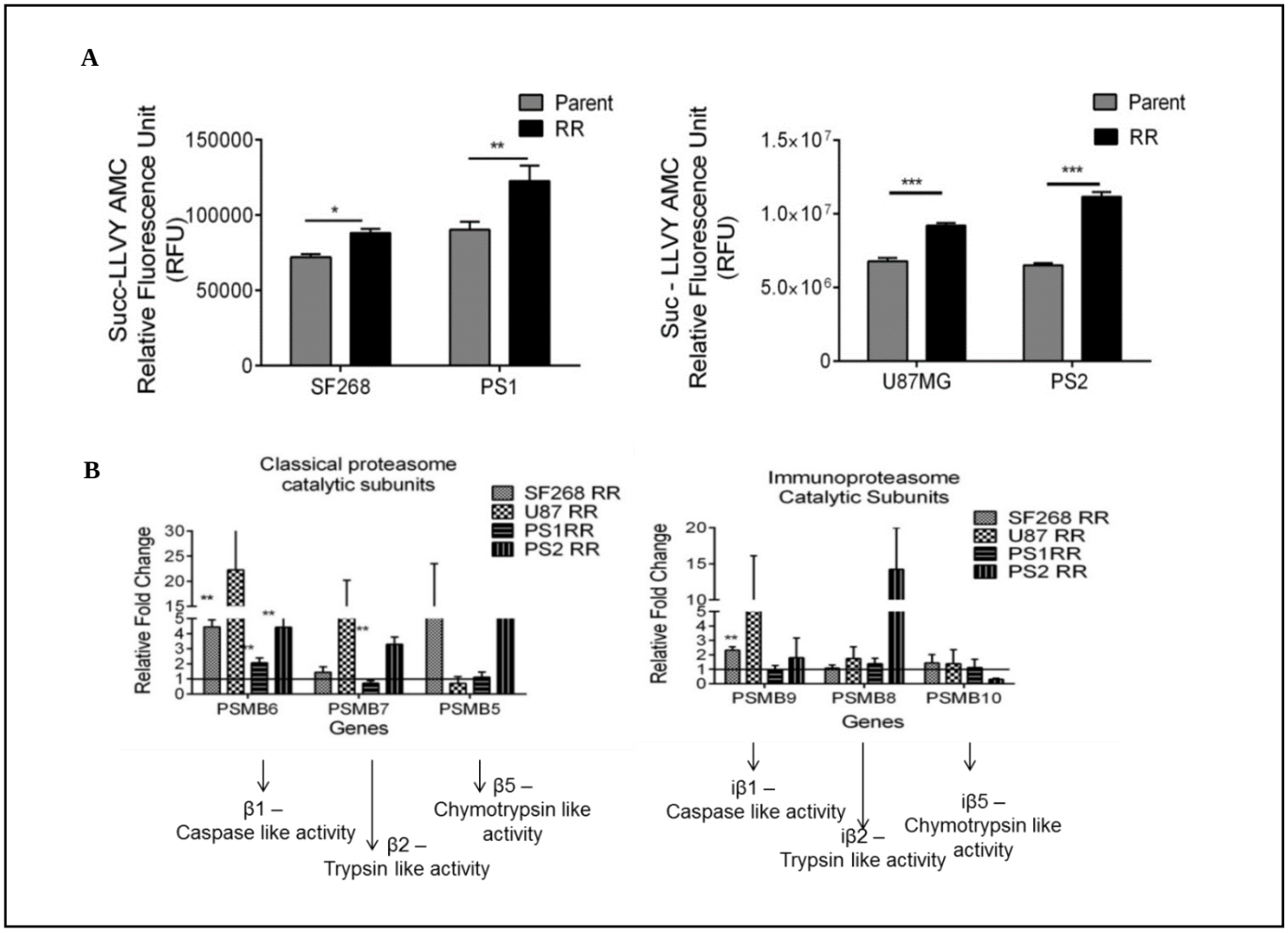

Figure 30 Proteasome activity and expression of beta catalytic subunits in RR cells.

(A)Data represents the chymotrypsin like proteasome activity measured using Succ-LLVY AMC florigenic substrate in the P and RR population of SF268, U87MG, PS1 and PS2. (B) The graph depicts the RPL19 normalised mRNA levels of classical and Immunoproteasome proteasome beta catalytic subunits respectively in the RR population of SF268, U87MG, PS1, and PS2 compared to the parent population

Most of the subunits belong to the classical proteasome. Hence the transcript levels of beta catalytic subunits: PSMB6 (β1- caspase like activity), PSMB7 (β2 – trypsin like activity) and PSMB5 (β5 – chymotrypsin like activity), were checked. PSMB6 transcript levels were elevated in the RR population of all the samples, PSMB7 and PSMB5 were elevated in at least one cell line and one patient sample. Proteomics data also identified a regulatory subunit of immunoproteasome (PSME1). Therefore, the mRNA levels of its catalytic subunits PSMB9, PSMB8 and PSMB10 were also determined (Figure 30 B). However, the transcript levels of

the three subunits were not significantly high in any of the samples. Since the RR population exhibited increased proteasome activity we wanted to analyze if the survival of RR cells was dependent on the proteasome activity. For this, we used bortezomib (BTZ), a pharmacological inhibitor of proteasome routinely used in the treatment of multiple myeloma. First, we determined the concentration of bortezomib at which proteasome activity was maximally inhibited with minimal cellular toxicity. For this proteasome activity of SF268 was assessed after 12 h. treatment of bortezomib at different concentrations (0.01nM to 1000nM). As seen from figure 31 A & B, 10nM of bortezomib was the minimum concentration at which significant inhibition of proteasome activity was observed and there was no significant cell death in RR as compared to the parent.

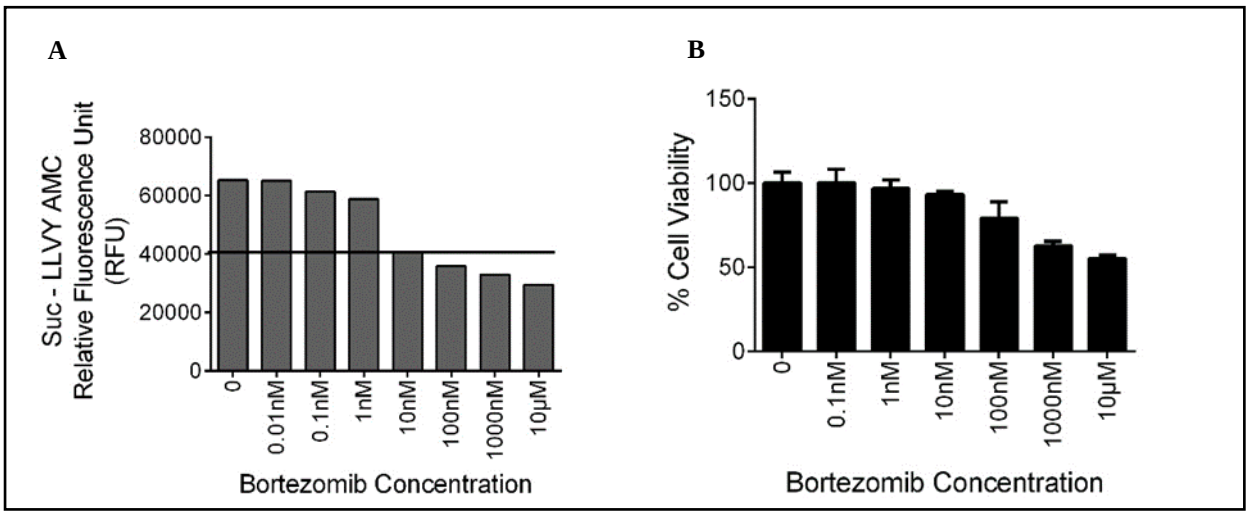

Figure 31 Dose determination of bortezomib in SF268

A & B) Proteasome activity inhibition and % cell viability at different concentrations of proteasome inhibitor – Bortezomib in SF268. (B) The graph shows the percentage of cells of SF268 and PS1 surviving at different doses of γ radiation with and without 10nM bortezomib in a clonogenic assay

Once the non-toxic concentration of bortezomib on parent cells was determined, we wanted to see if the inhibition of proteasome sensitizes the glioma cells to radiation. SF268 and PS1 cells were treated for 12 hrs. with 10nM bortezomib and their % cell survival was recorded at different doses of radiation. As shown in figure 32 A, bortezomib treatment significantly

reduced the D_0 dose of radiation from 5.07 Gy to 3.12 Gy and 4.4 Gy to 1.08 Gy for SF268 and PS1 respectively, showing that proteasome inhibition radiosensitizes glioma cells.

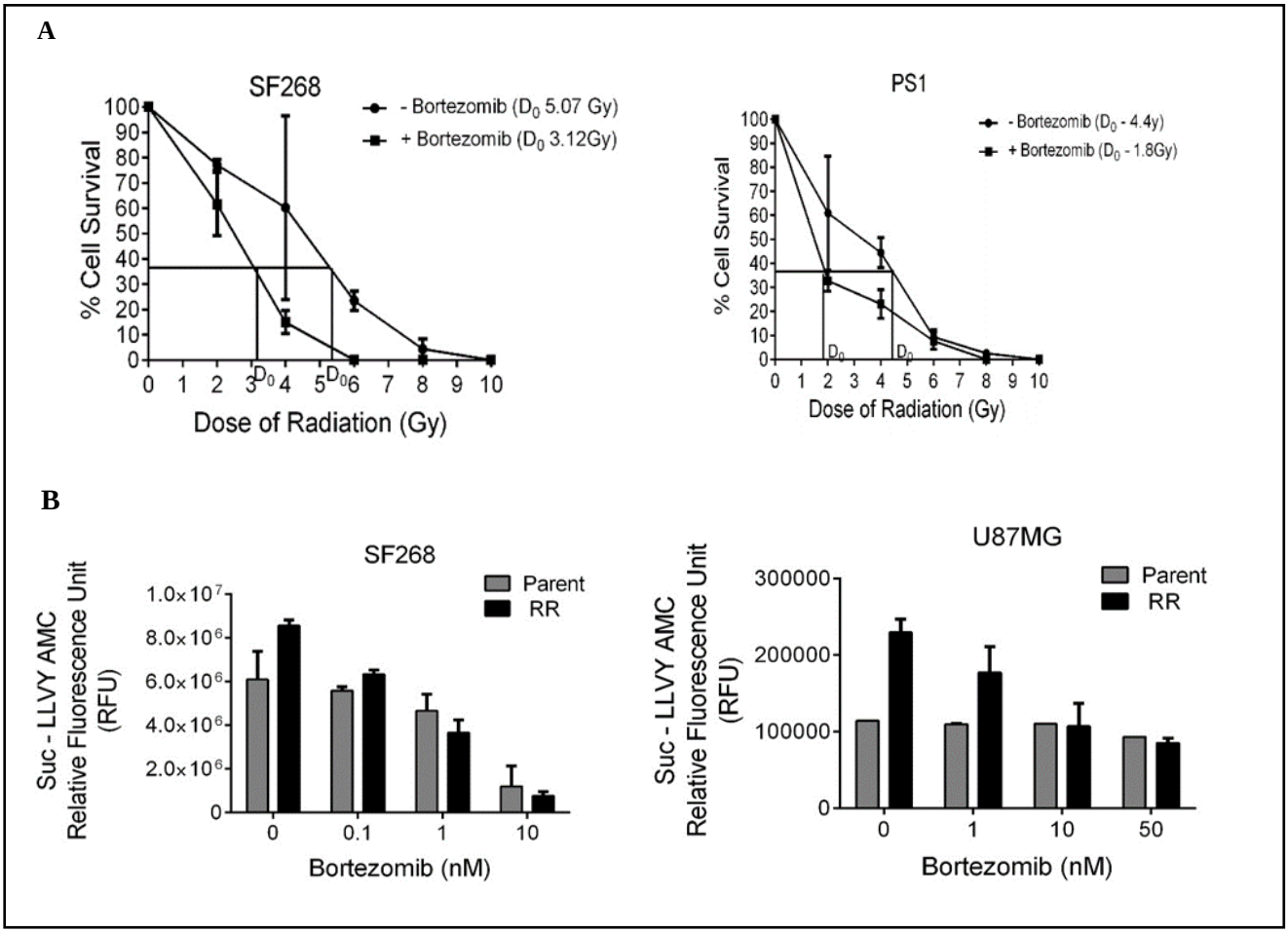

Figure 32 Effect of proteasome inhibition on proteasome activity in vitro in RR cells

(A) The graph shows the percentage of cells of SF268 and PS1 surviving at different doses of γ radiation with and without 10nM bortezomib in a clonogenic assay. (B) The bar graph shows proteasome activity in parent and RR cells of SF268 and U87 at different concentrations of the bortezomib as mentioned.

We then wanted to analyze the effect of bortezomib on RR population that has higher proteasome activity. For this, the parent and RR population of SF268 and U87 were treated with 0.1nM, 1nM and 10nM concentrations of bortezomib for 12 hrs. Following the treatment, cells were monitored for proteasome activity. Both parent and RR cells showed a gradual decrease in the activity of proteasomes with increasing concentration of the drug (Figure 32 B). However, 72 hours post drug treatment RR cells were significantly (8% SF268, 10% U87 and 23% PS1) more sensitive to proteasome inhibition compared to the parent population. PS2

showed similar % reduction in viability as compared to the parent population at 10nM (Figure 33 A, B, C & D).

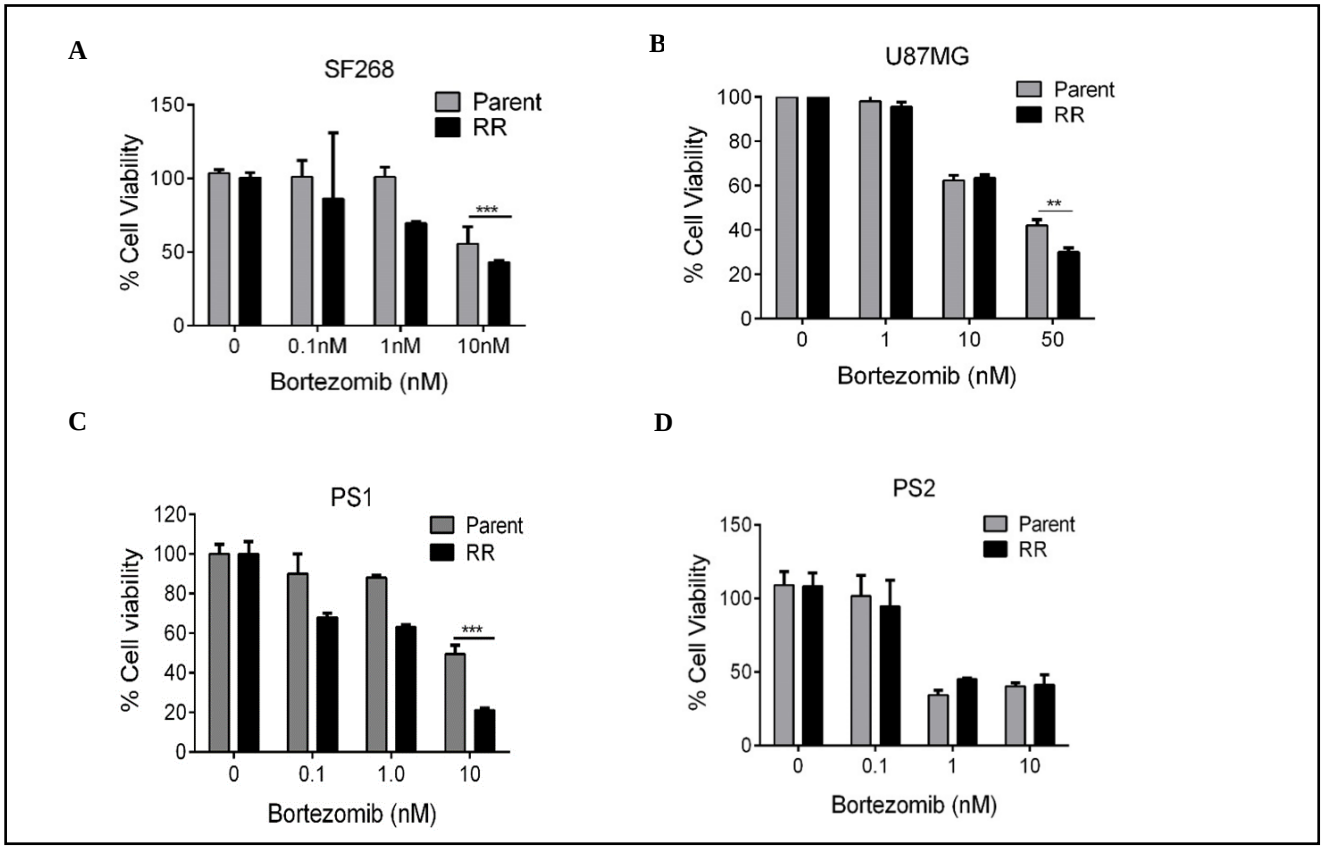

Figure 33 Effect of proteasome inhibition on cell viability of RR cells in vitro.

*Bar graph represents the percentage of viable cells (at 72hrs) as assessed by MTT assay at different concentrations of bortezomib in (A) SF268, (B) U87MG, (C) PS1 & (D) PS2. Cells were treated with bortezomib for 12 hrs. Results in each bar graph are the composite data from three independent experiments performed in triplicate (mean ± SEM); ***P = 0.001)*

We further wanted to determine if the proteasome targets were down-regulated in the RR population due to degradation via ubiquitin-mediated proteasome pathway. Down-regulated proteins were analyzed for the presence of annotated ubiquitin binding lysine residues. These proteins were downloaded from the Uniprot database (120) and parsed using in-house python scripts to determine the presence of curated ubiquitin binding sites. Of the 431 proteins, 14 proteins were found to harbor lysine residues which can undergo ubiquitin modification (Table 2).

GeneName	Protein Name	Relative Peptide Intensities in RR	Ub Position Glycyl lysine isopeptide	References
APP	Amyloid beta A4 protein	0.191	763	
HIST1H1B	Histone H1.5 (Histone H1a) (Histone H1b) (Histone H1s-3)	0.475	17	
HIST1H1B	Histone H1.5 (Histone H1a) (Histone H1b) (Histone H1s-3)	0.475	219	
HIST1H4A	Histone H4	0.477	13	
HIST1H4A	Histone H4	0.477	92	
KDM1A	lysine-specific histone demethylase 1A isoform b	0.478	503	Han X et al, Mol Cell. 2014 Aug
PEF1	peflin	0.508	137	McGourty CA et al, Cell. 2016 Oct
PPIA	peptidyl-prolyl cis-trans isomerase A	0.570	28	Visvikis O et al, FEBS J. 2008 Jan
RAC1	ras-related C3 botulinum toxin substrate 1 isoform Rac1	0.581	147	
RAN	GTP-binding nuclear protein Ran	0.601	71	
RBBP7	histone-binding protein RBBP7 isoform 2	0.602	4	
RBBP7	histone-binding protein RBBP7 isoform 2	0.605	159	
RPL10	60S ribosomal protein L10 isoform a	0.605	188	
RPS10	40S ribosomal protein S10	0.619	138	Sundaramoorthy E et al, Mol Cell. 2017 Feb 16

RPS10	40S ribosomal protein S10	0.626	139	Sundaramoorthy E et al, Mol Cell. 2017 Feb 16
TCEA1	transcription elongation factor A protein 1 isoform 1	0.626	55	
TDRKH	tudor and KH domain-containing protein isoform a	0.672	65	Cunningham et al, Nature Cell Biology 2015
TDRKH	tudor and KH domain-containing protein isoform a	0.672	76	Cunningham et al, Nature Cell Biology 2015
TDRKH	tudor and KH domain-containing protein isoform a	0.672	110	Cunningham et al, Nature Cell Biology 2015
TDRKH	tudor and KH domain-containing protein isoform a	0.672	112	Cunningham et al, Nature Cell Biology 2015
TDRKH	tudor and KH domain-containing protein isoform a	0.672	152	Cunningham et al, Nature Cell Biology 2015
TDRKH	tudor and KH domain-containing protein isoform a	0.672	175	Cunningham et al, Nature Cell Biology 2015
TDRKH	tudor and KH domain-containing protein isoform a	0.672	181	Cunningham et al, Nature Cell Biology 2015
TDRKH	tudor and KH domain-containing protein isoform a	0.672	187	Cunningham et al, Nature Cell Biology 2015
TDRKH	tudor and KH domain-containing protein isoform a	0.672	193	Cunningham et al, Nature Cell Biology 2015
TDRKH	tudor and KH domain-containing protein isoform a	0.672	256	Cunningham et al, Nature Cell Biology 2015
TDRKH	tudor and KH domain-containing protein isoform a	0.672	267	Cunningham et al, Nature Cell Biology 2015
TDRKH	tudor and KH domain-containing protein isoform a	0.672	479	Cunningham et al, Nature Cell Biology 2015

TDRKH	tudor and KH domain-containing protein isoform a	0.672	510	Cunningham et al, Nature Cell Biology 2015
TDRKH	tudor and KH domain-containing protein isoform a	0.672	529	Cunningham et al, Nature Cell Biology 2015
UBE2T	ubiquitin-conjugating enzyme E2 T	0.685	91	Alpi AF1 et al, Mol Cell. 2008 Dec 26
UBE2T	ubiquitin-conjugating enzyme E2 T	0.685	182	Alpi AF1 et al, Mol Cell. 2008 Dec 26

Table 2 Downregulated proteasome target proteins

List of downregulated proteins with ubiquitin binding lysine residues.

4.1.2.6 Proteasomes indirectly regulate RR cell survival via the NF-kB activation

One of the well-known substrates of the 26S proteasome is IκB-α which upon degradation leads to the activation of the transcription factor NF-kB. An increased proteasome activity should modulate the levels of activated NFkB in the RR population. Therefore, we checked for the levels of activated NFkB by western blot in the P and RR cells of cell lines and patient samples. Indeed, the RR cells displayed increased levels of activated NFkB in both the cell lines and PS1 (Figure 34 A & B).

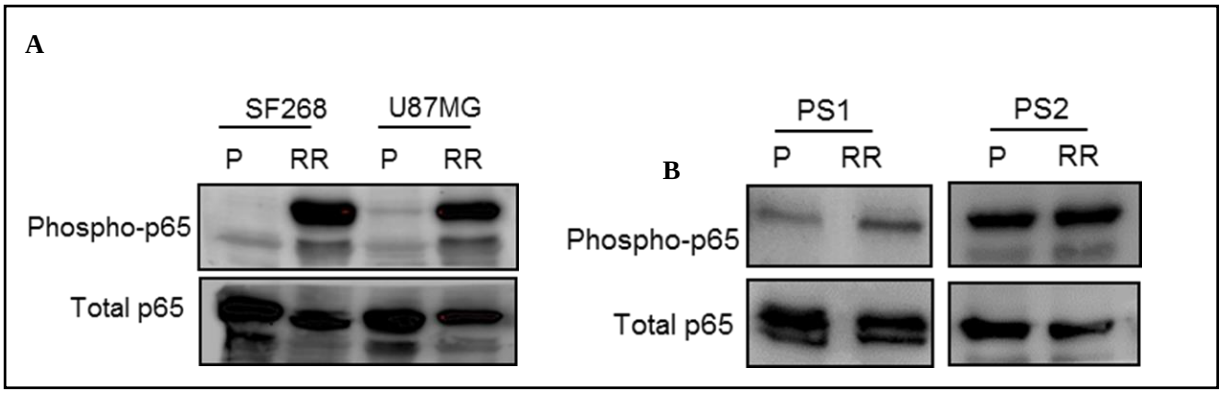

Figure 34 Western blot for protein expression of activated NfκB (phosphorylated p65) in the P (Parent) and RR (Radiation resistant) cells

(A) Cell line: SF268 and U87MG (B) Patient samples: PS1 and PS2 Total (T) total- p65 levels were used as loading controls

Furthermore, the transcript levels of 9 NFkB target genes (TNF-α, IL6, IkB-a, IFN-γ, ICAM1, COX2, NOD4, p16, SOD2) were screened in RR cells of the cell lines and patient sample by real-time PCR. A heat map representation of the 9 genes depicts upregulation of at least 6 genes out of the 9 in SF268, U87, and PS1 which also harbor increased expression of phospho-NFkB suggesting the presence of a transcriptionally active NFkB in RR cells (Figure 35).

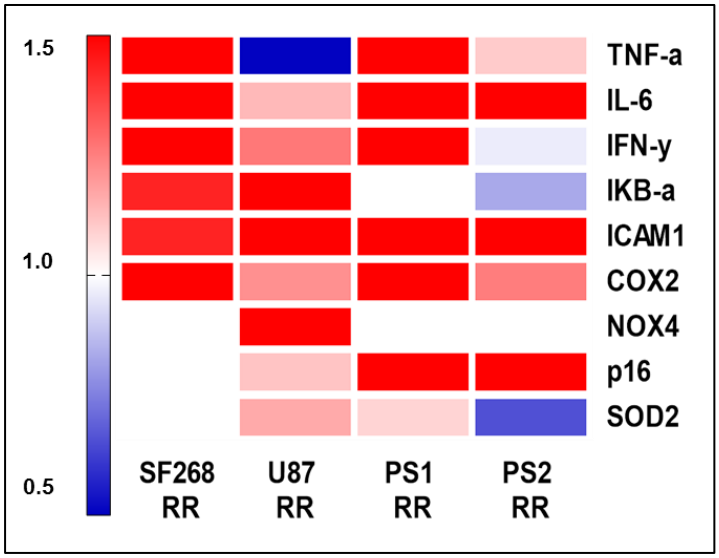

Figure 35 Heat map representation of gene expression values of NFkB target genes.

*The mRNA levels were assessed by qPCR in the RR population of SF268, U87, PS1, and PS2 compared to the parent population. GAPDH was used as internal control. Results are the composite data from three independent experiments performed in triplicate (mean ± SEM); *P = 0.05, **P = 0.01 and ***P = 0.001*

To directly assess the NFkB transcriptional activity in the RR cells of U87, we monitored the relative promoter activity of the luciferase-based NFkB reporter constructs in the P and RR cells. The RR cells showed a significant increase (20 fold) in NFkB transcriptional activity as compared to the parent population (P). Importantly, administration of the proteasome inhibitor (Bortezomib) in the P and RR cells diminished this activity by 1.5 and 3.0 fold demonstrating the dependency of NFkB activity on the proteasome activity. A synergistic inhibitory effect was observed in the presence of IkB-alpha construct and bortezomib in the P and RR cells. However, the RR cells displayed a much higher reduction as compared to the P cells (Figure 36)

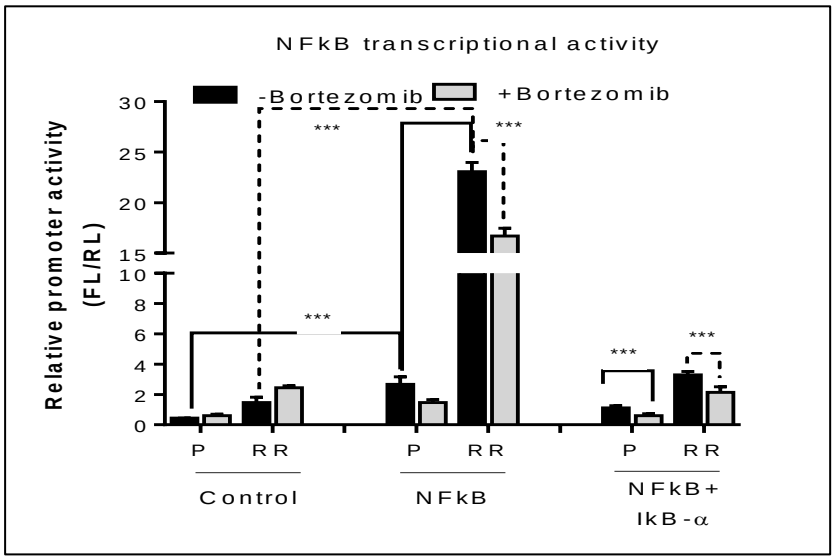

Figure 36 Luciferase based reporter assay for the transcriptional activity of NFkB

The NFkB firefly luciferase construct was transfected into (P) Parent and (RR) radioresistant cells then treated with bortezomib as indicated. As a control Con, A control plasmid was transfected with Renilla luciferase construct. The pTRIPZ IkB-alpha construct was used as NFkB suppressor. Luciferase values subsequent to normalization were plotted

4.1.2.7 Inhibition of Proteasome activity inhibits tumor formation and in vivo

We have shown that radiation resistant residual (RR) cells formed in our *in vitro* radiation resistant model systems retain their tumorigenic potential and re-grow to give rise to the recurrent tumor. We first wanted to analyze if the RR cells are capable of forming a tumour *in vivo* as well. For this pLenti6-luc2 U87MG cells (121) stably expressing luciferase were treated with the lethal dose of radiation 8Gy and RR cells were collected. The parent and RR cells were then stereotactically injected in the brain of 6-8 weeks old NOD/SCID mice. Tumor growth was monitored using bioluminescence imaging. As seen from figure 36 A & B RR cells were able to give rise to tumors and had greater tumorigenic potential as compared to the parent cells.

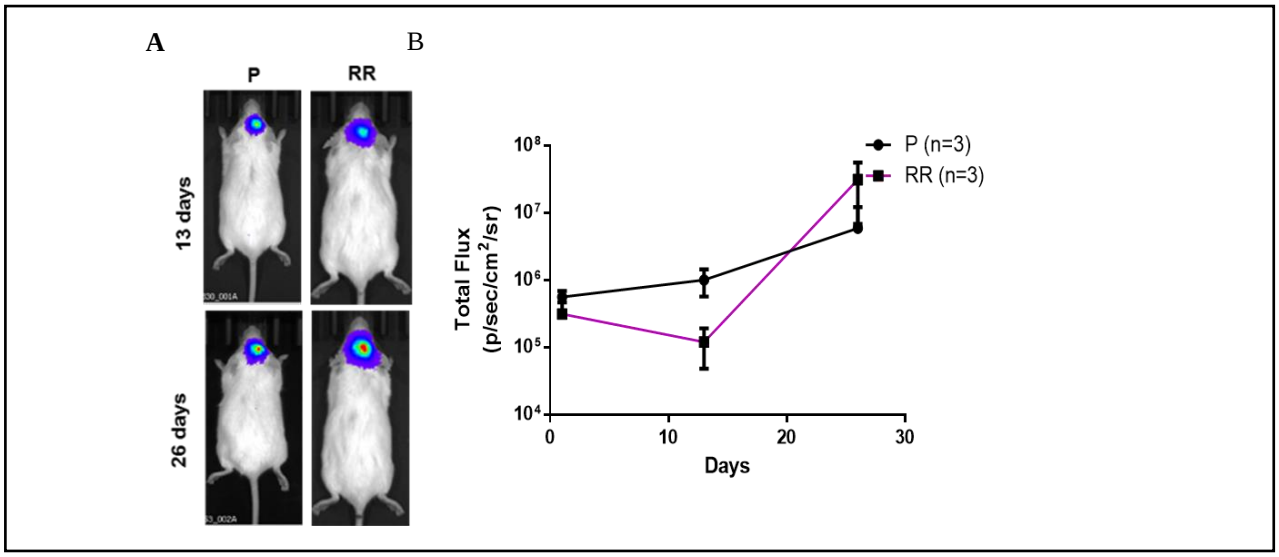

Figure 37 Tumorigenic potential of RR cells compared to P

(A) Representative bioluminescence images after orthotopic injection of U87MG-Luciferase labeled Parent (P) and Radiation Resistant (RR) cells. (B) The graph represents bioluminescence intensity plotted as total flux at different days post-injection.

We then evaluated the effect of proteasome inhibition on the tumorigenicity of the parent and RR cells. Since U87MG cells showed higher proteasome activity than the SF268 (Figure 30 A), hence they also required a higher concentration of bortezomib (50nM) for reducing the viability of their RR. Therefore for in vivo studies U87MG parent and RR cells were treated with 50nM bortezomib for 12hrs prior to injection. Tumor formation was monitored by bioluminescence. As expected at day 14 post-injection parent and RR cells treated with vehicle control or bortezomib showed almost similar growth, however, by day 33 while the parent cells treated with bortezomib had formed large tumors, the RR cells treated with bortezomib showed significantly reduced bioluminescence intensity (Figure 37 A). Presence of tumor cells was seen with Haematoxylin and Eosin staining in the brain slices of all the treatment groups of mice except for the brain tissue of mice treated injected with RR cells + bortezomib (Figure 37 B)

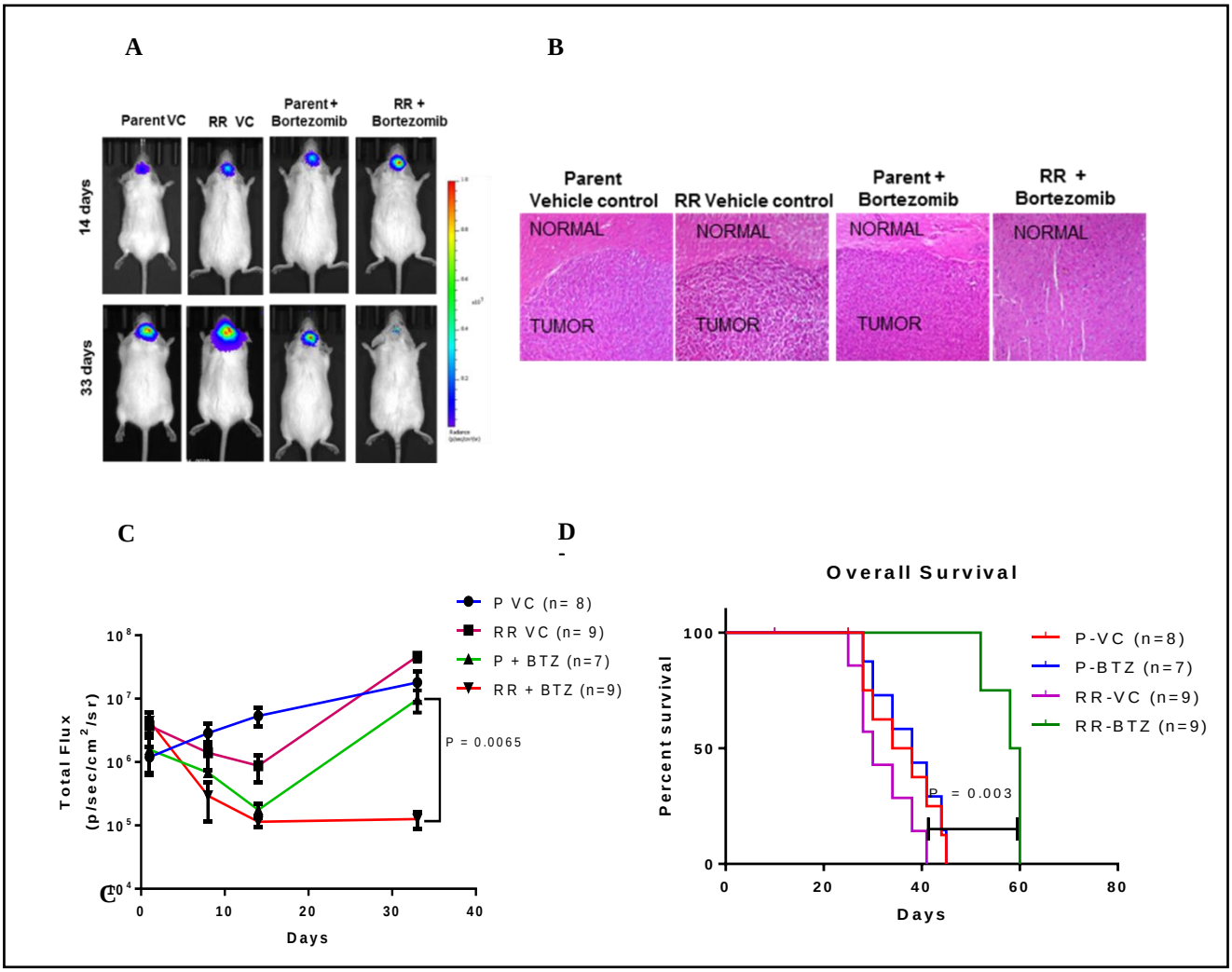

Figure 38 Tumorigenic potential of BTZ pretreated P and RR cells

(A) Bioluminescent images after orthotopic injection of U87MG-Luciferase labeled Parent (P) and Radiation Resistant (RR) cells treated with Vehicle Control (VC) and bortezomib. (B) Hematoxylin and eosin (H&E) staining of mice brain slices. Brain slices of the brain tissue from mice injected with Parent Vehicle control, RR Vehicle Control, Parent + Bortezomib, RR + Bortezomib cells were formalin fixed and paraffin embedded. Sections stained with H&E show regions infiltrated with tumor cells. All photomicrographs are shown with the same magnification. Bar = 100 µm. (C) The graph represents bioluminescence intensity at different days post injection of mice injected with P and RR cells pre-treated with bortezomib as compared to P and RR cells treated with vehicle control. 'n' represents a number of mice per group. (D) Kaplan Meier Curve for the overall survival of the mice in the pretreated study.

As represented in figure 37C, the mice injected with bortezomib treated RR cells showed a significant decline in bioluminescence as compared to the group injected with bortezomib treated P cells. Also, the overall survival of this group (RR-BTZ) was significantly higher than

that of the other three groups as shown in figure 4.16 D. Median survival of each group are as follows : P- VC – 36 days, P – BTZ – 38 days, RR – VC – 30 days, RR – BTZ – 58 days. Further, we did an intracranial injection of parental cells followed by radio therapy (fractionated dose of 14Gy) followed by intraperitoneal injection of bortezomib (0.5mg/Kg twice in a week for two weeks) as depicted in figure 39.

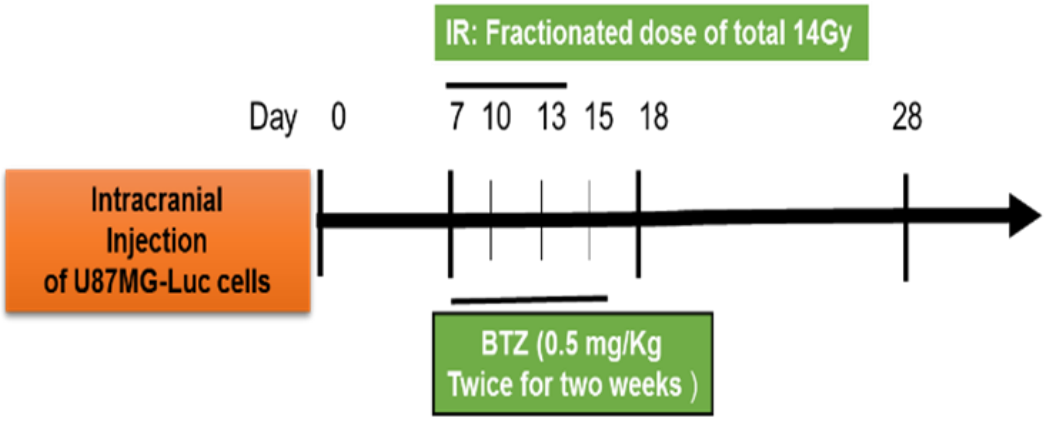

Figure 39 Schematic representation for studying the effect of intraperitoneal injections of bortezomib along with radiation treatment of mice intracranially injected with parent GBM cells.

IR – Radiation; BTZ – Bortezomib

Representative bioluminescence images from each group are shown in figure 40 A. The results show a significant reduction in bioluminescence of animals treated with radiation along with BTZ as compared to the radiation alone group (Figure 40 B). The disease-free survival of mice was significantly higher in the group treated with radiation and BTZ as compared to the radiated alone group (Figure 40 C).

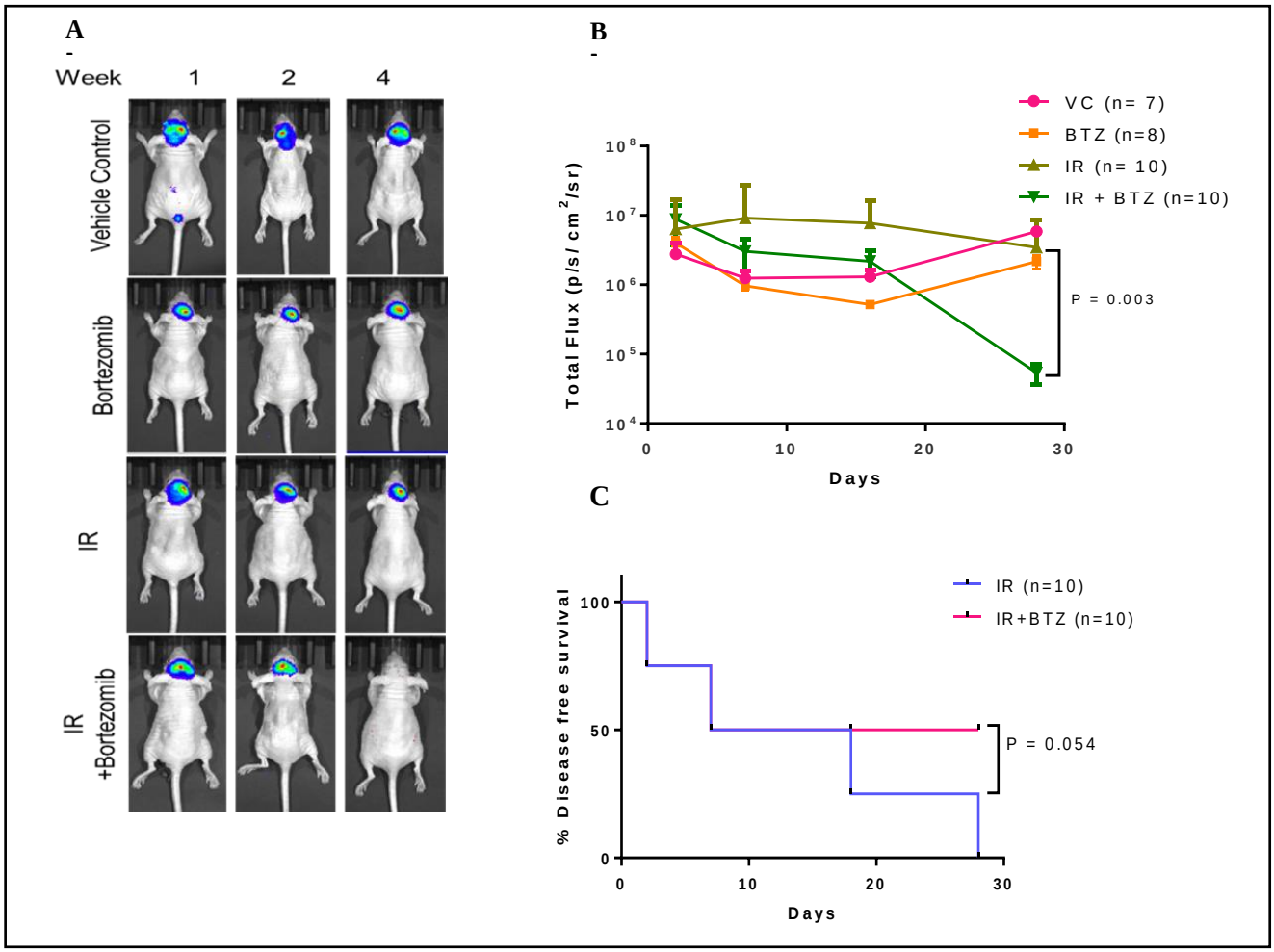

Figure 40 Effect of proteasome inhibition on the tumorigenic potential of the cells in vivo

(A) Representative bioluminescence images of tumor formation in the mice treated with IR and BTZ compared to the mice which were administered with Vehicle Control (VC), only BTZ and only IR.(B)Graphical representation of bioluminescence intensity recorded for mice treated with IR and BTZ compared to the mice which were administered only saline as Vehicle Control (VC), only BTZ, only IR (C) Kaplein Meier Curve for % tumor-free animals in the radiation and intraperitoneally administered BTZ study.

4.1.3 Discussion

Radioresistance and recurrence is currently an inevitable consequence in the field of glioblastoma. Until now, the mechanisms of radioresistance in glioblastoma have been explored in vitro and in vivo settings either immediately post radiation or after generation of repeated doses of radiation (acquired resistance) but not in the residual radiation-resistant cells. However, in this study, we focused on the processes deregulated in the innately radiation resistant residual (RR) population as we have previously shown that these are the cells responsible for relapse in glioblastoma (9). We performed iTRAQ based quantitative proteomic

analysis on the parent (P), innately radiation resistant residual (RR) and relapse (R) population. Amongst the many pathways, we found the proteasome pathway to be most significantly deregulated in the RR cells.

Proteasomes are well-known targets in cancer therapy owing to their role in maintaining homeostasis of proteins involved in cell cycle, signaling pathways regulating cell survival and apoptosis (122-125). Cancer cells harbor enhanced proteasome activity compared to their normal counterparts but the exact reason for this surge is still unknown. It is speculated that this escalation in proteasome activity is to cope with a crisis such as mutational events and chromosomal instabilities. Although proteasomes are identified as direct targets of radiation, their inhibition is short lived and thus the need for drugs targeting their enzymatic activity (111, 126, 127). Lower proteasome activity is shown to be a marker for a tumour initiating cells and stem cells (128). Proteasomes are also found to be downregulated in radio-resistant cells of breast cancer and prostate cancer established in vitro (126, 129, 130). Contrary to these reports, we observed an enhanced expression and activity of proteasomes in the innate radio-resistant residual cells of glioblastoma. Subsequently, we also identified 14 out of 431 downregulated proteins that harbor ubiquitin binding lysine residues. These proteins in the RR cells, we predict to be either ubiquitin adapters or direct targets of the ubiquitin-mediated proteasome machinery. This reduced number of proteins with ubiquitin binding attributes to the fact that proteasomes degrade a significant cellular portion by an ubiquitin-independent manner also which is still incompletely understood (112).

Bortezomib binds to the catalytic subunit of the 26S proteasome and preferentially inhibits the β5/chymotrypsin like activity of the proteasome. It is currently being used in the treatment of multiple myeloma (111, 131, 132). In GBM, it has been reported to sensitize the parent GBM cells to temozolomide and radiation treatment but after immediate exposure to the drug and radiation. However, in our study we show that the residual resistant cells that are formed after

a period of 5-7 days post radiation are more sensitive to proteasome inhibition compared to the parent cells, although, there is a differential response to proteasome inhibition amongst the cell lines (SF268, U87MG) and patient samples (PS1 & PS2) as depicted in Figure 5C. This could be due to the heterogeneity of GBM tumors. The subtle effect of bortezomib seen in vitro after 72hrs post-treatment is significantly enhanced in reducing tumorigenicity of the treated cells in vivo, suggesting a slow and prolonged effect of proteasome inhibition on the survival of the cells. Even though proteasome inhibition alone reduced cell viability of the parent cells *in vitro* but it did not effect the tumor burden *in vivo*. The difference in response *in vitro* and *in vivo* could be attributed to the *in vivo* microenvironment which is known to plays a major role in modulating the behaviour of tumor cells and efficacy of cancer drugs. A significant effect of proteasome inhibition was observed on the overall survival of mice which were injected with pre-treated RR-BTZ cells along with an increased % of tumour free mice when BTZ was administered intraperitoneally along with radiation as shown in figure 40 B & C. The increased levels of activated NFkB and its transcriptional activity in the RR cells correlate with previous reports where NFkB has been shown to promote radioresistance in glioblastoma and other cancers. It has been reported to trigger pro-survival and anti-apoptotic signals by transcriptional activation of over 200 genes including the pro-inflammatory cytokines, cell-cell adhesion molecules. We have observed cytokines such as TNF-α, IFN-γ, IL-6 and antioxidant genes such as COX2 levels increased in the RR. Its activation can occur via IkB-α degradation (Classical pathway) or the by TNF-α (alternative pathway) (113, 133, 134). However, the exact mechanism downstream to higher proteasome expression and NFkB activity in the RR cells needs to be further explored. Nonetheless, this study as illustrated in figure 41, establishes that

proteasomes aid the survival of the innate radiation resistant population via a NFkB pathway and hence can be valuable targets for precluding relapse in glioblastoma.

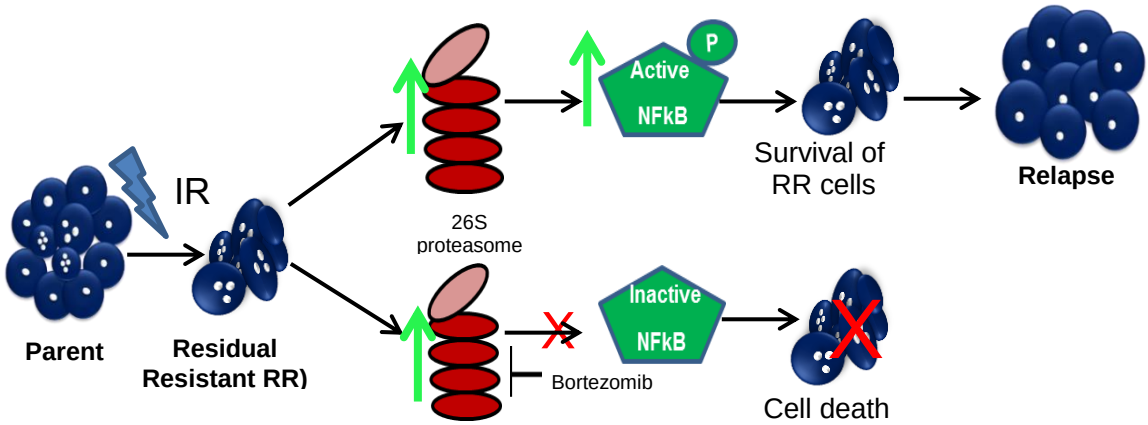

Figure 41 Proposed model for the study

4.2 Identification and functional validation of candidate protein 14-3-3 zeta in RR cells

4.2.1 Introduction

4.2.1.1 14-3-3 family

14-3-3 zeta belongs to the 14-3-3 family of proteins. 14-3-3 proteins are a class of highly conserved and ubiquitously expressed proteins. (135) These proteins are small acidic proteins with its molecular weight ranging from 27-30 kDa. These proteins are abundantly found in the brain but are also localized in all tissues including testes, liver, and heart. In terms of a eukaryotic cell, these proteins are largely found in the cytoplasmic compartment. However, they have also been spotted in the plasma membrane and intracellular organelles like the nucleus and the Golgi apparatus (136).

This family of proteins was identified by Moore and Perez in 1967 during the classification of brain proteins. These proteins were termed as '14-3-3' based on the fraction number on DEAE-cellulose chromatography and their migration position in starch gel electrophoresis. The name

14-3-3 was derived from the combination of its fraction number on DEAE-cellulose chromatography and its migration position in the subsequent starch–gel electrophoresis (137). In mammals, seven isoforms of 14-3-3 proteins (β, γ, ε, ζ, η, σ, and τ) have been found with each isoform encoded by a different gene and each having a unique mode of development and regulation of functions (138, 139). All the isoforms have a similar structure comprising of a dimerization region and a target binding region.

14-3-3 proteins exist as dimers, and each monomer in the dimer is composed of nine anti-parallel alpha helices with the dimer interface at the N-terminus.

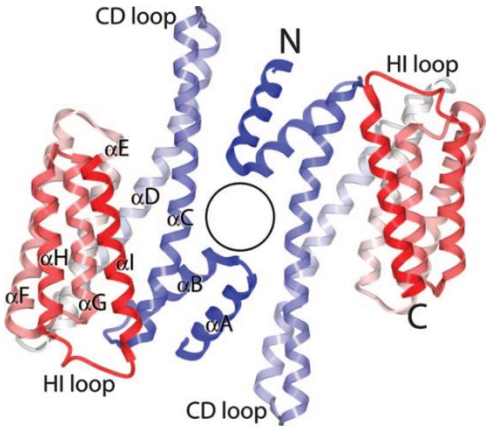

Figure 42 Structure of 14-3-3

The highly conserved residues reside in the concave inner surface of the grove and the variable residues are present in the N- terminal loop. The helices α C, α E, α G, and α I form a conserved peptide-binding groove (140, 141). They function through binding to phosphorylated serine/ threonine motifs, RSXpSXP (motif 1) and RXY/FXXpSXP (motif 2), where pS represents phosphoserine and X any amino acid, on their target proteins. (142, 143). 14-3-3 proteins are primarily phosphorylation-dependent for its regulation and phosphorylation is a key event in signaling pathways. Therefore, 14-3-3 interactions are largely regulated by the kinases and phosphatases that modulate the phosphorylation state of the target protein. Thus, they function

as adaptor proteins which play an essential role in regulating a large number of general and specialized signaling pathways.

These proteins bind to a variety of targets around the subcellular compartments which include the transcription factors, tumor suppressors, biosynthetic enzymes, cytoskeletal proteins and this diversity enables us to investigate and emerge with new mechanisms and roles of these proteins (144). They regulate their target proteins by inducing a conformational change in the protein, affecting protein activity or stability, facilitating protein complex formation, or altering protein subcellular localization.

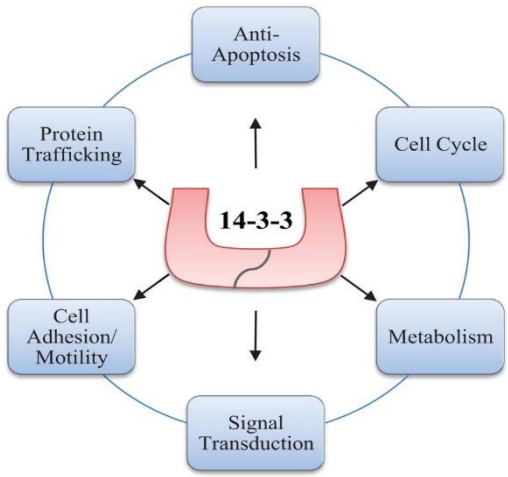

Figure 43 14-3-3 pathways to maintain normal cellular homeostasis.

(Image Courtesy – Expert Opin Ther Targets, 2010)

Since they are key regulators of cellular proliferation, differentiation, senescence, and apoptosis, hence they serve as potential targets in cancer therapy. Among the seven isoforms, 14-3-3sigma is stated as a tumor suppressor gene, while the other isoforms have been associated as an oncogene. 14-3-3 zeta amidst the six isoforms has been reported to be a prognostic marker and a potential therapeutic target.

4.2.1.2 Role of 14-3-3 ζ in cancer:

14-3-3 zeta plays a pivotal role in regulating multiple signaling pathways in cancer development, progression, and therapy resistance. It is overexpressed in various cancers and has been associated with poor prognosis, particularly in breast, lung and head and neck cancer.

Cancer types associated with 14-3-3 overexpression

Tumor Type	14-3-3 Isoform	Poor Prognosis
Breast	ζ	Yes
Lung	ζ, multiple	Yes
Pancreas	ζ	
Colon	ζ	
Esophageal	ζ	
Stomach	ζ	
Oral	ζ	
Head and Neck	ζ	Yes
Urothelial	ζ	
Renal	ε	
Brain, astrocytoma	β, η, multiple	
Brain, meningioma	multiple	
Chronic myeloid leukemia	ζ	
Diffuse large B cell lymphoma	ζ	
Papillomavirus-induced carcinomas	ζ	

Figure 44 Overexpression of 14-3-3 zeta in different cancers.

14-3-3 ζ is overexpressed in more than 40% of advanced breast cancer cases. It has been reported to promote metastasis in breast cancer by inhibiting RhoGDIα. Consequently, JiaXu et al showed that ζ can switch the role of TGF β from a tumor suppressor to a metastasis promoter by changing the partners of SMAD from p53 to Gli2. In head and neck squamous cell carcinoma (HNSCC), overexpression of 14-3-3 zeta and 14-3-3 sigma has been related to a high rate of recurrence. It has been shown to interact with Bad, p65 subunit of NF-κB and β-

catenin which facilitates cell proliferation, apoptosis, and adhesion in head and neck cancer. In another report by Macha, M. A et al it has been reported as a molecular target in guggulsterone induced apoptosis in head and neck cancer cells. In TSCC, overexpression of 14-3-3 zeta was associated with lymph node metastasis and poor prognosis through immunohistochemical studies. Silencing of 14-3-3 zeta reduced cell proliferation and migration of TSCC cells. In pancreatic cancers, overexpression of 14-3-3 zeta was found to be more in pancreatic adenocarcinoma (PCA) than in chronic pancreatitis (CP) which is one of the major risk factors of pancreatic cancer. These reports collectively show that 14-3-3 zeta acts as pro-survival signaling protein and hence serves as a potential target in cancer therapy. It is seen to be upregulated in many cancer and remains one of the principal reasons for poor prognosis of patients (145-149).

4.2.1.3 14-3-3 Zeta in Glioblastoma, Therapy Resistance, and Recurrence

In glioblastoma, according to the TCGA dataset, ζ is altered at mRNA and protein level in only 2.9% of cases. But, there was no significant correlation between overall survival and disease-free survival in these cases.

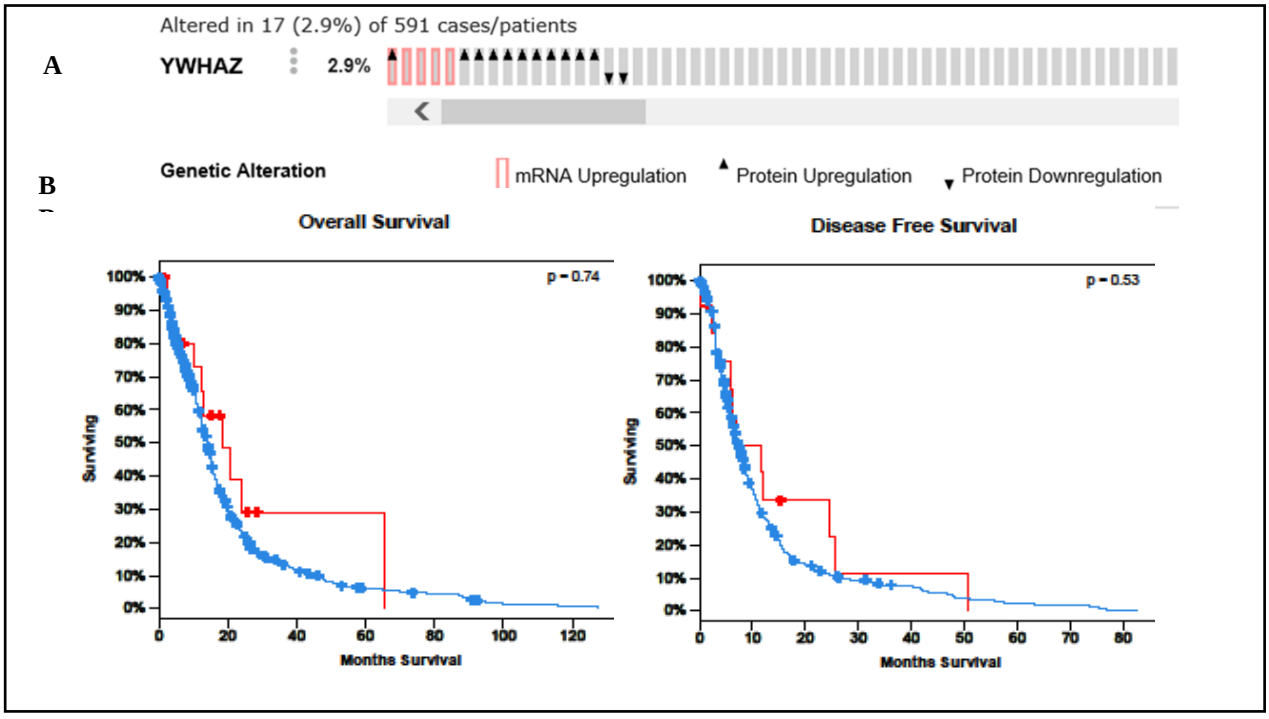

Figure 45 Expression of 14-3-3 ζ in TCGA patient samples dataset.

(A) Illustrative representation of mRNA and protein expression using cBioportal. (B) & (C) represent the overall survival and disease-free survival of patients overexpressing 14-3-3 ζ.

However, Yang et al in 2011 showed that 14-3-3 zeta positive expression is a prognosis indicator in patients with glioblastoma. Patients who were treated with surgery, radiation, and chemotherapy showed a positive 14-3-3 zeta expression in an immunohistochemical study. The 14-3-3 zeta also correlated with a short interval to tumor recurrence than the patients showing 14-3-3 zeta negative expression (150). This group later demonstrated in another study that 14-3-3 zeta positive cells show a higher cell viability, stronger invasion and a high therapy resistance with TMZ (151).

However, its role in promoting glioblastoma progression and radiation resistance has not been reported. In this study, we focused on exploring the functional role of 14-3-3 zeta in glioblastoma progression by identifying the binding partners of 14-3-3 zeta.

4.2.2 Results

4.2.2.1 Quantitative proteomic analysis revealed increased expression of 14-3-3 zeta in RR cells

While searching for candidate proteins amongst the differential proteins for further functional studies from our proteomic analysis, we analyzed all the 5 biological replicates for which proteomics was done. 14-3-3 zeta was found to be significantly upregulated (>1.5) in the RR cells of at least 4 of the biologically independent experiments of proteomic analysis (figure 46 A). The expression of 14-3-3 zeta was further confirmed by western blot in the P and RR cells of cell lines and patient samples (figure 46 B). 14-3-3 zeta was found to upregulated in RR cells of U87MG, SF268, PS1, and PS2. Thus, 14-3-3 zeta was considered to further understand its role in GBM progression and radio-resistance.

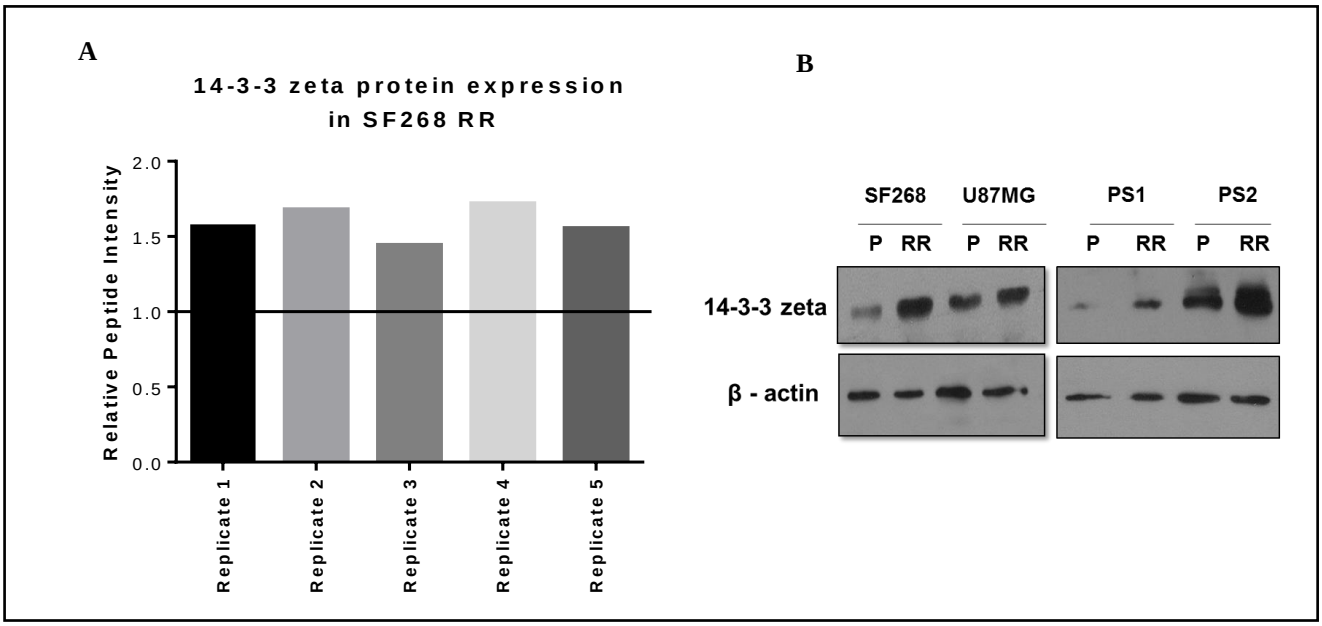

Figure 46 Expression of 14-3-3 zeta.

*A) 14-3-3 zeta relative peptide intensity values in SF268 RR in 5 biologically independent experiments of proteomic analysis. B) Western blot of 14-3-3 zeta in P (parent) and RR (Radio-resistant) cells of cell lines (SF268 and U87MG) and two patient samples (PS1, PS2). Beta-actin was used as loading control***.**

4.2.2.2 Identification of interacting partners of 14-3-3 ζ

Since 14-3-3 zeta belongs to the protein family which serves as adapter proteins by protein-protein interactions. We thus initiated an exploratory study to identify the interacting partners of 14-3-3 zeta in the RR cells. For this, GST tagged 14-3-3 zeta was expressed and purified from a bacterial system using pGEX 4T 14-3-3 ζ vector. The purity and identity of the protein were confirmed by mass spectrometry (Figure 47 A).

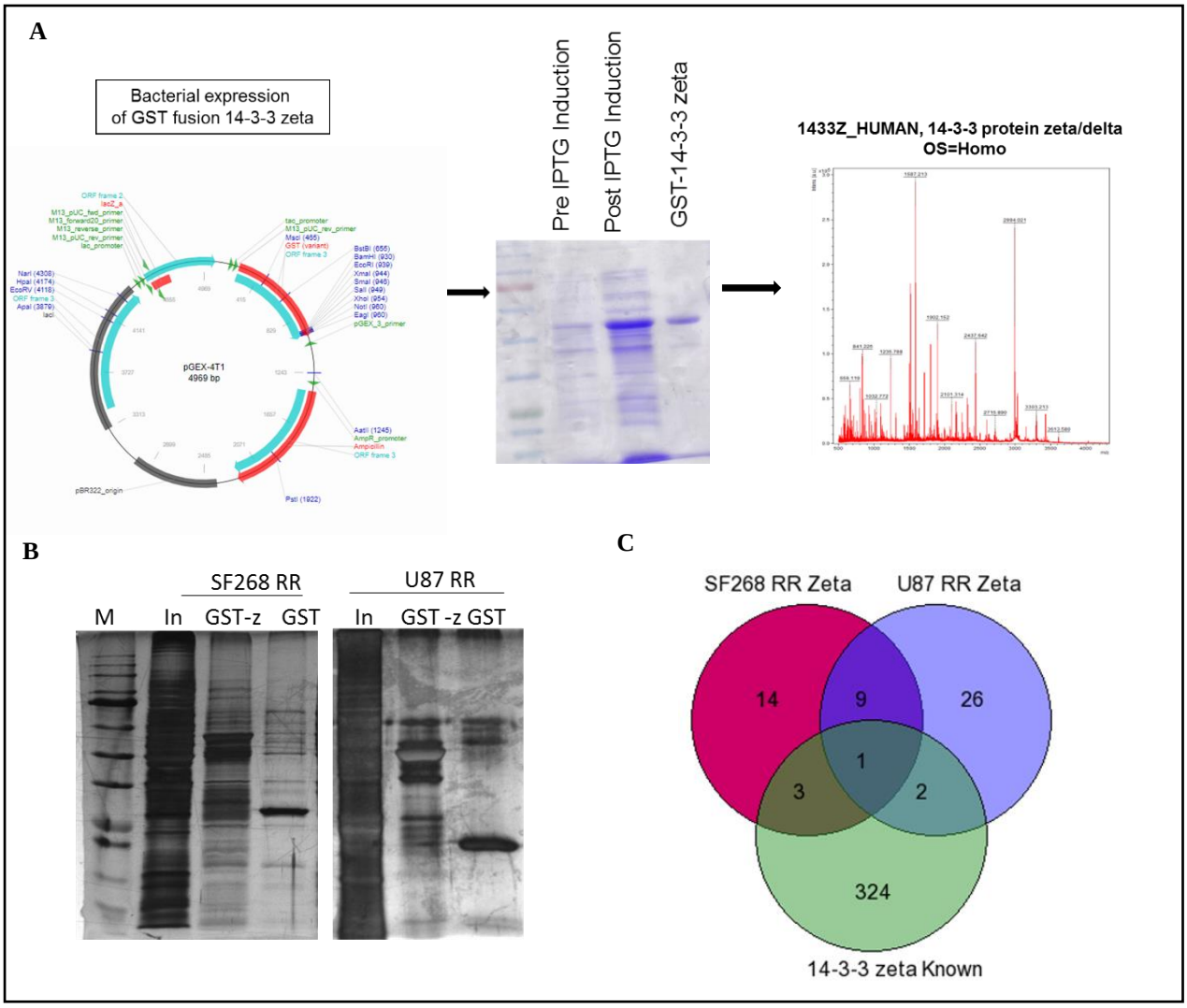

Figure 47 Identification of ζ interacting partners using GST pull down assay.

(A) Bacterial purification of GST tagged 14-3-3 ζ protein using pGEX 4T vector. The purified protein was confirmed for its purity and identity by extracting the protein from a Coomassie-stained gel and by mass spectrometry. (B) Silver-stained gel images of pull-down eluate for SF268 RR and U87MG RR using GST tagged 14-3-3 ζ (GST –z) and GST alone along with whole cell lysate as the input (In). (C) Venn diagram representing the common interacting proteins of 14-3-3 ζ identified in SF268 RR and U87MG RR. The third circle represents the known interacting partners of 14-3-3 ζ.

This purified protein was then incubated with whole cell lysates of SF268 RR and U87 RR cells and GST pull-down assay was performed. The empty pGEX 4T vector was used as a control. The eluted proteins were resolved on an SDS PAGE, silver stained, in-gel trypsin digested and run through LC-MS-MS for protein identification (Figure 47 B).

After performing at least 3 biologically independent experiments, 27 proteins were found to interact with 14-3-3 zeta in SF268 RR cells and 38 proteins were found to interact in U87MG

RR cells. According to the bio grid database, 14-3-3 zeta is known to interact with approximately 330 proteins. Thus, a gene set overlap was done to identify common interactors of ζ between SF268 and U87MG and to identify how many among the overlapping proteins were already known interactors (figure 47 C). In total, 15 proteins were common interacting proteins present in both SF268 and U87MG, of which 10 were novel binding partners and 5 proteins were known interacting partners of 14-3-3 zeta. The table below enlists all the 15 proteins that were identified. Interestingly, 12 out of the 15 proteins were also identified in our differential proteomic analysis as represented in table 3. 5. Among these 15 proteins are the proteins involved in glycolysis, TCA cycle, and ATP synthesis – GAPDH, MDH, ATP5A, PGK1, and ENO1. 2 proteins, catalase, and peroxiredoxin are known to aid the cells in overcoming oxidative stress (152). Annexin A2 and Serpin B12 are proteins involved in regulating cellular apoptosis as enlisted in table 4. Collectively, 14-3-3 zeta was found to interact with proteins involved in modulating metabolism, apoptosis and oxidative stress in the RR cells. Further functional experiments need to be performed to confirm and support this data set.

	Protein Name	Gene ID	iTRAQ
Unknown	Actin, cytoplasmic 2 OS	ACTG1	Yes
	Isoform 2 of Annexin A2 OS	ANXA2	Yes
	Zinc-alpha-2-glycoprotein OS	AZGP1	No
	Catalase OS	CAT	No
	Carbonyl reductase [NADPH] 1 OS	CBR1	Yes
	Elongation factor 1-gamma OS	EEF1G	Yes
	Glyceraldehyde-3-phosphate dehydrogenase, testis-specific OS	GAPDHS	Yes
	Malate dehydrogenase, mitochondrial OS	MDH2	Yes
	Serpin B12 OS	SERPINB12	No
Known	ATP synthase subunit alpha, mitochondrial OS	ATP5A1	Yes
	Phosphoglycerate kinase 1 OS	PGK1	Yes
	Alpha-enolase OS	ENO1	Yes
	Putative beta-actin-like protein 3 OS	POTEKP	No
	Peroxiredoxin-1 OS	PRDX1	Yes
	14-3-3 zeta	YWHAZ	Yes

Table 3 List of interacting proteins identified in RR cells

	Protein Name	Gene ID	iTRAQ
Metabolism	Glyceraldehyde-3-phosphate dehydrogenase, testis-specific OS	GAPDHS	Yes
	Malate dehydrogenase, mitochondrial OS	MDH2	Yes
	ATP synthase subunit alpha, mitochondrial OS	ATP5A1	Yes
	Phosphoglycerate kinase 1 OS	PGK1	Yes
	Alpha-enolase OS	ENO1	Yes
Antioxidant	Zinc-alpha-2-glycoprotein OS	AZGP1	No
	Catalase OS	CAT	No
	Peroxiredoxin-1 OS	PRDX1	Yes
	Carbonyl reductase [NADPH] 1 OS	CBR1	Yes
Cytoskeleton	Actin, cytoplasmic 2 OS	ACTG1	Yes
	Isoform 2 of Annexin A2 OS	ANXA2	Yes
	Putative beta-actin-like protein 3 OS	POTEKP	No
Others	Serpin B12 OS	SERPINB12	No
	Elongation factor 1-gamma OS	EEF1G	Yes
	14-3-3 zeta	YWHAZ	Yes

Table 4 List of interacting proteins functionally classified

4.2.2.3 Metabolic changes in the RR cells

Since 14-3-3 ζ showed plausible interactions with metabolic enzymes and antioxidants, the mitochondrial function of the RR cells was evaluated using the Seahorse XF Cell Mito Stress Test which measures oxygen consumption rate (OCR) of cells (figure 48 A). Sequential compound injections measure basal respiration, ATP production, proton leak, maximal respiration, spare respiratory capacity, and non-mitochondrial respiration rates. The RR cells showed an increase in proton leak compared to the parent cells and the non-mitochondrial respiration rate in SF268 RR cells was significantly higher as shown in figure 48 B & C.

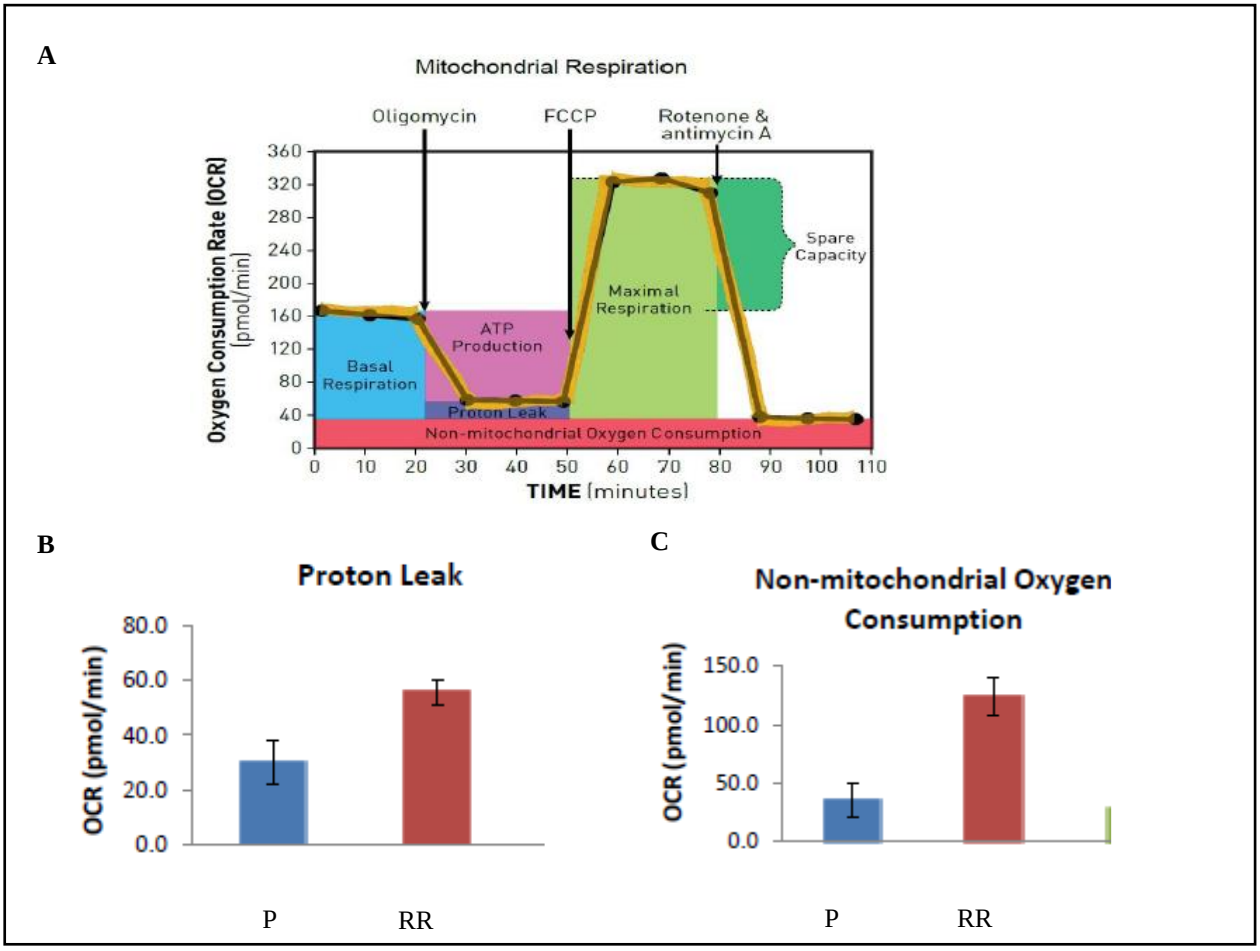

Figure 48 Mitochondrial function of RR compared to R.

A) Schematic presentation of the Mito stress assay performed on the SF268 RR cells. (B) Graphical representation of the proton leak and non-mitochondrial oxygen consumption

The increased proton leak in the RR cells demonstrates higher extracellular acidification rate. Additionally, electron microscopy revealed that the mitochondria of RR cells were significantly more in number and were elongated in morphology compared to the parent cells which harbor circular morphology (figure 49 A, B & C).

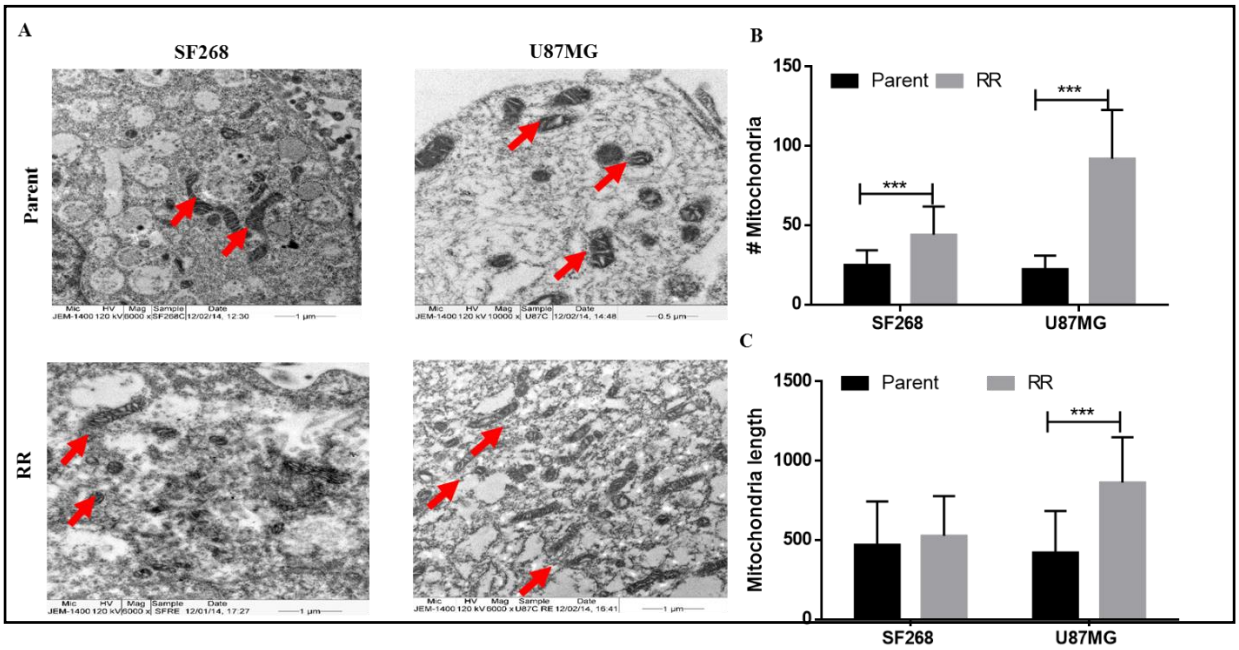

Figure 49 Mitochondrial morphology of P and RR cells.

***(A* Electron microscopy images of P and RR cells of SF268 and U87MG. (B) Graphical representation of the number of mitochondria in P and RR cells. (C) Graphical representation of length of mitochondria**

In conclusion, the findings in this study suggest a metabolic rewiring taking place in the RR cells. However, these outcomes need to be further confirmed by the 14-3-3 zeta knockdown cells to verify the role of 14-3-3 zeta in metabolic reprogramming of RR cells.

4.2.3 Discussion

14-3-3 proteins are well-known cancer therapeutic targets owing to their central role in regulating various cellular processes such as proliferation, apoptosis, signal transduction, migration, and invasion. In glioblastoma, various studies have reported a strong association

between 14-3-3 overexpression and glioma progression and therapy resistance. Also in our analysis, we found 14-3-zeta to be significantly upregulated in residual resistant cells that have an enhanced ability to survive and form relapse. Among the seven isoforms, 14-3-3 zeta was the only isoform found to be upregulated in the RR cells of all biologically independent proteomic analysis. The expression was confirmed by western blot in the RR cells of cell lines as well as primary cultures from the patient samples. Thus, excluding the fact that our findings could be just a cell line effect.

14-3-3 ζ is known to function in an interdependent manner via dynamic interactions with various proteins to regulate numerous cellular processes. Its diverse nature to dynamically interact with various proteins points towards a network of proteins influencing radio-resistance and relapse. Hence, to understand what processes it could be modulating we first chose to identify the interacting partners of 14-3-3 zeta in the RR cells. For this, a GST pull-down assay was performed with a purified form of GST tagged 14-3-3 ζ protein extract to identify interacting partners of 14-3-3 zeta in the RR cells of SF268 and U87MG. Amongst the proteins identified by mass spectrometry, 5 of the proteins were enzymes involved in metabolism such as Glycolysis (GAPDH, PGK1. ENO1), TCA cycle (MDH), ATP synthesis (ATP5A). The identification of these metabolic enzymes as 14-3-3ζ interacting proteins along with antioxidants such as CAT and PRDX1 indicates that 14-3-3ζ might be helping the RR cells to combat stress and survive. 14-3-3ζ has been reported to defend cells from numerous stresses, including chemotherapy-induced death, anoikis, and growth factor deprivation (153-155) S.E. Meek,et al in a seminal study in 2004 (156) using mammalian 14-3-3ζ as bait confirmed its interaction with metabolic enzymes such as pyruvate kinase M(PK), ATP-synthase(AS), glyceraldehyde-3-phosphate dehydrogenase (GAPDH), fatty acid synthase(FAS) and the bifunctional enzyme 6-phosphofructo-2-kinase/fructose-2,6-bisphosphatase (PFK-2). Concurrently, an independent experiment done in our lab to measure

the mitochondrial respiration rate of our RR cells revealed increased proton leak suggesting an increased extracellular acidification rate. We also observed the difference in the mitochondrial morphology in the RR cells compared to the parent cells in electron microscopy. The 14-3-3 proteins have been shown to regulate cellular metabolism (157). Furthermore, in a recent report is shown to regulate mitochondrial respiratory reserve in platelets regulating their bioenergy (158). In another study quantitative proteomic analysis of mitochondria from sensitive and resistant ovarian cancer cells have identified 14-3-3- zeta to be differentially present in the mitochondria of resistant cells (159). Taken together, these findings strongly suggest a plausible role of 14-3-3 zeta in regulating the metabolic processes in the RR cells which may confer resistance and recurrence. However, to support and confirm this hypothesis rigorous functional experiments need to be conducted. Nevertheless, the findings of this study have provided a new aspect of 14-3-3 ζ in glioblastoma which can be further explored.

5 Summary and Conclusion

5.1 Summary

Therapy resistance and recurrence in glioblastoma are inescapable conditions for a newly diagnosed glioblastoma patient. This is currently an escalating phenomenon in glioblastoma due to our inability to target residual radiation resistant (RR) cells which are invisible and inaccessible post initial treatment. We, therefore, recapitulated the clinical scenario of resistance in a cellular model developed from fresh primary GBM patient samples and cell lines. The model allowed us to capture 1) Parent cells 2) innately Radiation Resistant cells – less than 10% of the parent population and 3) Relapse (R) cells. A previously published study from our lab, Kaur E et al demonstrated that these RR cells were reversibly senescent for a short interval and enriched with MNGCs after exposure to a lethal dose of radiation. After being in a non-proliferative phase these RR cells resumed growth to form mononucleated relapse cells. The work done in this thesis stems from these findings to gain insight into the molecular mechanism of therapy resistance in glioblastoma using a proteomics approach. Following aspects were examined and recorded:

1. The aggressive nature of the relapse cells was tested on two cell lines (U87MG, SF268) by first monitoring the radiation response of the relapse cells by subjecting them to the second round of lethal dose of radiation. It was observed that the relapse cells responded in a similar manner as the parent cells. They also exhibited the presence of non-proliferative cells which remained undivided for about a week and grew back to form the second relapse population. The D_0 dose of the Parent, R1, R_2 cells shows an increasing trend. The relapse cells were found to be significantly more migrating as compared to the parent cells in both cell lines and patient samples. The relapse cells were also more invading than the parent cells in the cell lines. However, in patient samples, the relapse cells were equally invasive than their respective parent

counterparts. This could be attributed to heterogeneity of the tumor tissues and differential response of recurrent tumors to radiation.

2. The MNGCs found to be enriched in the RR cells were formed even when the glioblastoma cells were administered with a repeated exposure of radiation in 2Gy fractions and a daily dose of TMZ at the plasma concentration (25 µM). We observed that MNGCs and the transient non-proliferative phase is not just a consequence of a sudden exposure to high dose of radiation but they are formed even at a dose which is standardly used in the clinics. Thus, reflecting the phenomenon of a transient tumor dormancy before an aggressive relapse due to the presence of innately radio-resistant cells which are characterized by MNGCs.
3. The presence of MNGCs and the transient non-proliferative phase post-IR was not just restricted to glioblastoma. It was found to occur in breast cancer as well as colorectal cancer where these cells also displayed a similar response to a lethal dose of radiation. The RR cells formed in different cancer cell lines also exhibited increased expression of survival genes and SASPs.
4. A differential proteomic analysis using iTRAQ technology was performed on the parent, RR and R cells of SF268. Unsupervised clustering of the proteomics data identified protein clusters uniquely differential in each population. The RR cells harbored maximum genes to be uniquely differential as compared to P and R cells.
5. The RR cells showed a significant deregulation of the proteasome pathway in the three biologically independent proteomic analysis. The increased expression of the proteasome pathway was further confirmed by western blot analysis of proteasome subunits PSME1, PSMA7, and PSMB4. Along with increased expression, the RR cells also harbored enhanced proteasome activity in cell lines as well as patient samples.

6. Pharmacological inhibition of proteasome activity using the well-known FDA approved proteasome inhibitor – Bortezomib rendered the RR cells sensitive to radiation. A dose-dependent reduction in proteasome activity was observed in both P and RR cells. However, the cell viability of RR cells reduced more drastically as compared to the P cells after administration of the proteasome inhibitor in vitro.
7. The RR cells showed increased levels of activated phospho-p65 protein, a *bona fide* target of proteasomes as well as a significant increase (20 fold) in NFkB transcriptional activity as compared to the parent population (P) was also seen. Concurrently, at least 6 out of the 9 target genes of phospho-NFkB showed significantly increased expression in SF268, U87, and PS1
8. Administration of the proteasome inhibitor (Bortezomib) in the P and RR cells diminished this activity of NF-kB by 1.5 and 3.0-fold confirming the dependency of NFkB activity on the proteasome activity also suggesting an important role of NFKB in the survival of RR cells.
9. Most importantly, the therapeutic potential of using proteasomal inhibitors was established using an in vivo orthotopic GBM model. Firstly, the survival dependency of RR cells on proteasome function in vivo was demonstrated by orthotopically injecting BTZ pre-treated RR cells. These cells showed reduced tumorigenicity as compared to the group injected with BTZ pre-treated P cells along with a significant increase in their overall survival. Secondly, mice that developed GBM by intracranial injections of GBM cell line were administered a clinically relevant fractionated dose of radiation along with the intraperitoneal injection of BTZ. BTZ treated mice showed a significant increase in their disease-free survival along with reduced tumorigenicity as compared to the control group.

10. Apart from identifying proteasome pathway as a potential target for residual cells, the candidate-based approach revealed increased expression of 14-3-3 ζ in the RR cells compared to the P cells of GBM cell lines as well as patient samples. This protein regulates various cellular processes through dynamic interactions with its interacting partner. Hence in this study, GST fused ζ was used as bait for identifying the interacting partners of ζ in SF268 RR and U87MG RR population through GST pull-down assay followed by mass spectrometry. The data revealed plausible interactions with metabolic enzymes such as those involved in glycolysis, TCA cycle, ATP synthesis and antioxidants, cytoskeleton proteins. Since RR cells also show increased ATP production and the difference in their mitochondrial morphology, hence 14-3-3 zeta may have a role to play in the metabolic rewiring of the RR cells.

5.2 Conclusion

The aim of this study was to identify the processes deregulated in the innately radiation resistant residual (RR) population as we have previously shown that these are the cells responsible for relapse in glioblastoma. iTRAQ based quantitative proteomic analysis on the parent (P), innately radiation resistant residual (RR) and relapse (R) population revealed significantly deregulation of the proteasome pathway in the RR cells. Contrary to other reports, the RR cells displayed enhanced expression and activity of proteasome subunits, which triggered NFkB signaling. Pharmacological inhibition of proteasome activity led to impeded NFkB transcriptional activity, radio-sensitization of RR cells *in vitro*, and significantly reduced capacity to form orthotopic tumors *in vivo*. We demonstrate that a combination of proteasome inhibitor with radio-therapy abolish the inaccessible residual resistant cells thereby preventing GBM recurrence. However, the exact mechanism downstream to higher proteasome expression and NF-kB activity in the RR cells needs to be further explored. Nonetheless, this study establishes that proteasomes aid the survival of the innate radiation resistant population via a NFkB pathway and hence can be valuable targets for precluding relapse in glioblastoma. Apart from the

identification of biological processes governing the survival of RR cells, proteomic data revealed 14-3-3-zeta.overexpression of 14-3-3 zeta in the RR cells. In the quest to identify the broader functions of ζ via its interacting partners we found that it binds to metabolic enzymes, antioxidants, cytoskeletal proteins and apoptosis regulators. Since we also observe increased ECAR in the RR cells and changes in their mitochondrial morphology, it indicates that ζ might be curbing the metabolic processes in the RR cells to confer resistance and relapse. However, these findings need to be supported with more intricate results. To summarize, this study has revealed new insights into the radiation resistant residual cells and relapse cells that can be further explored for a deeper knowledge of radio resistance and recurrence in glioblastoma.

6 References

1. Bleeker FE, Molenaar RJ, Leenstra S. Recent advances in the molecular understanding of glioblastoma. Journal of neuro-oncology. 2012 May;108(1):11-27. PubMed PMID: 22270850. Pubmed Central PMCID: 3337398.
2. Stupp R1 MW, van den Bent MJ, Weller M, Fisher B, Taphoorn MJ, Belanger K, Brandes AA, Marosi C, Bogdahn U, Curschmann J, Janzer RC, Ludwin SK, Gorlia T, Allgeier A, Lacombe D, Cairncross JG, Eisenhauer E, Mirimanoff RO. Radiotherapy plus concomitant and adjuvant temozolomide for glioblastoma. N Engl J Med. 2005 March 10;352:9.
3. Stupp R1 HM, Mason WP, van den Bent MJ, Taphoorn MJ, Janzer RC, Ludwin SK, Allgeier A, Fisher B, Belanger K, Hau P, Brandes AA, Gijtenbeek J, Marosi C, Vecht CJ, Mokhtari K, Wesseling P, Villa S, Eisenhauer E, Gorlia T, Weller M, Lacombe D, Cairncross JG, Mirimanoff RO. Effects of radiotherapy with concomitant and adjuvant temozolomide versus radiotherapy alone on survival in glioblastoma in a randomised phase III study: 5-year analysis of the EORTC-NCIC trial. 2009;10.
4. Glas M, Rath BH, Simon M, Reinartz R, Schramme A, Trageser D, et al. Residual tumor cells are unique cellular targets in glioblastoma. Annals of neurology. 2010 Aug;68(2):264-9. PubMed PMID: 20695020. Pubmed Central PMCID: 4445859.
5. Kelley K, Knisely J, Symons M, Ruggieri R. Radioresistance of Brain Tumors. Cancers. 2016 Mar 30;8(4). PubMed PMID: 27043632. Pubmed Central PMCID: 4846851.
6. Weller M, Cloughesy T, Perry JR, Wick W. Standards of care for treatment of recurrent glioblastoma--are we there yet? Neuro-oncology. 2013 Jan;15(1):4-27. PubMed PMID: 23136223. Pubmed Central PMCID: 3534423.
7. Roy S, Lahiri D, Maji T, Biswas J. Recurrent Glioblastoma: Where we stand. South Asian journal of cancer. 2015 Oct-Dec;4(4):163-73. PubMed PMID: 26981507. Pubmed Central PMCID: 4772393.
8. Reardon DA. Therapeutic Advances in the Treatment of Glioblastoma: Rationale and Potential Role of Targeted Agents. The Oncologist. 2006;11(2):152-64.
9. Zhang X. Glioblastoma multiforme: Molecular characterization and current treatment strategy (Review). Experimental and Therapeutic Medicine. 2011.
10. Weller M, Cloughesy T, Perry JR, Wick W. Standards of care for treatment of recurrent glioblastoma--are we there yet? Neuro-Oncology. 2012;15(1):4-27.
11. Mangum R. Glioma Stem Cells and their Therapy Resistance. Journal of Carcinogenesis & Mutagenesis. 2012;01(S1).
12. Kanu OO, Mehta A, Di C, Lin N, Bortoff K, Bigner DD, et al. Glioblastoma multiforme: a review of therapeutic targets. Expert Opin Ther Targets. 2009 Jun;13(6):701-18. PubMed PMID: 19409033. Epub 2009/05/05. eng.
13. Wurth R, Barbieri F, Florio T. New Molecules and Old Drugs as Emerging Approaches to Selectively Target Human Glioblastoma Cancer Stem Cells. Biomed Res Int. 2014;2014:126586. PubMed PMID: 24527434. Pubmed Central PMCID: 3909978.
14. Roger Stupp MD, Warren P. Mason, M.D., Martin J. van den Bent, M.D.,, Michael Weller MD, Barbara Fisher, M.D., Martin J.B. Taphoorn, M.D.,, Karl Belanger MD, Alba A. Brandes, M.D., Christine Marosi, M.D.,, Ulrich Bogdahn MD, Jürgen Curschmann, M.D., Robert C. Janzer, M.D.,, Samuel K. Ludwin MD, Thierry Gorlia, M.Sc., Anouk Allgeier, Ph.D.,, Denis Lacombe MD, J. Gregory Cairncross, M.D., Elizabeth Eisenhauer, M.D.,, et al. Radiotherapy plus Concomitant and Adjuvant Temozolomide for Glioblastoma. The new england journal of medicine. 2005.
15. Kaur E, Rajendra J, Jadhav S, Shridhar E, Goda JS, Moiyadi A, et al. Radiation-induced homotypic cell fusions of innately resistant glioblastoma cells mediate their sustained survival and recurrence. Carcinogenesis. 2015 Jun;36(6):685-95. PubMed PMID: 25863126.
16. Zhang X, Zhang W, Cao WD, Cheng G, Zhang YQ. Glioblastoma multiforme: Molecular characterization and current treatment strategy (Review). Experimental and

therapeutic medicine. 2012 Jan;3(1):9-14. PubMed PMID: 22969836. Pubmed Central PMCID: 3438851.
17. Kumar DM, Patil V, Ramachandran B, Nila MV, Dharmalingam K, Somasundaram K. Temozolomide-modulated glioma proteome: role of interleukin-1 receptor-associated kinase-4 (IRAK4) in chemosensitivity. Proteomics. 2013 Jul;13(14):2113-24. PubMed PMID: 23595970.
18. ZHANG AWaG. Differential gene expression analysis in glioblastoma cells

and normal human brain cells based on GEO database. ONCOLOGY LETTERS. 2017 07 September;14.
19. Mann APM. Proteomics to study genes and genomes. NATURE. 2000;405 |.
20. Picotti P, Bodenmiller B, Aebersold R. Proteomics meets the scientific method. Nature methods. 2013 Jan;10(1):24-7. PubMed PMID: 23269373.
21. . !!! INVALID CITATION !!!
22. Khwaja FW, Reed MS, Olson JJ, Schmotzer BJ, Gillespie GY, Guha A, et al. Proteomic identification of biomarkers in the cerebrospinal fluid (CSF) of astrocytoma patients. J Proteome Res. 2007 Feb;6(2):559-70. PubMed PMID: 17269713. Pubmed Central PMCID: 2566942.
23. Vogel TW, Zhuang Z, Li J, Okamoto H, Furuta M, Lee YS, et al. Proteins and protein pattern differences between glioma cell lines and glioblastoma multiforme. Clinical cancer research : an official journal of the American Association for Cancer Research. 2005 May 15;11(10):3624-32. PubMed PMID: 15897557.
24. de Aquino PF, Carvalho PC, Nogueira FC, da Fonseca CO, de Souza Silva JC, Carvalho Mda G, et al. A Time-Based and Intratumoral Proteomic Assessment of a Recurrent Glioblastoma Multiforme. Frontiers in oncology. 2016;6:183. PubMed PMID: 27597932. Pubmed Central PMCID: 4992702.
25. Zhang P, Guo Z, Zhang Y, Gao Z, Ji N, Wang D, et al. A preliminary quantitative proteomic analysis of glioblastoma pseudoprogression. Proteome science. 2015;13:12. PubMed PMID: 25866482. Pubmed Central PMCID: 4393599.
26. Hudler P, Kocevar N, Komel R. Proteomic approaches in biomarker discovery: new perspectives in cancer diagnostics. TheScientificWorldJournal. 2014;2014:260348. PubMed PMID: 24550697. Pubmed Central PMCID: 3914447.
27. Kalinina J, Peng J, Ritchie JC, Van Meir EG. Proteomics of gliomas: initial biomarker discovery and evolution of technology. Neuro-oncology. 2011 Sep;13(9):926-42. PubMed PMID: 21852429. Pubmed Central PMCID: 3158015.
28. Collet B, Guitton N, Saikali S, Avril T, Pineau C, Hamlat A, et al. Differential analysis of glioblastoma multiforme proteome by a 2D-DIGE approach. Proteome science. 2011;9(1):16. PubMed PMID: 21470419. Pubmed Central PMCID: 3083325.
29. Niclou SP, Fack F, Rajcevic U. Glioma proteomics: status and perspectives. J Proteomics. 2010 Sep 10;73(10):1823-38. PubMed PMID: 20332038.
30. Thaker NG, Zhang F, McDonald PR, Shun TY, Lewen MD, Pollack IF, et al. Identification of survival genes in human glioblastoma cells by small interfering RNA screening. Molecular pharmacology. 2009 Dec;76(6):1246-55. PubMed PMID: 19783622. Pubmed Central PMCID: 2784725.
31. Hill JJ, Moreno MJ, Lam JC, Haqqani AS, Kelly JF. Identification of secreted proteins regulated by cAMP in glioblastoma cells using glycopeptide capture and label-free quantification. Proteomics. 2009 Feb;9(3):535-49. PubMed PMID: 19137551.
32. Furuta M, Weil RJ, Vortmeyer AO, Huang S, Lei J, Huang TN, et al. Protein patterns and proteins that identify subtypes of glioblastoma multiforme. Oncogene. 2004 Sep 2;23(40):6806-14. PubMed PMID: 15286718.

33. Smith JS JR. Genetic alterations in adult diffuse glioma: occurrence, significance, and prognostic implications. Front Biosci. 2000 Jan 1;5:D213-31.
34. Ohgaki HaK, P. Population-based studies on incidence, survival rates, and genetic alterations in astrocytic and oligodendroglial gliomas. J Neuropathol Exp Neurol 2005 (64): 479–89.
35. Society AC. Cancer Facts and Figures 2010. Atlanta American Cancer Society. 2010.
36. Thakkar J DT, Horbinski C, Ostrom QT, Lightner DD, Barnholtz-Sloan JS, et al. . Epidemiologic and molecular prognostic review of glioblastoma. Cancer Epidemiol Biomarkers Rev. 2014;23((10)):1985–96.
37. Morgan LL. The epidemiology of glioma in adults: a “state of the science” review. Neuro Oncol. 2015 Apr;17(4):623–4.
38. Ostrom QT GH, Fulop J, Liu M, Blanda R, Kromer C, Wolinsky Y, Kruchko C, Barnholtz-Sloan JS. CBTRUS Statistical Report: Primary Brain and Central Nervous System Tumors Diagnosed in the United States in 2008-2012. Neuro Oncol 2015 Oct;17
39. Ellor SV P-YT, Avgeropoulos NG. Glioblastoma: background, standard treatment paradigms, and supportive care considerations.

. J Law Med Ethics. 2014 42(2):171-82.
40. Munshi A JR. Therapy for glioma: Indian perspective. . Indian J Cancer 2009;46:127-31.
41. Wen PYaK, S. Malignant gliomas in adults. N Engl J Med 2008;359:492–507.
42. Blissitt PA AAoNN. Clinical practice guideline series update: care of the adult patient with a brain tumor. J Neurosci Nurs 2014 Dec;46(6):367-8.
43. Tyler C. Steed Merk JMT, Amanda R. Smith, Kunal Patel, Bob S. Carter, Valya Ramakrishnan, Anders M. Dale,, Lionel M. L. Chow, Alexander and Clark C. Chen. Differential localization of glioblastoma subtype: implications on glioblastoma pathogenesis. Oncotarget. 2016 April 01, 2016.
44. Johnson DR FS, Giannini C, Kaufmann TJ, Raghunathan A, Theodosopoulos PV, Clarke JL. . Case-based review: Newly diagnosed glioblastoma. . Neuro-Oncology Practice. 2015;2:106–21.
45. Alifieris C TD. Glioblastoma multiforme: Pathogenesis and treatment. Pharmacol Ther 2015 Aug 152.
46. A. L. Imaging in glioblastoma multiforme. . 2015
47. Young RM JA, Davis G, Sherman JH. Current trends in the surgical management and treatment of adult glioblastoma. Ann Transl Med 2015 Jun;3(9).
48. Network NCC. Clinical Practice Guidelines in Oncology: Central nervous system cancers 2015
49. Barani IJ LD. Radiation therapy of glioblastoma. Cancer Treat Res 2015;163:49-73.
50. Zhao S WJ, Wang C, Liu H, Dong X, Shi C, Shi C, Liu Y, Teng L, Han D, Chen X, Yang G, Wang L, Shen C, Li H. Intraoperative fluorescence-guided resection of high-grade malignant gliomas using 5-aminolevulinic acid-induced porphyrins: a systematic review and meta-analysis of prospective studies. PLoS One 2013;8(5).
51. Barone DG LT, Hart MG, Cochrane. Image guided surgery for the resection of brain tumours. Database Syst Rev. 2014 Jan 28; (1).
52. Cohen MH SY, Keegan P, Pazdur R. FDA drug approval summary: bevacizumab (Avastin) as treatment of recurrent glioblastoma multiforme. Oncologist 2009 Nov;14(11):1131-8.
53. Taal W OH, Walenkamp AM, Dubbink HJ, Beerepoot LV, Hanse MC, Buter J, Honkoop AH, Boerman D, de Vos FY, Dinjens WN, Enting RH, Taphoorn MJ, van den Berkmortel FW, Jansen RL, Brandsma D, Bromberg JE, van Heuvel I, Vernhout RM, van der

Holt B, van den Bent MJ. Single-agent bevacizumab or lomustine versus a combination of bevacizumab plus lomustine in patients with recurrent glioblastoma (BELOB trial): a randomised controlled phase 2 trial. Lancet Oncol 2014 15(9):943-53.
54. Stupp R TS, Kanner AA, Kesari S, Steinberg DM, Toms SA, Taylor LP, Lieberman F, Silvani A, Fink KL, Barnett GH, Zhu JJ, Henson JW, Engelhard HH, Chen TC, Tran DD, Sroubek J, Tran ND, Hottinger AF, Landolfi J, Desai R, Caroli M, Kew Y, Honnorat J, Idbaih A, Kirson ED, Weinberg U, Palti Y, Hegi ME, Ram Z. Maintenance Therapy With Tumor-Treating Fields Plus Temozolomide vs Temozolomide Alone for Glioblastoma: A Randomized Clinical Trial. JAMA 2015 Dec 15.
55. Mohammad Sami Walid M, PhD. Prognostic Factors for Long-Term Survival after Glioblastoma. The Permanente Journal. 2008;12(4).
56. Verhaak RG, Hoadley KA, Purdom E, Wang V, Qi Y, Wilkerson MD, et al. Integrated genomic analysis identifies clinically relevant subtypes of glioblastoma characterized by abnormalities in PDGFRA, IDH1, EGFR, and NF1. Cancer cell. 2010 Jan 19;17(1):98-110. PubMed PMID: 20129251. Pubmed Central PMCID: 2818769.
57. Houtan Noushmehr DJW, Kristin Diefes,Heidi S. Phillips, Kanan Pujara, Benjamin P. Berman,Fei Pan,Christopher E. Pelloski, Erik P. Sulman,Krishna P. Bhat, Roel G.W. Verhaak, Katherine A. Hoadley, D. Neil Hayes, Charles M. Perou, Heather K. Schmidt, Li Ding, Richard K. Wilson, David Van Den Berg, Hui Shen,Henrik Bengtsson, Pierre Neuvial, Leslie M. Cope, Jonathan Buckley, James G. Herman, Stephen B. Baylin, Peter W. Laird, Kenneth Aldape,and The Cancer Genome Atlas Research Network. Identification of a CpG Island Methylator Phenotype that Defines a Distinct Subgroup of Glioma. Cancer Cell. 2010 17(5):510–22. Epub May 18.
58. Chakravarti A, et al.,. Survivin enhances radiation resistance in primary human glioblastoma cells via caspase-independent mechanisms. . Oncogene, . 2004;23(45):7494-506.
59. Chakravarti A, et al., 15. The epidermal growth factor receptor pathway mediates resistance to sequential administration of radiation and chemotherapy in primary human glioblastoma cells in a RAS-dependent manner. Cancer Res, . 2002. ;62(15).
60. Ichimura K, et al., . Molecular pathogenesis of astrocytic tumours. . J Neurooncology. 2004; 70(2):137-60.
61. Chen J, R.M. McKay, and L.F. Parada, . Malignant glioma: lessons from genomics, mouse models, and stem cells. Cell. 2012;149(1):36-47.
62. Ines Crespo ALV, María Gonzalez-Tablas, María del Carmen Patino, Alvaro Otero, María Celeste Lopes, Catarina de Oliveira, Patricia Domingues, Alberto Orfao, Maria Dolores Tabernero. Molecular and Genomic Alterations in Glioblastoma Multiforme. The American Journal of Pathology. 2015;185(7):1820–33.
63. Bar E. E. CA, Lin A., et al. Cyclopamine-mediated Hedgehog pathway inhibition depletes stem-like cancer cells in glioblastoma. . Stem Cells. 2007;25(10):2524-33.
64. Clement V SP, Tribolet Nd, et al. . HEDGEHOG-GLI1 signaling regulates human glioma growth, cancer stem cell self-renewal, and tumorigenicity. . Curr Biol. 2007;17.
65. Jialiang Wang TPW, Justin D. Latha, Anita B. Hjelmeland, Xiao-Fan Wang, Rebekah R. White, Jeremy N. Rich, and Bruce A. Sullenger. Notch Promotes Radioresistance of Glioma Stem Cells. Stem Cells 2010;28(1):17-28.
66. Yu JB1 JH, Zhan RY1. Aberrant Notch signaling in glioblastoma stem cells contributes to tumor recurrence and invasion. Mol Med Rep. 2016;14(2):1263-8.
67. Massimo Squatrito CWB, Karim Helmy, Jason T. Huse, John H. Petrini, and Eric C. Holland. Loss of ATM/Chk2/p53 pathway components accelerates tumor development and contributes to radiation resistance in gliomas. Cancer Cell. 2010;18(6).

68. Wei Zhou MS, Guang-Hui Li, Yong-Zhong Wu, Ying Wang, Fu Jin, Yun-Yun Zhang, Li Yang, Dong-Lin Wang. Activation of the phosphorylation of ATM contributes to radioresistance of glioma stem cells. Oncology Reports. 2013;30:1793-801.
69. B. Pradet-Balade FB, H. Beug, E. W. Müllner, and J. A. Garcia-Sanz. Translation control: bridging the gap between genomics and proteomics? Trends in Biochemical Sciences. 2001;26(4):225-9.
70. Lage H. Proteomics in cancer cell research: an analysis of therapy resistance. Pathology, research and practice. 2004;200(2):105-17. PubMed PMID: 15237919.
71. UA K. Biomarker rediscovery in diagnostics. Expert Opin Med Diagn 2008;2(12):1391-400.
72. Basavaradhya Sahukar Shruthi PV, 1 and Selvamani2. Proteomics: A new perspective for cancer. Adv Biomed Res 2016;5(67).
73. E. Boja TH, R. Rivers et al. Evolution of clinical proteomics and its role in medicine. Journal of Proteome Research. 2011;10(1):66-84.
74. Kuster MBaB. Quantitative mass spectrometry in proteomics. Analytical and Bioanalytical Chemistry. 2012;404(4):937-8.
75. Aebersold RM. M. Mass spectrometry-based proteomics. Nature. 2003;422:198-207.
76. Bantscheff M, Schirle, M., Sweetman, G., Rick, J. & Küster, B. . Quantitative mass spectrometry in proteomics: a critical review. Anal Bioanal Chem. 2007;389:1017-31.
77. Albar LMaJP. Differential proteomics: An overview of gel and non gel based approaches. BRIEFINGS IN FUNCTIONAL GENOMICS AND PROTEOMICS. 2004;3(3):220-39.
78. Wiese S1 RK, Meyer HE, Warscheid B. Protein labeling by iTRAQ: a new tool for quantitative mass spectrometry in proteome research. Proteomics 2007;7(3):340-50.
79. W. W. Wu GW, S. J. Baek, and R. F. Shen,. Comparative study of three proteomic quantitative methods, DIGE, cICAT, and iTRAQ, using 2D gel- or LC-MALDI TOF/TOF. Journal of Proteome Research. 2006;5(3):651-8.
80. Furuta M WR, Vortmeyer AO, Huang S, Lei J, Huang TN, Lee YS, Bhowmick DA, Lubensky IA, Oldfield EH, Zhuang Z. . Protein patterns and proteins that identify subtypes of glioblastoma multiforme. . Oncogene. 2004;23:6806-14.
81. Khwaja FW1 RM, Olson JJ, Schmotzer BJ, Gillespie GY, Guha A, Groves MD, Kesari S, Pohl J, Van Meir EG. Proteomic identification of biomarkers in the cerebrospinal fluid (CSF) of astrocytoma patients. Journal of proteome research. 2007;6(2):559-70.
82. Uros Rajcevic‡ KP, Jaco C. Knol¶, Maarten Loos,,Se´ bastien Bougnaud, Oleg Klychnikov,KaWan L, Thang V. Pham, Jian Wang, Hrvoje Miletic, Zhao Peng, Rolf Bjerkvig, Connie R. Jimenez, and Simone P. Niclou. iTRAQ-based Proteomics Profiling Reveals Increased Metabolic Activity and Cellular Cross-talk in Angiogenic Compared with Invasive Glioblastoma Phenotype. Molecular & Cellular Proteomics 811. 2009.
83. de Saldanha da Gama Fischer J1 CCP, da Fonseca CO, Liao L, Degrave WM, da Gloria da Costa Carvalho M, Yates JR, Domont GB. Chemo-resistant protein expression pattern of glioblastoma cells (A172) to perillyl alcohol. Journal of Proteome Research. 2011;10(1):153-60.
84. Emmanuelle Com AC, Mélanie Lagarrigue, Sophie Michalak, Philippe Menei, Charles Pineau. Quantitative proteomic Isotope-Coded Protein Label (ICPL) analysis reveals alteration of several functional processes in the glioblastoma. Journal of Proteomics. 2012; 75(13):3898-913.
85. Polisetty RV, Gautam P, Sharma R, Harsha HC, Nair SC, Gupta MK, et al. LC-MS/MS analysis of differentially expressed glioblastoma membrane proteome reveals altered calcium signaling and other protein groups of regulatory functions. Molecular & cellular proteomics :

MCP. 2012 Jun;11(6):M111 013565. PubMed PMID: 22219345. Pubmed Central PMCID: 3433906.
86. Poonam Gautam. SCN, Manoj Kumar Gupta, Rakesh Sharma, Ravindra Varma Polisetty, Megha S. Uppin, Challa Sundaram, Aneel K. Puligopu, Praveen Ankathi, Aniruddh K. Purohit, Giriraj R. Chandak, H. C. Harsha, Ravi Sirdeshmukh. Proteins with Altered Levels in Plasma from Glioblastoma Patients as Revealed by iTRAQ-Based Quantitative Proteomic Analysis. PLoS One. 2012 August 22;7 (9).
87. Lescarbeau RS, Lei L, Bakken KK, Sims PA, Sarkaria JN, Canoll P, et al. Quantitative Phosphoproteomics Reveals Wee1 Kinase as a Therapeutic Target in a Model of Proneural Glioblastoma. Molecular Cancer Therapeutics. 2016;15(6):1332-43.
88. Aquino PF, Carvalho, P. C., Nogueira, F. C., da Fonseca, C. O. et al. A Time-Based and Intratumoral Proteomic Assessment of a Recurrent Glioblastoma Multiforme. Frontiers in oncology. 2016;6:183. PubMed PMID: 27597932. Pubmed Central PMCID: 4992702.
89. Rajaraman R et. al. Stem cells, senescence, neosis and self-renewal in cancer. Cancer Cell Int 2006.
90. Lathia J.D. VM, Rao M.S., Rich J.N. . Seeing is believing: Are cancer stem cells the loch ness monster of tumor biology? . Stem Cell Rev. 2011;7:227–37.
91. Dittmar T, Nagler C, Niggemann B, Zanker KS. The dark side of stem cells: triggering cancer progression by cell fusion. Current molecular medicine. 2013 Jun;13(5):735-50. PubMed PMID: 23642055.
92. Rycaj K. TDG. Cell-of-origin of cancer versus cancer stem cells: Assays and interpretations. Cancer Res,. 2015:4003–11.
93. Adorno-Cruz V. KG, Liu X., Doherty M., Junk D.J., Guan D., Hubert C., Venere M., Mulkearns-Hubert E., Sinyuk M., et al. Cancer stem cells: Targeting the roots of cancer, seeds of metastasis, and sources of therapy resistance. . Cancer Res,. 2015;75:924–9.
94. al. GRe. Isolation and characterization of tumorigenic, stem-like neural precursors from human glioblastoma. . Cancer Res,. 2004;64:7011-21.
95. al. FCMe. Human breast cancer cell lines contain stem-like cells that self-renew, give rise to phenotypically diverse progeny and survive chemotherapy. . Breast Cancer Res. 2008;10.
96. al. CJe. A restricted cell population propagates glioblastoma growth after chemotherapy. . Nature. 2012;488:522 - 6.
97. al. EPe. The role of cancer stem cells in breast cancer initiation and progression: potential cancer stem cell-directed therapies. Oncologist 2012;17:1394-401.
98. Nowak MJFHA. Glioblastoma stem-like cells: at the root of tumor recurrence and a therapeutic target Carcinogenesis. 2015;36(2):177-85.
99. Bao S WQ, McLendon RE, et al. . Glioma stem cells promote radioresistance by preferential activation of the DNA damage response. . Nature. 2006;444:756-60.
100. Peter Wend JDH, Ulrike Ziebold, Walter Birchmeier. Wnt signaling in stem and cancer stem cells. Seminars in Cell & Developmental Biology. October 2010;21(8):855-63.
101. al. TNe. Targeting cancer stem cells by inhibiting Wnt, Notch, and Hedgehog pathways. . Nat Rev Clin Oncol. 2011;8:97-106.
102. Johannes Möst LS, Gertraud Mayr, Annette Gasser, Alessandra Sarti and Manfred P. Dierich. Formation of Multinucleated Giant Cells In Vitro Is Dependent on the Stage of Monocyte to Macrophage Maturation. Blood. 1997;89:662-71.
103. Kawano H KT, Sato K , Goya T , Arikawa S , Wakisaka S Immunohistochemical study of giant cell in glioblastoma. Clinical Neuropathology. 1995;14:118-23.
104. Hosaka Mea. Giant cell formation through fusion of cells derived from a human giant cell tumor of tendon sheath. G J Orthop Sci. 2004;9:581-4.

105. Eom YWet a. Two distinct modes of cell death induced by doxorubicin: apoptosis and cell death through mitotic catastrophe accompanied by senescence-like phenotype. Oncogene. 2005;24:4765-77.
106. Barok Met a, R46. Trastuzumab-DM1 causes tumour growth inhibition by mitotic catastrophe in trastuzumab-resistant breast cancer cells in vivo. . Breast Cancer Res,. 2011;13.
107. Weihua Zet a. Formation of solid tumors by a single multinucleated cancer cell. Cancer. 2011;117:4092-9.
108. Hirai H, Arai T, Okada M, Nishibata T, Kobayashi M, Sakai N, et al. MK-1775, a small molecule Wee1 inhibitor, enhances anti-tumor efficacy of various DNA-damaging agents, including 5-fluorouracil. Cancer biology & therapy. 2010 Apr 1;9(7):514-22. PubMed PMID: 20107315.
109. Kaur E, Goda, J.S., Ghorai, A. et al. . Cell Oncol. 2018.
110. Suk K. Proteomic analysis of chemoresistance in glioblastoma. Current Neuropharmacology. 2012 (10):72-9.
111. McBride WH, Iwamoto KS, Syljuasen R, Pervan M, Pajonk F. The role of the ubiquitin/proteasome system in cellular responses to radiation. Oncogene. 2003 Sep 01;22(37):5755-73. PubMed PMID: 12947384.
112. Baugh JM, Viktorova EG, Pilipenko EV. Proteasomes can degrade a significant proportion of cellular proteins independent of ubiquitination. Journal of molecular biology. 2009 Feb 27;386(3):814-27. PubMed PMID: 19162040. Pubmed Central PMCID: 2649715.
113. Pahl HL. Activators and target genes of Rel/NF-kB transcription factors. Oncogene. 1999;18.
114. Songrong Ren MJS, Iuri D Louro, Peggy McKie-Bell et al. The p44S10 locus, encoding a subunit of the proteasome regulatory particle, is amplified during progression of cutaneous malignant melanoma. Oncogene. 2000;19:1419-27.
115. Chen L MK. Increased proteasome activity, ubiquitin-conjugating enzymes, and eEF1A translation factor detected in breast cancer tissue. Cancer Research. 2005;1(65):5599-606.
116. Rho JH QS, Wang JY, Roehrl MH. Proteomic expression analysis of surgical human colorectal cancer tissues: up-regulation of PSB7, PRDX1, and SRP9 and hypoxic adaptation in cancer. Journal of Proteome Research. 2008;7(7):2959-72.
117. A Arlt IB, C Schafmayer, J Tepel, S Sebens Müerköster et al. Increased proteasome subunit protein expression and proteasome activity in colon cancer relate to an enhanced activation of nuclear factor E2-related factor 2 (Nrf2). Oncogene. 2009;28:3983–96.
118. Della Donna LC, Pajonk F. Radioresistance of prostate cancer cells with low proteasome activity. The Prostate. 2012;1(72):868-74.
119. Smith L1 QO, Watson MB, Beavis AW, Potts D, Welham KJ, Garimella V, Lind MJ, Drew PJ, Cawkwell L. Proteomic identification of putative biomarkers of radiotherapy resistance: a possible role for the 26S proteasome? Neoplasia 2009;11(11):1194-207.
120. The UniProt C. UniProt: the universal protein knowledgebase. Nucleic acids research. 2017 Jan 04;45(D1):D158-D69. PubMed PMID: 27899622. Pubmed Central PMCID: 5210571.
121. Monika A. Jarzabek PCH, Kai O. Skaftnesmo, Emmet McCormack, Patrick Dicker, Jochen H.M. Prehn, Rolf Bjerkvig, and Annette T. Byrne. In Vivo Bioluminescence Imaging Validation of a Human Biopsy–Derived Orthotopic Mouse Model of Glioblastoma Multiforme. Molecular Imaging. 2013 May 12.
122. Burger AM, Seth AK. The ubiquitin-mediated protein degradation pathway in cancer: therapeutic implications. European journal of cancer. 2004 Oct;40(15):2217-29. PubMed PMID: 15454246.

123. Pajonk F, van Ophoven A, Weissenberger C, McBride WH. The proteasome inhibitor MG-132 sensitizes PC-3 prostate cancer cells to ionizing radiation by a DNA-PK-independent mechanism. BMC Cancer. 2005 Jul 07;5:76. PubMed PMID: 16001975. Pubmed Central PMCID: 1177933.
124. Qureshi N, Morrison DC, Reis J. Proteasome protease mediated regulation of cytokine induction and inflammation. Biochimica et biophysica acta. 2012 Nov;1823(11):2087-93. PubMed PMID: 22728331. Pubmed Central PMCID: 3465503.
125. Livneh I, Cohen-Kaplan V, Cohen-Rosenzweig C, Avni N, Ciechanover A. The life cycle of the 26S proteasome: from birth, through regulation and function, and onto its death. Cell research. 2016 Aug;26(8):869-85. PubMed PMID: 27444871. Pubmed Central PMCID: 4973335.
126. Pervan M IK, McBride WH. Proteasome Structures Affected by Ionizing Radiation. Molecular Cancer Research. 2005.
127. Pajonk Fea. Ionizing radiation affects 26s proteasome function and associated molecular responses, even at low doses. Radiotherapy and Oncology. 2001.
128. Tamari K, Hayashi K, Ishii H, Kano Y, Konno M, Kawamoto K, et al. Identification of chemoradiation-resistant osteosarcoma stem cells using an imaging system for proteasome activity. International journal of oncology. 2014 Dec;45(6):2349-54. PubMed PMID: 25269626.
129. Della Donna L, Lagadec C, Pajonk F. Radioresistance of prostate cancer cells with low proteasome activity. Prostate. 2012 Jun 01;72(8):868-74. PubMed PMID: 21932424. Pubmed Central PMCID: 3396561.
130. Smith L QO, Watson MB, Beavis AW, Potts D, Welham KJ, Garimella V, Lind MJ, Drew PJ, Cawkwell L. Proteomic Identification of Putative Biomarkers of Radiotherapy Resistance: A Possible Role for the 26S Proteasome? Neoplasia. 2009.
131. Crawford LJ, Walker B, Irvine AE. Proteasome inhibitors in cancer therapy. Journal of cell communication and signaling. 2011 Jun;5(2):101-10. PubMed PMID: 21484190. Pubmed Central PMCID: 3088792.
132. Teicher BA, Tomaszewski JE. Proteasome inhibitors. Biochemical pharmacology. 2015 Jul 01;96(1):1-9. PubMed PMID: 25935605.
133. Ahmed KM, Li JJ. NF-kappa B-mediated adaptive resistance to ionizing radiation. Free radical biology & medicine. 2008 Jan 01;44(1):1-13. PubMed PMID: 17967430. Pubmed Central PMCID: 2266095.
134. Cahill KE, Morshed RA, Yamini B. Nuclear factor-kappaB in glioblastoma: insights into regulators and targeted therapy. Neuro-oncology. 2016 Mar;18(3):329-39. PubMed PMID: 26534766. Pubmed Central PMCID: 4767244.
135. A A. 14-3-3 proteins: a historic overview. Semin Cancer Biol. 2006 Jun;16(3):162-72.
136. Boston PF, Jackson, P., & Thompson, R. J. . Human 14-3-3 Protein: Radioimmunoassay, Tissue Distribution, and Cerebrospinal Fluid Levels in Patients with Neurological Disorders. . Journal of neurochemistry. 1982;38(1475-1482).
137. Moore BW PV. In: Physiological and biochemical aspects of nervous integration. Carlson F, editor Englewood Cliffs, New Jersey: Prentice-Hall. 1967:343–59.
138. Chaudhri M SM, Aitken A Mammalian and yeast 14-3-3 isoforms form distinct patterns of dimers in vivo. Biochem Biophys Res Commun. 2003 (300:):679–85.
139. Jones DH LS, Aitken A. Isoforms of 14-3-3 protein can form homo- and heterodimers in vivo and in vitro: implications for function as adapter proteins. FEBS Lett 1995;368(1):55-8.
140. A.K. Gardino ea. Structural determinants of 14-3-3 binding specificities and regulation of subcellular localization of 14-3-3-ligand complexes: a comparison of the X-ray crystal structures of all human 14-3-3 isoforms. Semin Cancer Biol. 2006;16:173-82.

141. Xiaowen Yang ea. Structural basis for protein–protein interactions in the 14-3-3 protein family. PNAS. 2006 November 14;103(46):17237-42.
142. Muslin AJ, Tanner, J. W., Allen, P. M., and Shaw, A. S. . Interaction of 14-3-3 with signaling proteins is mediated by the recognition of phosphoserine. . Cell 1996;84(889-897).
143. Yaffe MB RK, Volinia S, Caron PR, Aitken A, Leffers H, Gamblin SJ, Smerdon SJ, Cantley LC. The structural basis for 14-3-3:phosphopeptide binding specificity. Cell. 1997 Dec 26;91(7):961-71.
144. Dougherty MK, & Morrison, D. K. Unlocking the code of 14-3-3. Journal of cell science. 2004;117(10):1875-84.
145. Matta A, DeSouza, L. V., Shukla, N. K., Gupta, S. D., Ralhan, R., & Siu, K. M. . Prognostic Significance of Head-and-Neck Cancer Biomarkers Previously Discovered and Identified Using iTRAQ-Labeling and Multidimensional Liquid Chromatography− Tandem Mass Spectrometry. . Journal of proteome research. 2008;7(5):2078-87.
146. Lin M, Morrison, C. D., Jones, S., Mohamed, N., Bacher, J., & Plass, C. . Copy number gain and oncogenic activity of YWHAZ/14-3-3ζ in head and neck squamous cell carcinoma. . International journal of cancer. 2009;125(3):603-11.
147. Macha MA, Matta, A., Chauhan, S. S., Siu, K. M., & Ralhan, R. 14-3-3 zeta is a molecular target in guggulsterone induced apoptosis in head and neck cancer cells. . BMC cancer. 2010;10(1).
148. Klemm C, Dommisch, H., Göke, F., Kreppel, M., Jepsen, S., Rolf, F., & Standop, J. Expression profiles for 14-3-3 zeta and CCL20 in pancreatic cancer and chronic pancreatitis. . Pathology-Research and Practice. 2014;210(6):335-41.
149. Jin LM, Han, X. H., Jie, Y. Q., & Meng, S. S. 14-3-3ζ silencing retards tongue squamous cell carcinoma progression by inhibiting cell survival and migration. . Cancer gene therapy. 2016;23(7).
150. Yang X, Cao, W., Zhou, J., Zhang, W., Zhang, X., Lin, W., & Wang, B. 14-3-3zeta positive expression is associated with a poor prognosis in patients with glioblastoma. Neurosurgery. 2011;68(4):932-9385.
151. Cao W. 14-3-3zeta positive cells show more tumorigenic characters in human glioblastoma. Turk Neurosurg,. 2016;26(6):813-7.
152. Péricles Arruda MLF, SouzabGecioni et al. A study of the relative importance of the peroxiredoxin-, catalase-, and glutathione-dependent systems in neural peroxide metabolism. Free Radical Biology and Medicine. 2011;51(1):69-77.
153. Vajira K. Weerasekara aDJP, a David G. Broadbent,a Jeffrey B. Mortenson,a Andrew D. Mathis,a Gideon N. Logan,a, John T. Prince aDMT, b J. Will Thompson,c Joshua L. Andersena. Metabolic-Stress-Induced Rearrangement of the 14-3-3 Interactome Promotes Autophagy via a ULK1- and AMPK-Regulated 14-3-3 Interaction with Phosphorylated Atg9. Molecular and Cellular Biology 2014;24:4379 – 88.
154. Zenggang Li JZ, Yuhong Du, Hae Ryoun Park, Shi-Yong Sun, Leon Bernal-Mizrachi, Alastair Aitken, Fadlo R. Khuri, and Haian Fu. Down-regulation of 14-3-3ζ suppresses anchorage-independent growth of lung cancer cells through anoikis activation. PNAS 2008;105:162-7.
155. Jing Lu HG, Warapen Treekitkarnmongkol, Ping Li, Jian Zhang, Bin Shi, Chen Ling, Xiaoyan Zhou, Tongzhen Chen, Paul J. Chiao, Xinhua Feng, Victoria L. Seewaldt, William J. Muller, Aysegul Sahin, Mien-Chie Hung,and Dihua Yu. 14-3-3ζ Cooperates with ErbB2 to Promote Progression of Ductal Carcinoma in Situ to Invasive Breast Cancer by Inducing Epithelial-Mesenchymal Transition. Cancer Cell. 2009;16(3):195-207.
156. Sarah E. M. Meek WSLaHP-W. Comprehensive Proteomic Analysis of Interphase and Mitotic 14-3-3-binding Proteins. Journal of biochemistry. 2004.

157. Rune Kleppea AM, Stein Ove Døskeland, Jan Haavik. The 14-3-3 proteins in regulation of cellular metabolism. Seminars in Cell & Developmental Biology. 2011;22(7):713-9.
158. Simone M. Schoenwaelder RD, Susan L. Cranmer, Hayley S. Ramshaw et al. 14-3-3ζ regulates the mitochondrial respiratory reserve linked to platelet phosphatidylserine exposure and procoagulant function. Nature communications. 2016;7.
159. Ming Chen HH, Haojie He, Wantao Ying, Xin Liu, Zhiqin Dai, Jie Yin, Ning Mao, Xiaohong Qian and Lingya Pan. Quantitative proteomic analysis of mitochondriafrom human ovarian cancer cells and theirpaclitaxel-resistant sublines. Cancer Science. 2015 106:1075-108.

7 Appendix

Appendix I

Gene Name	Sequence	
SURVIVIN	FORWARD	TCCACTGCCCCACTGAGAAC
	REVERSE	TGGCTCCCAGCCTTCCA
BCL-XL	FORWARD	GATCCCCATGGCAGCAGTAAAGCAAG
	REVERSE	CCCCATCCCGGAAGAGTTCATTCACT
BIRC3	FORWARD	TATGTGGGTAACAGTGATGA
	REVERSE	GAAACCACTTGGCATGTTGA
P21	FORWARD	GACACCACTGGAGGGTGACT
	REVERSE	ACAGGTCCACATGGTCTTCC
RHOC	FORWARD	AAGGATCAGTTTCCGGAGGT
	REVERSE	TAGTCTTCCTGCCCTGCTGT
RAC1	FORWARD	AACCAATGCATTTCCTGGAG
	REVERSE	TCCCATAAGCCCAGATTCAC
CDC42	FORWARD	ACGACCGCTGAGTTATCCAC
	REVERSE	CCCAACAAGCAAGAAAGGAG
VASP	FORWARD	GAAAACCCCCAAGGATGAAT
	REVERSE	GTTCTTCTCCCAGGGTCTCC
FLNB	FORWARD	CTGAGAGCCCACTCCAGTTC
	REVERSE	GGTGAAGGTGGCAGTTTTGT
RhoA	FORWARD	AAGGACCAGTTCCCAGAGGT
	REVERSE	GCTTTCCATCCACCTCGATA
FN1	FORWARD	TGGCCAGTCCTACAACCAGT
	REVERSE	CGGGAATCTTCTCTGTCAGC
PPP1R12A	FORWARD	GTTCCTACGGCAGTGACCAT
	REVERSE	GATCTGCGTCTCTCCCTGAC
ITGB5	FORWARD	TGCCTTGCTTGGAGAGAAAT
	REVERSE	AATCTCCACCGTTGTTCCAG
PSMB5	FORWARD	TCATGGATCGGGGCTATTCC
	REVERSE	GGTAGAGGTTGACTGCACCT
PSMB6	FORWARD	TATCATGGCCGTGCAGTTTG
	REVERSE	AGGTGTCAGCTTGTCAGTCA
PSMB7	FORWARD	CTGGCATCTTCAACGACCTG
	REVERSE	ACTGTGTATGGGCGGAGAAA
PSMB8	FORWARD	ACGTGGATGAACATGGGACT
	REVERSE	ATAGCCACTGTCCATGACCC
PSMB9	FORWARD	TTCACCACAGACGCTATTGC
	REVERSE	ACACCGGCAGCTGTAATAGT
PSMB10	FORWARD	CAAGAGCTGCGAGAAGATCC
	REVERSE	AACGCGTGTAGCTCCATCTT
IKB-α	FORWARD	CATCGTGGAGCTTTTGGTGTC
	REVERSE	AGCCCCACACTTCAACAGGAG

COX 2	FORWARD	TCCCTGAGCATCTACGGTTTG
	REVERSE	GTCTGGAACAACTGCTCATCAC
NOX 4	FORWARD	GCAGAGTTTACCCAGCACAA
	REVERSE	CAAAGCCAAGTCTGTGGAAA
P 16	FORWARD	GAGCAGCATGGAGCCTTC
	REVERSE	CATCATGACCTGGATCGG
SOD 2	FORWARD	ACCGAGGAGAAGTACCAGGA
	REVERSE	CTTCAGTGCAGGCTGAAGAG

8 Publications

www.oncotarget.com Oncotarget, 2018, Vol. 9, (No. 45), pp: 27667-27681

Research Paper

Enhanced proteasomal activity is essential for long term survival and recurrence of innately radiation resistant residual glioblastoma cells

Jacinth Rajendra[1,7], Keshava K. Datta[2], Sheikh Burhan Ud Din Farooqee[3,7], Rahul Thorat[5], Kiran Kumar[2], Nilesh Gardi[4], Ekjot Kaur[1,7], Jyothi Nair[1,7], Sameer Salunkhe[1,7], Ketaki Patkar[1], Sanket Desai[4,7], Jayant Sastri Goda[8], Aliasgar Moiyadi[6], Amit Dutt[4,7], Prasanna Venkatraman[3,7], Harsha Gowda[2] and Shilpee Dutt[1,7]

[1]Shilpee Dutt Laboratory, Tata Memorial Centre, Advanced Centre for Treatment, Research and Education in Cancer (ACTREC), Kharghar, Navi Mumbai, India

[2]Institute of Bioinformatics, International Technology Park, Bangalore, India

[3]Advanced Centre for Treatment, Research and Education in Cancer (ACTREC), Tata Memorial Centre (TMC), Kharghar, Navi Mumbai, India

[4]Integrated Genomics Laboratory, Advanced Centre for Treatment, Research and Education in Cancer, Tata Memorial Centre, Navi Mumbai, Maharashtra, India

[5]Laboratory Animal Facility, Advanced Centre for Treatment, Research and Education in Cancer (ACTREC), Tata Memorial Centre (TMC), Kharghar, Navi Mumbai, India

[6]Department of neurosurgery Tata Memorial Centre, Advanced Centre for Treatment, Research and Education in Cancer, Navi Mumbai, India

[7]Homi Bhabha National Institute, Training School Complex, Anushakti Nagar, Mumbai, India

[8]Department of Radiation Oncology, Tata Memorial Centre, Advanced Centre for Treatment, Research and Education in Cancer, Navi Mumbai, India

Correspondence to: *Shilpee Dutt,* ***email:*** *sdutt@actrec.gov.in*

Keywords: *glioblastoma; radio-resistant cells; recurrence; proteomic analysis; proteasomes*

Received: *August 28, 2017* ***Accepted:*** *April 25, 2018* ***Published:*** *June 12, 2018*

ABSTRACT

Therapy resistance and recurrence in Glioblastoma is due to the presence of residual radiation resistant cells. However, because of their inaccessibility from patient biopsies, the molecular mechanisms driving their survival remain unexplored. Residual Radiation Resistant (RR) and Relapse (R) cells were captured using cellular radiation resistant model generated from patient derived primary cultures and cell lines. iTRAQ based quantitative proteomics was performed to identify pathways unique to RR cells followed by *in vitro* and *in vivo* experiments showing their role in radio-resistance. 2720 proteins were identified across Parent (P), RR and R population with 824 and 874 differential proteins in RR and R cells. Unsupervised clustering showed proteasome pathway as the most significantly deregulated pathway in RR cells. Concordantly, the RR cells displayed enhanced expression and activity of proteasome subunits, which triggered NFkB signalling. Pharmacological inhibition of proteasome activity led to impeded NFkB transcriptional activity, radio-sensitization of RR cells *in vitro*, and significantly reduced capacity to form orthotopic tumours *in vivo*. We demonstrate that combination of proteasome inhibitor with radio-therapy abolish the inaccessible residual resistant cells thereby preventing GBM recurrence. Furthermore, we identified first proteomic signature of RR cells that can be exploited for GBM therapeutics.

INTRODUCTION

Glioblastoma is the most common and lethal primary brain tumour. Despite the multimodal therapy, tumour recurrence is major challenge in glioblastoma with patient survival less than 6 months post recurrence [1–4]. Recurrence in GBM is attributed to a subpopulation of cells that survive initial therapies and cause tumour re-growth [5, 6]. However, targeting residual resistant cells of glioma is challenging since they are invisible in MRIs post initial treatment and they are inaccessible from the patient biopsies for biological studies [7, 8]. We have previously reported development of a cellular model of radiation resistance using primary cultures from patient samples, which recapitulate the clinical scenario of resistance and enable us to capture residual radiation resistant (RR) cells [9] and understand their molecular mechanism of survival.

Since proteins are the ultimate biological effectors of the cells, in this study we have analyzed the total proteome of residual resistant cells of glioma [10–13]. Till date majority of proteomics studies in glioblastoma have focused on identification of differential proteins amongst different GBM cell lines, patient samples or within the same tumour to investigate the heterogeneity of glioblastoma, mechanism of chemoresistance and identification of diagnostic biomarkers [14–26]. However, none of these studies could identify survival mechanism of innately resistant cells due to their unavailability. This is the first report to identify the proteomic signature of residual resistant and the relapse cells of glioblastoma from cellular model. Data revealed a unique proteomic signature of RR and R cells with utmost clustering of deregulated genes uniquely in the RR cells. Contrary to previous reports which have shown a decrease in proteasome activity in radio resistant cells [27, 28], our data reveals that innately radio resistant GBM cells harbour increased expression of proteasomal subunits, enhanced proteasome activity and increased levels of proteasome substrate p-NFkB and concordant increase of NFkB target genes. We demonstrate pharmacological inhibition of proteasomal activity reduces NFkB transcriptional activity and radio sensitizes RR cells. Furthermore absence of proteasome activity in RR cells also significantly decreases their ability to form tumours *in vivo*. Together, our proteomics data has delineated proteasomal pathway as one of the plausible targetable mechanisms that significantly contribute to the survival of innate radiation residual cells via the NFkB signalling cascade.

RESULTS

Capturing innate radiation resistant (RR) and Relapse (R) cells from *in vitro* radiation resistant model

To capture and understand the survival mechanisms of residual resistant cells of GBM, that are diagnostically undetectable post treatment, we generated *in vitro* radiation resistant model derived from cell lines and patient samples [9] (Figure 1A). Using the same protocol, in this study first the glioblastoma cell lines (SF268 and U87MG) and two short term primary cultures of patient samples (PS1 and PS2) were subjected to their respective lethal dose of radiation (6.5 Gy, 8 Gy, 6 Gy, 6.5 Gy) as determined previously using clonogenic assay [9]. Post treatment initially the cells proliferate, but after 4–5 days post treatment more than 90% cells died leaving behind a small population (<10%) surviving cells. These cells are the innately radiation resistant residual cells (RR) which remain viable but non-proliferative for approximately 7–10 days and acquire Multinucleated Giant (MNGCs) phenotype. However, instead of undergoing mitotic catastrophe, RR cells resume growth to form the relapse (R) population. Figure 1B shows graphs for SF268 and PS1 growth pattern of RR cells. The parent (P), innately radiation resistant (RR) and relapse (R) cells obtained from SF268 were then subjected to quantitative proteomic analysis. The three populations obtained from U87MG, PS1 and PS2 were used for validation and functional studies.

Quantitative proteomic analysis radio resistant (RR) and relapse (R) cells

iTRAQ based quantitative proteomic analysis was performed on parent, RR and R cell population of SF268. Figure 1C illustrates the proteomics workflow. Equal amounts of protein from the Parent, RR and R populations was digested with trypsin and their tryptic peptides were labelled with 114, 115 and 116 isobaric reagents respectively for differential protein expression analysis. The iTRAQ-labelled peptide samples were pooled, fractionated and analyzed by LC-MS/MS. The data obtained was searched against National Centre for Biotechnology Information RefSeq database (version 52 40) using Protein Discoverer (version 1.4) using MASCOT and SEQUEST. Compared to parent cells 824 proteins were found to be differentially expressed in RR cells compared to parent cells out of which 393 proteins were up-regulated (fold change >1.5) and 431 proteins were downregulated (fold change <0.7) while 874 proteins were differentially expressed in relapse population of which 352 proteins were up-regulated (>1.5) and 522 proteins were downregulated (<0.7). 1,392 proteins were differentially regulated in R vs. RR out of which 747 proteins were upregulated (>1.5) and 645 were downregulated (<0.7) in the R population (Figure 1D). iTRAQ data was validated by analysing the expression levels of HRAS, EGFR, YBX3 (Figure 2A). Relative peptide intensity values of the three proteins from mass spectrometry showed concurrent expression with the western blot data (Figure 2B).

Unsupervised clustering of proteomics data identifies protein clusters uniquely differential in each population

Since a cell's phenotype is an outcome of a collective network of biological processes, it was hypothesized that proteins showing similar expression pattern will participate in similar biological processes. Therefore, we first identified the proteins showing co-expression, for which unique master differential gene list was compiled the at least one of the three binary comparison (RR Vs. P, R Vs. P, R Vs. RR) which comprise of 1773 genes. Unsupervised clustering was performed for these genes based on their respective relative protein abundance values as represented in a heat map. The expression pattern of each cluster is illustrated as a line plot (Figure 2C). Analysis segregated the data set into five clusters (C1-C5) out of which two major clusters, cluster 2 and cluster 3 represented proteins that were exclusively enriched with uniquely downregulated and upregulated proteins in the RR population, respectively. Cluster 2 represents 783 proteins and Cluster 3 represents 641 proteins. Clusters 1, 4 and 5 comprised of proteins that showed similar expression pattern in RR and R cells. 134 proteins were found to be downregulated in the RR and R as compared to the parent cells (cluster 1). The expression of 165 proteins remains at a basal level in the P and RR population however their expression declines in the R cells (cluster 4) and 70 proteins show an escalation in expression in the RR and R as compared to the P cells (cluster 5). Since we were interested to know how the RR cells survive, we focused on the proteins classified in cluster 2 and cluster 3 which comprised of proteins uniquely downregulated and upregulated in the RR cells, respectively.

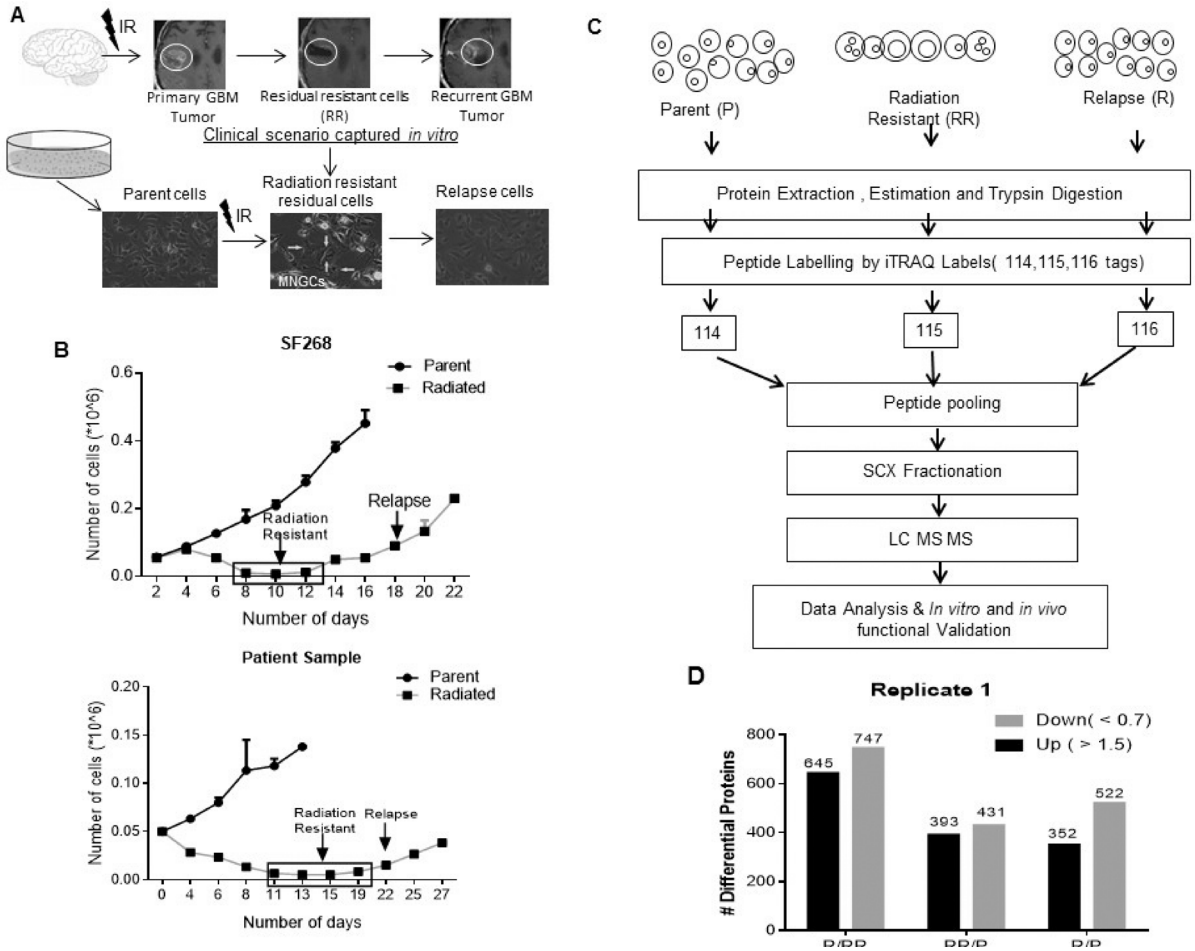

Figure 1: *In vitro* radiation resistant model. (**A**) The illustration depicts the clinical scenario in patient's pre and post treatment in which post-surgery there is a significant regression or complete abolishment of the tumor observed. However, in >90% cases tumor recurs. This clinical scenario was recapitulated in an *in vitro* model. The images represent the SF268 Parent, innate Radiation Resistant (RR) enriched with multinucleated giant cells (MNGCs) and Relapse (R) population. (**B**) Graph represents the growth kinetics of SF268 and Patient Sample post lethal dose of radiation. (**C**) A schematic representation of the proteomics workflow. (**D**) Graphical representation of the number of differential proteins identified in the RR and R w.r.t P and R w.r.t RR by the proteomic analysis. Results in each bar graph are the composite data from three independent experiments performed in triplicate (mean ± SEM)

Pathway analysis reveals deregulation of proteasome and protein turnover machinery proteins in RR population

To analyze the molecular pathway that might be involved in the survival and radiation resistance mechanisms of RR cell, pathway enrichment analysis of the deregulated proteins in RR population compared to parent population in cluster 2 and cluster 3 was done using KEGG and REACTOME database (Figure 2D). In total 42 pathways were deregulated in cluster 2, 33 pathways were deregulated in cluster 3. Interestingly, 11 pathways were commonly deregulated in both cluster 2 and 3 (Figure 2E). These pathways included glutathione metabolism, ribosome biogenesis in eukaryotes, RNA transport, spliceosome, and proteasome, protein processing in endoplasmic reticulum, regulation of actin cytoskeleton, non-alcoholic fatty liver disease (NAFLD), Alzheimer's disease, Huntington's disease and Epstein - Barr virus infection. Additionally, gene ontology and enrichment analysis of the entire differential proteins found in the RR compared to the parent cells, revealed 24 pathways enriched with upregulated (red circle) and downregulated proteins (green circle). Of these, 8 pathways were enriched with upregulated proteins and 16 pathways were enriched with downregulated proteins (Figure 3A). Out of the 8 pathways that were enriched with upregulated proteins, 5 statistically significant (Term P value < 0.05) pathways included Proteasome (8 proteins), Ubiquitin mediated proteolysis (10 proteins), Protein processing in Endoplasmic Reticulum (18 proteins), RNA Transport (17 proteins), oocyte meiosis (9 proteins). However, proteasome pathway was the most deregulated pathway based on the associated genes filter (k/K ratio). Proteomic analysis from three biological replicates also revealed significant deregulation of proteasome pathway in the RR population (Supplementary Figure 2 and Figure 3B). The data sets of all the replicates have been deposited to the ProteomeXchangeConsortium (http://proteomecentral.proteomexchange.org) via the PRIDE partner repository. The internal ID of submission is: px-submission #265394. A ProteomeXchange accession number will be generated after it has been loaded into the database. Proteasome subunits differential in all the four biological replicates have been represented in Table 1. Three subunits PSME1, PSMA7 and PSMB4 were used for validation by western blot (Figure 3C–3E).

RR cells display enhanced proteasome activity and survival dependency on proteasome activity *in vitro*

Since the RR population exhibited increased protein expression of proteasome subunits, we sought to observe if the expression correlated with proteasome activity. Therefore, proteasome activity was analysed in the parent and RR cells of SF268, U87MG, PS1 and PS2 using florigenic substrate Suc-LLVY-Amc. Indeed the RR population of SF268, U87MG, PS1 and PS2 showed 22.18%, 35.60%, 20.63% and 71.63 % increase respectively in the proteasome activity compared to the parent cells (Figure 4A). Among the 9 subunits overexpressed in the RR, 3 subunits are part of the 19S regulatory subunit–PSMC1, PSMD2, PSMD7;3 subunits of the 20 S core particle–PSMA1, PSMA7, PSMB4 and 1 subunits of the 11 S regulatory subunits–PSME1. Most of the subunits belong to the classical proteasome. Hence the transcript levels of beta catalytic subunits: PSMB6 (β1- caspase like activity), PSMB7 (β2-trypsin-like activity) and PSMB5 (β5-chymotrypsin-like activity), were checked. PSMB6 transcript levels were elevated in the RR population of all the samples, PSMB7 and PSMB5 were elevated in at least one cell line and one patient sample. Proteomics data also identified a regulatory subunit of immunoproteasome (PSME1). Therefore, the mRNA levels of its catalytic subunits PSMB9, PSMB8 and PSMB10 were also determined (Figure 4B). However, the transcript levels of the three subunits were not significantly high in any of the samples.

Since the RR population exhibited increased proteasome activity we wanted to analyze if the survival of RR cells was dependent on the proteasome activity. For this we used bortezomib (BTZ), a pharmacological inhibitor of proteasome routinely used in the treatment of multiple myeloma. First we determined the concentration of bortezomib at which proteasome activity was maximally inhibited with minimal cellular toxicity. For this proteasome activity of SF268 was assessed after 12 h. treatment of bortezomib at different concentrations (0.01 nM to 1000 nM). As seen from Figure 4C, 10 nM of bortezomib was the minimum concentration at which significant inhibition of proteasome activity was observed and there was no significant cell death in RR as compared to parent. Once the non-toxic concentration of bortezomib on parent cells was determined, we wanted to see if the inhibition of proteasome sensitizes the glioma cells to radiation. SF268 and PS1 cells were treated for 12 hrs with 10 nM bortezomib and their % cell survival was recorded at different doses of radiation. As shown in Figure 4D, bortezomib treatment significantly reduced the D_0 dose of radiation from 5.07 Gy to 3.12 Gy and 4.4 Gy to 1.08 Gy for SF268 and PS1 respectively, showing that proteasome inhibition radio sensitizes glioma cells. We then wanted to analyse the effect of bortezomib on RR population that have higher proteasome activity. For this the parent and RR population of SF268 and U87 were treated with 0.1 nM, 1 nM and 10 nM concentrations of bortezomib for 12 hrs. Following the treatment cells were monitored for proteasome activity. Both, parent and RR cells showed a gradual decrease in the activity of proteasomes with increasing concentration of the drug (Figure 5A and 5B). However, 72 hours post drug treatment RR cells were

significantly (8% SF268, 10% U87 and 23% PS1) more sensitive to proteasome inhibition compared to the parent population. PS2 showed similar % reduction in viability as compared to the parent population at 10 nM (Figure 5C).

Proteasomes indirectly regulate RR cell survival via the NFkB activation

We further wanted to determine if the proteasome targets were down-regulated in the RR population due to degradation via ubiquitin mediated proteasome pathway. Down regulated proteins were analysed for presence of annotated ubiquitin binding lysine residues. These proteins were downloaded from Uniprot database [29] and parsed using in-house python scripts to determine presence of curated ubiquitin binding sites. Of the 431 proteins, 14 proteins were found to harbour lysine residues which can undergo ubiquitin modification (Supplementary Figure 1). One of the well-known substrates of the 26 S proteasome is IκB-α which upon degradation leads to the activation of the transcription factor NFkB. An increased proteasome activity should modulate the levels of activated NFkB in the RR population. Therefore, we checked for the levels of activated NFkB by western blot in the P and RR cells of cell lines and patient samples. Indeed, the RR cells displayed increased levels of activated NFkB in both the cell lines and PS1 (Figure 5D). Furthermore, the transcript levels of 9 NFkB target genes (TNF-α, IL6, IkB-a, IFN-γ, ICAM1, COX2, NOD4, p16, SOD2) were screened in RR cells of the cell lines and patient sample by real-time PCR. A heat map representation of the 9 genes depicts upregulation of at least 6 genes out of the 9 in SF268, U87 and PS1 which also harbour increased expression of phospho-NFkB suggesting the presence of a transcriptionally active NFkB in RR cells (Figure 5E). To directly assess the NFkB transcriptional activity in the RR cells of U87, we monitored the relative promoter activity of the luciferase based NFkB reporter constructs in the P and RR cells. The

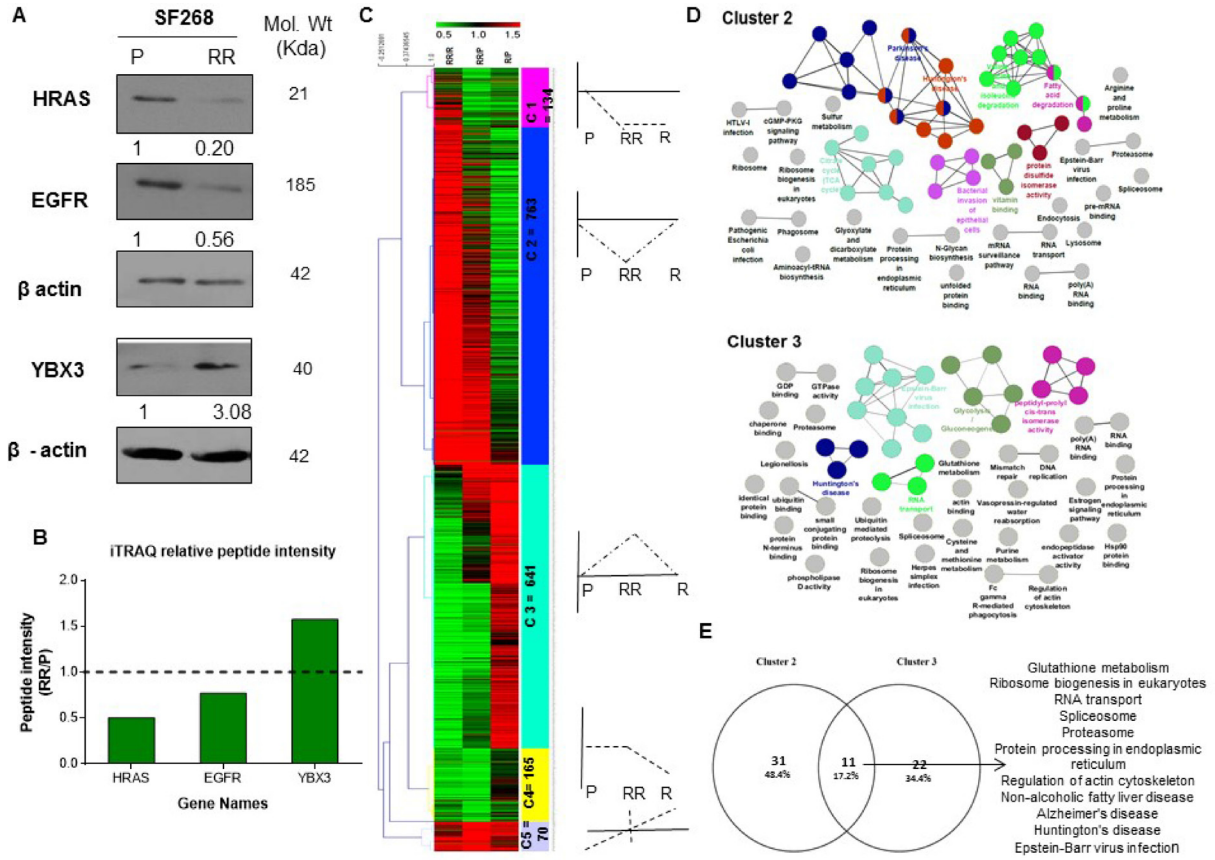

Figure 2: Proteomic analysis of the parent, radiation resistant and relapse population. (**A**) Western blots showing the expression of HRas, EGFR, YBX3 in Parent (P), Radiation Resistant (RR) and Relapse (R) population of SF268 cell line. β-actin was used as loading control. (**B**) Bar plot of the relative peptide intensity values of the mentioned proteins in RR/P and R/P as determined by iTRAQ. (**C**) Heat map representation of unsupervised hierarchical clustering of the proteins based on their relative peptide intensities in R w.r.t RR, RR w.r.t P and R w.r.t P. Red- Up-regulation >1.5, Green- Down-regulation <0.5. Heat map is divided into clusters with a dotted plot representing the expression pattern of proteins in each cluster. (**D**) Pathway analysis of the Genes in cluster 2 and cluster were collapsed into pathways using ClueGo and CluePedia plugin of Cytoscape with KEGG and REACTOME pathway databases. Each coloured circle represents a pathway enriched with upregulated and downregulated protein in the RR cells but non-differential in the R cells. (**E**) Venn diagram for the overlap of pathways between cluster 2 and cluster 3

RR cells showed a significant increase (20 fold) in NFkB transcriptional activity as compared to the parent population (P). Importantly, administration of the proteasome inhibitor (Bortezomib) in the P and RR cells diminished this activity by 1.5 and 3.0 fold demonstrating the dependency of NFkB activity on the proteasome activity. A synergistic inhibitory effect was observed in the presence of IkB-alpha construct and bortezomib in the P and RR cells. However, the RR cells displayed a much higher reduction as compared to the P cells (Figure 5F).

Inhibition of proteasome activity inhibits tumour formation and *in vivo*

We have shown that radiation resistant residual (RR) cells formed in our *in vitro* radiation resistant model systems retain their tumorigenic potential and re-grow to give rise to recurrent tumour. We first wanted to analyze if the RR cells are capable of forming tumour *in vivo* as well. For this pLenti6-luc2 U87MG cells [30] stably expressing luciferase were treated with the lethal dose of radiation 8Gy and RR cells were collected. The parent and RR cells were then stereo tactically injected in the brain of 6–8 weeks old NOD/SCID mice. Tumour growth was monitored using bioluminescence imaging. As seen from Figure 6A left panel and Figure 6C, RR cells were able to give rise to tumours and had greater tumorigenic potential as compared to the parent cells.

We then evaluated the effect of proteasome inhibition on the tumorigenicity of the parent and RR cells. Since U87MG cells showed higher proteasome activity than the SF268 (Figure 4A), hence they also required a higher concentration of bortezomib (50 nM) for reducing the viability of their RR. Therefore for *in vivo* studies U87MG parent and RR cells were treated with 50 nM bortezomib for 12 hrs prior to injection.

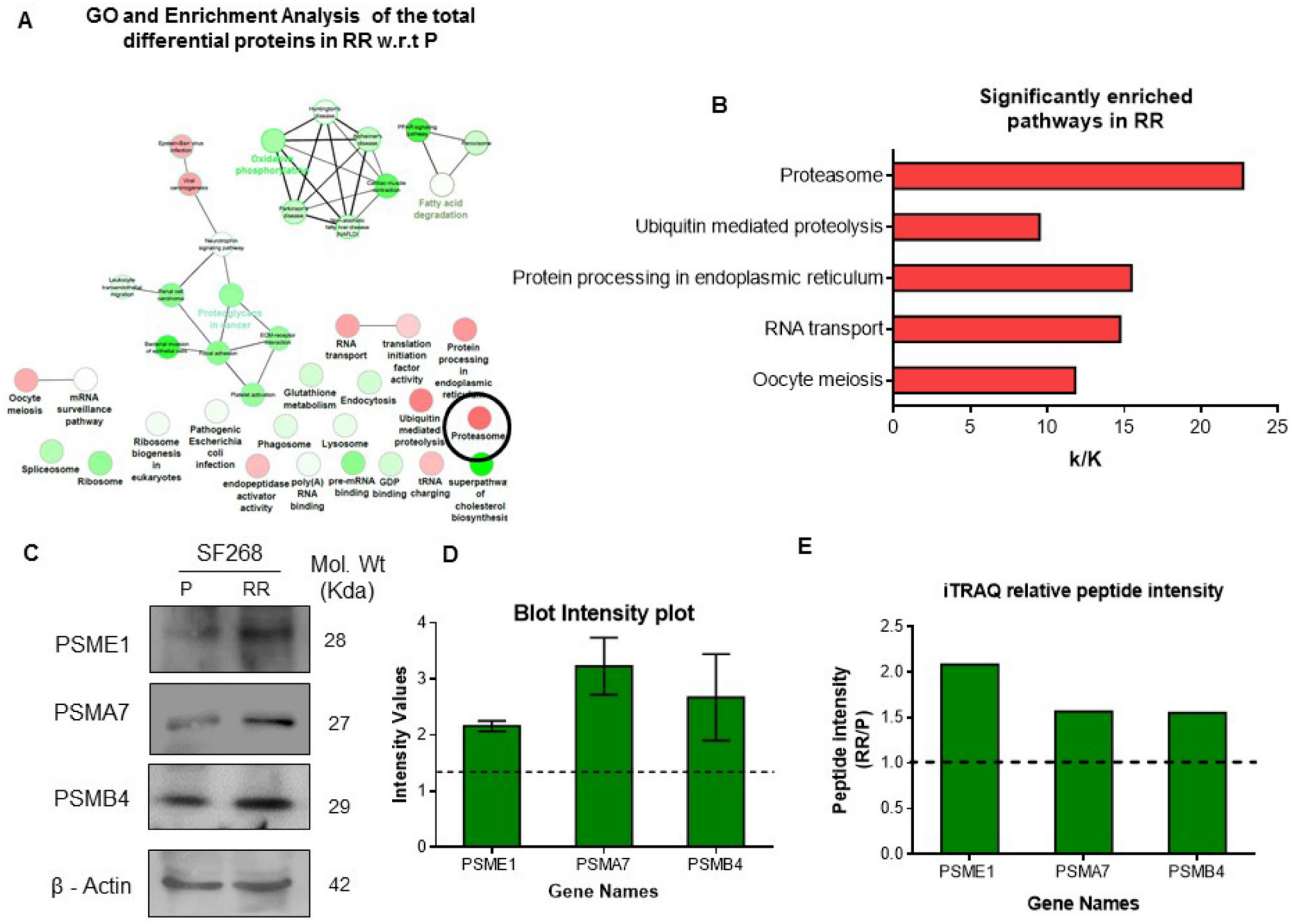

Figure 3: Deregulation of proteasome pathway in the radiation resistant population. (**A**) Pathway analysis of deregulated genes in Radiation Resistant (RR) vs. Parent (P) Genes deregulated in RR w.r.t P were collapsed into pathways using ClueGo and CluePedia plugin of Cytoscape with KEGG and REACTOME pathway databases. The colour gradient shows the number of genes of each group associated with the pathway. Equal proportions of the two clusters are represented in white. (**B**) KEGG pathways enriched with upregulated proteins according to their k/K ratio. k–Number of genes identified from the pathway, K–Total number of genes curated in the KEGG database for a pathway. (**C**) Western blot showing the expression of PSME1, PSMA7 and PSMB4 parent (P), Radiation Resistant (RR) and Relapse (R) cells of SF268. β-actin was used as loading control. (**D**) Band intensity plot for the proteins validated by western blot using IMAGE J software. (**E**) Shows the relative peptide intensity values of the three proteins from iTRAQ analysis.

Table 1: Represents the list of differential proteins identified in the proteasome pathway

Gene Symbol	Protein Description	Σ# Unique Peptides	Σ# PSMs	Fold Change in RR/P
REPLICATE 1				
PSME1	proteasome activator complex subunit 1 isoform 1 [Homo sapiens]	4	4	2.085
PSMD7	26S proteasome non-ATPase regulatory subunit 7 [Homo sapiens]	3	6	1.977
PSMA1	proteasome subunit alpha type-1 isoform 3 [Homo sapiens]	1	2	1.634
PSMD2	26S proteasome non-ATPase regulatory subunit 2 [Homo sapiens]	9	12	1.632
PSMA7	proteasome subunit alpha type-7 [Homo sapiens]	4	13	1.568
PSMB4	proteasome subunit beta type-4 [Homo sapiens]	2	4	1.550
PSMC1	26S protease regulatory subunit 4 [Homo sapiens]	6	10	1.518
PSMA3	proteasome subunit alpha type-3 isoform 2 [Homo sapiens]	2	4	0.656
PSMD14	26S proteasome non-ATPase regulatory subunit 14 [Homo sapiens]	3	4	0.593
REPLICATE 2				
PSMD9	26S proteasome non-ATPase regulatory subunit 9 isoform 1	4	6	1.88
PSMD10	26S proteasome non-ATPase regulatory subunit 10 isoform 1	6	9	1.523
PSMC1	26S protease regulatory subunit 4	19	57	1.381
PSMC6	26S protease regulatory subunit 10B	16	48	1.356
PSMD8	26S proteasome non-ATPase regulatory subunit 8	10	21	1.356
PSMA4	proteasome subunit alpha type-4 isoform 1	10	35	1.294
PSME2	proteasome activator complex subunit 2	12	30	1.281
PSMD13	26S proteasome non-ATPase regulatory subunit 13 isoform 1	19	47	1.243
PSMD7	26S proteasome non-ATPase regulatory subunit 7	10	19	1.227
PSMD12	26S proteasome non-ATPase regulatory subunit 12 isoform 1	22	44	1.207
REPLICATE 3				
PSMD9	26S proteasome non-ATPase regulatory subunit 9 isoform 1	5	7	3.587
PSMC5	26S protease regulatory subunit 8 isoform 1	21	54	1.525
PSMB10	proteasome subunit beta type-10 precursor	1	1	1.445
PSME2	proteasome activator complex subunit 2	9	29	1.41
PSMD6	26S proteasome non-ATPase regulatory subunit 6 isoform 2	19	30	1.382
PSMD4	26S proteasome non-ATPase regulatory subunit 4	12	27	1.362
PSMA3	proteasome subunit alpha type-3 isoform 1	9	25	1.326
PSMD8	26S proteasome non-ATPase regulatory subunit 8	9	19	1.321
PSMC6	26S protease regulatory subunit 10B	18	52	1.318
PSMD13	26S proteasome non-ATPase regulatory subunit 13 isoform 1	17	43	1.302
PSMB7	proteasome subunit beta type-7 precursor	5	17	1.278
PSMD2	26S proteasome non-ATPase regulatory subunit 2 isoform 1	31	74	1.257
PSMD14	26S proteasome non-ATPase regulatory subunit 14	13	23	1.222
PSMC4	26S protease regulatory subunit 6B isoform 1	17	49	1.217
REPLICATE 4				
PSMD9	26S proteasome non-ATPase regulatory subunit 9 isoform 1	6	10	1.95
PSME2	proteasome activator complex subunit 2	9	35	1.77
PSMD8	26S proteasome non-ATPase regulatory subunit 8	11	22	1.579
PSMD4	26S proteasome non-ATPase regulatory subunit 4	12	26	1.489
PSMD7	26S proteasome non-ATPase regulatory subunit 7	11	23	1.411
PSMC4	26S protease regulatory subunit 6B isoform 1	23	70	1.382

Columns from the right represent the gene symbol, protein description, #- number of unique peptides identified, number of peptide score matches (PSMs) and the fold change of the proteins in RR w.r.t P.

Tumour formation was monitored by bioluminescence. As expected at day 14 post injection parent and RR cells treated with vehicle control or bortezomib showed almost similar growth, however, by day 33 while the parent cells treated with bortezomib had formed large tumours, the RR cells treated with bortezomib showed significant reduced bioluminescence intensity (Figure 6A, right panel). Presence of tumour cells was seen with Haematoxylin and Eosin staining in the brain slices of all the treatment groups of mice except for the brain tissue of mice treated injected with RR cells + bortezomib (Figure 6B). As represented in Figure 6D, the mice injected with bortezomib treated RR cells showed a significant decline in bioluminescence as compared to the group injected with bortezomib treated P cells. Also, the overall survival of this group (RR-BTZ) was significantly higher than that of the other three groups as shown in Figure 6E. Median survival of each group are as follows: P- VC–36 days, P–BTZ–38 days, RR–VC–30 days, RR–BTZ–58 days. Further, we did intracranial injection of parental cells followed by radio therapy (fractionated dose of 14 Gy) followed by intraperitoneal injection of bortezomib (0.5 mg/Kg twice in a week for two weeks) as depicted in Figure 6F. Representative bioluminescence images from each group are shown in Figure 6G. The results show a significant reduction in bioluminescence of animals treated with radiation along with BTZ as compared to the radiation alone group (Figure 6H). The disease free survival of mice was significantly higher in the group treated with radiation and BTZ as compared to radiated alone group (Figure 6I).

Together these data confirmed that the proteasome inhibition *in vitro* and *in vivo* resulted in tumour reduction and abrogation of relapse.

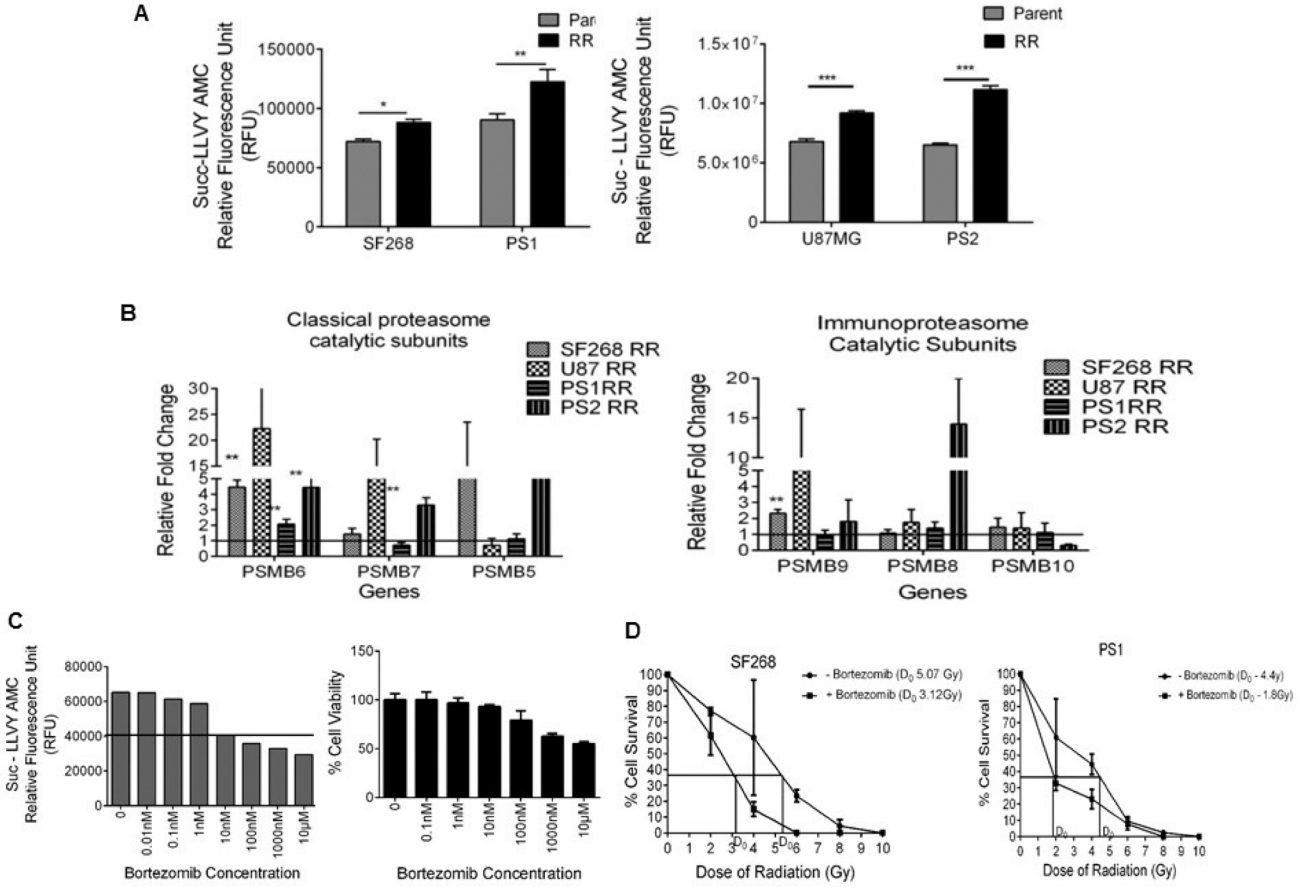

Figure 4: RR cells display enhanced proteasome activity and survival dependency on proteasomes *in vitro*. (**A**) Data represents the chymotrypsin like proteasome activity measured using Succ-LLVY AMC florigenic substrate in the P and RR population of SF268, U87MG, PS1 and PS2. (**B**) The graph depicts the RPL19 normalised mRNA levels of classical and Immunoproteasome proteasome beta catalytic subunits respectively in the RR population of SF268, U87MG, PS1, and PS2 compared to the parent population. (**C**) Proteasome activity inhibition and % cell viability at different concentrations of proteasome inhibitor–Bortezomib in SF268. (**D**) Graph shows percentage of cells of SF268 and PS1 surviving at different doses of γ radiation with and without 10 nM Bortezomib in a clonogenic assay. (D) Bar graph represents the percentage of viable cells (at 72 hrs) as assessed by MTT assay at different concentrations of Bortezomib. Cells were treated with Bortezomib for 12 hrs. Results in each bar graph are the composite data from three independent experiments performed in triplicate (mean ± SEM); $^{***}P = 0.001$c)

DISCUSSION

Radio resistance and recurrence is currently an inevitable consequence in the field of glioblastoma. Until now, the mechanisms of radio resistance in glioblastoma have been explored in *in vitro* and in *in vivo* settings either immediately post radiation or after generation of repeated doses of radiation (acquired resistance) but not in the residual radiation resistant cells. However, in this study we focused on the processes deregulated in the innately radiation resistant residual (RR) population as we have previously shown that these are the cells responsible for relapse in glioblastoma [9]. We performed iTRAQ based quantitative proteomic analysis on the parent (P), innately radiation resistant residual (RR) and relapse (R) population. Amongst the many pathways, we found the proteasome pathway to be most significantly deregulated in the RR cells.

Proteasomes are well known targets in cancer therapy owing to their role in maintaining homeostasis of proteins involved in cell cycle, signalling pathways regulating cell survival and apoptosis [31–34]. Cancer cells harbour enhanced proteasome activity compared to their normal counterparts but the exact reason for this surge is still unknown. It is speculated that this escalation in proteasome activity is to cope with crisis such as

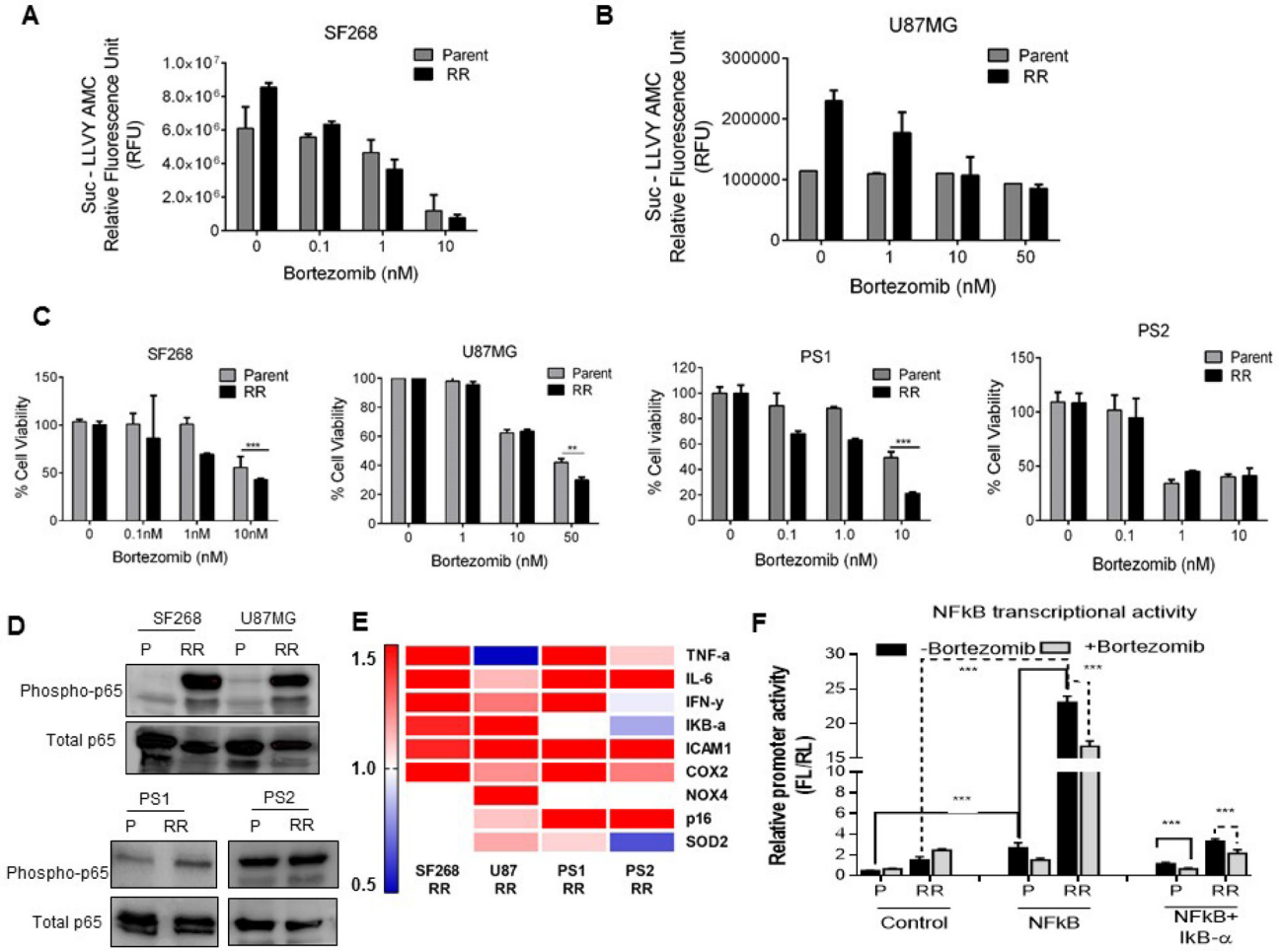

Figure 5: Proteasomes indirectly regulate RR cell survival via the NFkB activation. (**A** and **B**) Bar graph shows proteasome activity in parent and RR cells of SF268 and U87 at different concentrations of the Bortezomib as mentioned. (**C**) Bar graph represents the percentage of viable cells (at 72 hrs) as assessed by MTT assay at different concentrations of Bortezomib. Cells were treated with Bortezomib for 12 hrs. Results in each bar graph are the composite data from three independent experiments performed in triplicate ((mean ± SEM); $^{***}P = 0.001$) (**D**) Western blot represents the expression of phosphor- p65 in the P (Parent) and RR (Radiation resistant) cells of SF268, and U87MG, PS1 and PS2. Total (T) total- p65 levels were used as loading controls. (**E**) Heat map representation of gene expression values NFkB target genes by qPCR in the RR population of SF268, U87, PS1 and PS2 compared to the parent population. GAPDH was used as internal control. Results are the composite data from three independent experiments performed in triplicate (mean ± SEM); $^{*}P = 0.05$, $^{**}P = 0.01$ and $^{***}P = 0.001$ (**F**) Bortezomib treatment repressed the transcriptional activity of NFkB promoter luciferase constructs. The NFkB firefly luciferase construct was transfected into Parent and RR cells and then treated with Bortezomib as indicated. As a control Con A control plasmid was transfected with Renilla luciferase construct. The pTRIPZ IkB-alpha construct was used as NFkB suppressor. Luciferase values subsequent to normalization were plotted.

mutational events and chromosomal instabilities. Although proteasomes are identified as direct targets of radiation, their inhibition is short lived and thus the need for drugs targeting their enzymatic activity [28, 35, 36]. Lower proteasome activity is shown to be a marker for tumour initiating cells and stem cells [37]. Proteasomes are also found to be downregulated in radio-resistant cells of breast cancer and prostate cancer established *in vitro* [27, 35, 38]. Contrary to these reports, we observed an enhanced expression and activity of proteasomes in the innate radio-resistant residual cells of glioblastoma. Subsequently, we also identified 14 out of 431 downregulated proteins that harbour ubiquitin binding lysine residues (Supplementary Figure 1). These proteins in the RR cells, we predict to be either ubiquitin adapters or direct targets of the ubiquitin mediated proteasome machinery. This reduced number of proteins with ubiquitin binding attributes to the fact that proteasomes degrade a significant cellular portion by a ubiquitin independent manner also which is still incompletely understood [39].

Bortezomib preferentially inhibits the chymotrypsin like activity of proteasomes and is currently being

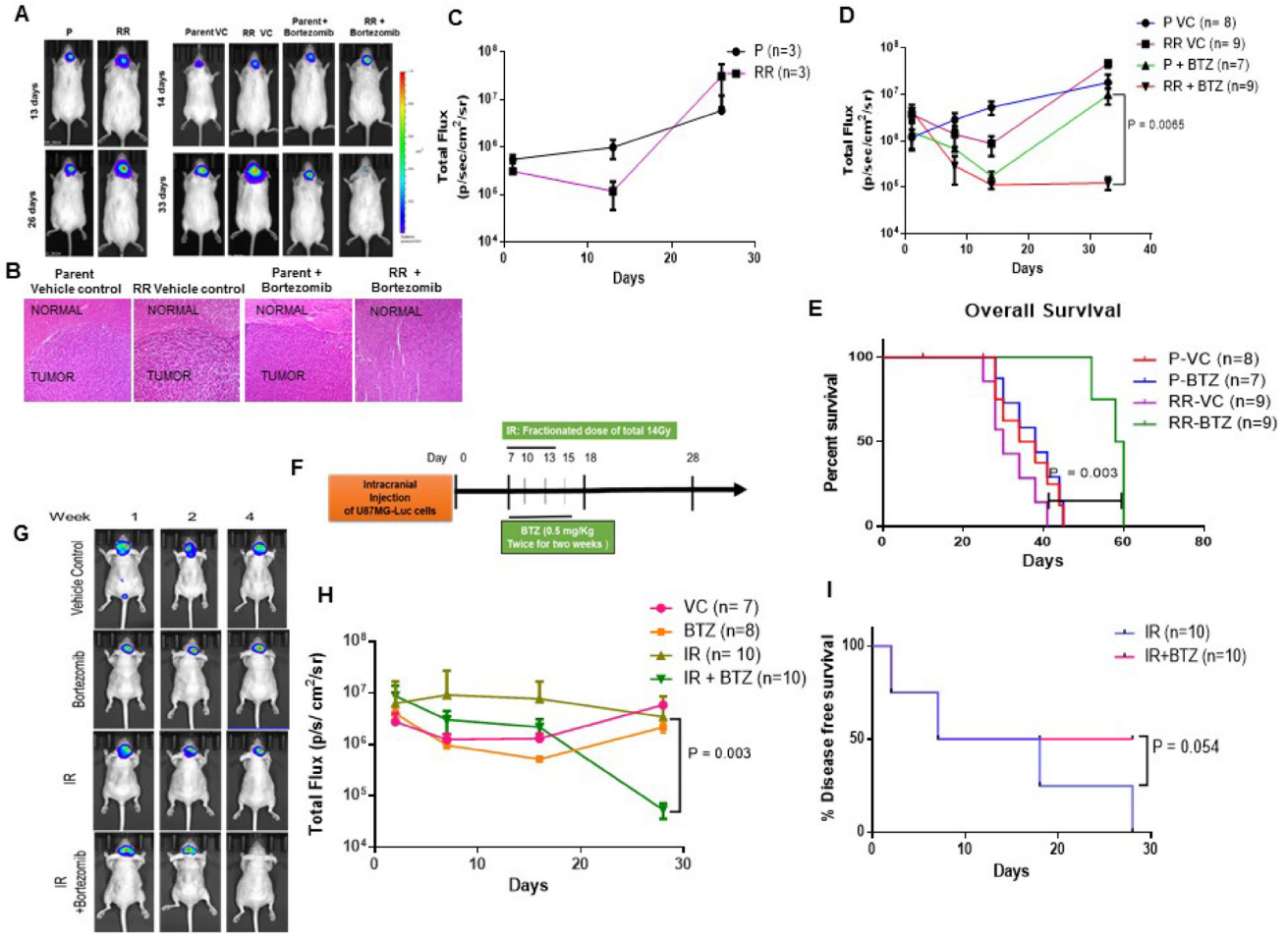

Figure 6: Proteasome inhibition reduces the tumorigenic potential of the cells *in vivo*. (**A**) Left panel - Representative bioluminescence images after orthotopic injection of U87MG-Luciferase labelled Parent (P) and Radiation Resistant (RR) cells. Right Panel - Bioluminescent images after orthotopic injection of U87MG-Luciferase labelled Parent (P) and Radiation Resistant (RR) cells treated with Vehicle Control (VC) and Bortezomib. (**B**) Hematoxylin and eosin (H&E) staining of mice brain slices. Brain slices of the brain tissue from mice injected with Parent Vehicle control, RR Vehicle Control, Parent + Bortezomib, RR + Bortezomib cells were formalin fixed and paraffin embedded. Sections stained with H&E show regions infiltrated with tumour cells. All photomicrographs are shown with the same magnification. Bar = 100 µm. (**C**) Graph represents bioluminescence signal at different days post injection in mice injected with P and RR cells. (**D**) Graph represents bioluminescence intensity at different days post injection of mice injected with P and RR cells pretreated with bortezomib as compared to P and RR cells treated with vehicle control. 'n' represents number of mice per group. (**E**) Kaplein Meier Curve for the overall survival of the mice in the pretreated study. (**F**) Schematic representation for studying the effect of intraperitoneal injections of bortezomib along with radiation treatment of mice intracranially injected with parent GBM cells. IR–Radiation; BTZ–Bortezomib. (**G**) Representative bioluminescence images of tumor formation in the mice treated with IR and BTZ compared to the mice which were administered with Vehicle Control (VC), only BTZ and only IR. (**H**) Graphical representation of bioluminescence intensity recorded for mice treated with IR and BTZ compared to the mice which were administered only saline as Vehicle Control (VC), only BTZ, only IR. (**I**) Kaplein Meier Curve for % tumor free animals in the radiation and intraperitoneally administered BTZ study.

used in the treatment for multiple myeloma [28, 40, 41]. In GBM, it has been reported to sensitize the parent GBM cells to temozolomide and radiation treatment but after immediate exposure to the drug and radiation [42]. However, in our study we show that the residual resistant cells that are formed after a period of 5–7 days post radiation are more sensitive to proteasome inhibition compared to the parent cells, although, there is a differential response to proteasome inhibition amongst the cell lines (SF268, U87MG) and patient samples (PS1 & PS2) as depicted in Figure 5C. This could be due to the heterogeneity of GBM tumours. The subtle effect of bortezomib seen *in vitro* after 72 hrs post treatment is significantly enhanced in reducing tumorigenicity of the treated cells *in vivo,* suggesting a slow and prolonged effect of proteasome inhibition on the survival of the cells. A significant effect of proteasome inhibition was observed on the overall survival of mice which were injected with pre-treated RR-BTZ cells along with an increased % of tumour free mice when BTZ was administered intraperitoneally along with radiation as shown in Figure 6H and 6I. The increased levels of activated NFkB and its transcriptional activity in the RR cells correlate with previous reports where NFkB has been shown to promote radio resistance in Glioblastoma and other cancers. It has been reported to trigger pro-survival and anti-apoptotic signals by transcriptional activation of over 200 genes including the pro inflammatory cytokines, cell-cell adhesion molecules. We have observed cytokines such as TNF-α, IFN-γ, IL-6 and antioxidant genes such COX2 levels increased in the RR. Its activation can occur via IkB-α degradation (Classical pathway) or the by TNF-α (alternative pathway) [43–45]. However, the exact mechanism downstream to higher proteasome expression and NFkB activity in the RR cells needs to be further explored. Nonetheless, this study as illustrated in Figure 7, establishes that proteasomes aid the survival of the innate radiation resistant population via NFkB pathway and hence can be valuable targets for precluding relapse in glioblastoma.

MATERIALS AND METHODS

Cell culture and drug treatment

GBM grade IV cell lines U87MG and SF268 were obtained from ATCC in 2011. These cell lines were last authenticated in the laboratory by short tandem repeat profiling based on eight markers in May 2014. The cell line was maintained in DMEM containing 10% (v/v) FBS, penicillin (200 U/ml), streptomycin (100 µg/ml) and incubated at 37° C in a humidified incubator with an atmosphere of 50 mL/L CO_2. Proteasome inhibitor was obtained from NATCO.

Cell synchronization and radiation treatment

The cells growing in 10% FBS containing media were washed with 1X PBS. The cells were incubated with 0.05% FBS containing DMEM for 72 hrs. After 72 hrs, cells were replaced by 10% FBS containing median and were irradiated using 60 Co γ-rays at the respective lethal dose.

Protein extraction

10 million cells of the Parent (P), Radiation Resistant (RR) and Relapse (R) cells were grown under normal growth conditions. The media was aspirated and the cells were washed thrice with cold 1 X PBS after which the cells were scraped and pelleted down. The cell pellet was suspended in 150 µl of 0.5% SDS Solution and sonicated with 10 pulses each for 10secs. The sonicated cells were centrifuged at 4000 RPM for 15 mins at 4° C and the supernatant was used for the proteomic analysis. The protein concentration was determined using bichoninic acid assay and equal amounts of protein from the 3 conditions were taken for further analysis.

iTRAQ labelling

Protein extracts from the untreated, radiation resistant and relapse cells were digested with trypsin and

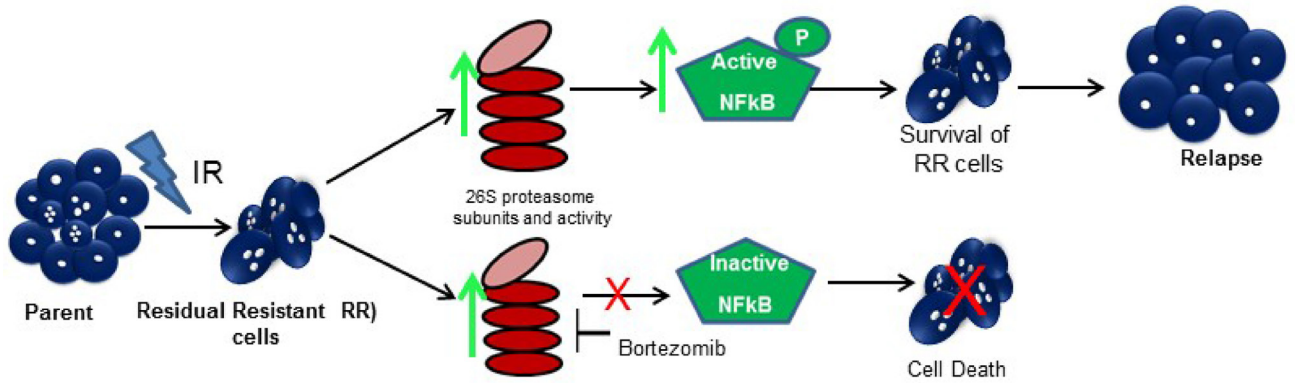

Figure 7: Proposed model for the study.

the peptides were labelled with iTRAQ reagents according to the manufacturer's instructions (iTRAQ Reagents Multiplex kit; Applied Biosystems/MDS Sciex, Foster City, CA). Briefly, 80 µg of protein from each sample was reduced, alkylated and digested with sequencing grade trypsin; (Promega, Madison, WI, USA). Peptides from P, RR and R were labelled with iTRAQ reagents containing 114, 115 and 116 reporter ions, respectively. The three labelled samples were pooled, vacuum-dried and subjected to fractionation by strong cation exchange (SCX) chromatography.

SCX fractionation

The pooled sample after iTRAQ labelling was resuspended in 1 ml of buffer A [10 mM KH2PO4, 25% (v/v) acetonitrile (ACN), pH 2.9] and separated on a SCX column (Zorbax 300-SCX, 5 µm, 2.1 mm ID × 50 mm, Agilent Technologies, Santa Clara, CA, USA) at a flow rate of 700 µl/min with a 40 min gradient [5 min, 0–5% buffer B (buffer A + 350 mM KCl); 5 min, 5–10%; 5 min, 10–23%; 5 min, 23–50%; 10 min, 50–100%; 10 min, 100% B]. One minute fractions were collected, vacuum-dried and desalted using C18 cartridge (Pierce, Rockford, USA) as per the manufacturer's instructions. After desalting, consecutive fractions were pooled to obtain a total of thirteen fractions for LC-MS/MS analysis.

LC-MS/MS analysis

Nanoflow electrospray ionization tandem mass spectrometric analysis of peptide samples was carried out using LTQ-Orbitrap Velos (Thermo Scientific, Bremen, Germany) interfaced with Agilent's 1200 Series nanoflow LC system. The chromatographic capillary columns used were packed with Magic C18 AQ (particle size 5 µm, pore size 100Å; Michrom Bioresources, Auburn, CA, USA) reversed phase material in 100% ACN at a pressure of 1000 psi. The peptide sample from each SCX fraction was enriched using a trap column (75 µm × 2 cm) at a flow rate of 3 µl/min and separated on an analytical column (75 µm × 10 cm) at a flow rate of 350 nl/min. The peptides were eluted using a linear gradient of 7–30% ACN over 65 min. Mass spectrometric analysis was carried out in a data dependent manner with full scans acquired using the Orbitrap mass analyser at a mass resolution of 60,000 at 400 m/z. For each MS cycle, twenty most intense precursor ions from a survey scan were selected for MS/MS and fragmentation detected at a mass resolution of 15,000 at m/z 400. The fragmentation was carried out using higher-energy collision dissociation (HCD) as the activation method with 40% normalized collision energy. The ions selected for fragmentation were excluded for 30 sec. The automatic gain control for full FT MS was set to 1 million ions and for FT MS/MS was set to 0.1 million ions with a maximum time of accumulation of 500 ms, respectively. For accurate mass measurements, the lock mass option was enabled.

Protein identification and quantitation

The MS data was analyzed using Proteome Discoverer (Thermo Fisher Scientific, Version 1.4). The workflow consisted of a spectrum selector and a reporter ion quantifier. MS/MS search was carried out using SEQUEST and MASCOT search algorithms against the NCBI RefSeq database (release 52 40) containing 31,811 proteins. Search parameters included trypsin as the enzyme with 1 missed cleavage allowed; oxidation of methionine was set as a dynamic modification while alkylation at cysteine and iTRAQ modification at N-terminus of the peptide and lysine were set as static modifications. Precursor and fragment mass tolerance were set to 20 ppm and 0.1.Da, respectively. False Discovery Rate (FDR) was calculated by searching the proteomic data against a decoy protein database. Only those Peptide Spectrum Matches (PSMs) that qualified a 1% FDR threshold were considered for further analysis. Unique peptide (s) for each protein identified was used to determine relative protein quantitation based on the relative intensities of reporter ions released during MS/MS fragmentation of peptides.

Bioinformatics analysis

Heat Map representation for the differential genes on the basis of their relative peptide intensities was constructed using MeV software (v 4.9.0). Unsupervised Hierarchical clustering of the genes was done using Pearson Correlation method. Functional annotation and Gene enrichment pathway analysis was done using Cytoscape (v 3.5.1) ClueGo (v 1.8) and CluPedia (v 1.0) plugin with default parameters. KEGG and REACTOME pathway databases were used for reference.

Western blot analysis

Cells were lysed using EBC lysis buffer (120 mM NaCl, 50 mM Tris-Cl (pH 8.0), 0.5% (v/v) Nonidet P-40, 50 µg/ml PMSF and protease, phosphatase inhibitor cocktail for 45 minutes on ice. The supernatant were collected and 40 ug of protein was used for immunoblotting using anti-YBX3 (rabbit; 1:1000; Pierce), anti-PSMB4 (rabbit; 1:1000; Pierce), and anti-PSMD10 (rabbit; 1:1000; Pierce), Actin (Sigma; 1:4000 dilutions), was used as a loading control. Immune-reactive proteins were visualized using an enhanced chemiluminescence (ECL) reagent (Pierce).

MTT cytotoxicity assay

5000 cells/well were seeded in 96 well plates for overnight. Bortezomib (Bortenat 2 mg; Natco Company) was added at different concentration i.e. 0.1 nM, 1 nM, 10 nM and 100 nM. After 72 hrs 10 µL of MTT reagent

(5 mg/ml in PBS, Himedia TC191-1G) was added to each well and incubated for 4 h. Crystals were dissolved using freshly prepared acidified isopropanol containing 10% tritonX-100. Optical density was measured at 570 nM by (SPECTROstar^{NANO}star spectrophotometer).

Proteasome activity assay

0.1 million cells were pelleted, washed twice with 1X PBS and resuspended in ATP buffer containing 50 mM Tris (pH 7.5), 5 mM MgCl2, 1 mMATP, 10% glycerol and protease inhibitor cocktail (Sigma). Cell suspensions were ultra-sonicated for four cycles of 5 s each (with 1 s break after each 2 s) at 30 kHz on ice. Proteasome activity was measured using 50 µM Suc-LLVY-7-amino-4-methyl coumarin substrate and fluorescence readings were taken at excitation 355 nm/emission 460 nm.

Trypan blue exclusion assay

0.1 million cells from all cultures were seeded in a 24 well plate and irradiated with the lethal dose of radiation. Viable cells from each well were counted every alternative day till 22 days to monitor the cell survival post radiation on a haemocytometer.

Orthotopic xenograft mouse experiments

All animal experiments were licensed through the Laboratory Animal Facility of ACTREC, TMC. Protocols were reviewed by the Institutional Animal Ethics Committee (IAEC). NUDE/SCID mice (6–8 weeks old) bred and maintained in an isolated facility within a specific pathogen-free environment were used for this study. 1×10^5 pLenti6-luc2 U87MG cells stably expressing luciferase were intracranially injected for generating the orthotopic GBM model and for studying the tumorigenicity of pre-treated Parent and RR cells. 2.5×10^5 pLenti6-luc2 U87MG stably expressing luciferase were intracranially injected for studying the effect of proteasome inhibitor along with radiation. In order to perform intracranial injection, the cells were suspended in 5 µl 1X PBS prior to injection and kept on ice until injected. Prior to injecting the cells intracranially, the mice were anesthetized using an injection mix of Ketamine (120 mg/kg)/Xylazine(mg/kg)/Saline and the mice was placed on the stereotaxic for stereotactic surgery. A 10 mm to 15 mm long incision was made on top of the skull. A small hole was drilled using a sterile 26 gauge sharp needle at 1 mm posterior to bregma and 2 mm lateral to coronal suture and 2.5 mm depth. The 5 µl cell suspension was then loaded onto the Hamilton syringe and injected at a rate of 1 µl per minute for a total of 6–8 minutes. The tumours were allowed to grow and animals were sacrificed using CO_2 at the onset of disease symptoms, such as weight and activity loss, and the brains were removed.

Radiation and drug treatment of orthotopic GBM mouse model.

The mice were divided into four groups post 7–10 days of intracranial injection: Vehicle control, bortezomib (Bortenat 2 mg, NATCO company), Radiated group, Radiation and BTZ group. Radiation was delivered to the whole brain of anesthetized mice, immobilized in a plastic chamber using 60Co γ-rays. A total dose of 14 Gy was administered over a period of 7 days. 0.5 mg/Kg of bortezomib was administered intraperitoneally twice in a week for 2 weeks.

Bioluminescence imaging of orthotopic tumor xenografts

Mice were anaesthetized with Ketamine/Xylazine and were administered luciferin (D-Luciferin potassium salt, 150 mg/kg, Calliper Life Sciences) via intraperitoneal injection. The images were acquired 10–12 minutes post injection. The time chosen was based on the pharmacokinetics of luciferin which defines that maximum luminescence emission and greatest sensitivity of detection will be obtained when cell luminescence is detected after 10–15 mins of injection of luciferin. The selected imaging time was maintained as constant among all the animals to be imaged. Regions of interest encompassing the intracranial area of signal were defined using Living Image software, and the total photons/s/sr/cm^2 (photons per second per steradian per square cm) was recorded.

Statistical methods

All data are represented as means ± standard error means (SEMs). The two-tailed Student's *t*-test was applied for statistical analysis. The Kaplan–Meier curve was plotted to generate the survival curves and to estimate the median survival values. Differences between survival curves were compared using a log-rank test.

ACKNOWLEDGMENTS

We thank Dr Neelam Shirsat and Dr Amit Dutt for providing the glioma cell lines. We acknowledge the funding from Department of Biotechnology (BT/PR4040/MDE/30/792/2012) and Tata Memorial Centre to SD

CONFLICTS OF INTEREST

Authors declare no conflicts of interest.

REFERENCES

1. Stupp R, Mason WP, van den Bent MJ, Weller M, Fisher B, Taphoorn MJ, Belanger K, Brandes AA, Marosi C, Bogdahn U, Curschmann J, Janzer RC, Ludwin SK, et al;

and European Organisation for Research and Treatment of Cancer Brain Tumor and Radiotherapy Groups; and National Cancer Institute of Canada Clinical Trials Group. Radiotherapy plus Concomitant and Adjuvant Temozolomide for Glioblastoma. The new england journal of medicine. 2005.

2. Stupp R, Hegi ME, Mason WP, van den Bent MJ, Taphoorn MJ, Janzer RC, Ludwin SK, Allgeier A, Fisher B, Belanger K, Hau P, Brandes AA, Gijtenbeek J, et al; European Organisation for Research and Treatment of Cancer Brain Tumour and Radiation Oncology Groups; National Cancer Institute of Canada Clinical Trials Group. Effects of radiotherapy with concomitant and adjuvant temozolomide versus radiotherapy alone on survival in glioblastoma in a randomised phase III study: 5-year analysis of the EORTC-NCIC trial. Lancet Oncol. 2009; 10:459-66.
3. Zhang X, Zhang W, Cao WD, Cheng G, Zhang YQ. Glioblastoma multiforme: molecular characterization and current treatment strategy (Review). Exp Ther Med. 2012; 3:9–14. Review https://doi.org/10.3892/etm.2011.367.
4. Reardon DA, Wen PY. Therapeutic advances in the treatment of glioblastoma: rationale and potential role of targeted agents. Oncologist. 2006; 11:152–64. https://doi.org/10.1634/theoncologist.11-2-152.
5. Glas M, Rath BH, Simon M, Reinartz R, Schramme A, Trageser D, Eisenreich R, Leinhaas A, Keller M, Schildhaus HU, Garbe S, Steinfarz B, Pietsch T, et al. Residual tumor cells are unique cellular targets in glioblastoma. Ann Neurol. 2010; 68:264–69.
6. Kelley K, Knisely J, Symons M, Ruggieri R. Radioresistance of Brain Tumors. Cancers. 2016; 8.
7. Weller M, Cloughesy T, Perry JR, Wick W. Standards of care for treatment of recurrent glioblastoma—are we there yet? Neuro-oncol. 2013; 15:4–27. https://doi.org/10.1093/neuonc/nos273.
8. Roy S, Lahiri D, Maji T, Biswas J. Recurrent Glioblastoma: where we stand. South Asian J Cancer. 2015; 4:163–73. https://doi.org/10.4103/2278-330X.175953.
9. Kaur E, Rajendra J, Jadhav S, Shridhar E, Goda JS, Moiyadi A, Dutt S. Radiation-induced homotypic cell fusions of innately resistant glioblastoma cells mediate their sustained survival and recurrence. Carcinogenesis. 2015; 36:685–95. https://doi.org/10.1093/carcin/bgv050.
10. Pandey A, Mann M. Proteomics to study genes and genomes. Nature. 2000; 405:837–46. https://doi.org/10.1038/35015709.
11. Chumbalkar V, Sawaya R, Bogler O. Proteomics: the new frontier also for brain tumor research. Curr Probl Cancer. 2008; 32:143–54. https://doi.org/10.1016/j.currproblcancer.2008.02.005.
12. Lage H. Proteomics in cancer cell research: an analysis of therapy resistance. Pathol Res Pract. 2004; 200:105–17. https://doi.org/10.1016/j.prp.2004.02.003.
13. Larance M, Lamond AI. Multidimensional proteomics for cell biology. Nat Rev Mol Cell Biol. 2015; 16:269–80. https://doi.org/10.1038/nrm3970.
14. Kalinina J, Peng J, Ritchie JC, Van Meir EG. Proteomics of gliomas: initial biomarker discovery and evolution of technology. Neuro-oncol. 2011; 13:926–42. https://doi.org/10.1093/neuonc/nor078.
15. Kumar DM, Patil V, Ramachandran B, Nila MV, Dharmalingam K, Somasundaram K. Temozolomide-modulated glioma proteome: role of interleukin-1 receptor-associated kinase-4 (IRAK4) in chemosensitivity. Proteomics. 2013; 13:2113–24. https://doi.org/10.1002/pmic.201200261.
16. Vogel TW, Zhuang Z, Li J, Okamoto H, Furuta M, Lee YS, Zeng W, Oldfield EH, Vortmeyer AO, Weil RJ. Proteins and protein pattern differences between glioma cell lines and glioblastoma multiforme. Clin Cancer Res. 2005; 11:3624-32. https://doi.org/10.1158/1078-0432.CCR-04-2115.
17. Hill JJ, Moreno MJ, Lam JC, Haqqani AS, Kelly JF. Identification of secreted proteins regulated by cAMP in glioblastoma cells using glycopeptide capture and label-free quantification. Proteomics. 2009; 9:535–49. https://doi.org/10.1002/pmic.200800257.
18. Furuta M, Weil RJ, Vortmeyer AO, Huang S, Lei J, Huang TN, Lee YS, Bhowmick DA, Lubensky IA, Oldfield EH, Zhuang Z. Protein patterns and proteins that identify subtypes of glioblastoma multiforme. Oncogene. 2004; 23:6806–14. https://doi.org/10.1038/sj.onc.1207770.
19. Fang X, Wang C, Balgley BM, Zhao K, Wang W, He F, Weil RJ, Lee CS. Targeted tissue proteomic analysis of human astrocytomas. J Proteome Res. 2012; 11:3937–46. https://doi.org/10.1021/pr300303t.
20. Deighton RF, Le Bihan T, Martin SF, Barrios-Llerena ME, Gerth AM, Kerr LE, McCulloch J, Whittle IR. The proteomic response in glioblastoma in young patients. J Neurooncol. 2014; 119:79–89. https://doi.org/10.1007/s11060-014-1474-6.
21. Com E, Clavreul A, Lagarrigue M, Michalak S, Menei P, Pineau C. Quantitative proteomic Isotope-Coded Protein Label (ICPL) analysis reveals alteration of several functional processes in the glioblastoma. J Proteomics. 2012; 75:3898–913. https://doi.org/10.1016/j.jprot.2012.04.034.
22. Polisetty RV, Gautam P, Sharma R, Harsha HC, Nair SC, Gupta MK, Uppin MS, Challa S, Puligopu AK, Ankathi P, Purohit AK, Chandak GR, Pandey A, Sirdeshmukh R. LC-MS/MS analysis of differentially expressed glioblastoma membrane proteome reveals altered calcium signaling and other protein groups of regulatory functions. Mol Cell Proteomics. 2012; 11:M111.013565.
23. Collet B, Guitton N, Saïkali S, Avril T, Pineau C, Hamlat A, Mosser J, Quillien V. Differential analysis of glioblastoma multiforme proteome by a 2D-DIGE approach. Proteome Sci. 2011; 9:16. https://doi.org/10.1186/1477-5956-9-16.
24. Niclou SP, Fack F, Rajcevic U. Glioma proteomics: status and perspectives. J Proteomics. 2010; 73:1823–38. https://doi.org/10.1016/j.jprot.2010.03.007.
25. Thirant C, Galan-Moya EM, Dubois LG, Pinte S, Chafey P, Broussard C, Varlet P, Devaux B, Soncin F, Gavard J,

Junier MP, Chneiweiss H. Differential proteomic analysis of human glioblastoma and neural stem cells reveals HDGF as a novel angiogenic secreted factor. Stem Cells. 2012; 30:845–53. https://doi.org/10.1002/stem.1062.

26. de Aquino PF, Carvalho PC, Nogueira FC, da Fonseca CO, de Souza Silva JC, Carvalho Mda G, Domont GB, Zanchin NI, Fischer Jde S. A Time-Based and Intratumoral Proteomic Assessment of a Recurrent Glioblastoma Multiforme. Front Oncol. 2016; 6:183.
27. Della Donna L, Lagadec C, Pajonk F. Radioresistance of prostate cancer cells with low proteasome activity. Prostate. 2012; 72:868–74. https://doi.org/10.1002/pros.21489.
28. McBride WH, Iwamoto KS, Syljuasen R, Pervan M, Pajonk F. The role of the ubiquitin/proteasome system in cellular responses to radiation. Oncogene. 2003; 22:5755–73. https://doi.org/10.1038/sj.onc.1206676.
29. The UniProt Consortium. UniProt: the universal protein knowledgebase. Nucleic Acids Res. 2017; 45:D158–69. https://doi.org/10.1093/nar/gkw1099.
30. Monika A. Jarzabek PCH, Kai O. Skaftnesmo, Emmet McCormack, Patrick Dicker, Jochen H.M. Prehn, Rolf Bjerkvig, and Annette T. Byrne. In Vivo Bioluminescence Imaging Validation of a Human Biopsy–Derived Orthotopic Mouse Model of Glioblastoma Multiforme. Molecular Imaging. 2013.
31. Burger AM, Seth AK. The ubiquitin-mediated protein degradation pathway in cancer: therapeutic implications. Eur J Cancer. 2004; 40:2217–29. https://doi.org/10.1016/j.ejca.2004.07.006.
32. Qureshi N, Morrison DC, Reis J. Proteasome protease mediated regulation of cytokine induction and inflammation. Biochim Biophys Acta. 2012; 1823:2087–93. https://doi.org/10.1016/j.bbamcr.2012.06.016.
33. Livneh I, Cohen-Kaplan V, Cohen-Rosenzweig C, Avni N, Ciechanover A. The life cycle of the 26S proteasome: from birth, through regulation and function, and onto its death. Cell Res. 2016; 26:869–85. https://doi.org/10.1038/cr.2016.86.
34. Pajonk F, van Ophoven A, Weissenberger C, McBride WH. The proteasome inhibitor MG-132 sensitizes PC-3 prostate cancer cells to ionizing radiation by a DNA-PK-independent mechanism. BMC Cancer. 2005; 5:76. https://doi.org/10.1186/1471-2407-5-76.
35. Pervan M, Iwamoto KS, McBride WH. Proteasome structures affected by ionizing radiation. Mol Cancer Res. 2005; 3:381–90. https://doi.org/10.1158/1541-7786.MCR-05-0032.
36. Pajonk F, McBride WH. Ionizing radiation affects 26s proteasome function and associated molecular responses, even at low doses. Radiother Oncol. 2001; 59:203–12. https://doi.org/10.1016/S0167-8140(01)00311-5.
37. Tamari K, Hayashi K, Ishii H, Kano Y, Konno M, Kawamoto K, Nishida N, Koseki J, Fukusumi T, Hasegawa S, Ogawa H, Hamabe A, Miyo M, et al. Identification of chemoradiation-resistant osteosarcoma stem cells using an imaging system for proteasome activity. Int J Oncol. 2014; 45:2349–54. https://doi.org/10.3892/ijo.2014.2671.
38. Smith L, Qutob O, Watson MB, Beavis AW, Potts D, Welham KJ, Garimella V, Lind MJ, Drew PJ, Cawkwell L. Proteomic identification of putative biomarkers of radiotherapy resistance: a possible role for the 26S proteasome? Neoplasia. 2009; 11:1194–207. https://doi.org/10.1593/neo.09902.
39. Baugh JM, Viktorova EG, Pilipenko EV. Proteasomes can degrade a significant proportion of cellular proteins independent of ubiquitination. J Mol Biol. 2009; 386:814–27. https://doi.org/10.1016/j.jmb.2008.12.081.
40. Crawford LJ, Walker B, Irvine AE. Proteasome inhibitors in cancer therapy. J Cell Commun Signal. 2011; 5:101–10. https://doi.org/10.1007/s12079-011-0121-7.
41. Teicher BA, Tomaszewski JE. Proteasome inhibitors. Biochem Pharmacol. 2015; 96:1–9. https://doi.org/10.1016/j.bcp.2015.04.008.
42. Thaker NG, Zhang F, McDonald PR, Shun TY, Lewen MD, Pollack IF, Lazo JS. Identification of survival genes in human glioblastoma cells by small interfering RNA screening. Mol Pharmacol. 2009; 76:1246–55. https://doi.org/10.1124/mol.109.058024.
43. Cahill KE, Morshed RA, Yamini B. Nuclear factor-κB in glioblastoma: insights into regulators and targeted therapy. Neuro-oncol. 2016; 18:329–39. https://doi.org/10.1093/neuonc/nov265.
44. Ahmed KM, Li JJ. NF-kappa B-mediated adaptive resistance to ionizing radiation. Free Radic Biol Med. 2008; 44:1–13. https://doi.org/10.1016/j.freeradbiomed.2007.09.022.
45. Pahl HL. Activators and target genes of Rel/NF-kappaB transcription factors. Oncogene. 1999; 18:6853–66. https://doi.org/10.1038/sj.onc.1203239.

Enhanced proteasomal activity is essential for long term survival and recurrence of innately radiation resistant residual glioblastoma cells

SUPPLEMENTARY MATERIALS

GeneName	Protein Name	Relative Peptide Intensities in RR	Ub Position Glycyl lysine isopeptide	References
APP	Amyloid beta A4 protein	0.191	763	
HIST1H1B	Histone H1.5 (Histone H1a) (Histone H1b) (Histone H1s-3)	0.475	17	
HIST1H1B	Histone H1.5 (Histone H1a) (Histone H1b) (Histone H1s-3)	0.475	219	
HIST1H4A	Histone H4	0.477	13	
HIST1H4A	Histone H4	0.477	92	
KDM1A	lysine-specific histone demethylase 1A isoform b	0.478	503	Han X et al, Mol Cell. 2014 Aug
PEF1	peflin	0.508	137	McGourty CA et al, Cell. 2016 Oct
PPIA	peptidyl-prolyl cis-trans isomerase A	0.570	28	Visvikis O et al, FEBS J. 2008 Jan
RAC1	ras-related C3 botulinum toxin substrate 1 isoform Rac1	0.581	147	
RAN	GTP-binding nuclear protein Ran	0.601	71	
RBBP7	histone-binding protein RBBP7 isoform 2	0.602	4	
RBBP7	histone-binding protein RBBP7 isoform 2	0.605	159	
RPL10	60S ribosomal protein L10 isoform a	0.605	188	
RPS10	40S ribosomal protein S10	0.619	138	Sundaramoorthy E et al, Mol Cell. 2017 Feb 16
RPS10	40S ribosomal protein S10	0.626	139	Sundaramoorthy E et al, Mol Cell. 2017 Feb 16
TCEA1	transcription elongation factor A protein 1 isoform 1	0.626	55	
TDRKH	tudor and KH domain-containing protein isoform a	0.672	65	Cunningham et al, Nature Cell Biology 2015
TDRKH	tudor and KH domain-containing protein isoform a	0.672	76	Cunningham et al, Nature Cell Biology 2015
TDRKH	tudor and KH domain-containing protein isoform a	0.672	110	Cunningham et al, Nature Cell Biology 2015
TDRKH	tudor and KH domain-containing protein isoform a	0.672	112	Cunningham et al, Nature Cell Biology 2015
TDRKH	tudor and KH domain-containing protein isoform a	0.672	152	Cunningham et al, Nature Cell Biology 2015
TDRKH	tudor and KH domain-containing protein isoform a	0.672	175	Cunningham et al, Nature Cell Biology 2015
TDRKH	tudor and KH domain-containing protein isoform a	0.672	181	Cunningham et al, Nature Cell Biology 2015
TDRKH	tudor and KH domain-containing protein isoform a	0.672	187	Cunningham et al, Nature Cell Biology 2015
TDRKH	tudor and KH domain-containing protein isoform a	0.672	193	Cunningham et al, Nature Cell Biology 2015
TDRKH	tudor and KH domain-containing protein isoform a	0.672	256	Cunningham et al, Nature Cell Biology 2015
TDRKH	tudor and KH domain-containing protein isoform a	0.672	267	Cunningham et al, Nature Cell Biology 2015
TDRKH	tudor and KH domain-containing protein isoform a	0.672	479	Cunningham et al, Nature Cell Biology 2015
TDRKH	tudor and KH domain-containing protein isoform a	0.672	510	Cunningham et al, Nature Cell Biology 2015
TDRKH	tudor and KH domain-containing protein isoform a	0.672	529	Cunningham et al, Nature Cell Biology 2015
UBE2T	ubiquitin-conjugating enzyme E2 T	0.685	91	Alpi AF1 et al, Mol Cell. 2008 Dec 26
UBE2T	ubiquitin-conjugating enzyme E2 T	0.685	182	Alpi AF1 et al, Mol Cell. 2008 Dec 26

Supplementary Figure 1: Downregulated proteasome target proteins. List of downregulated proteins with ubiquitin binding lysine residues.

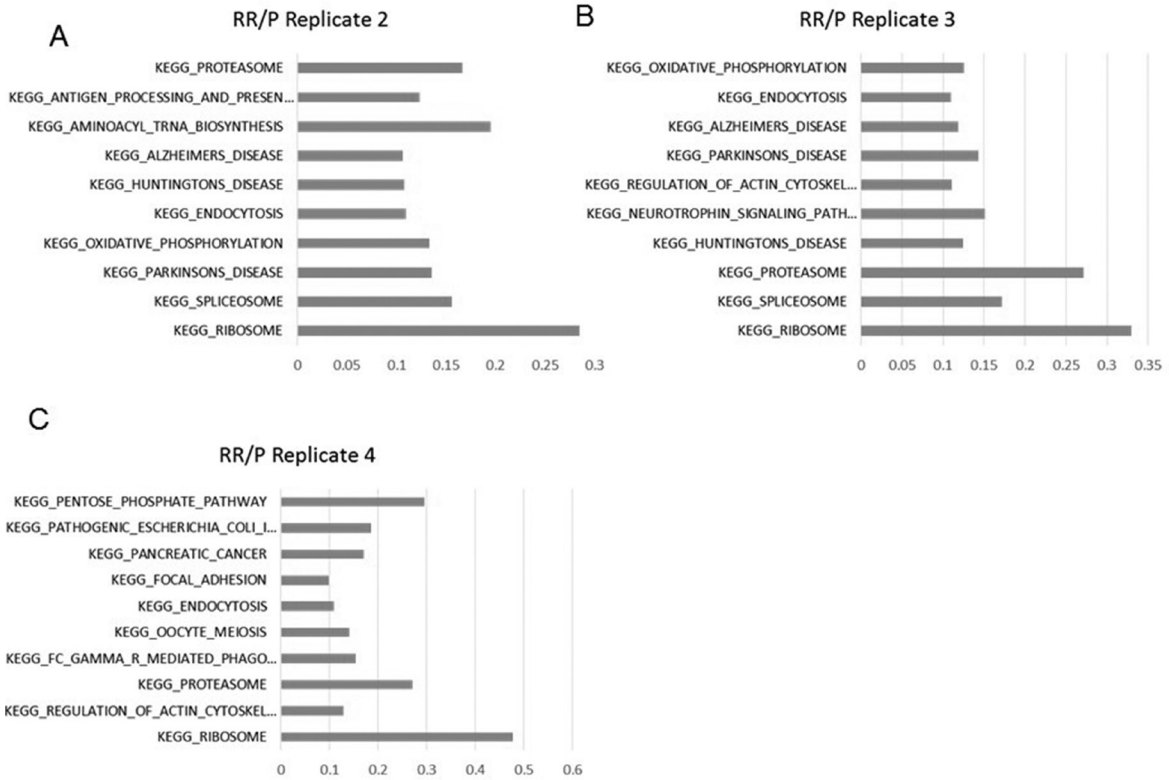

Supplementary Figure 2: Pathway analysis of deregulated proteins in all the biological replicates. (**A**) Pathway analysis of deregulated proteins in replicate 2. (**B**) Pathway analysis of deregulated proteins in replicate 3. (**C**) Pathway analysis of deregulated proteins in replicate 4.